OCS Study
MMS 2003-063

Coastal Marine Institute

Historical Reconstruction of the Contaminant Loading and Biological Responses in the Central Gulf of Mexico Shelf Sediments

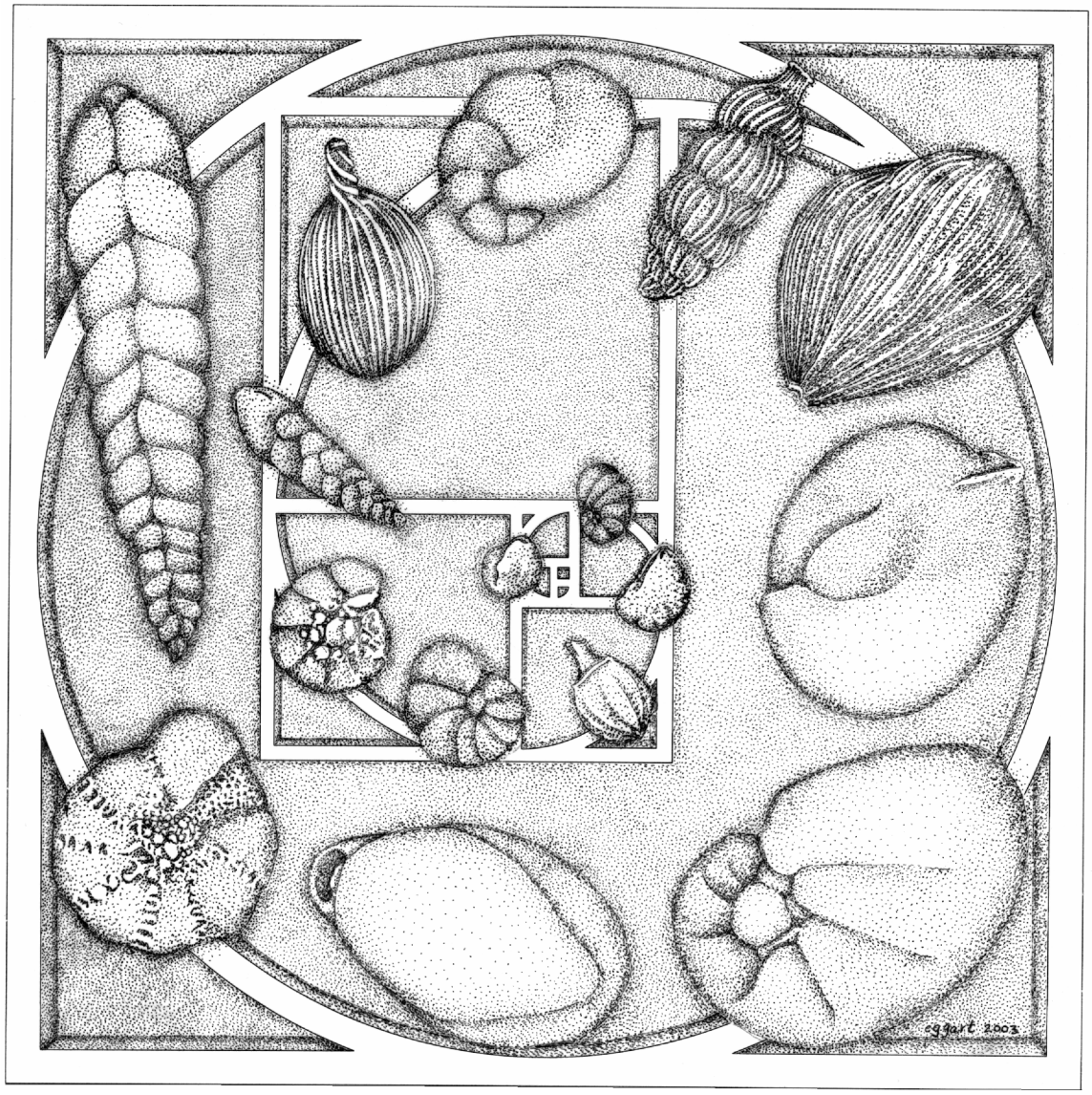

U.S. Department of the Interior
Minerals Management Service
Gulf of Mexico OCS Region

Cooperative Agreement
Coastal Marine Institute
Louisiana State University

OCS Study
MMS 2003-063

Coastal Marine Institute

Historical Reconstruction of the Contaminant Loading and Biological Responses in the Central Gulf of Mexico Shelf Sediments

Editors

R. Eugene Turner
Edward B. Overton
Nancy N. Rabalais
Barun K. Sen Gupta

October 2003

Prepared under MMS Contract
14-35-0001-30660-19930
by
Coastal Marine Institute
Louisiana State University
Baton Rouge, Louisiana 70803

Published by

U.S. Department of the Interior
Minerals Management Service
Gulf of Mexico OCS Region

Cooperative Agreement
Coastal Marine Institute
Louisiana State University

DISCLAIMER

This report was prepared under contract between the Minerals Management Service (MMS) and Louisiana State University, Coastal Ecology Institute. This report has been reviewed by the MMS and approved for publication. Approval does not signify that the contents necessarily reflect the views and policies of the Service, nor does mention of trade names or commercial products constitute endorsement or recommendation for use. It is, however, exempt from review and compliance with MMS editorial standards.

REPORT AVAILABILITY

Extra copies of the report may be obtained from the Public Information Office (Mail Stop 5034) at the following address:

U.S. Department of the Interior
Minerals Management Service
Gulf of Mexico OCS Region
Attention: Public Information Office (MS 5034)
1201 Elmwood Park Boulevard
New Orleans, Louisiana 70123-2394

Telephone Number: (504) 736-2519 or
1-800-200-GULF

CITATION

Suggested citation:

Turner, R.E., E.B. Overton, N.N. Rabalais, and B.K. Sen Gupta (eds.). 2003. Historical reconstruction of the contaminant loading and biological responses in the Central Gulf of Mexico shelf sediments. U.S. Dept. of the Interior, Minerals Management Service, Gulf of Mexico OCS Region, New Orleans, LA. OCS Study MMS 2003-063. 140 pp.

ACKNOWLEDGMENTS

The authors acknowledge and thank the many people who participated in the collection, analysis and discussions resulting in this conclusion, especially, Q. Dortch, B. Fry, D. Justic', J.M. Lee, T.A. Oswald, and E.M. Swenson, and the crew of the *R/V Pelican*.

ABOUT THE COVER

Artist, Mary Lee Eggart, depicts Louisiana foraminifers on a golden-mean spiral.

ABSTRACT

We documented changes in chemical contaminants and biological components of dated sediments collected from the central Gulf of Mexico continental shelf to evaluate the relative sources and concentrations. These include trace metals, selected organic compounds, phytoplankton pigments, diatom remnants and foraminifera.

The distribution of the selected organic compounds suggests a chronic contaminant loading from the river itself, from oil and gas exploration in the Gulf of Mexico, perhaps from natural seeps in the area, and the chronological usage of chlorinated agricultural pesticides. The total organochlorine pesticide and total poly aromatic hydrocarbon (PAH) concentrations begin increasing above background levels after World War II. The organochlorine pesticide concentrations peaked from the 1940's through the 1970's in most of the cores, but not all, and some were not dominated by any one pesticide. The petrogenic (petroleum in origin) PAHs were assessed by quantitating the total hopanes. The hopanes were present in almost all of the cores and began increasing after WWII. The prominent PAH analytes in most of the cores were pyrene, fluoranthene, and phenanthrene, which are associated with pyrogenic sources.

The fluctuations in the accumulation of Barium (Ba), but not Vanadium (V), are coincidental with the presumed use of barite on this shelf. The fluctuations in V concentration in the sediments are coincidental with the national consumption of V. Copper (Cu), Cadmium (Cd), and Zinc (Zn) concentrations in sediments fluctuate coincidentally with V, not Ba, thus indicating that the dominant source of these trace metals in offshore sediments are derived from riverine sources, and are not primarily from *in situ* industrial processes releasing them on the shelf. This is not to suggest that local site-specific contamination is not a significant management or health concern.

There is a general increase in chlorophyll *a*, pheopigments, zeaxanthin, fucoxanthin and most carotenoids over time, with the change gradual from 1955 to 1970, followed by a fairly steady increase to 1997. These patterns are consistent with the increased accumulation of diatom remnants in sediments. The increasing pigments and greater concentrations in areas where hypoxia is more likely to occur indicate an increase in eutrophication or a worsening of hypoxia or both.

The temporal trend in forminifera is one of diversity reduction and increasing dominance. No definite relationship could be established between the contaminant concentration in sediments and the composition of foraminiferal assemblage. The only match between a contaminant high and a diversity low was at the 1970-1975 level in one core; the significance of this match is unclear. Deformed Foraminifera, one indicator of extreme chemical pollution, are not present in either of the cores. On the other hand, the diversity and relative-abundance changes of foraminiferal species fit the model of progressively worsening seasonal hypoxia in the area.

These analyses indicate that both OCS development and riverine sources exert strong influences on the sediment constituents offshore, and that these influences may be independent of one another.

TABLE OF CONTENTS

ABSTRACT v

LIST OF FIGURES ix

LIST OF TABLES xiii

CHAPTER 1. INTRODUCTION 1.1

CHAPTER 2. ORGANICS ANALYSES 2.1
- Abstract 2.1
- Introduction 2.2
- Methodology 2.3
  - Preparation and Extraction 2.3
  - Instrument Configuration and Calibration 2.4
  - Quantitative Analysis 2.5
  - Quality Assurance (QA)/Quality Control (QC) 2.5
  - Instrumental QA/QC 2.6
- Results 2.6
  - Organochlorine Pesticides (OC) and Polychlorinated Biphenyls (PCB's) 2.7
  - Polycyclic Aromatic Hydrocarbons (PAH's) 2.10
  - Individual Core Results 2.15
- Discussion 2.16
  - Organochlorine (OC) Pesticides 2.18
  - Polycyclic Aromatic Hydrocarbons (PAH's) 2.18
- Recommendations 2.19

CHAPTER 3. TRACE METAL, C, N AND BIOLOGICALLY-BOUND SILICATE IN DATED SEDIMENTS FROM THE LOUISIANA CONTINENTAL SHELF 3.1
- Abstract 3.1
- Introduction 3.2
- Methods 3.3
  - Sediment Dating 3.3
  - Diatom Remains 3.4
  - Total Organic Carbon 3.4
  - Trace Metals 3.4
  - Grain Size 3.4
  - Mineral Production and Use 3.5
- Results and Discussion 3.5
  - Sediment Accretion Rates 3.5
  - General Sediment Quality Near and Far from the Mississippi River Delta 3.6
  - Trace Metals 3.6

TABLE OF CONTENTS
(continued)

Diatom Remains and Organic Content 3.10
Summary 3.11

CHAPTER 4. ECOSYSTEM HISTORY REVEALED THROUGH PRESERVED PHYTOPLANKTON PIGMENTS 4.1
Abstract 4.1
Introduction 4.1
Study Area 4.2
Methods 4.4
Sediment Grain Size Analysis 4.4
Chloropigments by High Performance Liquid Chromatography (HPLC) 4.4
Results and Discussion 4.5
Sediment Grain Size 4.5
Phytoplankton Pigments 4.6
Summary 4.16

CHAPTER 5. HISTORICAL RECONSTRUCTION OF THE CONTAMINANT LOADING AND BIOLOGICAL RESPONSES IN THE CENTRAL GULF OF MEXICO SHELF SEDIMENTS: FORAMINIFERA 5.1
Abstract 5.1
Introduction 5.1
Materials and Methods 5.2
Results and Discussion 5.3
Species Diversity 5.3
Species Distribution 5.4
Community Change 5.13
Additional Data 5.18
Significant Stratigraphic Trends and Interpretations 5.22
Summary and Conclusions 5.23

CHAPTER 6. LITERATURE CITED 6.1

CHAPTER 7. APPENDICES 7.1

Appendix A. Total Organochlorine Pesticide Histograms 7.3
Appendix B. Organochlorine Pesticide Concentrations for Sediment Cores 7.9
Appendix C. Total Organochlorine Pesticide Histograms by Decade 7.15
Appendix D. Total PAH Histograms 7.19
Appendix E. PAH Concentrations for Sediment Cores 7.25
Appendix F. Total PAH Histograms by Decade 7.33
Appendix G. Total PAH vs. Estimated Total Hopane Concentrations by Core and Date 7.41

LIST OF FIGURES

Figure 1.1. The production of oil and gas in southern Louisiana in 1941, 1964 and 1981 ..... 1.1

Figure 1.2. The oil and produced water production for leases in the Gulf of Mexico OCS. The mean water depth of new oil leases in the Gulf of Mexico, by year. The percentage of oil spilled of the total production in the Gulf of Mexico, by year 1.2

Figure 2.1. Location of the core samples analyzed for organic contaminants 2.3

Figure 2.2. Total organochlorine (OC) pesticide and breakdown product distributions in the core samples collected from the Mississippi Delta Bight prior to 1950 and after 1950 ..... 2.9

Figure 2.3. Total OC pesticide concentrations prior to the 1950's, after the 1950's and the overall totals in OCS cores collected from the Mississippi Delta Bight 2.9

Figure 2.4. Total PAH concentrations prior to 1950, after 1950 and overall totals from core samples collected in the Mississippi Delta Bight 2.12

Figure 2.5. Estimated total hopane concentrations prior to the 1950's, after the 1950's and the overall total from core samples collected from the Mississippi Delta Bight 2.13

Figure 2.6. Total PAH (petrogenic PAH's) distributions in the core samples collected from the Mississippi Delta Bight prior to 1950 and after 1950 ..... 2.14

Figure 2.7. Estimated total hopanes (petrogenic PAH's) distributions in the core samples collected from the Mississippi Delta Bight prior to 1950 and after 1950 ..... 2.14

Figure 3.1. Sampling locations where sediment cores were collected 3.3

Figure 3.2. The vertical distribution of ^{210}Pb in six cores collected for this study 3.5

Figure 3.3. Sedimentation rates (cm yr^{-1}) west of the Mississippi River delta 3.6

Figure 3.4. The relationship between sediment density and organic content and aluminum and sand 3.6

LIST OF FIGURES
(continued)

Figure 3.5. The relationship between the concentration (µg g^{-1}) of vanadium and barium in six sediment cores 3.7

Figure 3.6. The normalized concentration of barium (µg Ba / g Al) in six dated sediment cores from various depth zones on the Louisiana shelf 3.8

Figure 3.7. The normalized concentration of vanadium (µg V / g Al) in six dated sediment cores from various depth zones on the Louisiana shelf..... 3.9

Figure 3.8. The relationship between the percent carbon and nitrogen in dated sediments from six cores (dry weight basis) 3.11

Figure 3.9. The concentration of percent biogenic silica (Bsi) and % carbon vs. dated horizon for sediments from the continental shelf west of the Mississippi River delta in 10 to 100 m water depth 3.12

Figure 3.10. Core locations in the MDB where increasing concentrations of %BSi or %C were observed in the last three decades 3.13

Figure 4.1. Frequency distribution of hypoxic bottom-water during mid-summer for years 1985-2001 with core stations superimposed 4.2

Figure 4.2. Vertical distribution of % sand, % silt and % clay for cores as indicated..... 4.5

Figure 4.3. Vertical distribution of chlorophyll *a* and chlorophyll *a*/pheopigment ratio (Chla/Pheo) for cores E30-1, E50-1, E60-2, F35-2 and D50G 4.7

Figure 4.4. Vertical distribution of zeaxanthin and zeaxanthis/ß-carotene ratio for cores E30-1, E50-1, E60-2, F35-2 and D50G 4.8

Figure 4.5. Vertical distribution of fucoxanthin and diadinoxanthin for cores E30-1, E50-1, E60-2, F35-2 and D50G..... 4.9

Figure 4.6. Vertical distribution of alloxanthin and diatoxanthin for cores E30-1, E50-1, E60-2, F35-2 and D50G 4.10

Figure 4.7. Vertical distribution of chloropigments in core D50G; chla (chlorophyll *a*), total phaeo (total phaeopigments), Fuco (fucoxanthin), Ddx (diadinoxanthin), allo (alloxanthin), Diato (diatoxanthin), Lutein, zea (zeaxanthin), Cantha (canthaxanthin), B-caro (ß-carotene)..... 4.11

LIST OF FIGURES
(continued)

Figure 4.8. Vertical distribution of chloropigments in core I3; chla (chlorophyll *a*), total pheo (total phaeopigments), Fuco (fucoxanthin), Ddx (diadinoxanthin), Diato (diatoxanthin), Lutein, zea (zeaxanthin), B-caro (ß-carotene) 4.12

Figure 4.9. Trend of average Secchi disk depth on the Louisiana shelf west of the Mississippi River delta 4.15

Figure 5.1. Core locations 5.2

Figure 5.2. Distribution of species richness through time. A, core E60; B, core F35 .....5.4

Figure 5.3. Distribution of Shannon-Wiener diversity index through time. A, core E60; B, core F35 .....5.6

Figure 5.4. Distribution of dominant species through time. A, core E60; B, core F35 .....5.7

Figure 5.5. Distribution of *Ammonia–Elphidium* Index in Core F35 .....5.8

Figure 5.6. Distribution of relative abundances of *Bulimina marginata, Cancris sagra, Fursenkoina pontoni, Saccammina diflugiformis, and Uvigerina hispido-costata* in core E60 .....5.8

Figure 5.7. Distribution of relative abundances of *Bulimina marginata and Bolivina lowmani* in core F35 .....5.9

Figure 5.8. Distribution of relative abundances of *Quinqueloculina*. Core E60; core E35 .....5.10

Figure 5.9. Distribution of relative abundances of agglutinated and porcelaneous species groups, core E60 .....5.11

Figure 5.10. Distribution of relative abundances of agglutinated and porcelaneous species groups, core F35 .....5.12

Figure 5.11. Cluster analysis of E60 foraminiferal data; dendrogram for 12 cases 5.13

Figure 5.12. Cluster analysis of F35 foraminiferal data; dendrogram for 33 cases 5.14

Figure 5.13. Eigenvalues scree plot for E60 foraminiferal data 5.15

Figure 5.14. Factor loadings, Factor 1/Factor2 core E60 .....5.16

LIST OF FIGURES
(continued)

Figure 5.15. Factor loadings, Factor 1/Factor3 (A) and Factor 2/Factor 3 (B), core E60 .....5.17

Figure 5.16. Plots of factor scores against time, core E60. A, Factor 1. B, Factor 2.....5.17

Figure 5.17. Distribution of relative abundance of *Quinqueloculina*; core G27 .....5.19

Figure 5.18. Cluster analysis of BL10 core data, dendrogram for 51 cases 5.20

LIST OF TABLES

Table 2.1. Physical and chemical information from samples from the Mississippi Delta Bight 2.7

Table 2.2. Target OC pesticides and breakdown products, PCB's in the core samples 2.8

Table 2.3. Target PAH's in the originally proposed GC/MS-SIM method 2.10

Table 2.4. Target PAH's and oil biomarkers in GC/MS-SIM oil fingerprinting method 2.11

Table 3.1. Results from a simple linear regression analysis of the relationship between Cd, Cu, and Zn (Y) versus both vanadium and barium (x) in dated sediments from six core samples from the Louisiana shelf 3.10

Table 4.1. The taxonomic origin of pigments from Louisiana shelf sediment cores and their relative concentrations in algal groups 4.3

Table 4.2. Likelihood of exposure to hypoxia for each station based on mid-summer cruise data and more frequent observations off Terrebonne Bay 4.4

Table 4.3. Results of linear regressions among sediment pigments, sediment biogenic silica and Mississippi River annual nitrate load 4.13

Table 5.1. Eigenvalues for E60 foraminiferal data 5.15

Table 5.2. Factor loadings for 12 foraminiferal taxa in core E60. ..... 5.16

Table 5.3. Factor scores for 12 samples in core E60 ..... 5.18

Table 5.4. Eigenvalues for BL10 foraminiferal data 5.21

Table 5.5. Factor loadings for 18 foraminiferal species from core BL10 ..... 5.21

CHAPTER 1

INTRODUCTION

Oil and gas recovery from the northern Gulf of Mexico started in earnest after WWII, beginning in shallow water. Offshore production on the Outer Continental Shelf (OCS) at the turn of the last century was primarily off the Louisiana coast, and amounted to more than 600 million barrels of oil annually (1 bbl. = 42 gal.) and new leases were located in an average 100 m water depth (Figures 1.1 and 1.2, top). This non-renewable resource recovery was accompanied by a volume of produced water slightly larger than the oil recovered (Figure 1.2, middle). The percentage of oil spilled has declined since the peak in the mid-1970s, to the point where it is now about 0.005 % of the produced volume (Figure 1.2, bottom). Not all of this spilled oil is recovered where it is spilled. The produced water, the oil spilled and chemicals used in the mineral recovery phase have received some attention because of potential ecosystem impacts on this biologically-rich environment.

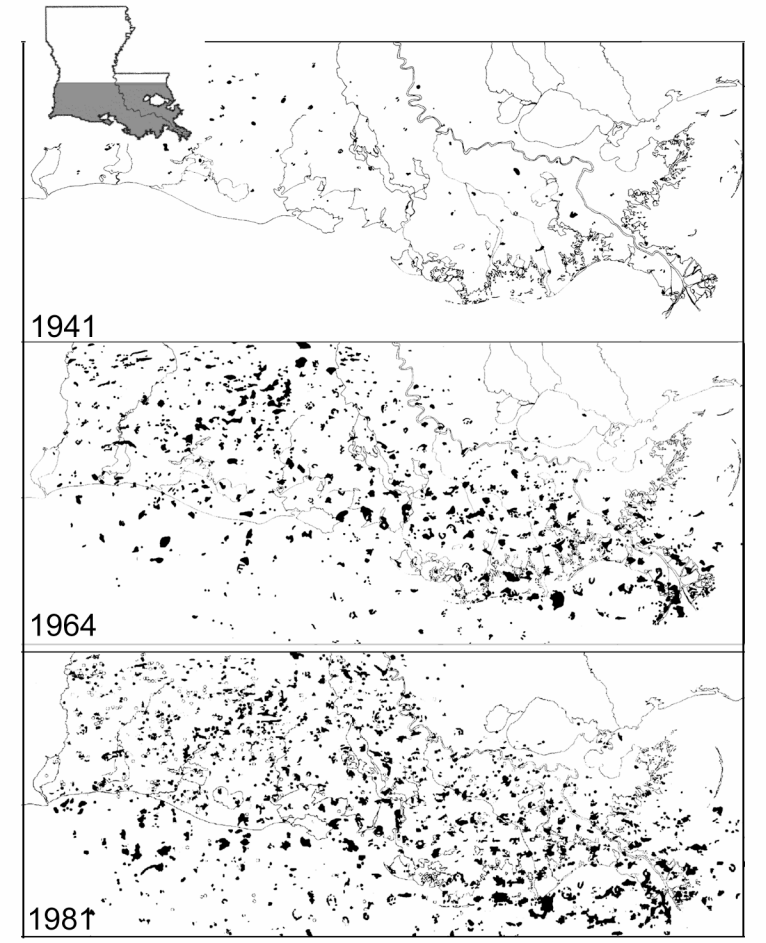

Figure 1.1. The production of oil and gas in southern Louisiana in 1941, 1964 and 1981 (from the Louisiana Geological Survey).

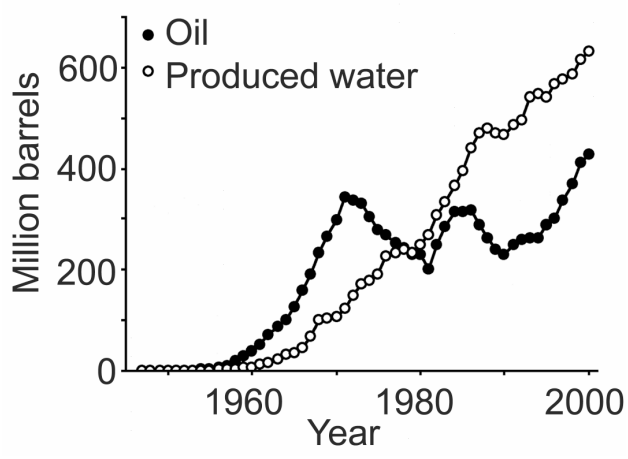

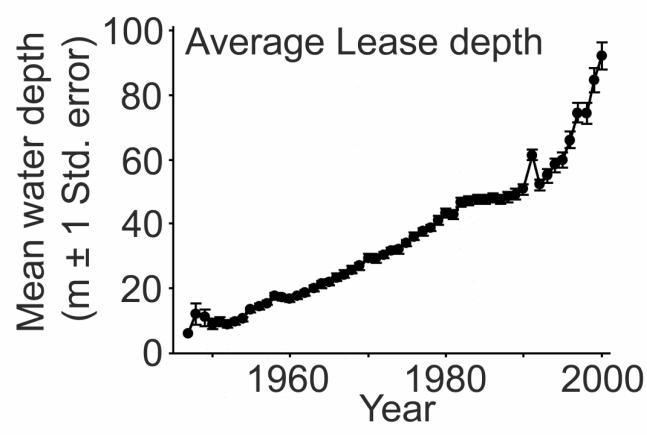

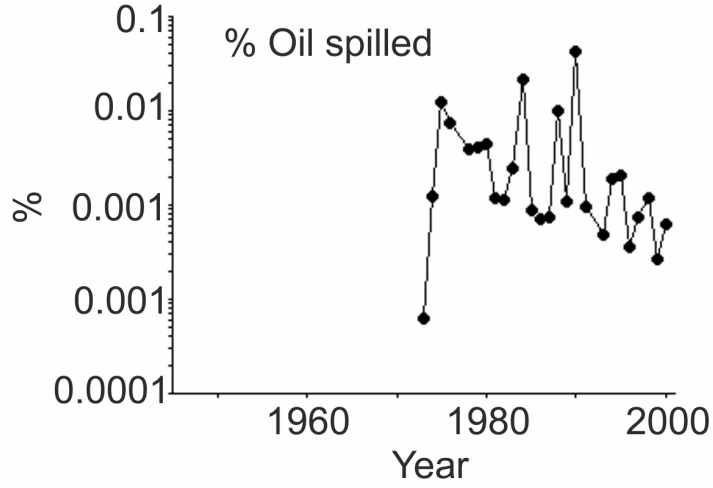

Figure 1.2. Top: The oil and produced water production for leases in the Gulf of Mexico OCS. Middle: The mean water depth of new oil leases in the Gulf of Mexico, by year. Bottom: The percentage of oil spilled of the total production in the Gulf of Mexico, by year. Data are from the U.S. Minerals Management Service (2003) and the U.S. Coast Guard (2003).

A pervasive, continuing, and confounding feature of the OCS Program and continental shelf investigations involves evaluation of the relative influences of these oil and gas recovery efforts against a background of regional forcing functions, such as riverine sources, climate, and estuarine exchanges that vary 'naturally' and have also changed over decades from landscape-scale influences (Bender et al. 1979). In other words, is the *in situ* release of contaminants as significant as the changes occurring from landuse changes in the Mississippi River watershed, and can they be detected against a background that includes a substantial natural variability. These influences complicate estimations of the more localized releases of oil and gas drilling and production operations. Whether containinant releases are significant in terms of background or 'natural' amounts is an issue complicated by transport and degradation processes. A National Academy of Sciences report on MMS offshore studies, the Rowe and Turner (1989) recommendations, and Bender et al. (1979) contain similar conclusions: (1) basic information on the ecosystem is missing, (2) a broad analysis is informative, and more interdisciplinary studies, especially of long-term nature, are required, (3) the benthos is a repository of long-term trends, and (4) the role of the Mississippi River must be teased out of the more localized impacts by oil and gas recovery efforts.

In this context, we attempted to document changes in chemical contaminants of the central Gulf of Mexico continental shelf sediments, the biogeochemical signature of ecosystem changes found within them, and the biological response by the foraminiferal community. We place these changes within the framework of the regional influence of the Mississippi River, oil and gas recovery efforts, and the natural variability of the ecosystem. The approach was to analyze constituents in dated sediment cores. The work required: (1) careful collection of sediment cores from the continental shelf, (2) dating these cores in meaningfully long increments, (3) determination of sediment N, P and organic C, and trace metals and organic compounds, including petroleum biomarkers within core segments, and (4) quantitative estimation of benthic foraminiferal species abundances.

The questions we addressed included:

- What are the historical changes in contaminant storage of the Outer Continental Shelf (OCS) ecosystem?
- Are the anticipated biomarkers of petroleum sources localized or regional; are they temporally isolated in the sediment core?
- To what depth contour and distance downstream of the Mississippi River plume do these influences, if any, extend?
- Are these changes reflected in the assemblages of benthic foraminifera and other ecosystem indicators?

The report is divided into four (4) chapters addressing aspects of these questions on this shelf. Our primary analyses is of the constituents in dated sediments before mineral recovery activity began up to the mid-1990s. Chapter 2 (Organic Analyses; Overton, Miles, and Ashton) examines three main categories of pollutants or bio-indicators: total polycyclic aromatic hydrocarbons, or PAHs, (indicative of pyrogenic PAHs), total hopanes (indicative of petrogenic PAHs) and total organochlorine pesticides. Chapter 3 (Trace Metal, C, N and Biologically-bound Silicate in Dated Sediments from the Louisiana Continental Shelf; Turner, Milan,

Rabalais) documents the regional changes in trace metals and in biological materials (carbon, nitrogen, biogenic silica) in time and space. Chapter 4 (Ecosystem History Revealed through Preserved Phytoplankton Pigments; Rabalais, Atilla and Normandeau) and Chapter 5 (Historical Reconstruction of the Contaminant Loading and Biological Responses in the Central Gulf of Mexico Shelf Sediments: Foraminifera; Sen Gupta and Platon) examines two different aspects of the planktonic record.

CHAPTER 2

ORGANICS ANALYSES

Edward B. Overton, M. Scott Miles, and Buffy M. Ashton
Department of Environmental Studies, Louisiana State University

ABSTRACT

The distribution of selected organic compounds within ten dated cores taken from the Mississippi Delta Bight off coastal Louisiana suggests a chronic contaminant loading from several sources including the river itself, oil and gas exploration in the central Gulf of Mexico (GOM) shelf area, natural seeps, and the historical usage of chlorinated agricultural pesticides. Data interpretations were broken down into three main categories: total organochlorine (OC) pesticides; total polycyclic aromatic hydrocarbons, or PAH's, (indicative of pyrogenic PAH's); and estimated total hopanes (indicative of petrogenic hydrocarbons). The sediments were also analyzed for polychlorinated biphenyls (PCB's); however, PCB's were not detected at part per billion levels. Therefore, data analyses focused on the OC pesticides, the PAH's and the petrogenic hydrocarbons. The total OC pesticide and PAH concentrations begin increasing above background levels after World War II. The estimated total hopanes, which are considered to be petroleum biomarkers, were present in almost all of the cores; however, the concentrations show a gradual increase after the 1950's, especially in the vicinity of transect "E".

Gas Chromatography/Electron Capture Detection (GC/ECD) was used to obtain the OC pesticide data. Gas Chromatography/Mass Spectrometry (GC/MS) was used to obtain both the pyrogenic PAH and petrogenic hydrocarbon data. The initial GC/MS method was based on a combination of Technical Memorandum NMFS F/NWC-92 and the U.S. EPA analytical methods for detecting target PAH analytes. This methodology was appropriate for isolating PAH compounds of pyrogenic origin; however, it was inadequate for isolating compounds indicative of petrogenic sources. Therefore, a more detailed GC/MS methodology, which includes certain parent PAH compounds, their alkyl homologs, and the hopanes and steranes, was employed to confirm the presence of petrogenic contamination and help in the determination of the contamination sources.

The purpose of analyzing the sediment cores for OC pesticides, PAH's and hopanes was to document the contamination changes of the central GOM, Outer Continental Shelf (OCS) sediments and try to place the changes within the framework of the regional influence of the Mississippi river and/or oil and gas exploration activities. Based on the distribution of these organic analytes, the Mississippi River is a regional source of the OC pesticides and the pyrogenic PAH's. On the other hand, the hopanes detected in the sediment cores represent a local influence of natural geologic hydrocarbon seeps, or oil and gas exploration in the GOM. Atmospheric input of the targeted contaminants appears to be minimal to none.

INTRODUCTION

Organic contaminants are introduced into the sediment column by four main transport processes:

- Aeolian transport of fossil fuels and wood combustion products followed by deposition on the sea surface and subsequent sedimentation;
- Riverine transport of combined point and non-point sources of input;
- Direct introduction of waste materials via anthropogenic activities such as pipeline and oil spills or barge disposal; and,
- Resuspension of materials reaching coastal marine sediment via bullet one and two followed by deposition in settling areas (Boehm and Farrington 1984).

The contaminants of concern, once associated with the suspended solids in the water column, are eventually deposited attached to these sediments (Santschi et al. 2001). Hence, in theory, sediment cores can provide valuable information regarding the history of persistent contamination and the changes in chemical contamination throughout the course of time. The purpose of analyzing the sediment cores for organochlorine (OC) pesticides, PAH's and other petroleum related hydrocarbons was to document these changes in central Gulf of Mexico Outer Continental Shelf sediments and try to place the changes within the framework of the relative influences of oil and gas recovery efforts compared to the regional influence of the Mississippi River, and to some extent, atmospheric influences.

The agricultural use of OC pesticides began in 1945 with broad scale applications of DDT (dichlorodiphenyltrichloroethane) (Reich et al. 1986). DDT was the most widely used pesticide in this first generation pesticide class because it was the most effective and had the longest lasting efficacy. Additionally, it was very common to mix DDT with other pesticides such as lindane (hexachlorocyclohexane) to treat a wide range of insect pests. Other organochlorine pesticides were mixtures of several OC pesticides. For example, chlordane, or technical chlordane, was 60-75% chlordane (in the *cis* and *trans* isomeric forms) and 25-40% related compounds such as *trans*-nonachlor and heptachlor. The target OC pesticides in this study (with the exception of lindane which is still used in head lice treatments) are no longer registered for use in the United States and were phased out in the 1970's and 1980's. However, due to their persistence in the environment they are still detectable in several environmental matrices.

Oil and gas production in the Gulf of Mexico began in 1947 and peaked in 1971. Production then declined through the late 1970's until the 1980's, during which production peaked again in 1984. In the late 1980's, the price of oil collapsed as a result of sharp increases in crude oil prices associated with declines in output and increases in inflation in many industrialized countries. Initially, Gulf of Mexico production began in the shallower depths (<330 m) of the OCS and it wasn't until the 1990's that production platforms began to move into deeper waters. The Gulf of Mexico is rich in subsurface gas and oil fields and has been one of the mainstays of the United States oil industry. This has been attributed to rapid sediment deposition, active salt deformation and sea floor seeps which contribute to the vertical migration of oil and gas (Sassen et al. 2001). The target PAH's and petrogenic hydrocarbons in this study are compounds common in oil; however, they can also be common in other types of hydrocarbon waste (i.e. industrial waste or creosote contamination). Compounds universal in crude oils and petroleum products that are commonly used for the exclusive identification of these types of products in the

environment are called oil biomarkers. These compounds include the alkyl homologs of certain PAH parent compounds and the triterpane and steranes. Oil biomarkers are important oil constituents because they are generally more resistant to environmental weathering than most of the other oil compounds. Additionally, oil biomarker distribution can be unique for each type of oil and each different geographic source of petroleum, which results in each oil having a unique oil fingerprint.

METHODOLOGY

We analyzed sediments for the distribution of selected organic compounds within ten dated cores taken from the central GOM-OCS Bight area west of the Southwest Pass of the Mississippi River off coastal Louisiana (Figure 2.1). One of the cores sampled, I3, does not appear in the figure.

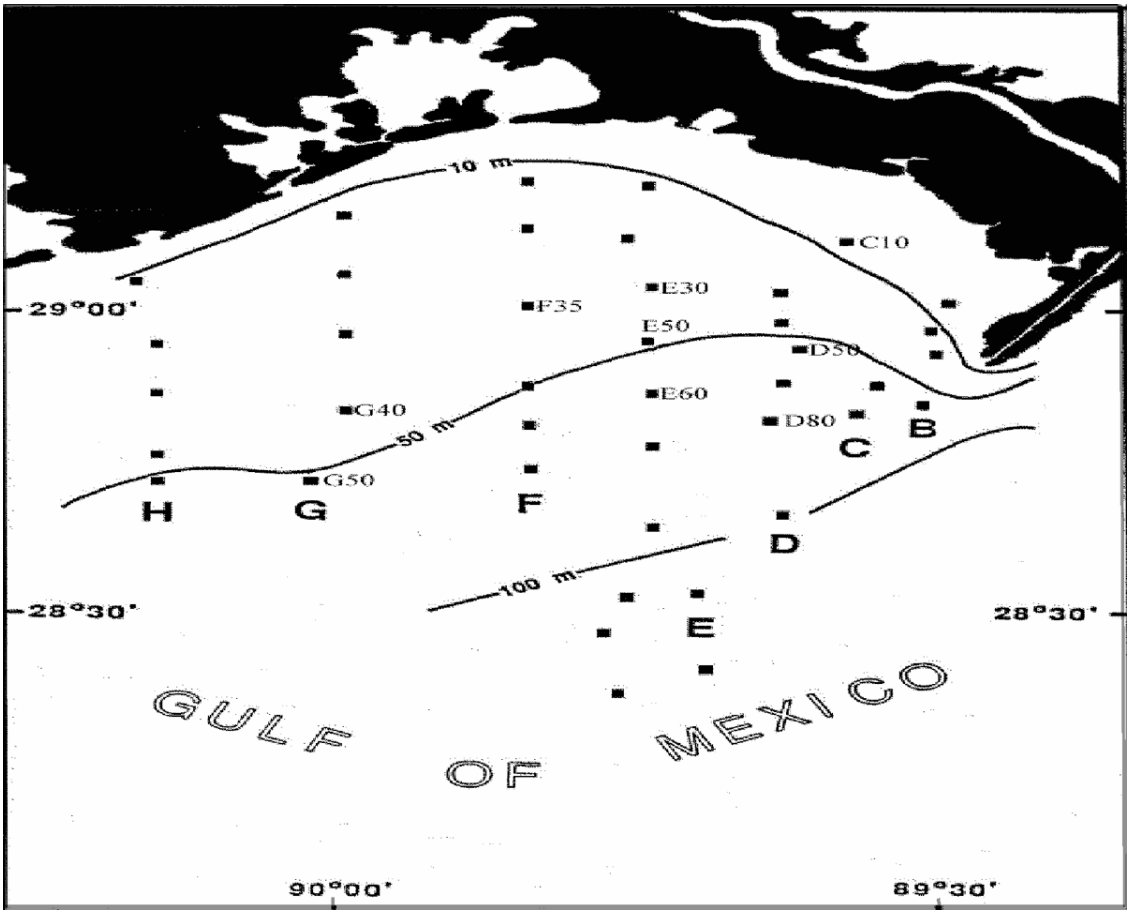

Figure 2.1. Location of the core samples analyzed for organic contaminants.

Preparation and Extraction

The sediment samples, when received by LSU-DES, were free of extraneous materials such as pebbles, weeds, etc. The samples were weighed to 10 g, if possible. If 10 g were not available, the whole sample was weighed. The samples were then extracted with dichloromethane (DCM) and spiked with surrogate standards at a final extract concentration of 200 μg ml^{-1}. The samples

were then placed in an ultrasonic bath for 15 minutes. The DCM was filtered through a funnel containing anhydrous sodium sulfate into a round bottom flask. This extraction procedure was repeated two more times for each core section/depth. The combined decantates were concentrated to 2.0-mL using a combination of rotary evaporation and Kuderna-Danish concentrator tubes.

Alumina/silica gel chromatographic columns were prepared for the clean-up of the concentrated extracts. Silica gel was activated at 170ºC for 12 hours and partially deactivated with 3% (v/w) distilled water. Five grams of silica gel was slurry packed in dichloromethane over 10 g of alumina, previously activated at 400ºC for 4 h and partially deactivated with 1% distilled water (v/w). The final extracts, in hexane, were concentrated using Kuderna-Danish tubes heated in a water bath at 60ºC to a final volume of 1.0-mL.

After initial full scan GC/MS analysis of representative samples of the individual core sections showed non-detection of the OC pesticides, PCB's and PAH's, 5-6 section *extracts* within each core were combined to lower analyte detection limits. Representative samples of the combined sections, after concentration to 2.0-mL, were then run on the GC/MS in selected ion monitoring mode (SIM). Analyte detection was still low, so the combined extracts were then concentrated to a final volume of either 1.0-mL for cores E30, E50, E60, and F35, or 0.1-mL for the remaining cores.

Instrument Configuration and Calibration

GC/ECD

Because analyte detection limits were low for the OC pesticides and PCB's on the GC/MS, the samples were prepared for analysis on a HP5890 GC with an electron capture detector (ECD). The GC was operated in temperature program mode with the initial column temperature of 120ºC, held for 3 minutes, then increased to 200ºC at a rate of 15ºC/minute and held at this temperature for 8 minutes. The temperature was then increased to 270ºC at a rate of 3ºC/minute and held at this final temperature for 1.00 minute. The injector temperature was set at 250ºC and only high-temperature, low thermal bleed septa were used. The ECD was maintained at 290ºC.

Several of the samples that contained OC pesticides concentrations >2 ug g^{-1} were run on a HP6890 GC-ECD/NPD in the Formulations Laboratory in the Louisiana State University Agricultural Chemistry Department for secondary column confirmation. The oven temperature program parameters were the same as described above. The injector was set at 265ºC and the ECD was maintained at 350ºC. The injection was split at a ratio of 2:1. The column was a HP-608 (30 m x 0.53 mm ID x 0.5 μm film). As mentioned previously, PCB's were not detected at ppb levels, and therefore, only the OC pesticide data from the GC/EDC was quantitated and evaluated.

GC/MS

A HP5890 GC/5971 MSD operated in selected ion monitoring mode (SIM) was configured with a DB-5 high resolution capillary column (30 meter x 0.25 mm ID x 0.25 micron film, J&W Scientific). The GC flow rates were adjusted to provide the optimal separation. For the PAH's, the GC was operated in temperature program mode with the initial column temperature of 60ºC

held for 3 minutes, then increased to 320ºC at a rate of 10ºC/minute and held at the upper temperature for 5 minutes. The injector temperature was set at 250ºC and only high-temperature, low thermal bleed septa were used. The interface to the MS was maintained at 280ºC. The GC/MS parameters were the same for the OC pesticides and PCBs; however, the ion groups were changed to reflect the analytes of interest. The method for GC/MS full scanning analysis on representative samples from each core was also the same, except the MS was operated in full scan mode and not in SIM mode.

Quantitative Analysis

OC Pesticides

The concentrations of the target OC pesticides were determined by an external standard method. Using EPA SWP Method 8081B as a guideline, a single point calibration using a calibration standard near the mid-point of the expected range of the OC pesticides was performed. Verification of the calibration was performed at least once each 12-hour shift by injecting a calibration verification standard prior to conducting any sample analyses. The concentration of each OC pesticide compound was calculated to two (2) significant figures.

PAH's

The concentrations of the target PAH's were determined by an internal standard method and response factors calculated from a 3-point calibration curve using commercially available standards for the analytes of interest. The concentration of each PAH compound was calculated to two (2) significant figures. Background levels of analytes and percent recoveries (60-120%) for each surrogate standard were monitored throughout the analyses. The internal standards were 2-fluorobiphenyl and terphenyl-d_{14}, and the surrogate standards were naphthalene-d_8, acenaphthene-d_{10}, phenanthrene-d_{10}, chrysene-d_{12}, and perylene-d_{12}.

Quality Assurance/Quality Control

General QA/QC

Reagent grade or pesticide grade chemicals/solvents were used in all the extractions and analyses. The standard solutions and sample extracts were stored in polytetrafluoroethylene (PTFE)-sealed vials, in a refrigerator at a temperature of 4ºC. All glassware and labware was washed in hot, soapy water; rinsed with tap water and distilled water; rinsed with methanol and then dichloromethane; and placed in an oven set at 130ºC overnight prior to any sample preparation and extraction.

Analytical QA/QC

An extraction blank was prepared with each set of extracted samples to insure that there was no contamination from the solvents, glassware, or laboratory equipment used during the concentration procedures.

All method blanks, duplicates, and sediment samples were spiked with surrogate standards prior to extraction. The surrogate recoveries were acceptable if they fell within the range of 60-120% (EPA acceptance criteria).

Instrumental QA/QC

GC/ECD

A daily calibration standard was the first injection of each sequence on the GC/ECD, which was then followed by a hexane blank. The calibration was verified at least once each 12-hour shift. If the results from these injections verified proper instrument performance, the analysis of samples continued; however, if the daily standard indicated instrumental problems, then no further analytical work was performed until the instrument was restored to good operating condition.

The identities of all analytes were established using correlation of their retention times in the samples to the daily retention time window. Retention time windows were established to allow for minor shifts in absolute retention times as a result of sample loadings and normal chromatographic variability. For quantification of analytes of interest, daily calculation of calibration factors for each analyte at one calibration level was used to check the percent relative standard deviation, or %RSD (a measure of precision). The %RSD of the calibration factors for each analyte had to be within acceptable QC limits on a daily basis (i.e., %RSD must be <15% each day to be considered acceptable).

GC/MS

The MS was tuned to PFTBA (perfluorotributylamine, the most commonly used tuning compound required for automatic tuning of the instrument) prior to each set of analyses. If the tune was significantly different from prior tune parameter values, the instrument was checked for malfunctions (e.g., air leaks, worn septum, dirty liner, etc.) and returned to normal operating conditions. Appropriate internal standards were added just before GC/MS analysis to verify that the injection was made correctly.

The identities of all analytes were established using correlation of their retention times and mass spectral data. For quantification of analytes of interest, three concentration levels for each analyte were used for the initial calibration curve. The linearity and %RSD was calculated for each analyte and found to be within the acceptable limits. The same GC operating conditions were used for the initial calibration curve and for the sample extracts.

A daily calibration standard (at one concentration level) was the first injection after the tune, followed by a blank. If the results from these injections verified proper instrument performance, the analysis of samples continued; however, if the daily standard indicated instrumental problems, then no further analytical work was performed until the instrument was restored to good operating condition.

RESULTS

Table 2.1 is a summary table for the cores analyzed and displays the pertinent physical and chemical information for each core analyzed.

Table 2.1

Physical and chemical information from samples from the Mississippi Delta Bight.

PHYSICAL			CHEMICAL		
Core	**Core Dates**	**Sedimentation Rate**	**Total PAH's (Pyrogenic PAH's)**	**Estimated Total Hopanes (Petrogenic Hydrocarbons)**	**Total OC Pesticides**
C10	1974-1989	1.00 cm yr^{-1}	230 ng g^{-1}	81 ng g^{-1}	0.00 ng g^{-1}
D50G	1777-1997	1.24 cm yr^{-1}	2400 ng g^{-1}	1100 ng g^{-1}	0.81 ng g^{-1}
D80	1974-1997	0.46 cm yr^{-1}	5300 ng g^{-1}	1100 ng g^{-1}	2200 ng g^{-1}
E30	1960-1997	1.10 cm yr^{-1}	110 ng g^{-1}	3100 ng g^{-1}	3400 ng g^{-1}
E50	1938-1997	1.00 cm yr^{-1}	380 ng g^{-1}	4100 ng g^{-1}	13000 ng g^{-1}
E60	1931-1997	0.74 cm yr^{-1}	120 ng g^{-1}	4400 ng g^{-1}	99 ng g^{-1}
F35	1945-1997	0.84 cm yr^{-1}	180 ng g^{-1}	2200 ng g^{-1}	140 ng g^{-1}
G40	1806-1989	0.12 cm yr^{-1}	900 ng g^{-1}	140 ng g^{-1}	44 ng g^{-1}
G50	1896-1916	0.15 cm yr^{-1}	330 ng g^{-1}	52 ng g^{-1}	3500 ng g^{-1}
I3	1934-1999	0.46 cm yr^{-1}	790 ng g^{-1}	170 ng g^{-1}	700 ng g^{-1}

Organochlorine Pesticides (OC) and Polychlorinated Biphenyls (PCB's)

The concentrations of OC pesticides and PCB's in the samples were below the GC/MS detection limit, even in the SIM mode. Even though it was not originally described in the scope of work, the extracts were re-analyzed using a GC with electron capture detector (ECD). This method, GC/ECD, is 10 to 100 times more sensitive for OC pesticides than the GC/MS-SIM analytical procedure and is generally preferred for these types of chlorinated compounds. The drawback to GC/ECD is that the identification of the target OC pesticides and PCB's is by retention time and the chromatographic behavior of many of the targeted OC pesticides can result in co-elution. Compound identification determined from the retention times of a single-column analysis are generally confirmed on a second column (LSU-DES analysis confirmation was obtained from analyses performed at the LSU-Agricultural Chemistry Formulations Laboratory). The target OC pesticides and PCB's are listed in Table 2.2. The OC pesticides in the list include both parent pesticides and their common breakdown products. Several of the OC pesticides were detected using GC/ECD; however, PCB's were not present at ppb levels.

Table 2.2

Target OC pesticides and breakdown products, and PCB's in the core samples.

Target OC Pesticides		**Target PCB's**	
Aldrin	Heptachlor Epoxide	Dichlorobiphenyl	Nonachlorobiphenyl
cis-Chlordane	Hexachlorobenzene	Trichlorobiphenyls	Decachlorobiphenyl
2,4'-DDD, 4,4'-DDD	Lindane (γ-BHC)	Tetrachlorobiphenyl	
2,4'-DDE, 4,4'-DDE	Mirex	Pentachlorobiphenyl	
2,4'-DDT, 4,4'-DDT	*trans*-Nonachlor	Hexachlorobiphenyl	
Dieldrin	Endrin	Heptachlorobiphenyl	
Heptachlor		Octachlorobiphenyl	

The OC pesticide concentrations peaked from the 1940's through the 1970's in most of the cores. Some cores, C10 for example, had no OC pesticides present. Cores along the "D" transect (D50G and D80) were not dominated by any one pesticide. The cores along transect "E" (E30, E50, and E60) were dominated by cis-chlordane, one of the isomers present in technical chlordane (primarily used for termite control). There was only one core analyzed from transect "F" and it was also dominated by cis-chlordane. The two cores along transect "G" (G40 and G50) had different dominating OC pesticides throughout the core profile. The last core, I3 (not shown in Figure 2.1), was dominated by dieldrin, a pesticide primarily used in insecticidal laquers for wood preservation (Rose 1963) and as a soil insecticide (Thomson 1979).

The estimated date ranges of the sediment cores correspond to, and the highest concentrations of the OC pesticides are consistent with, the time periods in which most of these compounds were still approved for use. Core E30 has the highest concentrations of OC pesticides after these compounds were no longer approved for usage. Histograms of the total OC pesticide distribution and the tabular OC pesticide data for each core and composited sections are given in Appendices A and B respectively. Figure 2.2 is a 3-D plot with the x and y axes oriented to the coast of Louisiana by core transect and shelf depth. Figure 2.3 is a histogram that displays the same data set in a 2-D format. These graphical representations clearly display the difference in distribution of the total OC pesticides prior to the 1950's and after the 1950's in the OCS study area. OC pesticide concentrations broken down by decade, beginning with the 1940's through the 1990's, are in Appendix C.

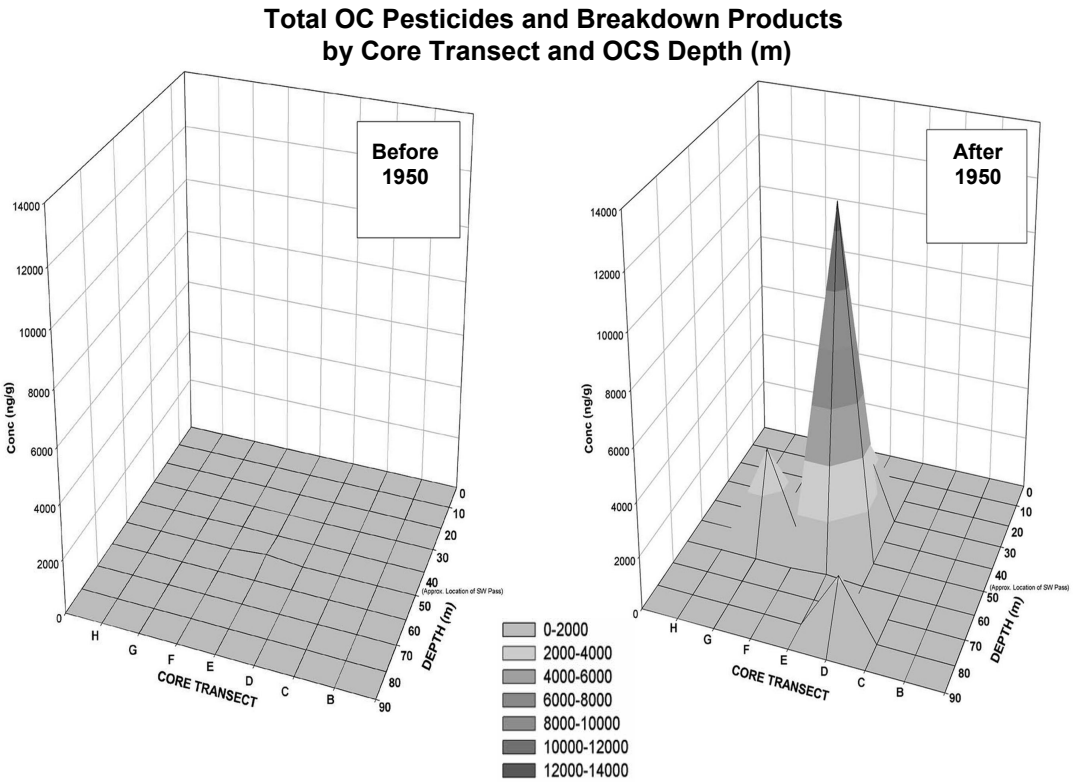

Figure 2.2. Total organochlorine (OC) pesticide and breakdown product distributions in the core samples collected from the Mississippi Delta Bight prior to 1950 (left) and after 1950 (right).

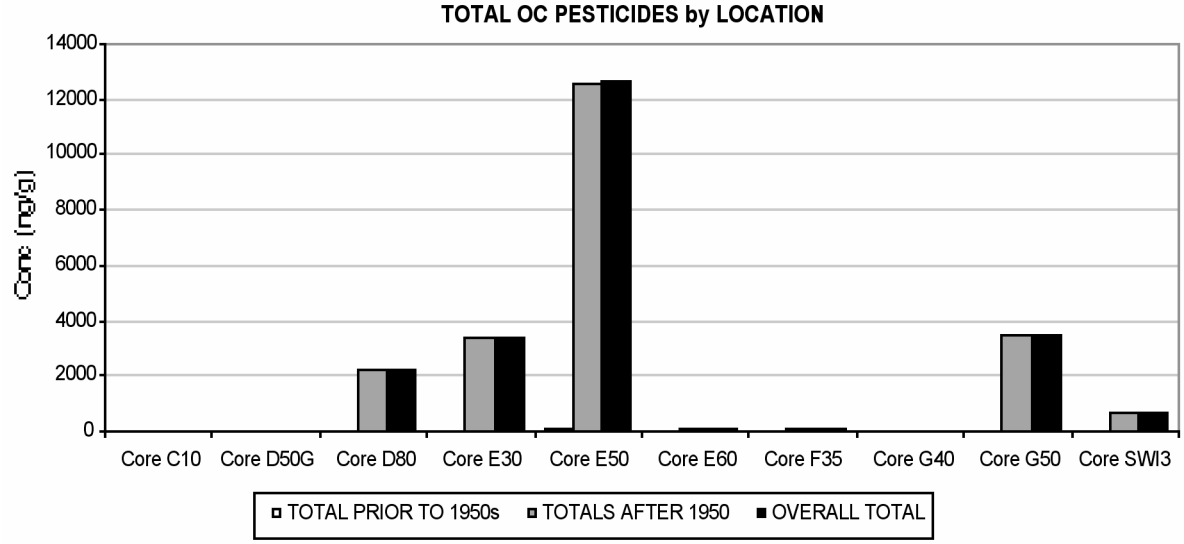

Figure 2.3. Total OC pesticide concentrations prior to the 1950's (front), after the 1950's (middle) and the overall totals (back) in OCS cores collected from the Mississippi Delta Bight.

Due to the levee system of the Mississippi River in Louisiana, no pesticides used for agricultural purposes in Louisiana enter the Mississippi River. Therefore, the pesticides detected in the sediment cores are most likely from the upper Mississippi River basin. This area of the

Mississippi River basin is the largest and most intensively farmed region in the nation (Goolsby and Pereira 1995). There were five sections of core samples that contained significantly elevated levels of the OC pesticides. These samples seemed to contain pesticides with three distribution patterns. Pattern "A" in the 1976-1978 section of D80 contained a total of 2100 ng g^{-1} total pesticides comprised mostly of nonachlor (an ingredient in technical chlordane), chlordane, dieldrin, endrin and the DDT's. Pattern "B", in the 1993-1997 section of core E30, contained a total of 2100 ng g^{-1} total pesticides comprised of lindane, heptachlor, aldrin, chlordane and dieldrin. Pattern "C" in sections of cores from transect E50 (1959-1964 and 1948-1953) and G50 (1956-1989) contained the full list of target OC pesticides with concentrations of 7000, 4800 and 3500 ng g^{-1} respectively.

It is not likely that Mississippi River is the source of these elevated levels of OC pesticides because the high octanol/water partition coefficients (K_{ow}) of these compounds limits the movement of the pesticides once deposited. The K_{ow} of many PAH's are within a similar range as the OC pesticides; therefore, if sediment deposition patterns were a factor the same spikes in the PAH concentrations would be apparent, which they are not. The OC pesticides are very persistent in the environment and would not easily degrade in an anaerobic sediment matrix. Hence, these OC pesticides were most likely directly deposited in these areas as opposed to originating from the river and moving west across the shelf with the dilution plume. On the other hand, the date ranges that correspond with the elevated levels of OC pesticides in these core sections indicate that they are not related to oil and gas recovery efforts.

Polycyclic Aromatic Hydrocarbons (PAH's)

The concentrations of PAH's in the sediment cores analyzed by LSU-DES range from 5.5 ng g^{-1} to 1200 ng g^{-1}. A total of 24 compounds, shown in Table 2.3, were targeted in the originally proposed GC/MS-SIM methodology (NOAA Technical Memorandum NMFS F/NWC-92 and EPA SWP-846). Several of these PAH's were detected; mainly fluoranthene and pyrene. Despite the fact that the target PAH's in Table 2.3 are common oil constituents, they may also indicate other sources of pollution. Therefore, the original methodology was not able to distinguish contamination related to oil and gas recovery efforts from other pollution sources.

Table 2.3

Target PAH's in the originally proposed GC/MS-SIM method.

Naphthalene	Fluoranthene
2-Methyl Naphthalene	Pyrene
1-Methyl Naphthalene	Benzo (a) Anthracene
2,3,5-Trimethyl Naphthalene	Chrysene
2,6-Dimethyl Naphthalene	Benzo (b) Fluoranthene
Acenaphthylene	Benzo (k) Fluoranthene
Acenaphthene	Benzo (e) Pyrene
Biphenyl	Benzo (a) Pyrene
Fluorene	Perylene
Phenanthrene	Indeno (1,2,3-cd) Pyrene
Anthracene	Dibenzo (a,h) Anthracene
1-Methyl Phenanthrene	Benzo (g,h,i) Perylene

For further investigation, all of the sample extracts were re-analyzed with a GC/MS-SIM oil fingerprinting method (modified U.S. EPA SWP-846 method 8270) developed by Louisiana State University-Department of Environmental Studies/Response and Chemical Assessment Team (LSU-DES/RCAT). This oil fingerprinting method includes several of the original target PAH's in Table 2.3; however it has been expanded to include dibenzothiophene (DBT; a sulfur related PAH), PAH alkyl homologs and other oil biomarker compounds such as the hopanes and steranes (Table 2.4). It was evident that after data from these additional analyses were examined, that much more information regarding the nature of the PAH and petrogenic contamination was gained using the oil fingerprinting method compared to the originally proposed analytical method. The oil fingerprinting method provided valuable information regarding the presence of petrogenic hydrocarbons that would have been overlooked by the originally proposed method.

Accordingly, PAH data interpretations were broken down into two categories: total PAH's, indicative of pyrogenic PAH's, obtained from the original GC/MS method; and estimated total hopanes, indicative of petroleum related hydrocarbons, obtained from the GC/MS oil fingerprinting method. In an effort to obtain additional petrogenic source data, other oil biomarker compounds (i.e., the total C-3 DBT's versus the total C-3 Phenanthrenes; a sulfur to non-sulfur ratio) obtained from the fingerprinting method were examined; however, the estimated total hopanes provided the best petrogenic data trends.

Table 2.4

Target PAH's and oil biomarkers in GC/MS-SIM oil fingerprinting method.

Acenaphthylene	C-3 Dibenzothiophenes	C-2 Naphthobenzothiophenes
Acenaphthene	Dibenzo(a,h)Anthracene	C-3 Naphthobenzothiophenes
Anthracene	Fluoranthene	Normal Alkanes (nC_{10}-nC_{35})
Benzo(a)Anthracene	Fluorene	Perylene
Benzo(a)Pyrene	C-1 Fluorenes	Phenanthrene
Benzo(b)Fluoranthene	C-2 Fluorenes	C-1 Phenanthrenes
Benzo(e)Pyrene	C-3 Fluorenes	C-2 Phenanthrenes
Benzo(g,h,i) Perylene	Hopanes	C-3 Phenanthrenes
Benzo(k)Fluoranthene	Indeno(1,2,3-cd)Pyrene	C-4 Phenanthrenes
Chrysene	Naphthalene	Pyrene
C-1 Chrysenes	C-1 Naphthalenes	C-1 Pyrenes
C-2 Chrysenes	C-2 Naphthalenes	C-2 Pyrenes
C-3 Chrysenes	C-3 Naphthalenes	C-3 Pyrenes
Dibenzothiophene	C-4 Naphthalenes	C-4 Pyrenes
C-1 Dibenzothiophenes	Naphthobenzothiophene	Steranes
C-2 Dibenzothiophenes	C-1 Naphthobenzothiophenes	

The pyrogenic PAH data trend shows a gradual increase in these contaminants over the course of time, and suggests a chronic contaminant loading from the Mississippi River. Total PAH concentrations begin increasing above background levels after the World War II era (See Figure 2.4). Histograms of the <u>total</u> PAH distribution, the tabular PAH data for each core and

composited sections, and the PAH distributions by decade are given in Appendices D, E and F respectively.

On the other hand, the distribution of the petrogenic PAH's (estimated total hopane concentrations) indicate contamination from oil and gas exploration in the Gulf of Mexico, and perhaps from natural geologic hydrocarbon seeps in the area. The hopanes, assessed by quantitating the total hopanes, were present in almost all of the cores; however, the hopane concentrations began increasing after the WWII era (Figure 2.5), especially in the vicinity of transect E.

All hydrocarbon levels are used to indicate relative loading of the respective samples since no data are available to correlate hydrocarbon loading with initial source input levels. This being said, the postulation is that pyrogenic loading is predominately associated with riverine inputs, while petrogenic loading is associated with production and exploration activities or possibly natural geologic hydrocarbon seeps in the vicinity of transect E in the study area.

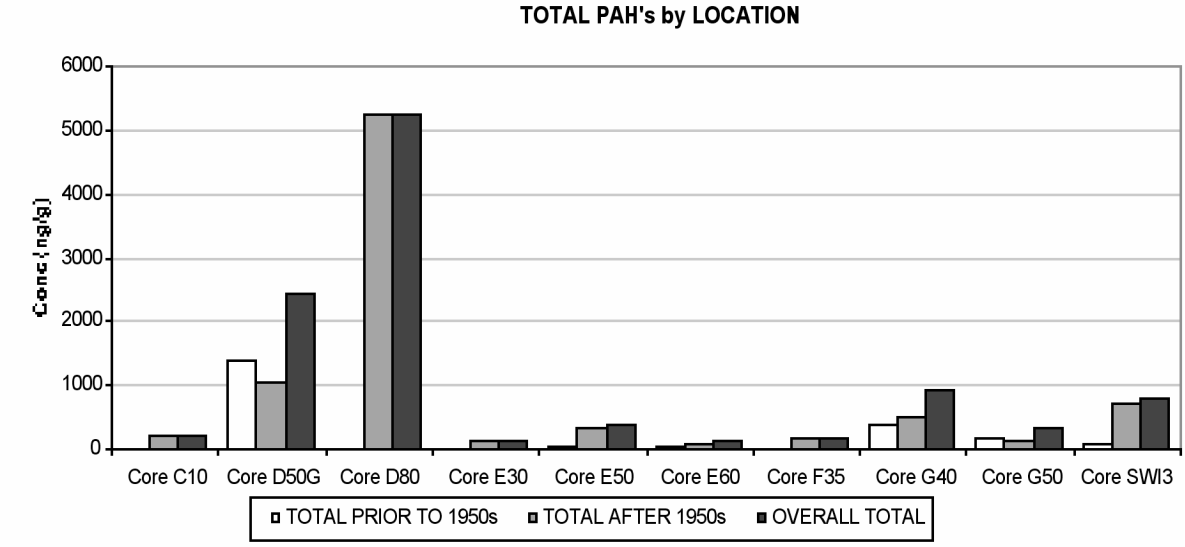

Figure 2.4. Total PAH concentrations prior to 1950 (front), after 1950 (middle) and overall totals (back) from core samples collected from the Mississippi Delta Bight.

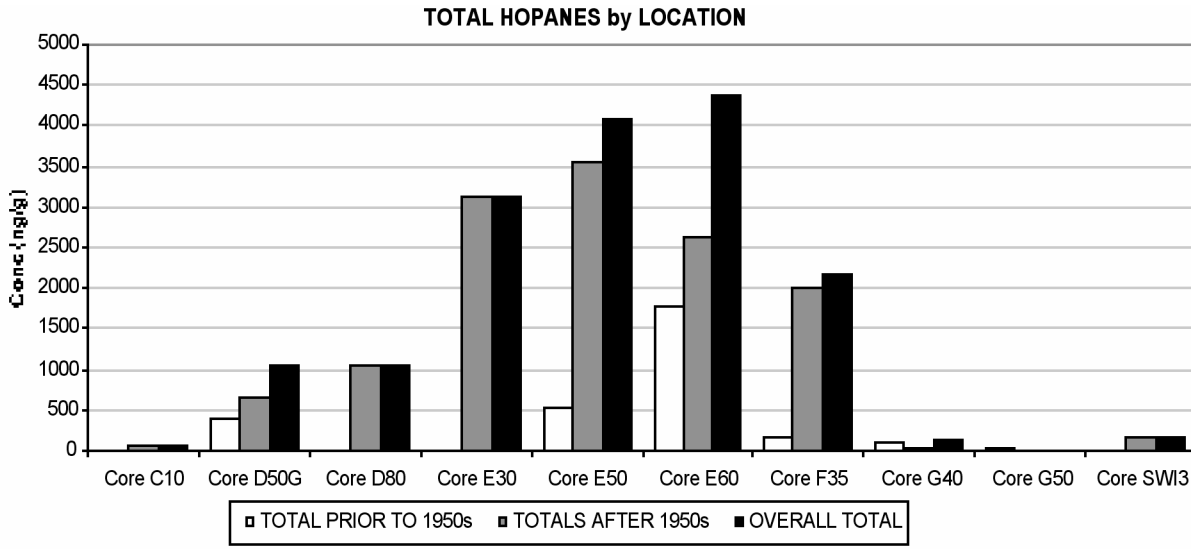

Figure 2.5. Estimated total hopane concentrations prior to the 1950's (front), after the 1950's (middle) and the overall total (back) from core samples collected from the Mississippi Delta Bight.

Figures 2.6 and 2.7 are 3-D plots with the x and y axes oriented to the coast of Louisiana by core transect and OCS depth (as displayed in Figure 2.1). Figure 2.6 displays the total PAH distribution in the study area of the OCS prior to the 1950's and after the 1950's. On the other hand, Figure 2.7 displays the estimated total hopanes in the same manner. Appendix G contains trend data that compares the total PAH's (pyrogenic in nature) to the estimated total hopane concentrations (petrogenic in nature) for each core by core depth. An inverse relationship exists between the pyrogenic PAH's and the petrogenic hydrocarbons; generally, when the total pyrogenic PAH's were high, the petrogenic hopanes were low. This correlation is supported by the fact that the greatest amount of sediment deposition is occurring near the mouth of the Mississippi River (see Figure 3.3 in the next chapter).

Theoretically, heavier suspended particles are going to settle out in the shelf area closest to the mouth of the river and, as a result the concentrations of contaminants adsorbed on the sediments from the river are going to be higher near the source of the sediment plume and will decrease as the sediment plume moves west. The highest concentrations of pyrogenic PAH's occur in transect D, which is within an area of higher sediment deposition off the mouth of the Mississippi River. The concentrations of pyrogenic PAH's begin to decrease in transects west of transect D, until they increase once again in transects G and I3. This increase is probably due to estuarine run-off in the area that contains pyrogenic PAH's from marsh-burning practices. The lowest pyrogenic PAH concentrations are in transects E and F; however, these transects have the highest estimated total hopanes concentrations. For that reason, it is believed that oil and gas recovery and/or natural geologic hydrocarbon seeps are concentrated in this vicinity and are local sources of petrogenic contamination.

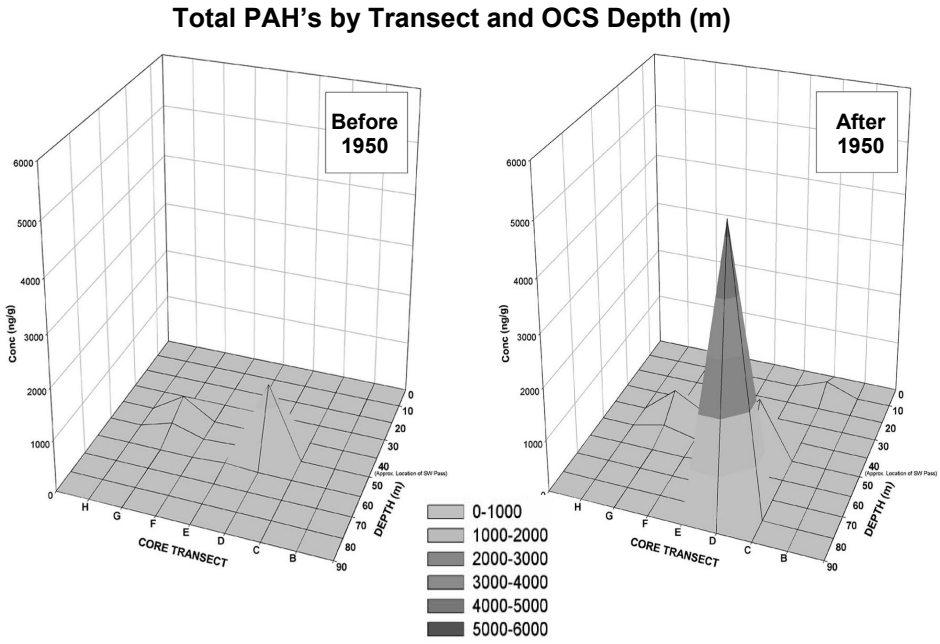

Figure 2.6. Total PAH (pyrogenic PAH's) distributions in the core samples collected from the Mississippi Delta Bight prior to 1950 (left) and after 1950 (right).

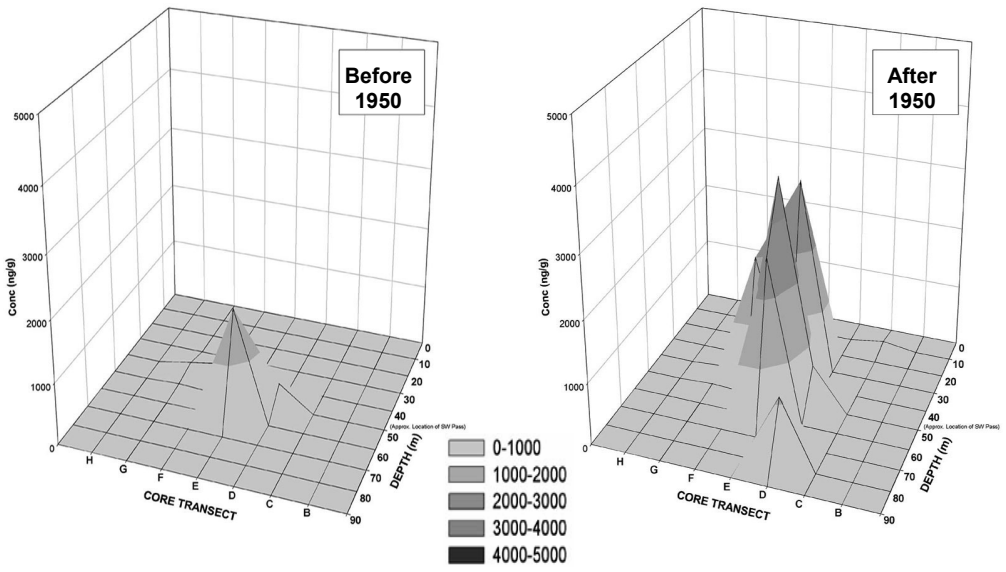

Figure 2.7. Estimated total hopanes (petrogenic PAH's) distributions in the core samples collected from the Mississippi Delta Bight prior to 1950 (left) and after 1950 (right).

Individual Core Results

Core C10

No OC pesticides were detected in this core. The most dominant PAH's in core C10 were pyrene, fluoranthene, phenanthrene, and 1-methyl phenanthrene. The highest concentration of PAH's (130 ng g^{-1}) was in sections 24-34 (ca. 1978-1974).

Core D50G

The only OC pesticide detected in this core was DDT (0.81 ng g^{-1}) in sections 63-75 (ca. 1947-1937). The most dominant PAH's in core D50G were pyrene, fluoranthene, phenanthrene, anthracene and benzo(k)fluoranthene. The highest concentration of PAH's (490 ng g^{-1}) was in sections 38-48 (ca. 1967-1959).

Core D80

There were several OC pesticides and their associated breakdown products detected throughout the core depth including: heptachlor, aldrin, cis-chlordane, endrin, DDD, trans-nonachlor, dieldrin, DDT and DDE. The highest concentrations of OC pesticides (2100 ng g^{-1}) were in sections 37-42 (ca. 1978-1976). Pyrene, fluoranthene, phenanthrene, and fluorene were the most dominant PAH's within core D80. Sections 25-30 (ca. 1984-1981) had the highest concentration of PAH's (1200 ng g^{-1}). The OC pesticides were first detected in sections 19-24 (ca. 1986-1984) and were present throughout the rest of the core depth.

Core E30

OC pesticides were detected in all sections of core E30 and include: cis-chlordane, hexachlorobenzene, aldrin, heptachlor, heptachlor epoxide, trans-nonachlor, dieldrin, and lindane. The highest concentrations of the OC pesticides (2100 ng g^{-1}) were in sections 1-5 (ca. 1997-1993). The most dominant PAH's in core E30 were chrysene, benzo(a)anthracene, benzo(k)fluoranthene, benzo(e)pyrene, benzo(g,h,i)perylene, fluoranthene, pyrene, benzo(b)fluoranthene, and perylene. The highest concentration of PAH's, 26 ng g^{-1}, was in sections 11-15, dating from 1987-1982.

Core E50

The OC pesticides were first detected in sections 6-10 (ca. 1992-1987) and were present throughout the rest of the core depth. All of the target OC pesticides were detected in this core. Sections 31-35 had the highest concentration of OC pesticides, 7000 ng g^{-1}, of all the cores. The date range for these sections is 1964-1959. The most dominant PAH's in core E50 were benzo(g,h,i)perylene, chrysene, fluoranthene, benzo(a)anthracene, perylene, pyrene, benzo(b)fluoranthene, benzo(e)pyrene, indenopyrene, dibenzo(a,h)anthracene, and benzo(a)pyrene. Sections 21-25, dating from 1975-1970, contained the highest concentrations of PAH's (140 ng g^{-1}).

C*ore E60*

OC pesticides detected in sections 1-15 (ca. 1997-1977) and sections 21-35 (ca. 1975-1948) included cis-chlordane, heptachlor epoxide, DDT, aldrin, trans-nonachlor, endrin, DDD, and heptachlor. Sections 31-35 contained the highest concentrations of OC pesticides (31 ng g^{-1}) and dated from 1954-1948. Chrysene, fluoranthene, pyrene, perylene, benzo(a)anthracene, and

phenanthrene were the most dominant PAH's in core E60. Sections 46-47 (ca. 1933-1931) had the highest concentration of PAH's (28 ng g^{-1}).

Core F35

Core F35 had OC pesticides present throughout the depth of the core. The most dominant pesticide was cis-chlordane, followed by DDD, endrin, trans-nonachlor, and heptachlor epoxide. The sections with the highest OC pesticide concentrations (33 ng g^{-1}) were 16-20 (ca. 1976-1971). The most dominant PAH's in core F35 were benzo(a)anthracene, chrysene, benzo(g,h,i)perylene, benzo(a)pyrene, perylene, indeno(1,2,3-cd)pyrene, fluoranthene, pyrene, dibenzo(a,h)anthracene, and benzo(e)pyrene. The highest PAH concentrations, a total of 67 ng g^{-1}, were in sections 26-30 dating from 1963-1957.

Core G40

The most dominant OC pesticides in Core G40 were DDD, hexachlorobenzene, dieldrin, trans-nonachlor, DDT, cis-chlordane, lindane, endrin and aldrin. OC pesticides were detected throughout the depth of the core, but sections 1-6 contained the highest concentrations, 44 ng g^{-1}. Core G40 was dominated by the PAH's perylene, fluoranthene, pyrene, 1-methyl phenanthrene, and phenanthrene. The highest concentration of PAH's (510 ng g^{-1}) was in sections 1-6 (ca. 1989-1939).

Core G50

OC pesticides were present in sections 1-5 of Core G50 and included: heptachlor epoxide, DDT, endrin, aldrin, DDD, trans-nonachlor, cis-chlordane, dieldrin, lindane, DDE, and heptachlor. The concentration of OC pesticides in these sections was 3500 ng g^{-1}. The dominant PAH's in core G50 were pyrene, phenanthrene, fluoranthene, and perylene. The highest concentration of PAH's (140 ng g^{-1}) was in sections 1-5 (ca. 1989-1956).

Core I3

The most dominant OC pesticide in core I3 was dieldrin, followed by heptachlor epoxide and heptachlor. Other pesticides detected include: hexachlorobenzene, aldrin, DDT, endrin, DDD, and lindane. The OC pesticides were present throughout the depth of the core. Sections 13-17 (ca. 1969-1959) had OC pesticide concentrations of 460 ng g^{-1}. Core I3 was dominated by the following PAH's: pyrene, phenanthrene, 1-methyl phenanthrene, and fluoranthene. Sections 13-17 (ca. 1969-1959) had the highest concentrations of PAH's—230 ng g^{-1}.

DISCUSSION

The Mississippi river drains the largest and most intensely farmed region in the United States. Concerns over the adverse effects from anthropogenic activities (e.g., expanding populations; industries; agricultural practices) on the water quality of the Mississippi River began to emerge after World War II (Goolsby and Pereira 1995), and by the 1960's a decline in the water quality along with many other adverse side effects of urbanization were evident. The results from these anthropogenic activities are distributed in the sediments deposited on the OCS by the Mississippi River. PAH's and OC pesticides normally adsorb onto suspended particles in the water column

and are transported and deposited as sediments. Therefore, OCS sediment cores can, theoretically, be used to retrace the history of chemical contamination over a period of time.

Trends apparent in the data show that the levels of OC pesticide contamination were consistent with the beginning and peak application of these first generation pesticides, and that the PAH contamination, both pyrogenic and petrogenic, gradually increase as time progresses beginning around the time of oil exploration (around 1950). Atmospheric input of the targeted contaminants appears to be minimal to none due to the fact that some of the contaminants were not distributed equally throughout the study region. The Mississippi River is the principle source of the OC pesticides and the pyrogenic PAH's. Due to the levees in Louisiana, state agricultural run-off does not generally enter this river system; therefore, the OC pesticides detected in the sediment cores were due to a regional influence.

There were two anomalies present in the total OC pesticide concentrations in core E50, sections 31-35 (ca.1964-1959) and 41-45 (ca.1953-1948), and core G50, sections 1-5 (ca.1989-1956). The total pesticide concentrations in the aforementioned sections were almost an order of magnitude higher than the other core's total pesticide concentrations. All target OC pesticides were detected in these sections of E50 and G50. It is not likely the Mississippi River is the source of these elevated levels of OC pesticides because the K_{ow} of these compounds limits the movement of the pesticides once deposited. If sediment deposition patterns were a factor, the same spikes in the total PAH concentrations would be apparent because the K_{ow} of many PAH's are within a similar range as the OC pesticides. Hence, these OC pesticides were most likely directly deposited in these areas as opposed to originating from the river and moving west across the shelf with the sediment dilution plume. The OC pesticides are very persistent in the environment and would not easily degrade in an anaerobic sediment matrix. Therefore, all of the target OC pesticides and breakdown products would be distributed in the neighboring core transects with similar shelf depth. It is possible that factors such as annual usage, spring flux, the phase out of OC pesticides in the late 1970's and 1980's, flood events, limited-biodegradation, gravity-driven sediment transport and post-depositional mixing from storm surges contributed to the variations in the OC pesticides from core to core within the study area. On the other hand, the date ranges that correspond with the elevated levels of OC pesticides in these core sections indicate that they are not related to oil and gas recovery efforts.

The pyrogenic PAH's have an inverse relationship with the petrogenic hydrocarbons; generally, when the total PAH's were high, the hopanes (representing the petrogenic-related hydrocarbons) were low or below the total PAH's. Since the heavier suspended particles are going to settle out in the shelf area closest to the mouth of the river, the concentrations of contaminants adsorbed on the sediments from the river are going to be higher near the source of the sediment plume and will decrease as the sediment plume moves west. The highest concentrations of pyrogenic PAH's occur in transect D, which is within an area of higher sediment deposition off the mouth of the Mississippi River. The concentrations of pyrogenic PAH's begin to decrease in transects west of transect D, until they increase once again in transects G and I3 (probably related to marsh-burning practices and estuarine run-off). Transects E and F have the lowest pyrogenic PAH concentrations; however, the highest estimated total hopanes concentrations. For that reason, it is believed that the hopanes represent a local influence of natural geologic hydrocarbon seeps or oil and gas exploration.

Organochlorine (OC) Pesticides

The target OC pesticides in this study are no longer registered for agricultural use in the United States and their presence in the sediment cores is indicative of their environmental persistence. Examination of the estimated K_{oc} (octanol/water partition coefficient) values for theses compounds indicate that they are generally immobile or slightly mobile in soils/sediment. Previous studies of sediments from the Mississippi River and Gulf of Mexico have indicated that concentrations of *individual* OC pesticides can vary from 0.49 ng g^{-1} to as high as 900 ng g^{-1} (Laska et al. 1976; Murray et al. 1981). The concentrations of *total* OC pesticides in the sediment cores analyzed by LSU-Department of Environmental Studies range from 0.61 ng g^{-1} to 7000 ng g^{-1}. Outside of the fact that cores E50 and G50 had high concentrations of the OC pesticides, the rest of the pesticide concentrations in the cores were consistent with other historical reconstruction of contaminant loading studies (Barber and Writer 1998; Carr et al. 1996; Santschi et al. 2001). The OC pesticides and associated breakdown products commonly found throughout all of the cores were heptachlor epoxide, cis-chlordane, endrin, 4-4'-DDD, and 4,4'-DDT.

The majority of pesticides used in the Mississippi River basin, both presently and historically, are applied in the upper part of the basin, mainly in Illinois, Iowa, Indiana, eastern Nebraska, and southern Minnesota (Goolsby and Pereira 1995). The major crops in these states are corn and soybean. The OC pesticides used for these crops prior to their phase out in the late 1970's and the 1980's might have included: DDT; dieldrin; lindane; endrin; aldrin; and heptachlor (Rose 1963). Again, it is important to note that the levee system in the state of Louisiana prevents agricultural runoff from entering the Mississippi River. Therefore, any of the OC pesticides present in the OCS are from agricultural runoff in the Midwest and possibly the Atchafalaya. Some of the OC pesticides of local interest that may have been used prior to their ban in the U.S. included: lindane (cotton); DDT (cotton; soybeans; sugar cane; mosquitoes); aldrin (cotton; sugar cane; beetles that eat strawberry seeds); endrin (cotton); heptachlor (mosquitoes; cotton; sugar cane) (Rose 1963). The OC pesticide list was very similar on a regional and local level, probably due to the fact that this "first generation" of pesticides worked extremely well on a very broad range of pests and were very persistent.

Polycyclic Aromatic Hydrocarbons (PAH's)

The results of the PAH analyses performed by LSU-DES appear to be consistent with research from other historical reconstructions of contaminant loading (Barber and Writer 1998; Boehm and Farrington 1984; Carr et al. 1996; Overton et al. 1986; Santschi et al. 2001). The concentrations of PAH's in the sediment cores analyzed by LSU-DES range from 5.5 ng g^{-1} to 1200 ng g^{-1}. The dominance of fluoranthene and pyrene in the total PAH concentration, and also the presence of the benzofluoranthenes and benzopyrenes indicates an assemblage of combustion-PAH-dominated sediments. The PAH compounds on the original target compound list were ineffective at distinguishing petrogenic from pyrogenic hydrocarbon contamination since the list did not include typical oil biomarkers, such as dibenzothiophene (DBT), the alkyl homologs of the parent PAH's, and the hopanes and steranes. Alkyl homologs of the PAH compounds, as well as the pentacyclic hopane and sterane type compounds, are known to be associated with petroleum sources, and quantifying the "total" hopanes proved to be very valuable in distinguishing regional influences from local influences.

RECOMMENDATIONS

Many of the important PAH's (DBT, the alkyl homologues, hopanes and steranes) were excluded in the proposed Technical Memorandum NMFS F/NWC-92 and EPA SWP-846 GC/MS-SIM method used in this research. These compounds are very important oil biomarkers because they provide valuable oil fingerprint information and remain detectable and relatively unchanged in oil residues after natural environmental weathering processes (Ashton et al. 2000; Philip and Oung 1988). Analyzing for these biomarkers in the sediment samples allows OCS activities to be discriminated from non-OCS activities; mainly due to the fact that the biomarkers can be quantitated, background levels of petrogenic activity can be determined and variations from background can be distinguished. Much more information could be gained, as far as OCS versus non-OCS activities are concerned, if future sediment cores were analyzed for the target compounds listed in Table 2.2. These target analytes are part of an oil fingerprinting GC/MS-SIM method developed by LSU-DES/RCAT to determine whether spilled oil can be matched to a suspected source oil. This fingerprinting method is a modified version of U.S. EPA SW-846 Method 8270.

The proposed methodology for detecting the OC pesticides by GC/MS would have been prudent if the concentrations of the pesticides were greater than 10 $\mu g\ g^{-1}$ (parts per million). Unfortunately, most of the pesticide concentrations were below this level. Therefore, any future OC pesticide analysis should be done by GC/ECD (U.S. EPA SW-846 Method 8081B). Furthermore, normalization of the OC pesticide concentrations in the sediments to the TOC may provide additional information regarding the distribution patterns in the OCS.

Future studies should also consider taking larger core samples and have more sampling points. A few additional cores in transect F, especially in the 50m area of the shelf, would have provided more information relating to the contaminant distribution pattern along the shelf and the relation of the distribution between transects E and G. Larger core samples would provide larger sediment samples to be divided for the various analyses that were performed in this project. A larger sample size would also allow for a lower detection limit of the trace organic compounds targeted.

CHAPTER 3

TRACE METAL, C, N AND BIOLOGICALLY-BOUND SILICATE IN DATED SEDIMENTS FROM THE LOUISIANA CONTINENTAL SHELF

R. Eugene Turner and C.S. Milan
Coastal Ecology Institute, and Department of Oceanography and Coastal Sciences
Louisiana State University
and
N.N. Rabalais
Louisiana Universities Marine Consortium

ABSTRACT

The development of the OCS for oil and gas recovery started in the 1950s and peaked in the 1990s, while moving further offshore and into deeper waters. We examined the sedimentary record offshore for indicators of industrial by-products of OCS development and of national industrial products, primarily using Vanadium (V) and Barium (Ba) concentrations normalized for Aluminum (Al). Barium is primarily used in drilling muds in Barite, whereas V is an important strengthening component of metal alloys, including steel. The fluctuations in the accumulation of Ba, but not V, are coincidental with the presumed use of Barite. The fluctuations in V concentration in the sediments are coincidental with the national consumption of V. Copper (Cu), Cadmium (Cd), and Zinc (Zn) concentrations in sediments fluctuate coincidentally with V, not Ba, thus indicating that the dominant source of these trace metals in offshore sediments are derived from riverine sources, and are not primarily from *in situ* industrial processes releasing them on the shelf. This is not to suggest that local site-specific contamination is not a significant management or health concern.

The hypoxic zone that consistently covers much of this continental shelf in summer is attributed to N loading from the Mississippi River. Increased nitrogen loading from river to shelf stimulates diatom production whose subsequent loading to the bottom layer and metabolism results in oxygen being depleted faster than it is replaced. In the last two decades there has been an increased accumulation of organic matter in sediments near the mouth of the Mississippi River. This coupling between river water, surface water and bottom water has recently expanded westward towards the Texas coast, west of the Atchafalaya River delta. The accumulation of Biologically-bound silica (BSi) and carbon in dated sediments is not coincidental with variations in either V or Ba consumption rates.

These analyses indicate that both OCS development and riverine sources exert strong influences on the sediment constituents offshore, and that these influences may be independent of one another.

INTRODUCTION

Both small and large oil spills are a ubiquitous consequence of oil and gas recovery and transportation in the coastal zone (National Research Council 2003). But there are also other contaminants released that are of concern, whose accumulation in sediments is used to reconstruct the historical pollutant loading rates, at least in a relative way (Bricker 1993; Ravichandran et al. 1995; Cochran et al. 1998; Santschi 2001). The temporal and spatial significance of potential contamination from Outer Continental Shelf (OCS) activities in the northern Gulf of Mexico remains a vexing problem for management. The *in situ* release of contaminants may or may not be as significant as the changes occurring from landuse changes in the Mississippi River watershed, and be undetectable against a background that includes a substantial natural variability. Landuse changes in the Mississippi River watershed resulted in coastal eutrophication and contributed to a larger, more severe and longer lasting hypoxic water mass in the bottom layer of the same region (Turner and Rabalais 1994a). These changes may be more significant to the shelf ecosystem than those resulting from contaminant releases related to OCS development. However, without knowledge of these larger scale influences, we may be subject to overly simplistic arguments, and remain profoundly uncertain about management impacts, hence remedial strategies. In this context, we attempted to document the changes in trace metals and organics produced *in situ* within the central Gulf of Mexico continental shelf.

We were interested in how the historical accumulations of trace metals, especially V and Ba, varied in relationship to the production and consumption of these metals. Vanadium is alloyed with other metals to strengthen them, particularly in the manufacture of steel. This steel is used to build the skeleton of oil and gas platforms (http://www.mii.org/Minerals/photovan.html, Mineral Information Institute). Barite ($BaSO_4$) is an important additive for oil-well drilling mud, which is a "weighting agent" that is crushed and mixed with water and other materials and pumped into the drill hole. Its weight counteracts the force of the oil and gas when it is released from the ground, which allows the rig operators to prevent explosive releases of the oil and gas during recovery. Over 75% of barite consumption in the U.S. is for this drilling application (http://www.mii.org/Minerals/photovan.html, Mineral Information Institute). If the source of V or B in the sediments were influenced by either local or riverine sources, then variations in the sediment record might be observed to fluctuate with variations in either national consumption patterns (V or Ba) or in shelf-wide application of drilling mud (Ba) or oil and gas well structural development (V). Interpretations of changes in Zn, Cu, or Cd (and other pollutants) depend on knowledge of these source-accumulation relationships. Lastly, we attempted to document the sedimentary accumulation of diatoms (measured as the residual silica in the buried frustules, also known as the biologically-bound silica, or BSi) and organic matter produced *in situ* within the region where sediments for the trace metal analyses were collected, if not the same sample. This effort was meant to help frame the controlling impact of the Mississippi River on the biological productivity in the oil and gas recovery operations.

METHODS

Sediments were collected using aged steel tubing with sharpened ends that were carefully pushed into a box core with a twisting motion to reduce compactions, which was always less than 10%. Sample locations (Figure 3.1) are from the region of locally high sedimentary carbon, sediment phytoplankton pigments from *in situ* phytoplankton production (marine origin), and BSi (about 1% TOC, 28.1 µg g dry weight^{-1}, and 0.6% BSi, respectively). These sediments were directly downstream and beneath the Mississippi River's dilution plume, and their constituents reflect the *in situ* primary production and subsequent transport of organics from surface to bottom waters very near the river delta (Turner and Rabalais 1994a). One sample was taken further west beyond where the Atchafalaya river debouches onto the shelf (about 91.5 º W). Six cores are described herein that were collected in 1997, or later. Additional samples were from a suite of archived cores collected in April 1989.

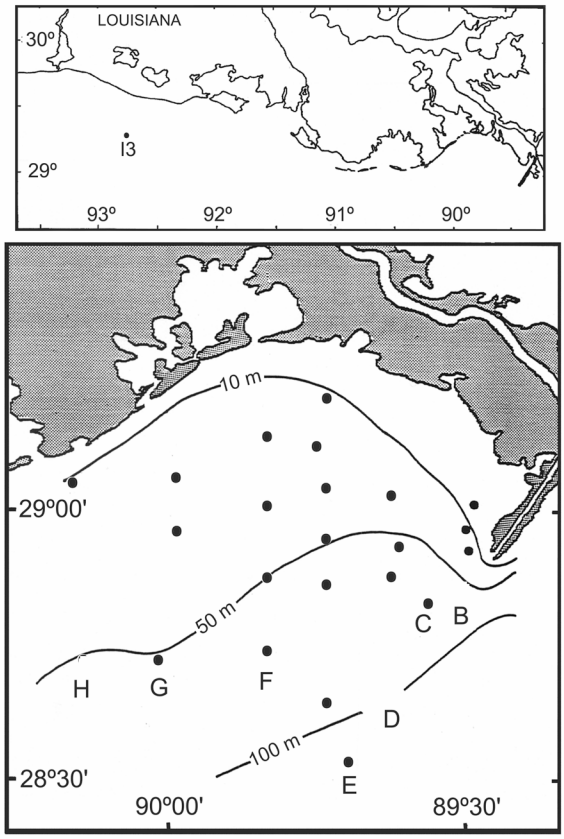

Figure 3.1. Sampling locations where sediment cores were collected. All but one (I3) are from the western side of the Mississippi River delta. The letters correspond to sampling transects.

Sediment Dating

Sediment cores were analyzed for residual chemical and biological remnants. Sediment dating involved ^{210}Pb isotope counts in a non-destructive manner using a Princeton Gamma-Tech 60

mm diameter intrinsic germanium "N" type coaxial detector (40% efficiency) interfaced to an EG&G Ortec 92X spectrum master integrated gamma-spectroscopy system. This unit provides detector power, signal acquisition and amplification of 4096 channels and is equipped with an automatic sample changer for 40 samples. Calculations of accretion rates are based upon the decay constant of ^{210}Pb and the decay and non-decay-corrected activities of ^{210}Pb with depth (Nittrouer et al. 1979). Estimates beyond the 200 yBP limit of the method using the approaches applied here assume linear accumulation rates, which may not always be the case.

Cores were cut into 0.5 to 2 cm sections, depending on need. Samples were set aside (weighed and measured to determine proportional representation of a whole sample) for non-destructive analyses (e.g., foraminifera).

Diatom Remains

Diatoms accumulate silica in their frustrules which remain after death. Biologically-bound silica (BSi) was estimated using the methods described by DeMasters (1981). Aliquots of dried sediments were digested at 85º C in 50 ml polypropylene centrifuge tubes, using a 2% solution of $NaCO_3$, and subsampled at 1, 2, 3 and 5 hours. The intercept of a linear regression analysis of silicate concentrations vs. time was used to estimate the concentration of BSi. This method assumes that BSi digests within 1 hour, but that non-biologically bound silica continues to dissolve at a slower rate over the next several hours. The method is an indirect means to obtain relative measures of diatom density in sediments and has been successfully applied in the region by Turner et al. (1994a) and Parsons et al. (2002).

Total Organic Carbon

Sediment samples for total organic carbon (TOC) were ground and the carbonate material removed by using hydrochloric acid. Subsamples for analysis were weighed on a Cahn micro-balance and analyzed with a Control Equipment Elemental Analyzer, Model 240 XA with a multi-sampler injector. Duplicate samples for the maximum and minimum TOC readings for each run were performed for quality control. Some samples were combusted in a Carlo Erba elemental analyzer coupled to a Thermoquest Delta Plus isotope ratio mass spectrometer functioning as a continuous flow system (Barrie and Prosser 1996) to determine C, N and S quantities.

Trace Metals

Samples for trace metal analyses were digested in nitric acid, hydrogen peroxide and hydrochloric acid (EPA Method 3050B) prior to analysis by inductively coupled plasma atomic emission spectrometry (ICP-AES). Simple linear regression analyses were made using the concentration of V and Ba versus Cd, Cu and Zn. The Adjusted Coefficient of Determination (Adj. R^2) was accepted only if $p < 0.01$. Metals were normalized to Al to compensate for variations in clay content, which is a standard analytical approach (e.g., Ravichandran et al. 1985; Santschi et al. 2001).

Grain Size

Grain size distributions down to 0.3 µm. were determined using a Coulter Multisizer with 256 channelizer capability and using 280 µm, 140 µm and 50 µm aperture tube sizes. Samples were sieved through 20-µm Nitex before analysis with the 50-µm aperture tube. Coulter Accucomp

software was used to overlay distributions from each tube, and sand, silt and clay fractions were identified using the final combined distribution. Coarser samples were sieved to isolate larger sand particles unsuitable for Coulter Multisizer analysis. Where appropriate, these sand measurements were combined with the Coulter Multisizer data, assuming a constant particle density for the sand fraction, to produce a total grain size distribution.

Mineral Production and Use

Data on annual U.S. industrial production and apparent consumption (a combination of data on production, exports, imports and net change in stockpiles) for V and barite is from Kelly et al. (2001). These data were plotted by year since 1900 and compared to the estimated concentration of the various constituents for sediments dated as described above.

RESULTS AND DISCUSSION

Sediment Accretion Rates

Sediment accretion rates for six cores were determined using the vertical distribution of ^{210}Pb (Figure 3.2). The accretion rates ranged between 0.41 (I3, western shelf) and 1.24 cm yr^{-1}. The accretion rate for 34 sediment cores collected in the region shown in Figure 3.1 was 0.99 ±1.22 cm yr^{-1} (mean ± 1 Std. Dev.). The highest sedimentation rates are along transects B and C (Figure 3.1), and the rates decline in a westward direction (Figure 3.3).

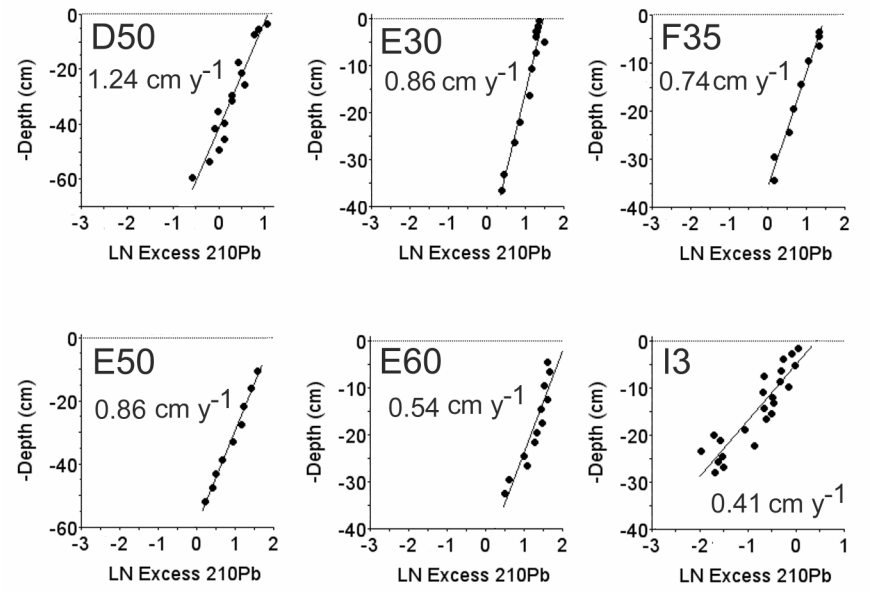

Figure 3.2. The vertical distribution of ^{210}Pb in six cores collected for this study. Other sediments were also used from dated cores described by Turner and Rabalais (1994a). A simple linear regression of the Ln Excess Sed_{210} vs. depth (cm) is shown (exclusive of the surface mixed layer), with the estimated sediment accumulation rate (cm yr^{-1}).

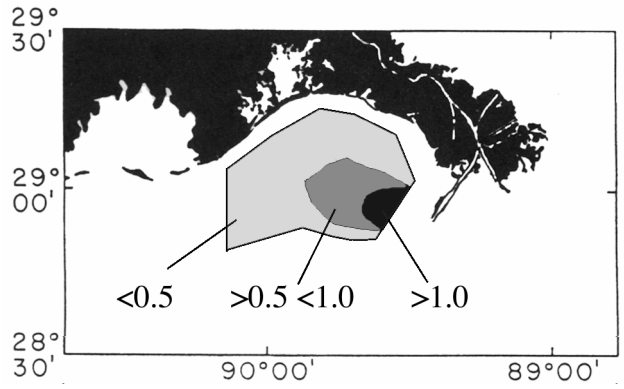

Figure 3.3. Sedimentation rates (cm yr^{-1}) west of the Mississippi River delta (unpublished data of the Principal Investigators, and substantiated by several others, including Eadie et al. 1994; Nelson et al. 1994; Blackwelder et al. 1996).

General Sediment Quality Near and Far from the Mississippi River Delta

The sediments within the Mississippi Delta Bight (MDB), where all but one of the sediment cores reported here came from, had a different organic, density, silt and clay content than did core I3, which came from the western shelf (Figure 3.4). Compared to the western shelf (core I3) the MDB sediments tended to have more organic content, a lower density, a higher concentration of Al, and more sand.

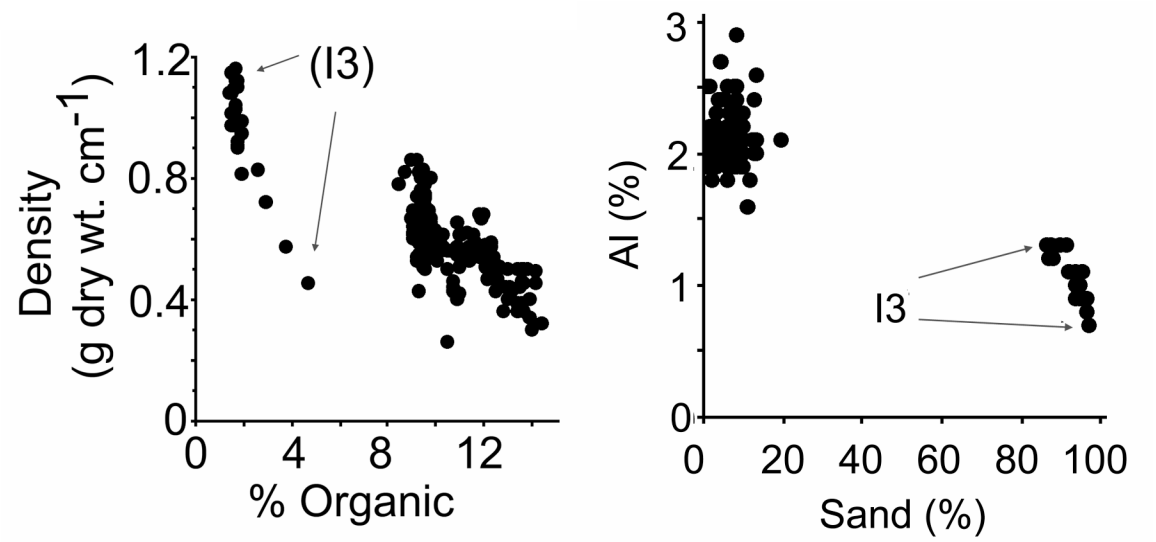

Figure 3.4. The relationship between sediment density and organic content (left panel) and aluminum and sand (right panel). The samples from core I3 (western Louisiana shelf) are indicated in each panel. All the other samples are from the Mississippi Delta Bight.

Trace Metals

There was no statistically-significant relationship between the concentration of V and Ba in any set of sediments from an individual core, or, from the aggregated set of data from all six cores (Figure 3.5). This is an important observation used in a subsequent discussion concerned with

the historical accumulation of V and Ba as they are related to fluctuations in source materials from the Mississippi River watershed and from oil and gas recovery *in situ*. If V and Ba were from only one of these two sources (atmospheric transport for these metals is presumed to be insignificant, but it may be quite important for other metals, e.g., Pb (Trefrey et al. 1985), and if the source amounts were proportional over the last 100 years, and otherwise behave the same during deposition and post-burial, then there would be a significant relationship between V and Ba concentration. This direct relationship was not observed, which does not prove that different sources were important.

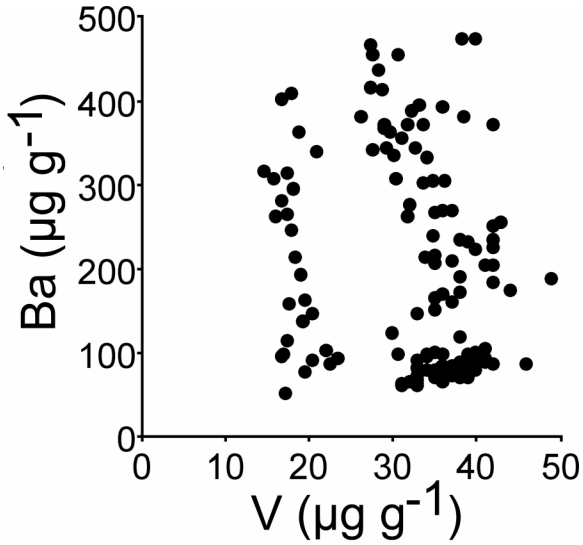

Figure 3.5. The relationship between the concentration (µg g^{-1}) of vanadium and barium in six sediment cores. No correlation is found between the two variables when analyzed by individual core or when aggregated together.

The accumulation of Ba in sediments rises and falls with the national production and consumption rate of Barite (Figure 3.6). Variations in barite use are coincidental with the rise of oil and gas recovery efforts on this shelf. Barite is primarily used as an additive to assist in the safe recovery of the mineral product. Higher concentrations of Ba in sediments and Ba consumption begins in the late 1940s, there is a peak in the early 1980s, and then a decline thereafter. Cores E50 and E60 had a rise about a decade apart, which may reflect the expansion of drilling activities into deeper waters (Figure 1.2). The cores from the MDB collected in the shallowest water (E30 and F35) were not deep enough to retrieve samples from before the 1970s. Some details of the annual peaks and troughs in production/consumption are not well-preserved in the sedimentary record, presumably due to mixing, but also, perhaps, to issues related to the field application of drilling muds, and post-application downstream transport to the west. The lag between the rise and fall in production and the subsequent variations in core I3 is about two to three years, which could be due to bioturbation in the surface layer. An additional complication is that sediment dating may not be either precise enough or sedimentation rates sufficiently consistent from year-to-year (e.g., from hurricane influences) to capture a signal varying among a few years.

The accumulation of V in sediments rises and falls with its national production and consumption rate (Figure 3.7). There are six valleys and peaks in the national V production rate which appear to be present in the sedimentary record, though not dramatically so in all cases. A lag of a few years and about a decade between industrial production and accumulation in sediments is suggested for the region near, and far, from the Mississippi River, respectively.

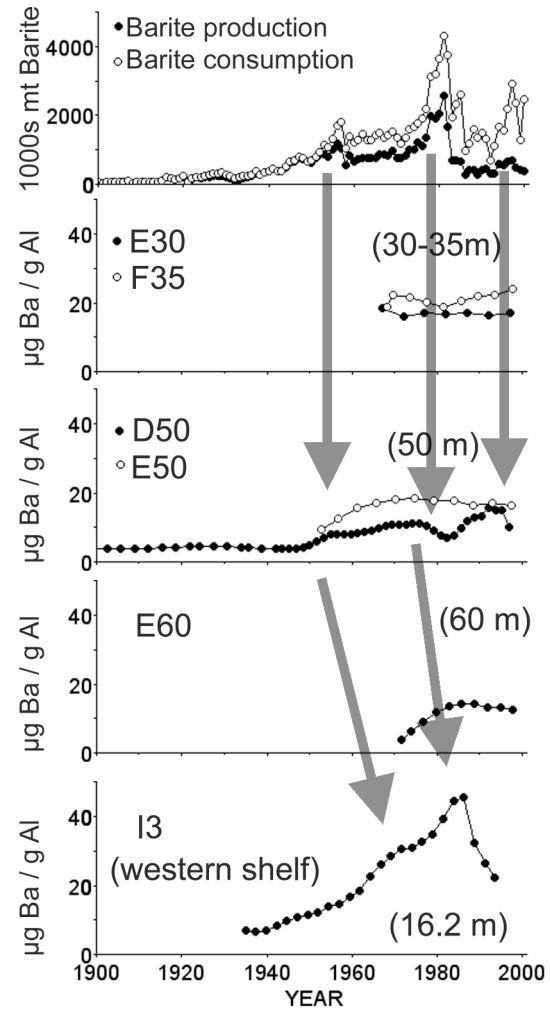

Figure 3.6. The normalized concentration of barium (µg Ba / g Al) in six dated sediment cores from various depth zones on the Louisiana shelf. The industrial production and consumption of barium in the United States is shown in the top panel. Possible coincidental peaks in the industrial production and the appearance of vanadium in sediments are indicated with the lightly shaded arrows. A lag of < 2 years and about a decade between industrial production and accumulation in sediments is suggested for the region near (E30, F35, D50, and D60), and far (I3), from the Mississippi River, respectively.

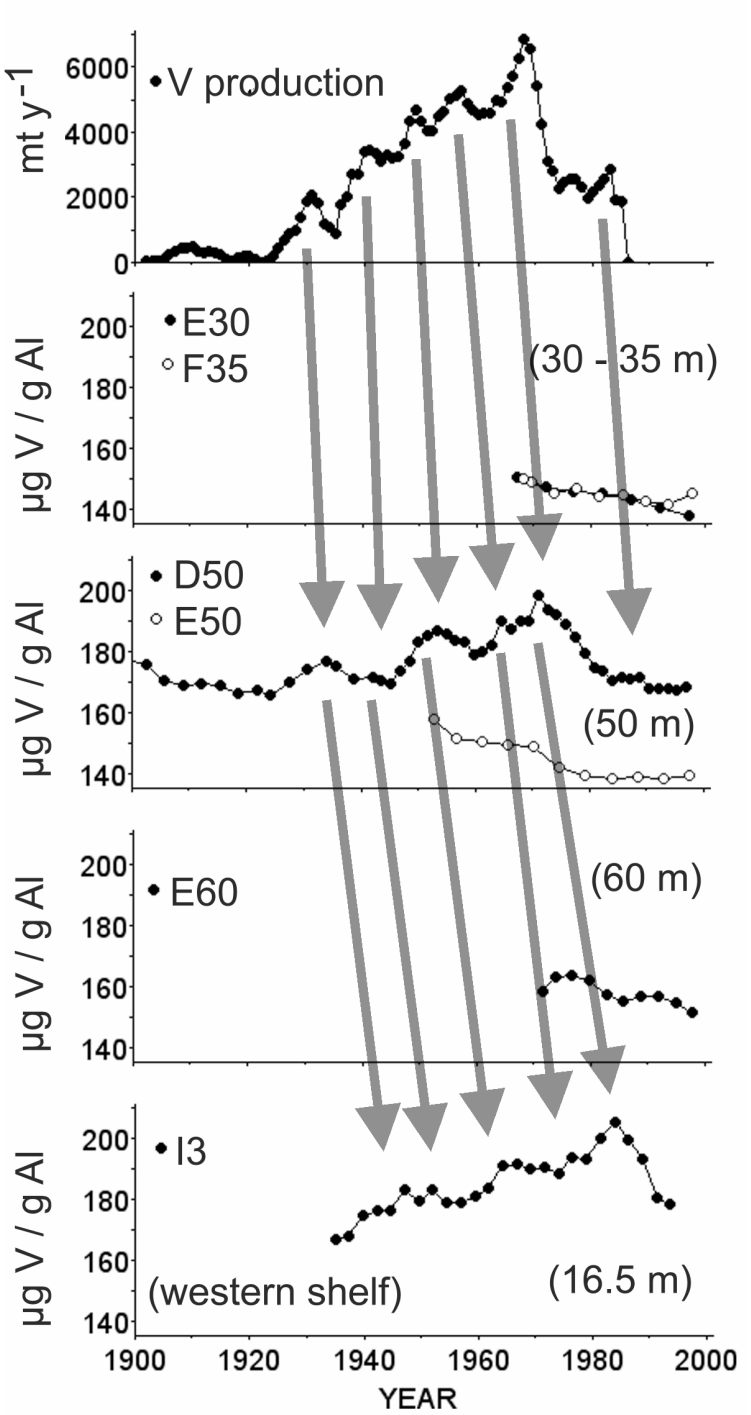

Figure 3.7. The normalized concentration of vanadium (µg V / g Al) in six dated sediment cores from various depth zones on the Louisiana shelf. The industrial production of vanadium in the United States is shown in the top panel. Possible coincidental peaks in the industrial production and the appearance of vanadium in sediments are indicated with the lightly shaded arrows. A lag of a few years and about a decade between industrial production and accumulation in sediments is suggested for the region near (E30, F35, D50, and D60), and far (I3), from the Mississippi River, respectively.

The concentration of Cu, Cd and Zn were strongly and positively correlated (Adj. $R^2 > 0.5$), with the concentration of V in all the cores (Table 3.1). The relationship between the concentration of Cu, Cd and Zn were also positively correlated with Ba concentration, but weakly so (Adj. $R^2 < 0.15$). This suggests that the factors controlling the accumulation of these three elements is more similar to the suite of factors affecting V than to Ba concentrations on this shelf.

Table 3.1

Results from a simple linear regression analysis of the relationship between Cd, Cu, and Zn (Y) versus both vanadium and barium (x) in dated sediments from six core samples from the Louisiana shelf. The Adjusted R^2 value is shown if the relationship is both positive (a direct relationship) statistically-significant at $p < 0.05$. N.S. = not significant. The total sample number is between 63 and 145 sample pairs. The more significant correlation between Cu, Cd and Zn for either V and Ba is highlighted in **bold**.

	V	Ba
Cu	**0.80**	0.14
Cd	**0.74**	0.09
Zn	**0.54**	0.08

The temporal variations in the accumulation of Ba appears to vary concurrently with the production and use of barite on this shelf, implying, but not proving, a cause-and-effect relationship. Some calculations may help determine if sufficient barite is released to account for the observed concentration in the sediments. We assumed that the average impacted area is a generous 100,000 km^2, that barite is 48% Ba, and that the use on the shelf is 75% of the consumption rate for 1990 to 2000 (1,732,636 mt). The average density of all sediment samples (n = 174) is 0.63 g cm^{-3}, and the average sedimentation rate for 34 cores is 0.99 cm yr^{-1}. The average Ba concentration was 192 µg g^{-1} (dry wt), of which 150 µg Ba g^{-1} was assumed to be recent accumulation that is above a 'background' historical concentration (pre-1900s). A sedimentary 'capture rate' of 15 % of the barite used would explain a 150 µg g^{-1} change in Ba concentration above this background amount. Similar sedimentary capture efficiencies could be estimated for other constituents of drilling mud, if the proportional amounts (relative to Ba) were known. However, the proportional amounts are not well-known, partly because of variations among operators and product evolution, and also because of proprietary protections.

Diatom Remains and Organic Content

The carbon and nitrogen content of sediment in all six cores is strongly related (Figure 3.8), and there is no obvious distinction in the C/ N ratio among cores, despite the differing sand, carbon and clay content (Figure 3.4).

The amount of BSi and carbon in sediments among cores varies considerably across the shelf (Figure 3.9). Some locations had a rise in either or both BSi and carbon in recent decades,

whereas others did not. The location of the sampling sites with increases in BSi or %C is in the center of the sample grid, which is also where the most frequent occurrence of summer hypoxia occurs (Figure 4.1). The areas without increases are outside the area that most frequently experiences hypoxic water formation in the summer. This result is consistent with the conclusion that the organic matter which is consumed in the bottom waters to create low oxygen conditions is also accumulating in the sediments. The concentration of BSi increased steeply in the last decade for core I3 (west of the Atchafalaya River), which is later than occurred in all analyses of cores collected in the MRB (Figure 3.9). The implication is that the size of the hypoxic zone is expanding in a westerly direction, as predicted by the application of a Streeter-Phelps model of nitrogen loading and hypoxic zone size (Scavia et al. 2003).

The amount of carbon stored in the sediments from 1970 to 1990 was estimated using the average sedimentation rate mentioned earlier (0.99 cm y^{-1}), the average carbon content in sediments dated >1980, and the dry density. The average accumulation rate is 64 g C m^{-2} y^{-1}.

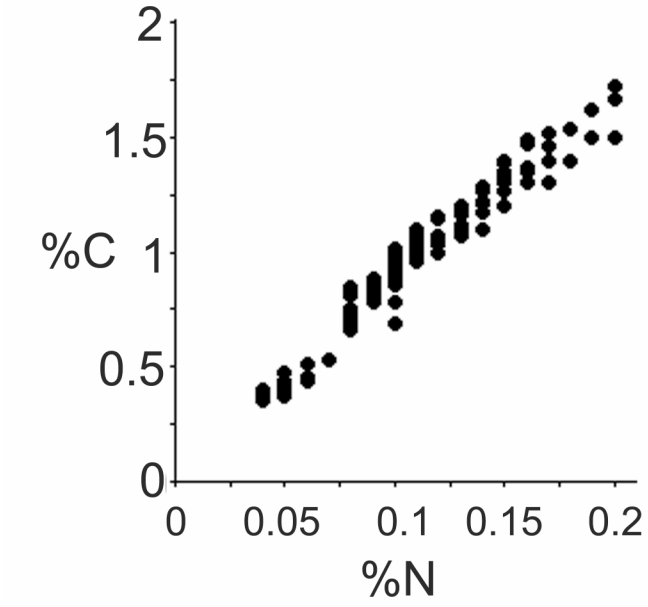

Figure 3.8. The relationship between the percent carbon and nitrogen in dated sediments from six cores (dry weight basis).

SUMMARY

The development of the OCS for oil and gas recovery started in the 1950s and peaked in the 1990s, while moving further offshore into deeper waters. The sedimentary record offshore shows fluctuations in the accumulation of Ba that are coincidental with the presumed use of Barite, a primary industrial application in OCS development. The fluctuations in V concentration in the sediments are not coincidental with Ba, but they are coincidental with the national consumption of V. Cu, Cd, and Zn concentrations in sediments fluctuate coincidentally with V, not Ba, thus indicating that the dominant source of these trace metals in offshore sediments are derived from riverine sources, and are not primarily from *in situ* industrial processes releasing them on the shelf. This is not to suggest that local site-specific contamination is not a significant management or health concern.

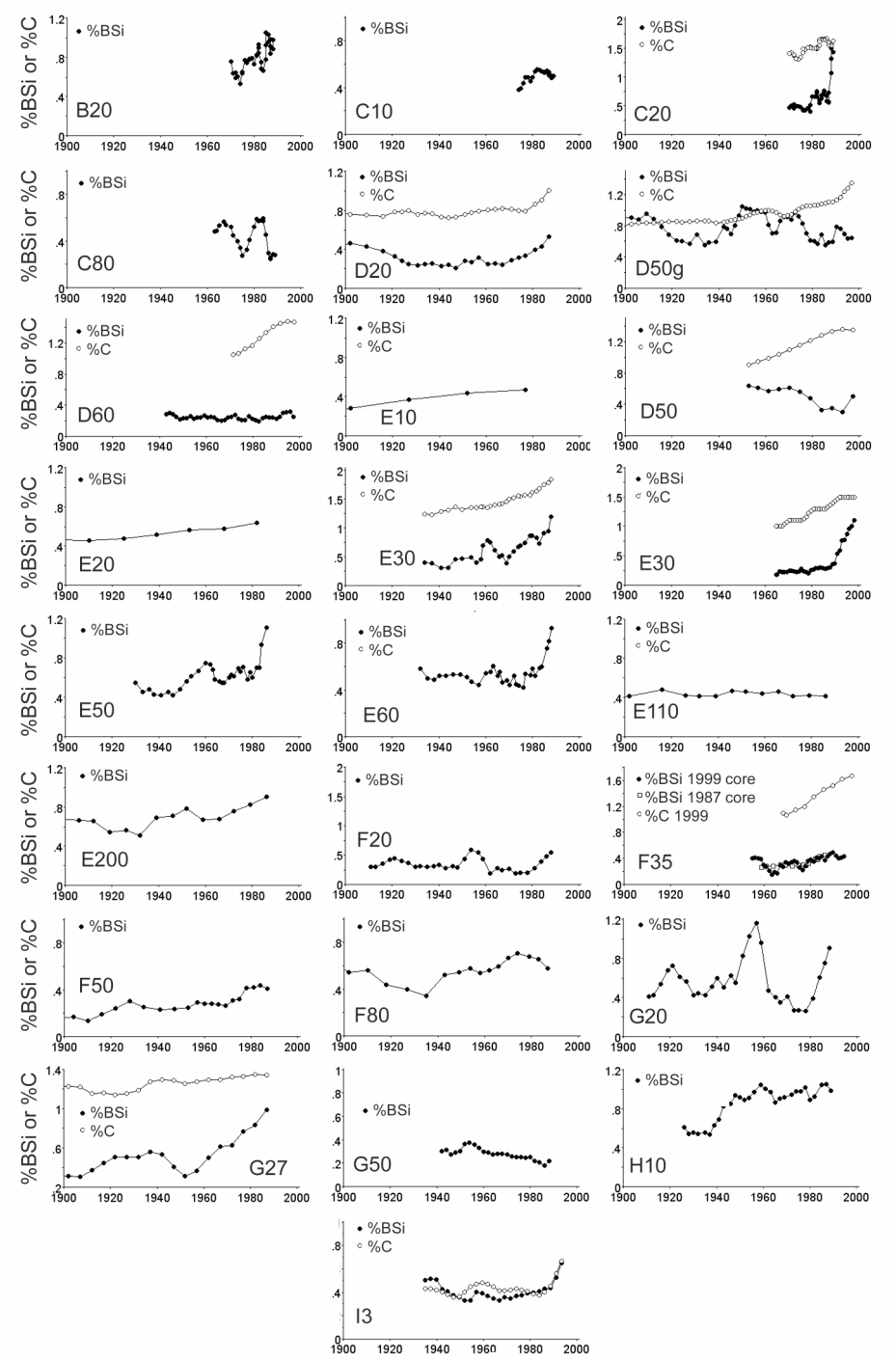

Figure 3.9. The concentration of percent biogenic silica (BSi) and % carbon vs. dated horizon for sediments from the continental shelf west of the Mississippi River delta in 10 to 100 m water depth. The data are for a 3 year running average. The letter is the transect shown in Figure 3.1. The number with the letter is the water depth, except for core I3 (16.2 m). Stations F35 and D50 have data from multiple cores (from different sampling dates).

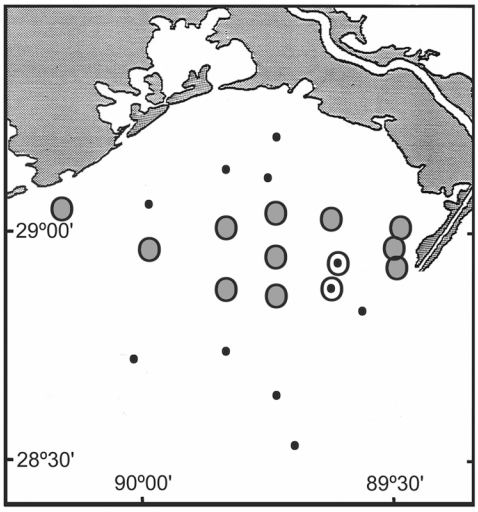

Figure 3.10. Core locations in the MDB where increasing concentrations of %BSi or %C were observed in the last three decades (data in Figure 3.9).

The hypoxic zone that covers much of the shelf in summer is attributed to loading of nitrogen from the Mississippi River (Rabalais et al. 2002b). Higher nitrogen loading from river to shelf increases surface production of diatoms whose organic loading to the bottom layer and subsequent metabolism results in oxygen being depleted faster than it is replaced. This coupling between river water, surface water and bottom water, therefore, extends from the MRB and westward off the Texas coast. Thus the influence of the river is demonstrably significant to the whole shelf, and not the region within a few tens of kms of the river's mouth.

CHAPTER 4

ECOSYSTEM HISTORY REVEALED THROUGH PRESERVED PHYTOPLANKTON PIGMENTS

Nancy N. Rabalais, Nazan Atilla, Claire Normandeau
Louisiana Universities Marine Consortium

ABSTRACT

Pigments determined by high performance liquid chromatography (HPLC) provide useful information concerning water column and epibenthic plant and microbial communities in both extant communities and accumulated sediments in lakes, estuaries and the ocean. Chlorophyll *a* provides an estimate of overall biomass, and carotenoid pigments provide taxonomic biomarkers characteristic of phytoplankton. HPLC pigments have proven useful in identifying the components of microphytobenthic communities and documenting the change of phytoplankton communities in freshwater and marine environments. We examined the pigments preserved in sediment cores to document the changes in phytoplankton community composition, phytoplankton abundance, and conditions of hypoxia over time. Carbon accumulated in sediments of the Louisiana continental shelf in water depths of 20 to 60 m are primarily marine phytoplankton sourced and represent the history of phytoplankton communities in the overlying water. There is a general increase in chlorophyll *a*, pheopigments, zeaxanthin, fucoxanthin and most carotenoids over time, with the change gradual from 1955 to 1970, followed by a fairly steady increase to 1997, the time the cores were collected. The highest chloropigment concentrations were in cores E30, E50 and F35, which were located in areas more likely to be exposed to seasonal hypoxia. The increasing pigments and greater concentrations in areas where hypoxia is more likely to occur indicate an increase in eutrophication or a worsening of hypoxia or both.

INTRODUCTION

Pigments determined by high performance liquid chromatography (HPLC) provide useful information concerning water column and epibenthic plant and microbial communities in both extant communities and accumulated sediments in lakes, estuaries and the ocean. Chlorophyll *a* provides an estimate of overall biomass, and carotenoid pigments provide taxonomic biomarkers characteristic of phytoplankton (Table 4.1; summarized in Jeffrey et al. 1997). HPLC pigments have proven useful in identifying the components of microphytobenthic communities (e.g., Cariou-Le Riaux-Gobin et al. 1987; Cariou-Le Gall and Blanchard 1995; Buffan-Dubau and Carman 2000a) and documenting the change of phytoplankton communities over time in freshwater and marine environments (e.g., Züllig 1981; Hodgson et al. 1997, 1998; Bianchi et al. 2000, 2002). In the case of reconstructing historic changes in phytoplankton, knowing the presence or absence of particular taxa in dated sediment cores or their change in abundance (biomass) can help identify the influence of natural variability or human-induced changes in water quality.

STUDY AREA

The distribution of the sediment cores in relation to the frequency of present-day bottom-water hypoxia (dissolved oxygen less than 2 mg l^{-1}, for the period 1985-2001) is shown in Figure 4.1. This frequency distribution represents hypoxia at the time of the mid-summer cruise, but not severity or seasonal progression for the remainder of the year. Based on the distribution for mid-summer hypoxia and knowledge of the depths at which hypoxia is likely to occur at other times of the year, the likelihood of hypoxia at each of the stations can be predicted (Table 4.2).

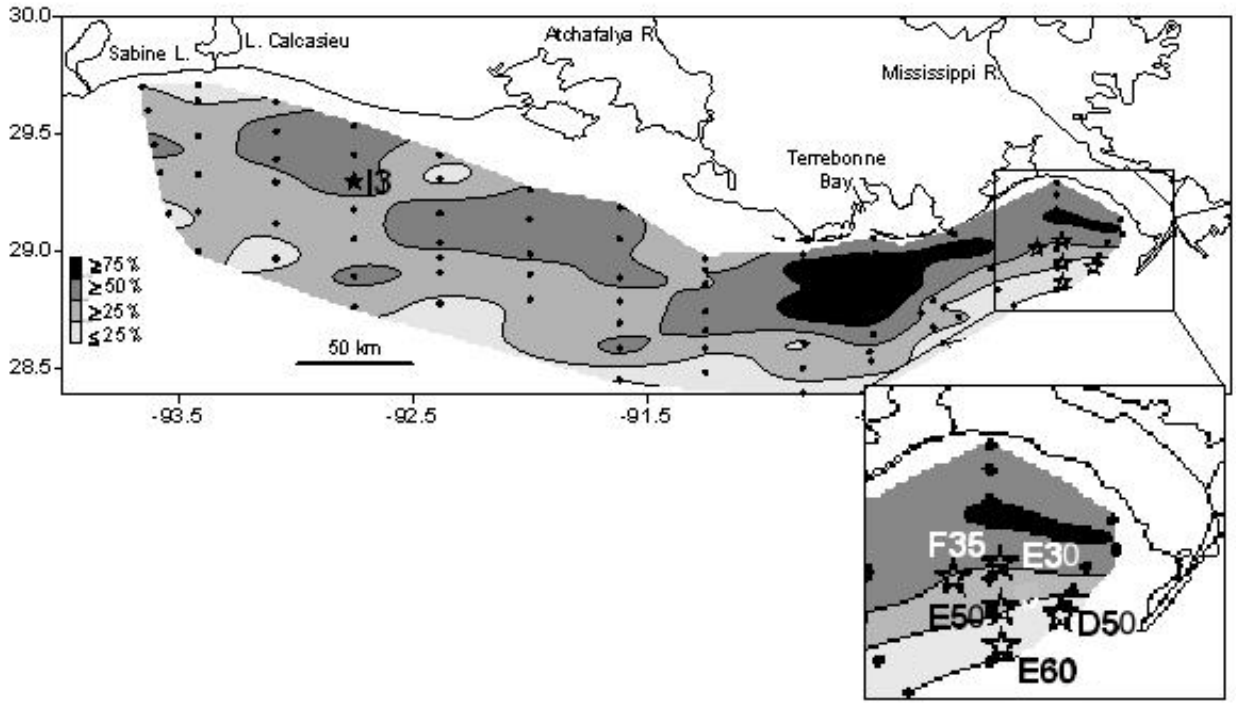

Figure 4.1. Frequency distribution of hypoxic bottom-water during mid-summer for years 1985-2001 (modified from Rabalais et al. 2002a) with core stations superimposed.

Table 4.1

The taxonomic origin of pigments from Louisiana shelf sediment cores and their relative concentrations in algal groups as identified by Jeffrey and Mantoura (1997).

		Algal Division/Class										
Pigment	abbreviation	Cyanophyta[1]	Rhodophyta	Cryptophyta	Chlorophyceae	Prasinophyceae	Euglenophyta	Eustigmatophyta	Bacillariophyta	Dinophyta[2]	Prymnesiophyceae	Chrysophyceae
Chlorophylls												
Chlorophyll a	chla	+	+	+	+	+	+	+	+	+	+	+
Pheophytin a	pheoa	Chlorophyll degradation products										
Pheophytin b	pheob	Chlorophyll degradation products										
Pheophytin a-like	phea-l	Chlorophyll degradation products										
Carotenes												
ß-carotene	bcaro	-			-	-	-	-	o	o	o	o
Xanthophylls												
Alloxanthin	allo			+							+	+
Canthaxanthin	canth	1										
Diadinoxanthin	ddx						+		+	+	+	+
Diatoxanthin	diato							o	o	o	o	o
Fucoxanthin	fuco								+	2	+	+
Lutein	lutein				+	-						
Peridinin	peri									+		
Violaxanthin	viola				+	+		+				
Zeaxanthin	zea	+	+		-			o				

1 Many freshwater filamentous cyanophytes have a wide range of carotenoids, not found in the picoplanktonic cyanobacteria (e.g., echinenone, canthaxanthin, see Nichols (1973) as reported in Jeffrey and Mantoura (1997)).
2 Several dinoflagellates have no trace of peridinin but have pigments characteristic of their endosymbionts (Jeffrey and Mantoura 1997).
+ = major pigment
- = minor pigment
o = trace pigment

METHODS

Sediment Grain Size Analysis

Sediment grain size analysis was determined on sediments from which the organic matter was removed either by combustion of dried, ground sediments or by treatment of wet sediment with 3.5% H_2O_2). For some samples, the coarse fraction was dry sieved and the fine fraction was determined with a Coulter Multisizer with 256 channelizer capability. For other samples, the sediments were dispersed in sodium hexametaphosphate (2.55 g l^{-1} H_2O) overnight, then wet sieved through a 63 m sieve to collect the sand fraction. The mud fraction was divided into %silt and %clay by timed gravimetric extraction of dispersed sediments (Folk 1974).

Chloropigments by High Performance Liquid Chromatography (HPLC)

Plant pigments were extracted and analyzed by high performance liquid chromatography (HPLC) according to the methods of Wright et al. (1991). Pigments were extracted with a combination of sonication and 100% acetone. The filtered extract (0.2 m) was injected into a Waters HPLC equipped with a 600 Controller and 600 Pump, 996 Photodiode Array Detector, and 474 Fluorescence Detector. The use of three columns (Waters Nova-Pak C_{18} 3.9 x 150 mm, a Rainin Microsorb C_{18}, and a Vydac Reverse-Phase C_{18}) maximized peak separation.

Table 4.2

Likelihood of exposure to hypoxia for each station based on mid-summer cruise data and more frequent observations off Terrebonne Bay (Rabalais et al. 2002b).

	Relative Hypoxia Exposure			
Station	**High**	**High-Med**	**Medium**	**Low**
I3	X			
E30		X		
F35		X		
E50			X	
D50				X
E60				X

Pigment identification was determined by comparing retention times and visible absorption spectra of pigments with pure standards. Chlorophyll *a* and *b* and ß–carotene were purchased from Sigma Chemical Co. Peridinin, fucoxanthin, zeaxanthin, violaxanthin, alloxanthin, diadinoxanthin, echinenone, canthaxanthin, lutein, and neoxanthin were purchased from The International Agency for C^{14} Determination, VKI Water Quality Institute, Denmark. Standards of chlorophyll *a* and *b* were converted to pheophytin *a* and *b* by acidification and standards of pheophorbides *a* and *b* and chlorophyllide *a* were obtained by the method detailed in Buffan-Dubau and Carman (2000b). Pigment concentrations were expressed as g g dry $sediment^{-1}$.

RESULTS AND DISCUSSION

Sediment Grain Size

Sediments from all cores from the MDB (D50, E30, E50, E60, and F35) were primarily silts, averaging 80% silt with variable clay and sand proportions (Figure 4.2). Sediments in the core from the southwestern Louisiana shelf (I3) were primarily sands, averaging > 90%, with a finer fraction at the surface and a clayey layer in the lower section (pre-1950s).

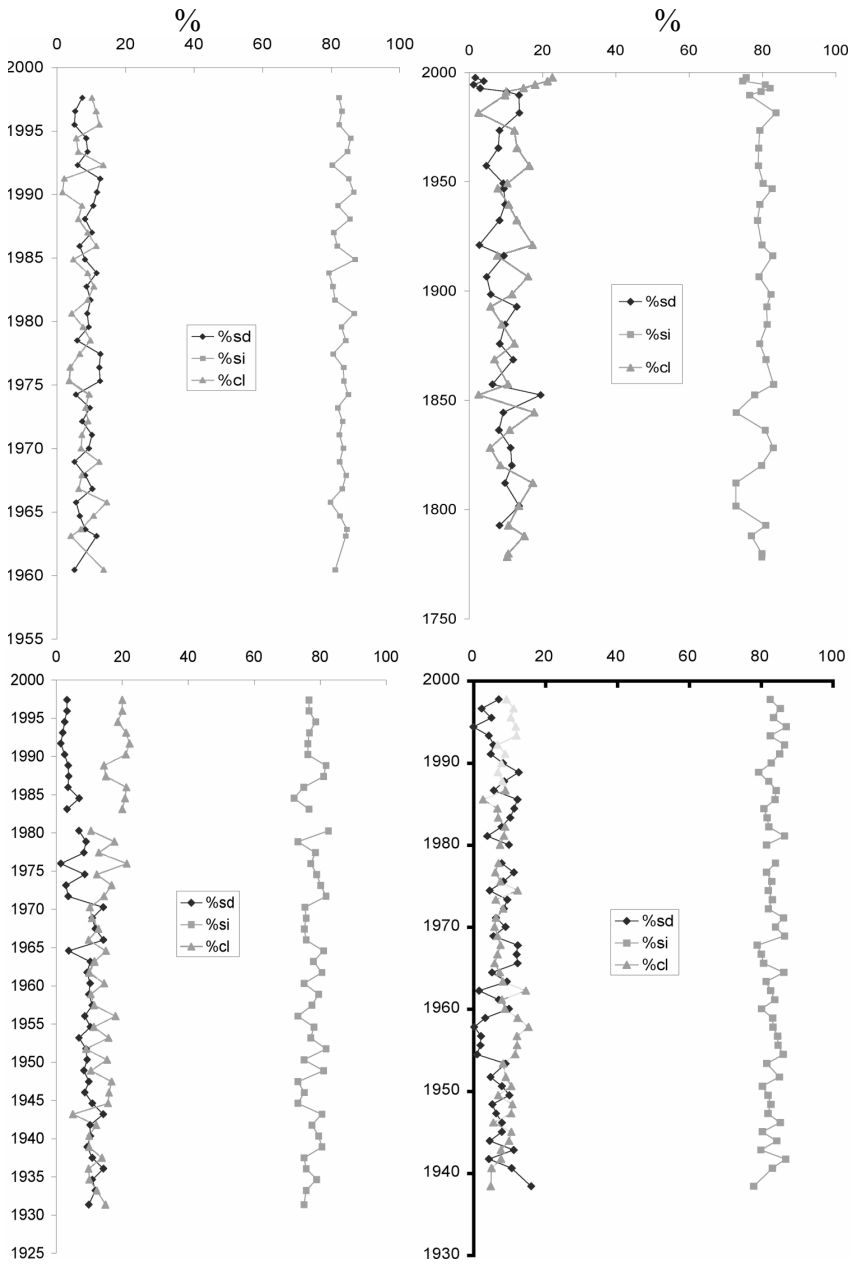

Figure 4.2. Vertical distribution of % sand, % silt and % clay for cores as indicated.

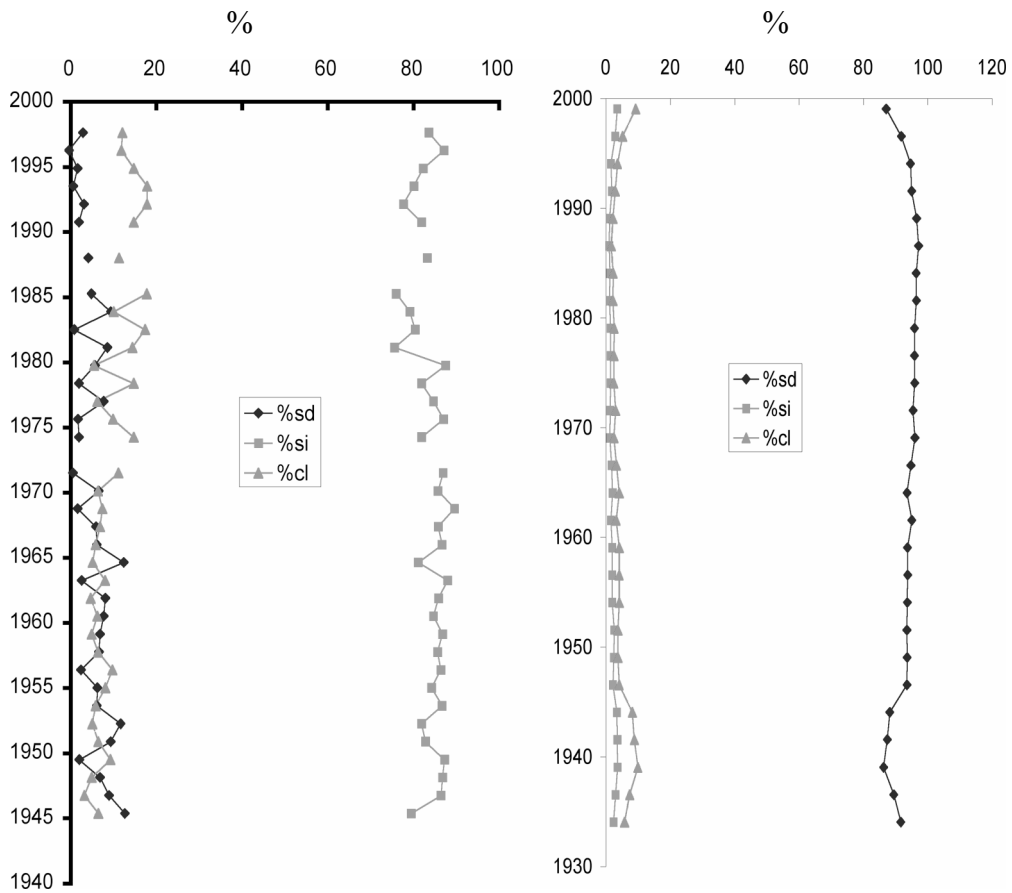

Figure 4.2. Vertical distribution of % sand, % silt and % clay for cores as indicated (continued).

Phytoplankton Pigments

Source of Pigments

Sources of organic carbon accumulated in Louisiana shelf sediments can potentially come from the water column, microphytobenthos, and terrestrial, marsh or submersed plants. The stable carbon isotope measurements of cores from the MDB, however, indicate that the overwhelming source of the carbon in accumulated sediments is marine phytoplankton and not allochthonous carbon in the source of terrestrial carbon from the drainage system of the Mississippi River or from export of marsh plant detritus from the coastal wetlands (Turner and Rabalais 1994a). Stable carbon isotope ratios for the core from the southwest Louisiana shelf indicate the same marine phytoplankton source (B. Fry, unpublished data). Thus, changes in the chloropigments in the sediments represent changes in the phytoplankton community in the overlying water column.

Time Sequences of Pigments

There is a general increase in chlorophyll *a*, pheopigments, zeaxanthin, fucoxanthin and most carotenoids over time, with the change gradual from 1955 to 1970, followed by a fairly steady increase (Figures 4.3-4.8). The concentrations are greater in E30, E50, and F35 than in E60 and D50, comparable to their relative listing for likelihood of hypoxia exposure as High-Medium and

Medium compared to Low (Table 4.2). The only distinguishing rise or fall in carotenoid concentrations occurred in E30 at 1988. Carotenoids were dramatically lower in1988 than before or after. The 1988 date corresponds with a period of severe drought in the Mississippi River basin, 100-yr low river discharge, and low nutrient loads.

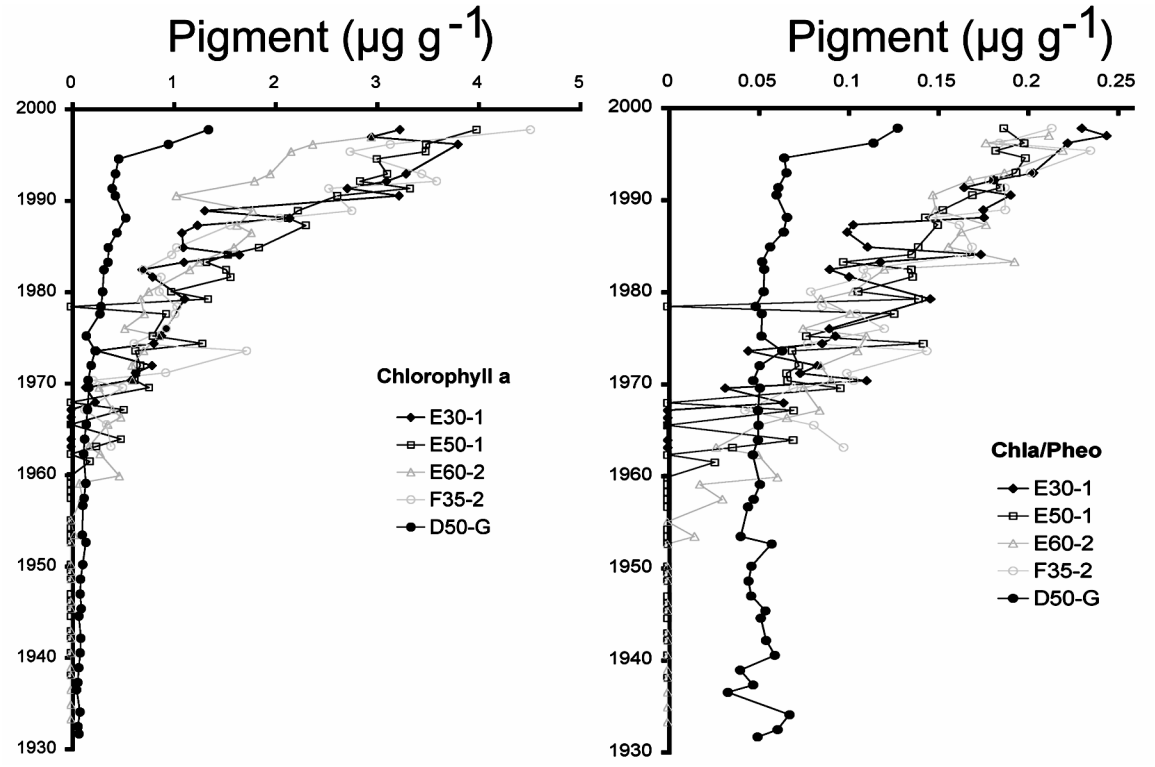

Figure 4.3. Vertical distribution of chlorophyll *a* and chlorophyll *a*/pheopigment ration (Chla/Pheo) for cores E30-1, E50-1, E60-2, F35-2 and D50G.

The longer D50G core taken with a gravity corer contains sediments dated to 1785 (Figure 4.7). Most carotenoids and chlorophyll *a* concentrations did not increase in the core until the 1970-period. Zeaxanthin (cyanobacteria) and ß-carotene concentrations showed a rise in more recent sediments beginning in the 1940s. There were also indications of historical cyanobacterial abundance in the 1785 to 1820 period and a rise then decrease for the 1860 to 1940 period with the peak concentrations occurring in the 1885 to 1935 period.

The degradation products of chlorophylls are pheopigments. As chlorophyll degradation proceeds, the ratio of chlorophyll *a*/pheopigments will decrease. Chlorophyll *a* degrades more slowly in hypoxic/anoxic conditions than in oxic conditions (Sun et al. 1991, 1993). Thus, a high chlorophyll *a*/pheopigment ratio may indicate high deposition rates of chlorophyll *a* or hypoxic/anoxic conditions of the overlying water. The chlorophyll *a*/pheopigment ratio increased with newer sediments in an up-core direction, but varied by core (Figure 4.3). The ratio generally increased gradually from mid-1950s for core E60, since 1960 for core E50, and since 1965 for core E30. Core F35 was not deep enough to sample sediments prior to 1962, but

the ratio was high at that point. These results indicate an increase in eutrophication, hypoxia, or both post-1950 with a dramatic rise post-1970.

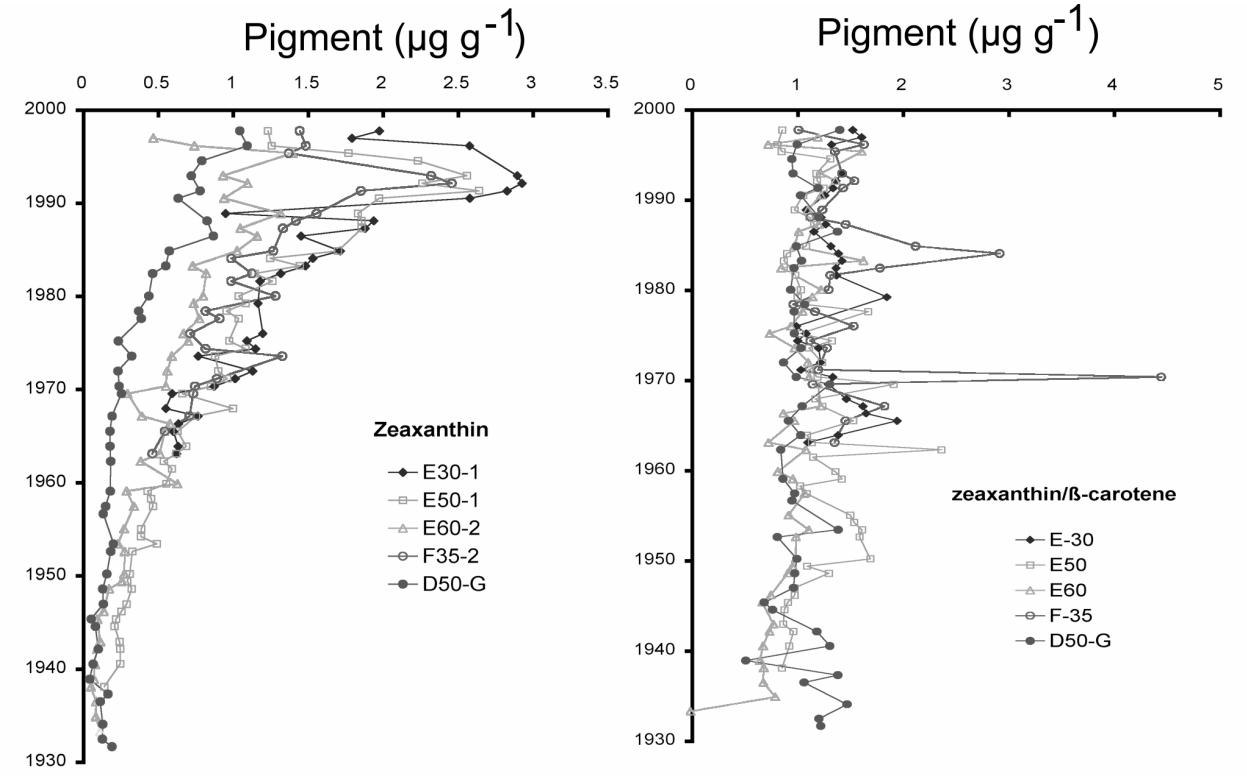

Figure 4.4. Vertical distribution of zeaxanthin and zeaxanthis/ß-carotene ratio for cores E30-1, E50-1, E60-2, F35-2 and D50G.

Specificity of Pigments

Of the chlorophylls, only chlorophyll *a* was detected in the sediments. Chlorophyll *b* is unlikely to be present because it is unstable in sediments. The presence of pheophorbide *b* indicated that chlorophyll *b* was at one time present in the water column. The highest overall concentration of pheopigments, however, was due to those derived from chlorophyll *a*.

Lutein, along with chlorophyll *b*, signifies the presence of detrital material from chlorophytes and vascular plants, but does not decay as rapidly as chlorophyll *b* (Bianchi et al. 1991). Lutein was present in relatively low and fairly uniform concentrations throughout the vertical depth of the cores in the MDB (example for D50 in Figure 4.7) and minimal in core I3 (Figure 4.8). The low concentrations of lutein would, therefore, represent a minimal contribution of terrestrial-sourced or freshwater phytoplankton to the accumulated carbon on the shelf. For those cores that pre-date 1950, there was an increase in the amount of lutein in the sediments beginning in the 1960-1970 period. Because lutein is fairly stable in anoxic sediments (Abele-Oeschger 1991), the increase in its concentration post 1960-1970 could signify increasing anoxic conditions in the sediments.

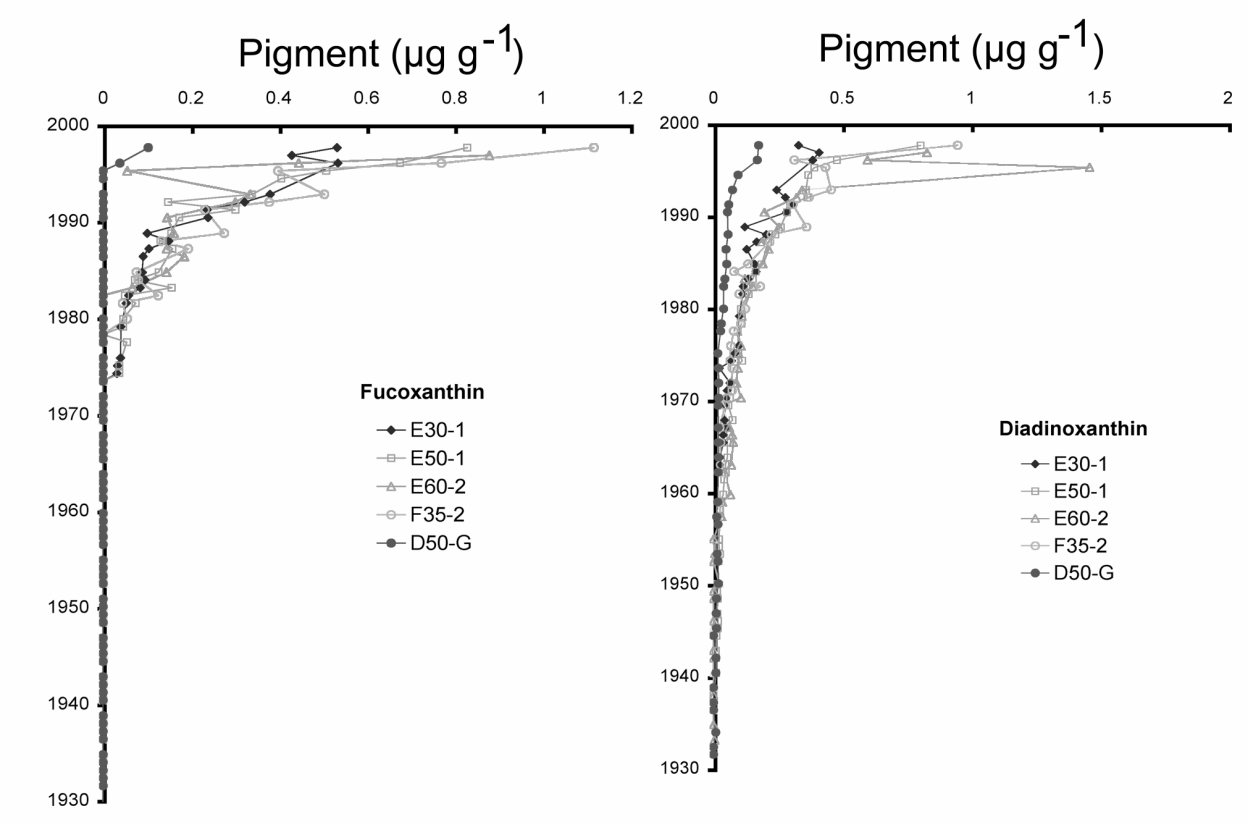

Figure 4.5. Vertical distribution of fucoxanthin and diadinoxanthin for cores E30-1, E50-1, E60-2, F35-2 and D50G.

The lack of the biomarker for prymnesiophytes and low values for the dinoflagellate biomarker, peridinin, indicated that the fucoxanthin present in the sediments originated from diatoms. The only station with trace amounts of peridinin that would indicate historic dinoflagellate blooms was I3. This station is closest to areas along the southwestern Louisiana coast and upper Texas coast (Figure 4.1) that experience periodic *Karenia brevis* or *Gymonodinium sanguineum* blooms (Harper and Guillen 1989; Dortch et al. 1999; Q. Dortch, unpubl. data). Other pigments that represented high biomass of phytoplankton were zeaxanthin (cyanobacteria) and ß-carotene (ubiquitous among several algae). Lower concentrations (and their representative phytoplankton taxa) were represented by diatoxanthin (trace in diatoms, dinoflagellates, prymnesiophytes, and raphidophytes), alloxanthin (cryptophytes), diadinoxanthin (primarily diatoms, dinoflagellates, prymnesiophytes, and raphidophytes), and canthaxanthin (some cyanobacteria) (Table 4.1).

Because of differential degradation of chloropigments (Leavitt 1993), the proportion of one pigment to another cannot be used as a proxy for relative biomass of phytoplankton taxa over time. The differences in rate of change among the carotenoids are evident in the few correlations between individual pigments (Table 4.3). The time course of any individual pigment, however, can be an indicator of change in the productivity of a taxa.

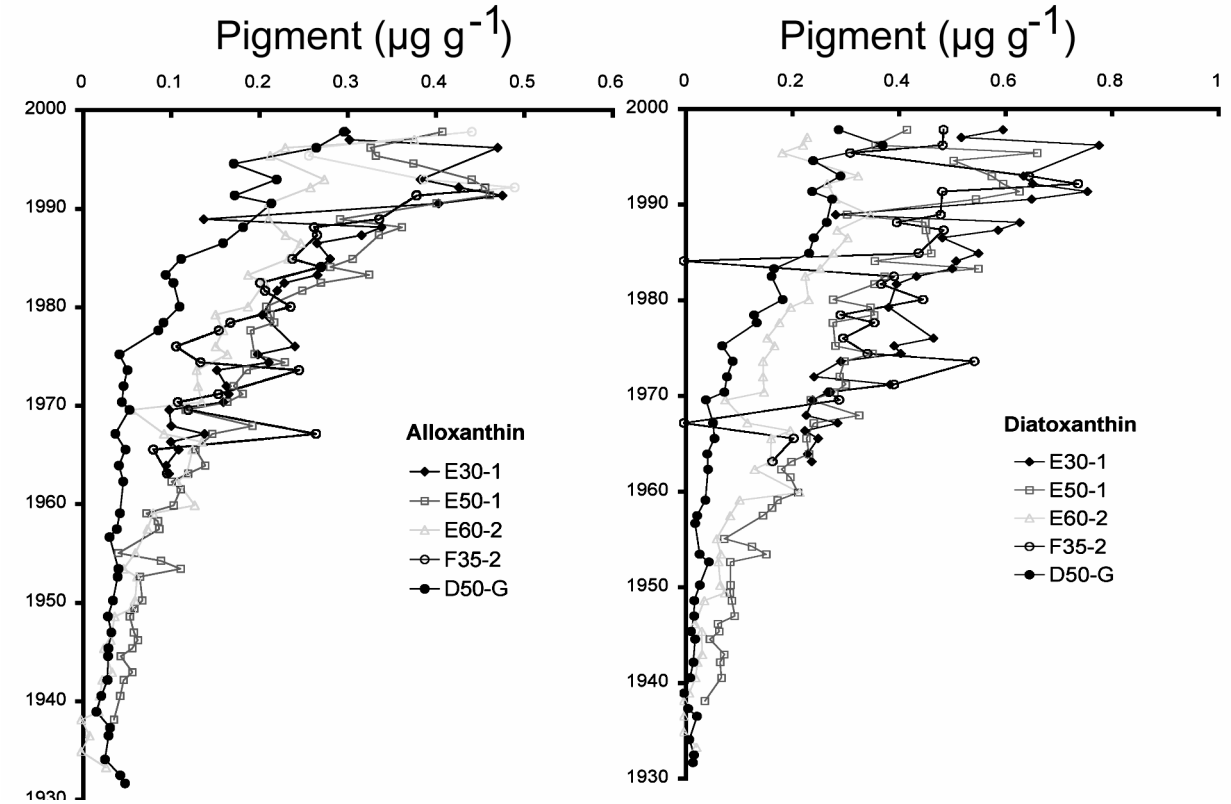

Figure 4.6. Vertical distribution of alloxanthin and diatoxanthin for cores E30-1, E50-1, E60-2, F35-2 and D50G.

Mississippi Delta Bight

Chlorophyll *a* decreased at a faster rate with depth than many of the carotenoid pigments (e.g., fucoxanthin, zeaxanthin, and ß-carotene) consistent with the fact that the chlorophylls are more labile than the carotenoids (Hodgson et al. 1997). Overall, carotenoids increased through time (more production) but some at a faster rate (differences in degradation or productivity of specific taxa or both).

Fucoxanthin (diatoms) was present in all cores (Figure 4.5) in the post-1970 period with the exception of core D50G in which concentrations were minimal in all but the upper two slices (Figure 4.6). Fucoxanthin is known to degrade more quickly than chlorophyll *a* (Klein and Riaux-Gobin 1991; Cariou-LeGall and Blanchard 1995), and its absence prior to the 1950s may be due to its degradation rather than a lack of diatom production. However, both fucoxanthin and chlorophyll *a* declined at similar rates indicating an increase in production of diatoms since the 1970s. Under anoxic conditions in lakes (Züllig 1981; Hodgson et al. 1997 1998), fucoxanthin was preserved. Therefore, it is not unreasonable to also hypothesize that a reason for the increase in fucoxanthin since the 1970s would be increasing overlying water anoxia and that its relative change over time indicated periods of eutrophication and anoxia (Züllig 1981).

Zeaxanthin (cyanobacteria) was present at trace levels through the depth of all cores with no peaks prior to the early 1950s, a gradual rise from 1950 to 1970, and a greater rate of increase since 1970 (Figure 4.4). There was also an indication of high concentrations during the early 1990s consistent with the flood of the Mississippi River in 1993. The increase of the relatively stable pigment zeaxanthin (Züllig 1981; Bianchi et al. 2000) would indicate an increase in cyanobacterial populations in more recent times. The lack of historic peaks, similar to those seen in paleostratigraphy from the Baltic (Bianchi et al. 2000), would indicate that cyanobacteria were not a major biomass component of the phytoplankton community of the shelf prior to the 1950s. This is confirmed by the zeaxanthin/ ß-carotene ratios (Bianchi et al. 2000), which show no trends over long periods, mostly between 1 and 1.5, and no exceptionally high peaks that would indicate cyanobacterial biomass (Figure 4.4).

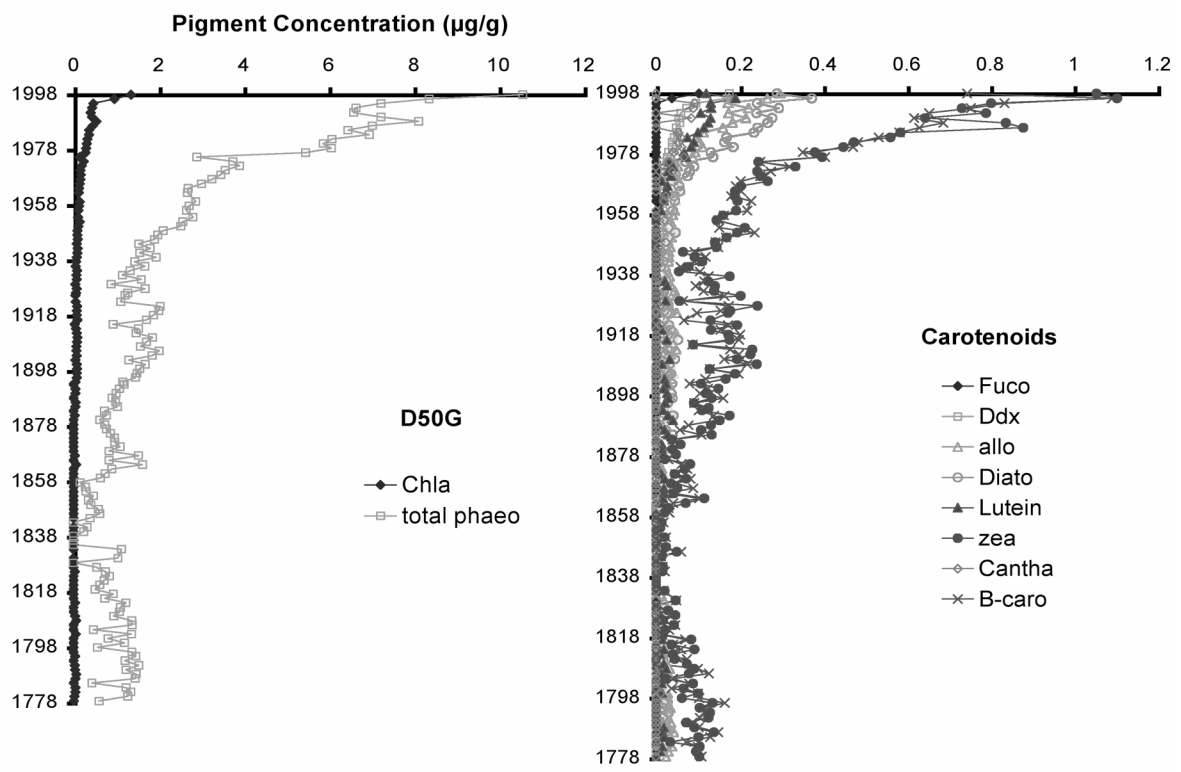

Figure 4.7. Vertical distribution of chloropigments in core D50G; chla (chlorophyll *a*), total phaeo (total phaeopigments), Fuco (fucoxanthin), Ddx (diadinoxanthin), allo (alloxanthin), Diato (diatoxanthin), Lutein, zea (zeaxanthin), Cantha (canthaxanthin), B-caro (ß-carotene).

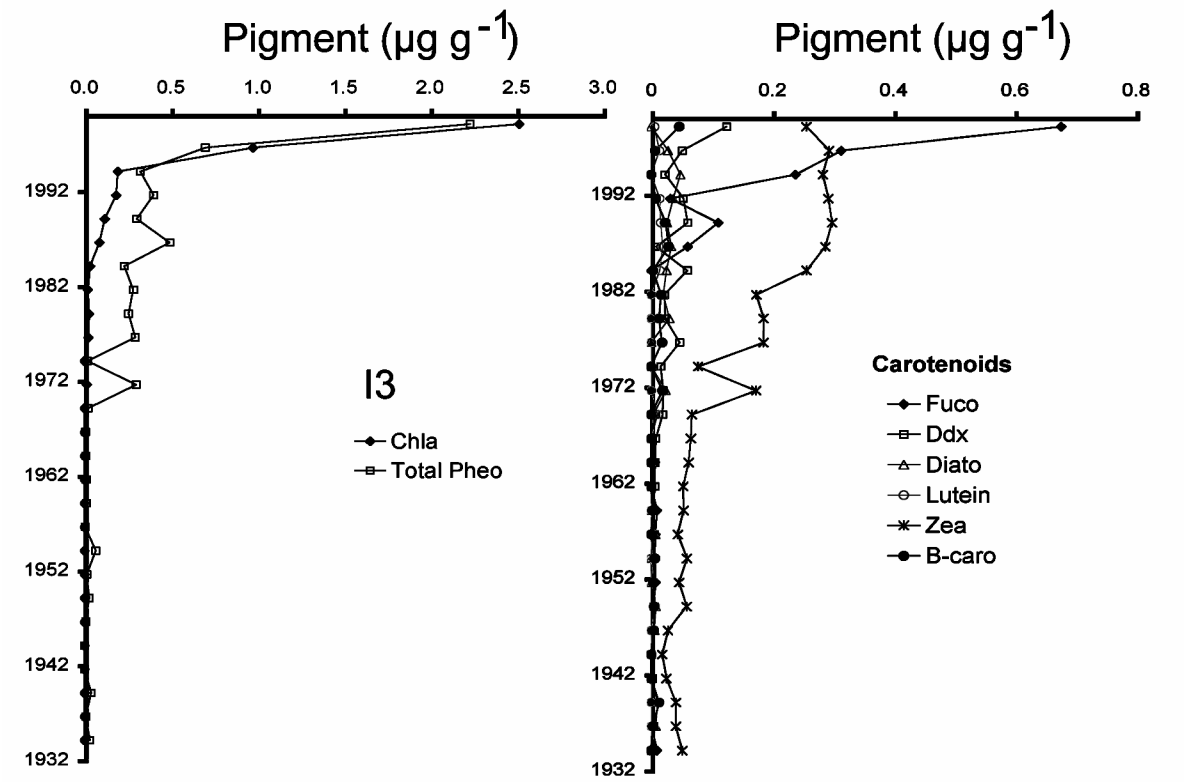

Figure 4.8. Vertical distribution of chloropigments in core I3; chla (chlorophyll *a*), total pheo (total phaeopigments), Fuco (fucoxanthin), Ddx (diadinoxanthin), Diato (diatoxanthin), Lutein, zea (zeaxanthin), B-caro (ß-carotene).

Alloxanthin concentrations begin to rise after 1950 in all cores from the MDB. Peaks in the sediment record from the early 1950s to present indicate aperiodic cryptophyte blooms (Figure 4.6). Diatoxanthin (a trace carotenoid in several algal groups) followed a similar pattern to alloxanthin (Figure 4.6). Diadinoxanthin (indicative of several algal groups) concentrations increased slowly since 1970 then more rapidly after 1985 (Figure 4.5).

Southwestern Louisiana Shelf

The sedimentary nature and chloropigments of core I3 from the southwestern shelf were sufficiently different from those of the MDB cores to segregate those results from the other cores (Figure 4.8). The sediments of the I3 core were primarily sands as opposed to silts for all others (Figure 4.2), and the pigment concentrations were the lowest of all the cores. Zeaxanthin was the dominant carotenoid as in the other cores, but ß-carotene was not a major component as it was with cores from the Mississippi Delta Bight (MDB). This means that the zeaxanthin/ ß-carotene ratio was much higher in the I3 core than the cores from the bight, a ratio of 10 to 40 versus 1-1.5, respectively, and that significant cyanobacterial blooms have occurred in this area since 1970. The chlorophyll *a*/pheopigment ratio increased steadily from the 1970s indicating increasing euthrophication or worsening hypoxic conditions or both. The trace levels of lutein indicate that terrestrially-derived plant materials are not a significant source of carbon accumulating in the sediments of core I3.

Table 4.3

Results of linear regressions among sediment pigments, sediment biogenic silica and Mississippi River annual nitrate load (from 1969 to 1997). Underlined values are for $R \geq 0.90$, significant at $p < 0.05$.

CORE D50G	1	2	3	4	5	6	7	8
1 Diadinoxanthin	1							
2 Diatoxanthin	0.85	1						
3 Fucoxanthin	0.76	0.41	1					
4 Alloxanthin	0.91	0.95	0.59	1				
5 Zeaxanthin	0.89	0.96	0.51	0.96	1			
6 Chlorophyll a	0.96	0.85	0.82	0.92	0.9	1		
7 BSi	0.35	0.46	0.12	0.42	0.44	0.43	1	
8 Nitrate	0.51	0.68	0.23	0.55	0.67	0.47	0.5	1

CORE F35	1	2	3	4	5	6	7	8
1 Diadinoxanthin	1							
2 Diatoxanthin	0.52	1						
3 Fucoxanthin	0.93	0.46	1					
4 Alloxanthin	0.76	0.59	0.69	1				
5 Zeaxanthin	0.64	0.81	0.58	0.88	1			
6 Chlorophyll a	0.9	0.69	0.88	0.84	0.82	1		
7 BSi	0.57	0.7	0.55	0.46	0.57	0.52	1	
8 Nitrate	0.33	0.11	0.34	0.46	0.3	0.29	0.08	1

CORE E60	1	2	3	4	5	6	7	8
1 Diadinoxanthin	1							
2 Diatoxanthin	0.44	1						
3 Fucoxanthin	0.59	0.49	1					
4 Alloxanthin	0.64	0.92	0.72	1				
5 Zeaxanthin	0.6	0.92	0.34	0.85	1			
6 Chlorophyll a	0.78	0.82	0.8	0.94	0.8	1		
7 BSi	0.31	0.02	0.18	0.14	0.11	0.21	1	
8 Nitrate	0.36	0.62	0.26	0.69	0.62	0.55	0.12	1

Table 4.3

Results of linear regressions among sediment pigments, sediment biogenic silica and Mississippi River annual nitrate load (from 1969 to 1997). Underlined values are for $R \geq 0.90$, significant at $p < 0.05$. (continued)

CORE E50	1	2	3	4	5	6	7	8
1 Diadinoxanthin	1							
2 Diatoxanthin	0.73	1						
3 Fucoxanthin	0.95	0.61	1					
4 Alloxanthin	0.84	0.95	0.7	1				
5 Zeaxanthin	0.73	0.94	0.59	0.96	1			
6 Chlorophyll a	0.93	0.86	0.87	0.93	0.88	1		
7 BSi	0.01	0.03	0.13	0.08	0.13	0.03	1	
8 Nitrate	0.46	0.52	0.44	0.57	0.46	0.55	0.24	1

CORE E30	1	2	3	4	5	6	7	8
1 Diadinoxanthin	1							
2 Diatoxanthin	0.87	1						
3 Fucoxanthin	0.94	0.77	1					
4 Alloxanthin	0.88	0.98	0.78	1				
5 Zeaxanthin	0.87	0.94	0.80	0.97	1			
6 Chlorophyll a	0.95	0.88	0.93	0.90	0.93	1		
7 BSi	0.86	0.63	0.94	0.63	0.66	0.84	1	
8 Nitrate	0.42	0.56	0.32	0.47	0.41	0.36	0.27	1

Relationships with Other Indicators of Productivity

The increase in concentration of chlorophyll *a* and fucoxanthin should be consistent with an increase in BSi as an indicator of diatom production as seen in prior results from the MDB (Turner and Rabalais 1994a) and Charlotte Harbor sediments (Turner et al. 2001). Most BSi profiles for sediments, however, were fairly uniform and did not show a positive relationship with chloropigments (R values well below 0.5). The exception was station E30, the station most likely to be in the epicenter of biogenic silica accumulation and surface sediment chlorophyll *a* concentrations (Turner and Rabalais 1994a). BSi and fucoxanthin were positively related ($R = 0.94$, $p < 0.05$). The relationships of BSi to chlorophyll *a* and other carotenoids for core E30 were also positive, but not significant.

Surface water productivity in the MDB has increased since the 1950s as indicated by several water column and sediment indicators. These include increase in diatom-based production (Turner and Rabalais 1994a, b), accumulation of marine-origin carbon (Eadie et al. 1994), and decrease in Secchi disk depth (Figure 4.9; Rabalais et al. 2002c). The decrease in water clarity is not due to an increase in suspended sediment concentration, because the suspended sediment concentration of the Mississippi River has been reduced by 50% since 1950 when the largest natural sources of sediments in the drainage basin were cut off from the Mississippi River main stem by the construction of large reservoirs on the Missouri and Arkansas Rivers (Meade 1995).

Mississippi River nitrate load is closely correlated with indicators of productivity in the overlying water column (Justic' et al. 1993, 1996) and hypoxia in bottom waters (Scavia et al. 2003), and should therefore be correlated with similar indicators in the sediment cores. None of the correlations, however, were significant (Table 4.3). This is likely the result of a much shorter time frame for the Mississippi River nitrate load data (back to 1969) when nitrate had already increased over historic values, versus the sediment core data that date back to at least 1930 for stations D50, E50 and E60 but only to the early 1960s for stations E30 and F35 (where hypoxia is more likely to occur). This is also the reason the R-values for correlations with the longer time sequence for D50, E50 and E60 were higher than the values for E30 and F35 where hypoxia is more likely to occur.

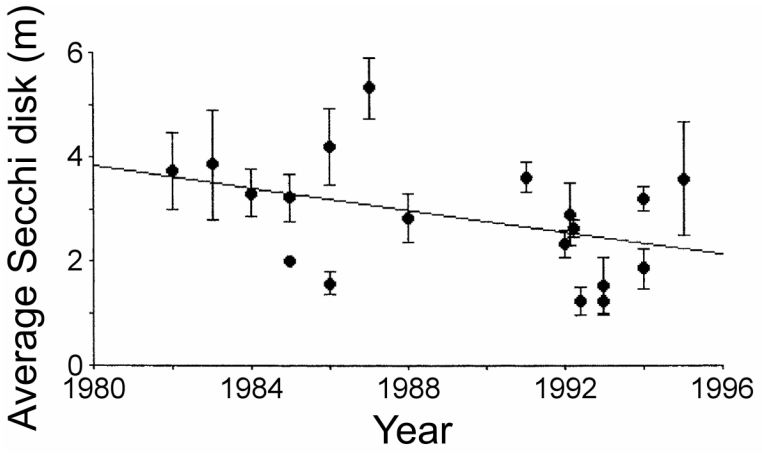

Figure 4.9. Trend of average Secchi disk depth on the Louisiana shelf west of the Mississippi River delta. The data are restricted to stations with surface water salinity between 20 and 25 psu and depths between 10 and 100 m. The slope of the regression line is significant at the 8% level of significance. The error bars are ±1 s.e. (From Rabalais et al. 2002c).

Relationships with Indicators of Hypoxia

The results of foraminiferan cluster analyses for core E60 indicate trends similar to a proposed evolution of seasonal hypoxia (Blackwelder et al. 1966) with a significant change in foraminiferal composition in the middle of the 20th century. The increases in chloropigments for core E60 also began in the 1955-1960 period. There were no clear clusters of foraminiferans in the F35 core, because the time sequence was not long enough. However, the chlorophyll *a* concentrations in that core, beginning in early 1960, indicated already elevated levels suggestive of increased production or worsening hypoxia or both. The increasing trend in relative abundances of the foraminiferan, *Buliminella morgani*, in cores F35 and E60 as a consequence of progressive hypoxia are paralleled by increases in chloropigments.

Bacterial chloropigments from a sediment core collected in a chronic area of hypoxia in 27 m water depth 50 km west of the MDB study area (Chen et al. 2001) confirmed a worsening of hypoxia since the early 1960s consistent with results of several other workers (Nelsen et al.

1994; Rabalais et al. 1986; Sen Gupta et al. 1996). The concentrations of chloropigments in sediment cores from the MDB, which date back only to 1963 but are likely to experience Medium-High hypoxia (E 30, F 35; Table 4.2), are elevated, consistent with the findings of Chen et al. (2001) and the several foraminiferan studies.

SUMMARY

The carbon accumulated in sediments of the Louisiana continental shelf in water depths of 20 to 60 m are primarily from marine phytoplankton and contains the history of phytoplankton communities in the overlying water. There is a general increase in chlorophyll *a*, pheopigments, zeaxanthin, fucoxanthin and most carotenoids over time, with the change gradual from 1955 to 1970, followed by a fairly steady increase to 1997, the time the cores were collected. The highest chloropigment concentrations were in cores E30, E50 and F35, which were located in areas more likely to be exposed to seasonal hypoxia. The increasing pigments and greater concentrations in areas where hypoxia is more likely to occur indicate an increase in eutrophication, or a worsening of hypoxia, or both.

CHAPTER 5

HISTORICAL RECONSTRUCTION OF THE CONTAMINANT LOADING AND BIOLOGICAL RESPONSES IN THE CENTRAL GULF OF MEXICO SHELF SEDIMENTS: FORAMINIFERA

Barun K. Sen Gupta
Department of Geology and Geophysics, Louisiana State University
and
Emil Platon
Energy and Geoscience Institute, University of Utah

ABSTRACT

Two cores, F35 and E60, were processed for the investigation of benthic Foraminifera; seventy four species were identified. Foraminiferal data reported by previous workers from two other Louisiana shelf cores were also examined for comparison. Core F35 covers the time span of 1943-1997, E60 1915-1997. In both cores the temporal trend is one of diversity reduction and dominance increase. Cluster analysis of foraminiferal relative abundance data from E60 shows significant assemblage changes in between the 1915-1936, 1938-1978 and 1979-1997 time intervals. No definite relationship could be established between the contaminant concentration in sediments and the composition of foraminiferal assemblage. The only match between a contaminant high (PAH 37 ng g^{-1}, OC pesticides 35 ng g^{-1}) and a diversity low was at the 1970-1975 level in core F35; the significance of this match is unclear. Deformed Foraminifera, one indicator of extreme chemical pollution, are not present in either of the cores. On the other hand, the diversity and relative-abundance changes of foraminiferal species fit the model of progressively worsening seasonal hypoxia in the area.

INTRODUCTION

Nearshore benthic Foraminifera are sensitive indicator organisms of marine environments and environmental stresses. Their meiofaunal size and substantial population densities facilitate quantitative studies of these species. In addition, the calcitic shells of many Foraminifera are much better preserved in the sedimentary record than the aragonitic shells of invertebrates such as molluscs. Some species of Foraminifera are tolerant of many environmental stresses, including oxygen depletion and various forms of toxicity, and may be present in substrates that are devoid of other shelled organisms. Dominance shifts in benthic foraminiferal assemblages have been recorded in many nearshore areas affected by industrial or municipal pollution, and a reduction in diversity has been noticed in extreme cases. In this context, we investigated the distribution of benthic Foraminifera in two Gulf of Mexico box cores in order to (a) assess the possible effects of hydrocarbon contamination on these shelled protozoans (because of toxicity or oxygen depletion) and (b) interpret environmental changes in historical time that affected foraminiferal microhabitats. Comparisons were made with published data from two other cores taken from the same area.

MATERIALS AND METHODS

The locations of the cores used for the present study (as well as those of two other cores from which comparable data were available) are shown in Figure 5.1. Box cores were collected in April 1997 from 35 and 60 m water depths (stations F35 and E60). After retrieval, each box core was examined for disturbance, and was recognized as undisturbed if the overlying water was clear and invertebrate tracks were visible at the sediment surface. Subsamples from each box core were obtained with 7-cm diameter plastic tubes and sliced at 1-cm intervals. Approximately half of these 1-cm slices became the primary samples for this study. Selected samples were washed over a 63 μm sieve and dried. The resulting residuum was split with a microsplitter to provide an aliquot of approximately 300 shells of benthic Foraminifera. All of these specimens were picked and identified at the species level.

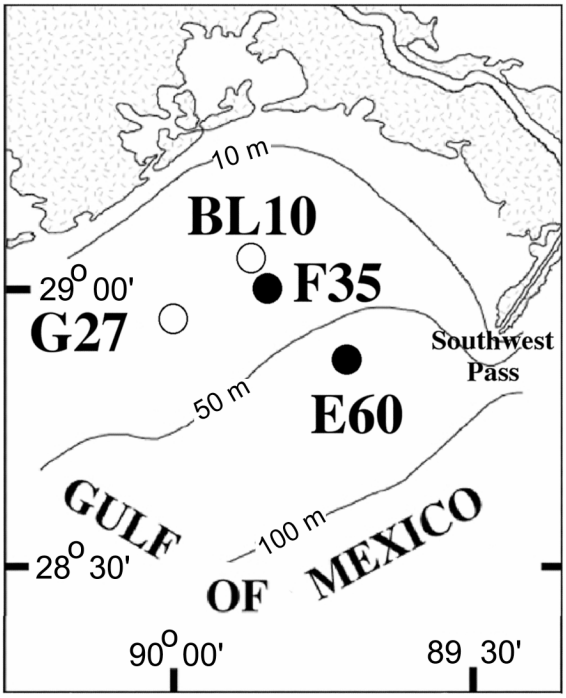

Figure 5.1. Core locations. Cores F35 and E60 were taken in spring 1997 (primary material for this study); BL10, core 10 of Blackwelder et al. (1996); G27, core studied by Sen Gupta et al. (1996) and Rabalais et al. (1996). Water depths: F35, 35 m; E60, 60 m; BL10, 29 m; G27, 27 m.

Parameters such as distribution of taxa (species and/or higher level), species diversity (see below), and univariate and multivariate responses were examined. The chosen sampling intervals for the foraminiferal study were linked to the time spans represented by the cores and the sampling intervals for petroleum biomarkers. In the core-top samples, living Foraminifera was recognized by the Rose Bengal stain.

Species diversity was assessed by two measures computed from the foraminiferal counts: (1) species richness (S), i.e., the number of species present in the sample or aliquot, and (2) Shannon Wiener Index given by the equation $H(S) = -\sum p_i \ln p_i$, where p_i is the proportion of the i^{th} species. Simple linear regression (SLR) and multivariate analyses (Cluster Analysis, Principal Components Analysis) of foraminiferal data were performed in order to find additional clues to historical changes in the composition of the benthic foraminiferal community. Absolute ages of samples were estimated on the basis of accumulation rates calculated by ^{210}Pb dating (R. E. Turner, personal communication). The characteristics of sediments in Louisiana Bight that make ^{210}Pb analysis a reliable technique for determining accumulation rates include (1) high deposition rates (> 1 mm/yr); (2) shallow mixed surface zone (< 15 cm); (3) high proportions of silt and clay (> 40%), and (4) negligible effect of bioturbation. Thus, in the ^{210}Pb profiles, an extended radioactive decay region between the surface mixed layer and the lower region of background activities allow the determination of sediment accumulation rates (R. E. Turner, personal communication).

RESULTS AND DISCUSSION

Species Diversity

Seventy four species of benthic Foraminifera were identified, 42 from F35 and 55 from E60; 23 species were present in both cores. Plots of species richness are in Figure 5.2. Three intervals can be distinguished in the species-richness curve for core E60. During the first interval, 1915-1936, a relatively high number (27-29) of benthic foraminiferal species populated the habitat. Species richness decreased steadily from 27 in 1936 to 12 in 1970 and then remained nearly constant at values that averaged 10.6 for the rest of the investigated time interval (1976-1997). The decreasing trend of the number of benthic foraminiferal species at E60 was tested with simple linear regression (SLR). This procedure, performed at 95 % confidence, explained 92% of the data variability (correlation coefficient, $r = 0.92$) and showed that the species richness increased with the core depth with a β (slope) value of 0.47. At the 35-m station (core F35), species richness decreased from 23 to 7 between 1943 and 1948 and remained at a relatively low level during the subsequent period (1948-1997), with a mean of 8. The SLR for F35 (species richness against depth) could explain only 30% of the data variability. Thus, the decreasing trend in species richness in F35 (with the exception of the highest value recorded for the oldest sample) is not as evident as in E60.

Trends of Shannon-Wiener index (Figure 5.3) are similar to those of species richness. In E60, this diversity index decreased steadily from 2.29 in 1915 to 0.81 in 1997, whereas in F35 the value changed from 1.74 in 1943 to 1.31 in 1948. Most subsequent values remained between 1.3 and 1.5, but a pronounced minimum value of 0.38 was attained around 1973. This drop in the Shannon-Wiener Index is due to a significant reduction in the number of minor components of the foraminiferal assemblage. Regression analysis of E60 data shows (with 95% confidence) that diversity index increased downcore. The SLR's "best fit" explained 92% of the response variable. No significant pattern of diversity change can be deciphered from the SLR analysis performed on the F35 data.

Species Distribution

Dominant Species

Stratigraphic distributions of the three dominant species, *Buliminella morgani*, *Nonionella basiloba*, and *Epistominella vitrea*, are shown in Figure 5.4. The sum of proportions of these species in E60 ranges between 0.62 and 0.94, with a mean of 0.86. An increasing trend of this sum is evident especially between 1915 and 1945. A significant increase in the relative abundance of *Buliminella morgani* between 1988 and 1997 is also noticeable. In F35, the sum of the relative abundances of *Buliminella morgani*, *Epistominella vitrea,* and *Nonionella basiloba* shows an increasing trend between 1943 and 1955. Two pronounced drops occurred in 1970 and 1976. During the second half of the century, these three hyaline species comprise, on average, as much as 91% of the foraminiferal assemblages in both of the cores.

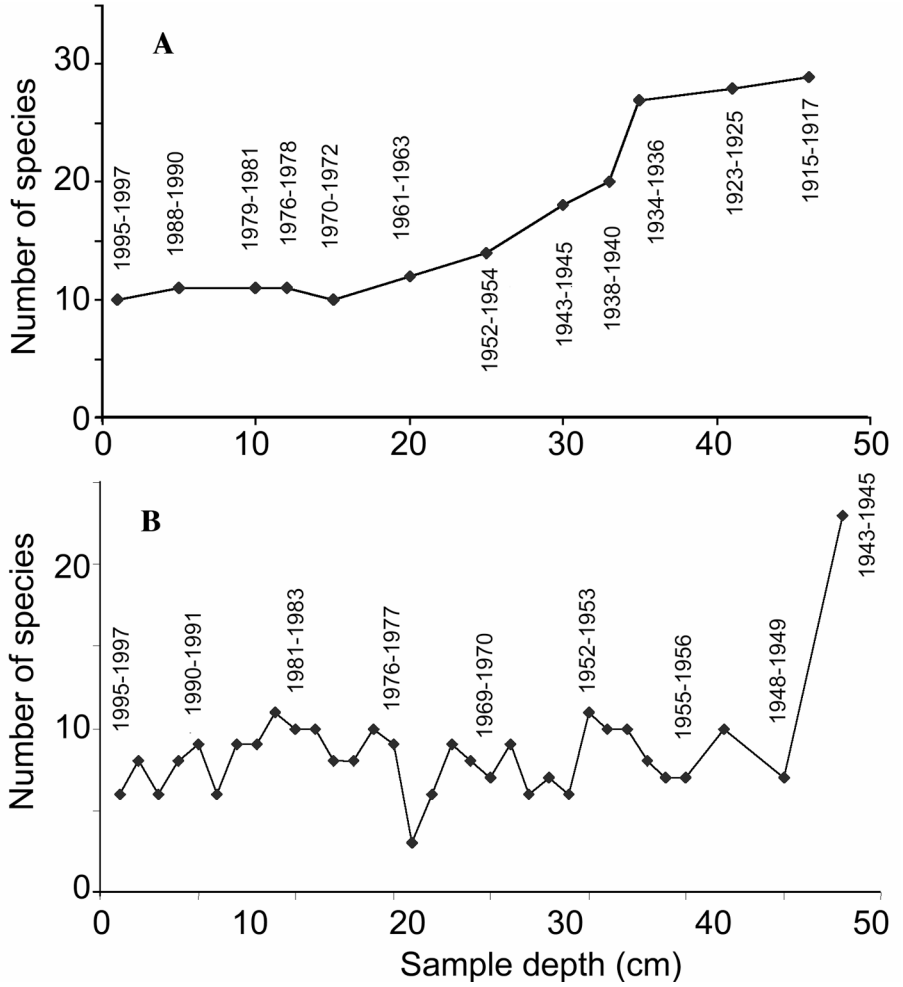

Figure 5.2. Distribution of species richness through time. A, core E60; B, core F35.

Ammonia and Elphidium

The *Ammonia-Elphidium* foraminiferal index (or A-E index, given by NA/(NA + NE)X100) is regarded as an indicator of oxygen stress (Sen Gupta et al. 1996). Its value stays above 60% in most F35 samples, and above 80% in the youngest part (1979-1997) of this core (Figure 5.5). Because of the low numbers of both *Ammonia* (<12 per sample) and *Elphidium* (<6 per sample, with one exception), however, the fluctuations of the A-E index are difficult to interpret; neither of the two taxa are present in 7 samples, thus resulting in a zero value of the index. The A-E index reaches a maximum value (100) in several samples towards the top of the core due to the lack of *Elphidium* specimens. In E60, only two specimens of *Ammonia* were found; there was no *Elphidium*.

Minor Species

Some species of benthic Foraminifera in E60 have low relative abundances, but they occur in a significant number of samples. The plot in Figure 5.6 shows the relative abundance distributions of *Bulimina marginata, Cancris sagra, Fursenkoina pontoni, Saccammina difflugiformis, and Uvigerina hispido-costata.* It is evident that the relative abundances of all these species decreased especially between 1915 and 1945. Relative abundances of *Bolivina lowmani* and *Bulimina marginata* from F35 are plotted in Figure 5.7. These proportions are highly variable through time.

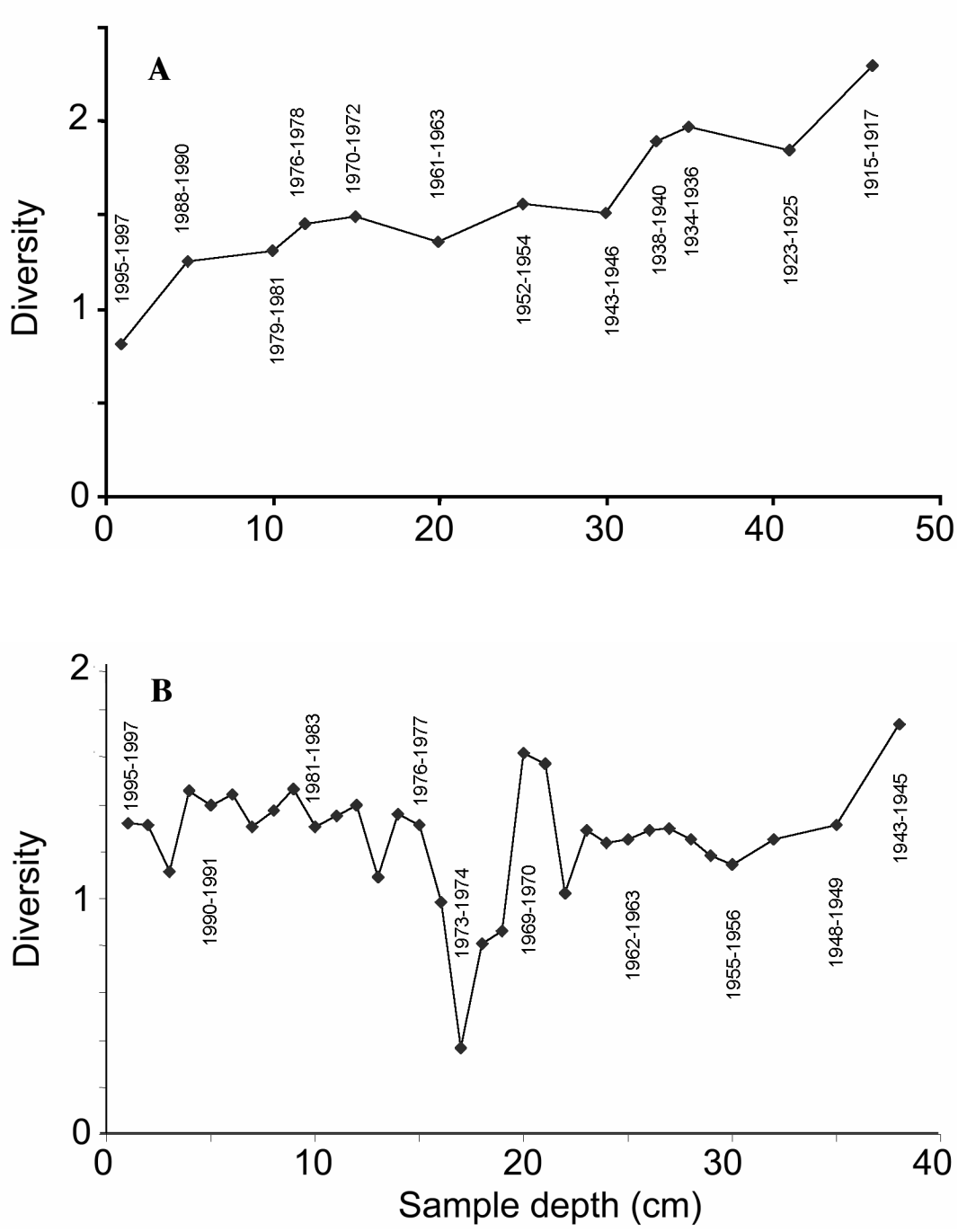

Figure 5.3. Distribution of Shannon-Wiener diversity index through time. A, core E60; B, core F35.

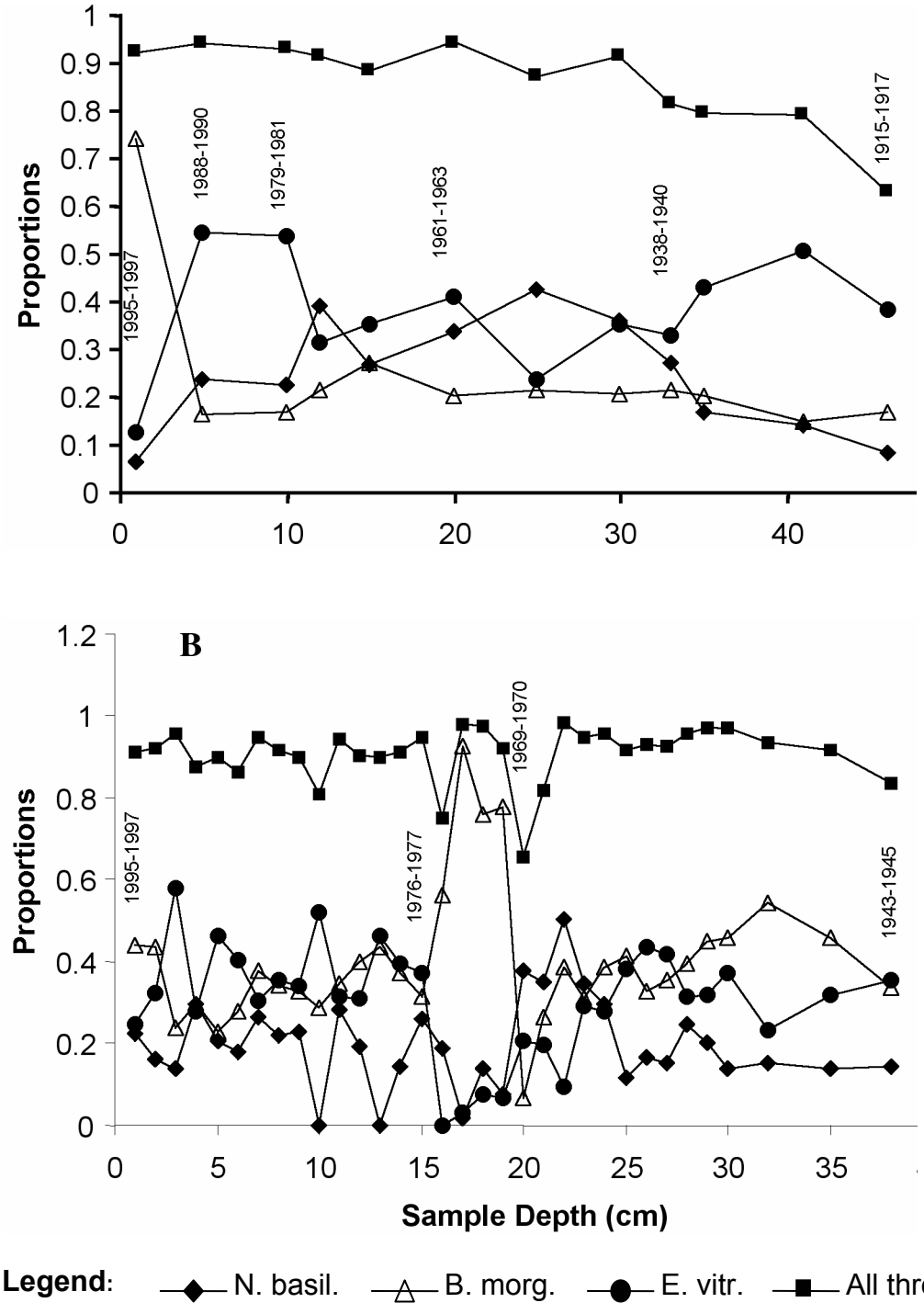

Figure 5.4. Distribution of dominant species through time. A, core E60; B, core F35.

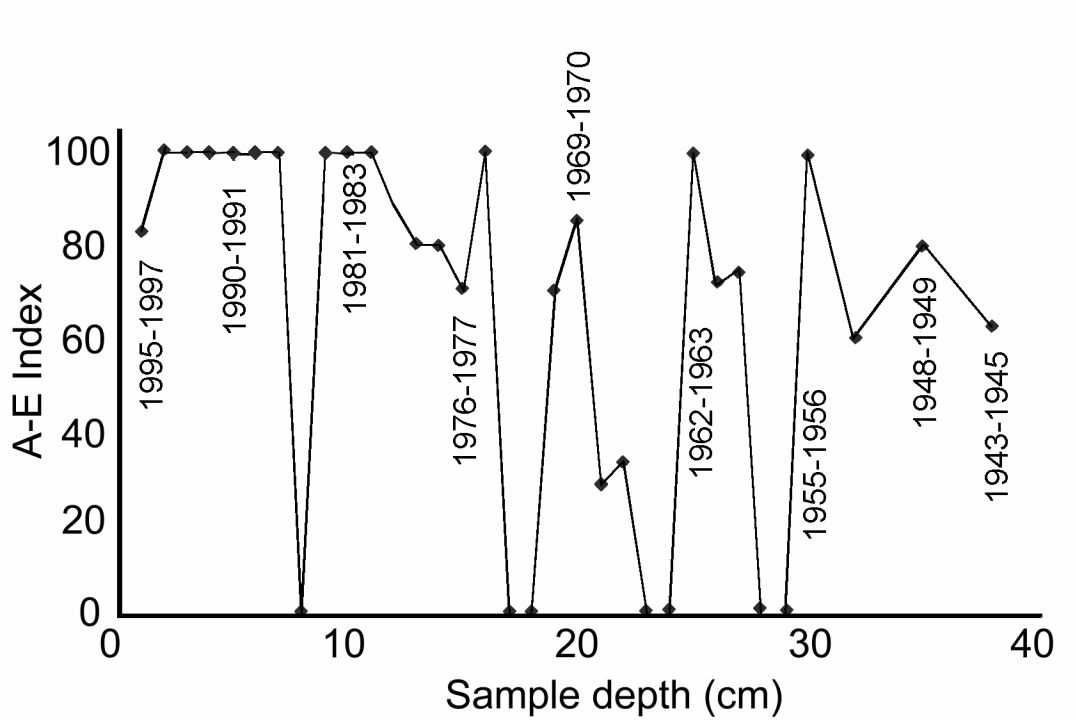

Figure 5.5. Distribution of *Ammonia–Elphidium* Index in Core F35. The maximum value of 100 is for samples where no *Elphidium* was found; the zero value is for samples in which both *Ammonia* and *Elphidium* were absent.

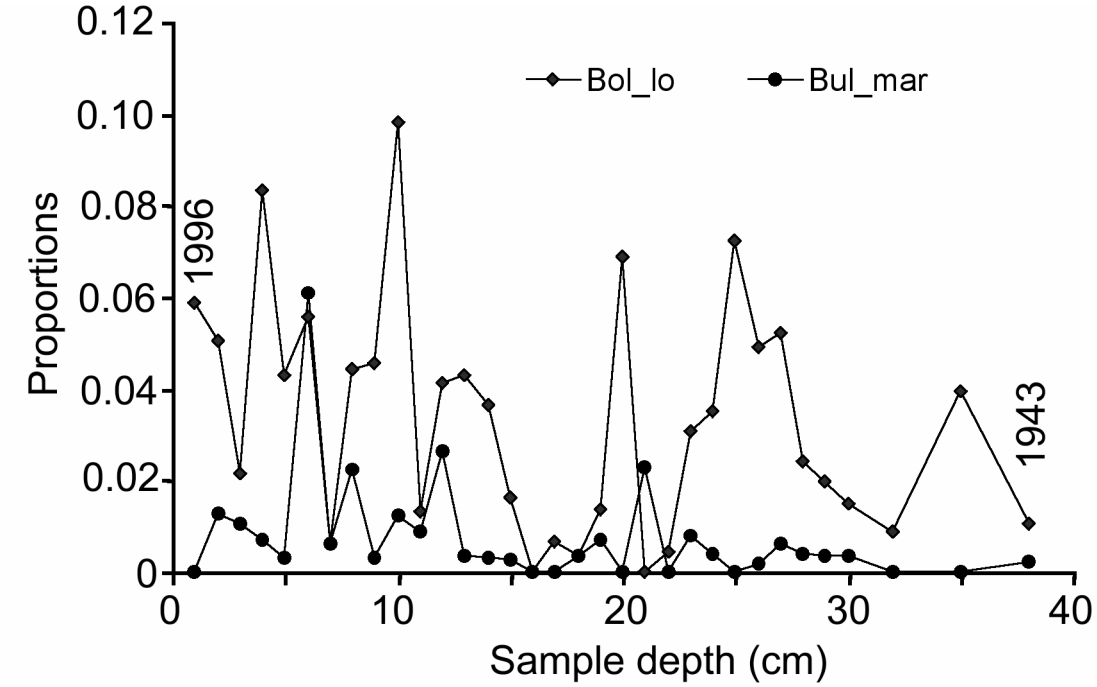

Figure 5.6. Distribution of relative abundances of *Bulimina marginata, Cancris sagra, Fursenkoina pontoni, Saccammina diflugiformis, and Uvigerina hispido-costata* in core E60.

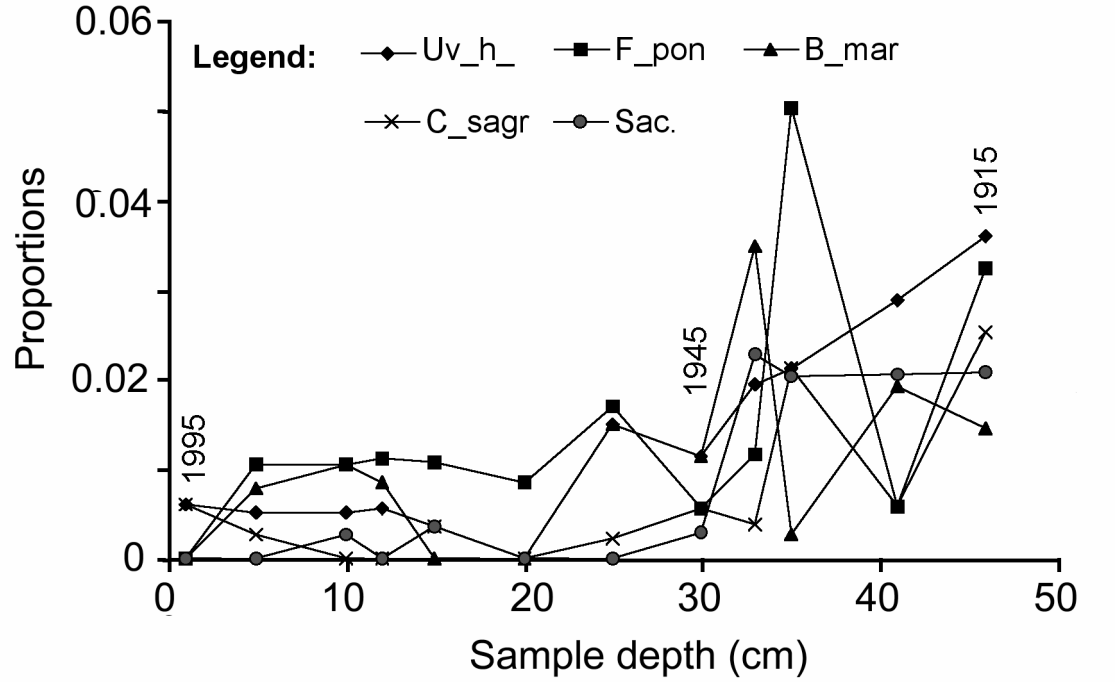

Figure 5.7. Distribution of relative abundances of *Bulimina marginata and Bolivina lowmani* in core F35.

Quinqueloculina

For the time periods represented by the two cores, *Quinqueloculina* is a minor taxon with persistent stratigraphic trends (Figure 5.8). At station E60, it was present in very low numbers before 1943, but absent later. At the shallower F35 station, *Quinqueloculina* is sporadically present, reaching a proportion of about 0.03 in 1943 and proportions between 0.003 and 0.01 in the post 1975 period; it was absent in the 1948-1975 time interval.

Agglutinated and Porcelaneous Groups

Foraminiferal orders with agglutinated shells (Astrorhizida, Lituolida, Textulariida) and porcelaneous shells (Miliolida, which includes the genus *Quinqueloculina*) suffered a decline, or even disappeared, in water depths between 35 and 60 m during the past century on this shelf. At E60, the proportion of the agglutinated group dropped from 0.08 in 1915 to 0.006 in 1943, whereas that of the porcelaneous group declined from 0.06 to 0.003 during the same time span (Figure 5.9). During the subsequent period, up to 1997, both groups were extremely rare or absent at this site. The historical record of benthic Foraminifera at F35 m is shorter than the one at E60, but reduced proportions of agglutinated and porcelaneous taxa are still apparent (Figure 5.10). Here the proportion of agglutinated taxa was 0.06 in 1943, but zero during the 1990s, whereas that of porcelaneous taxa was about 0.04 in 1943 and, with one exception, also zero for the 1990s.

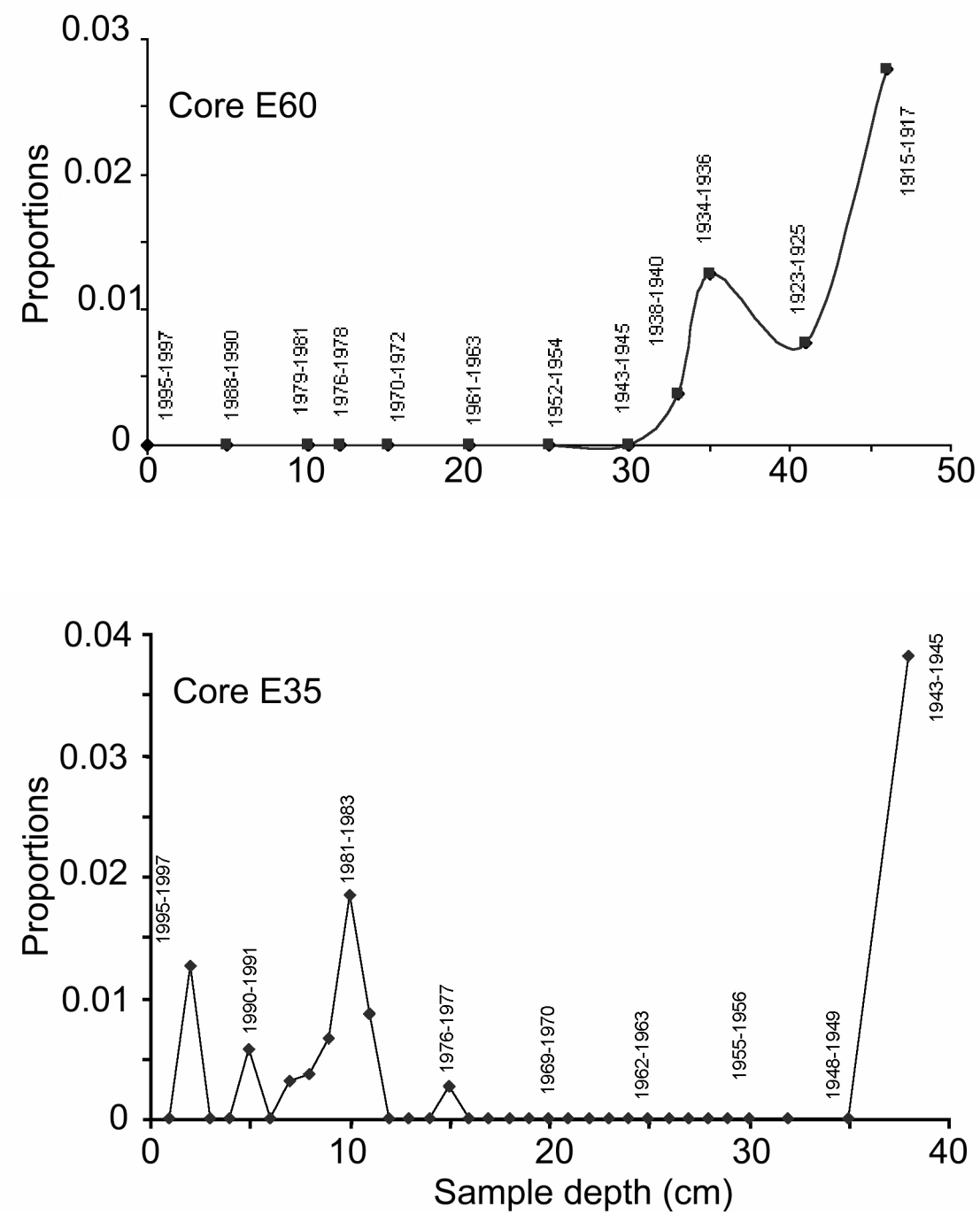

Figure 5.8. Distribution of relative abundances of *Quinqueloculina*. Top, core E60; bottom, core E35.

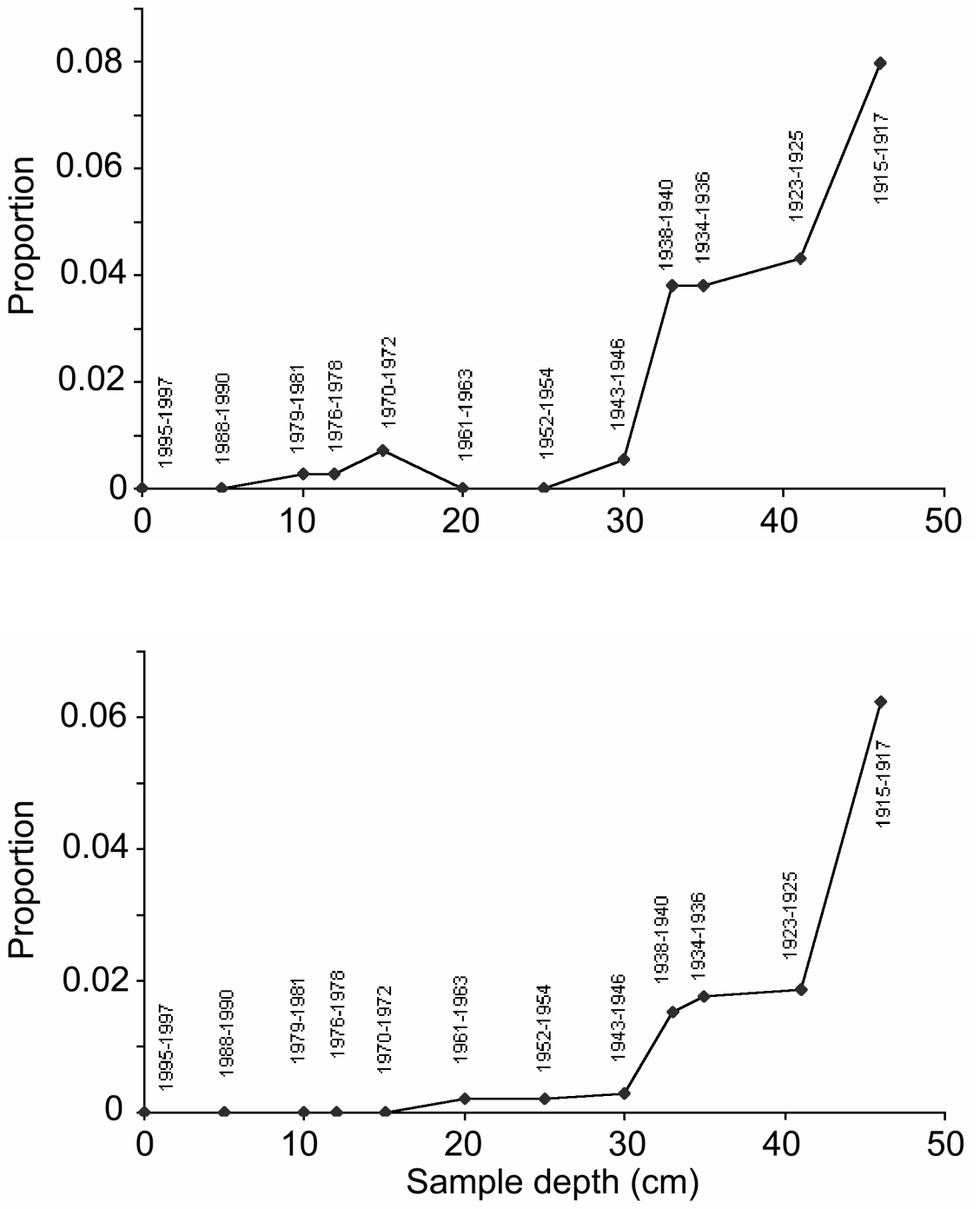

Figure 5.9. Distribution of relative abundances of agglutinated (top) and porcelaneous (bottom) species groups, core E60.

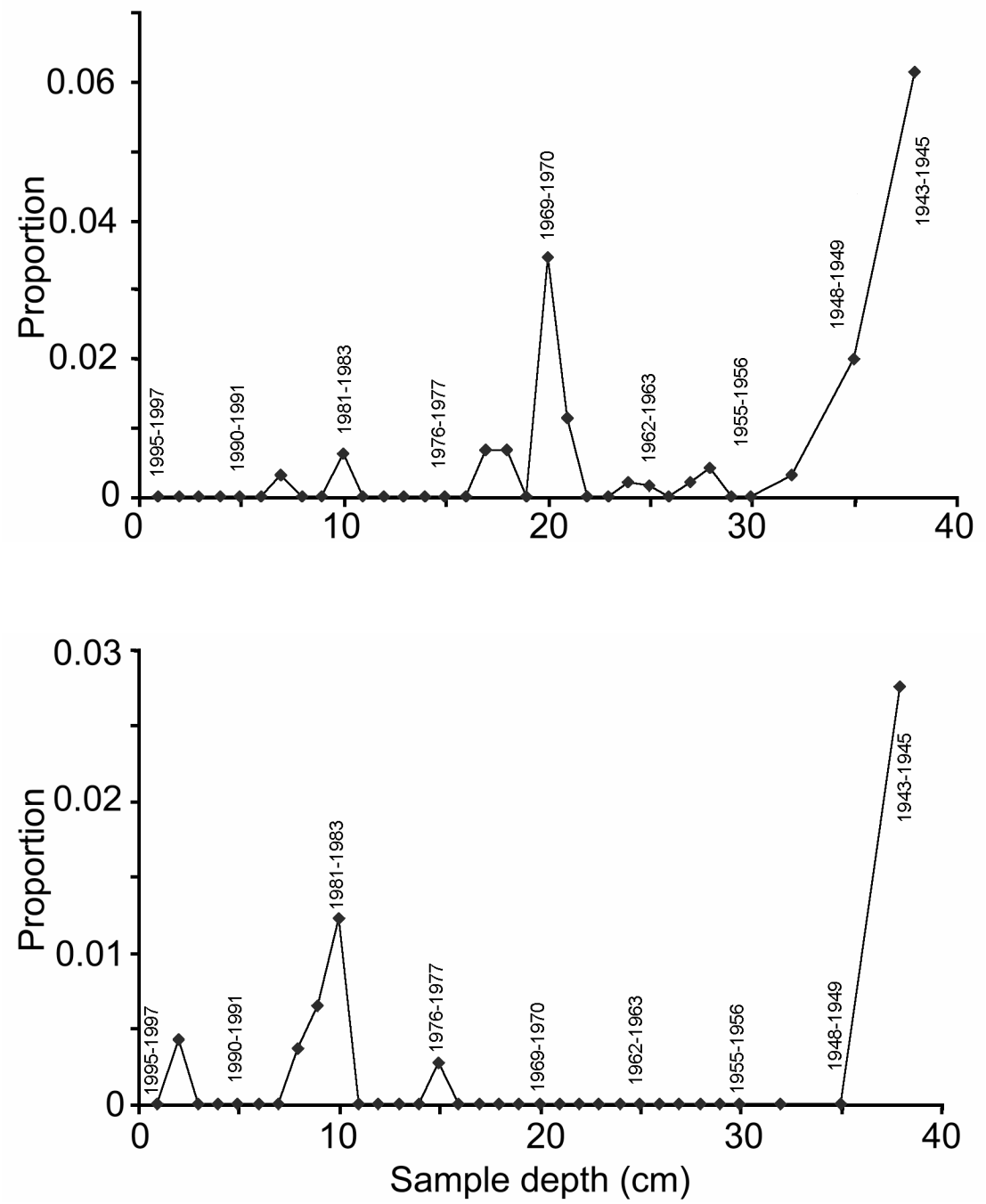

Figure 5.10. Distribution of relative abundances of agglutinated (top) and porcelaneous (bottom) species groups, core F35.

Community Change

A Cluster Analysis (CA) procedure was applied to foraminiferal data from E60 and F35. In addition, Principal Components Analysis (PCA) was used in the analysis of the E60 data. Three main clusters are present (Figure 5.11). They correspond to the intervals 1915-1936, 1938-1978 and 1979-1997, and thus agree well with the distribution trend of the species richness. Major changes in the benthic foraminiferal assemblage at this location took place within the 1936-1938 and 1978-1979 intervals.

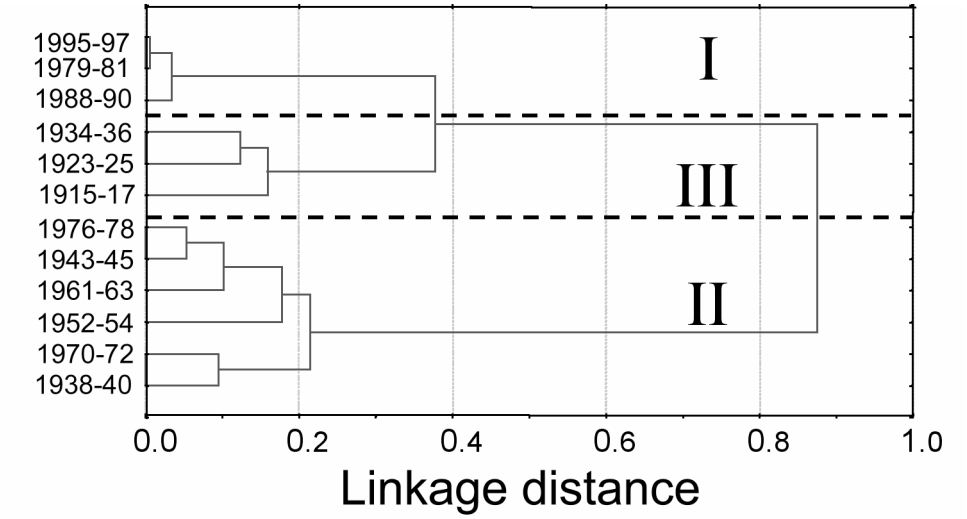

Figure 5.11. Cluster analysis of E60 foraminiferal data; dendrogram for 12 cases. Linkage procedure, Ward's Method; correlation coefficient, Euclidean distance.

The cluster diagram for F35 core data (Figure 5.12) shows no meaningful major clusters of the samples. It is noticeable that temporally successive samples representing the 1970-1975 time interval belong to an isolated cluster whose distance from the other clusters is relatively large. This is due to a very low representation of minor components in the 4 samples of the 1970-1975 cluster. The core-bottom (1943) sample whose high species richness makes it different from the rest of the F35 samples has an anomalous placement within the dendrogram. The numerical similarity between this sample and others in the same cluster (1959, 1960, 1977) is caused by the absence of certain species rather than by a very similar species content. Overall, the lack of any meaningful clustering of the foraminiferal data of F35 is partly due to the short time interval covered by the analyzed samples. However, as shown by species richness, a shift in the benthic foraminiferal content could have taken place prior to 1948. A longer stratigraphic record is needed in order to better determine when such a shift occurred.

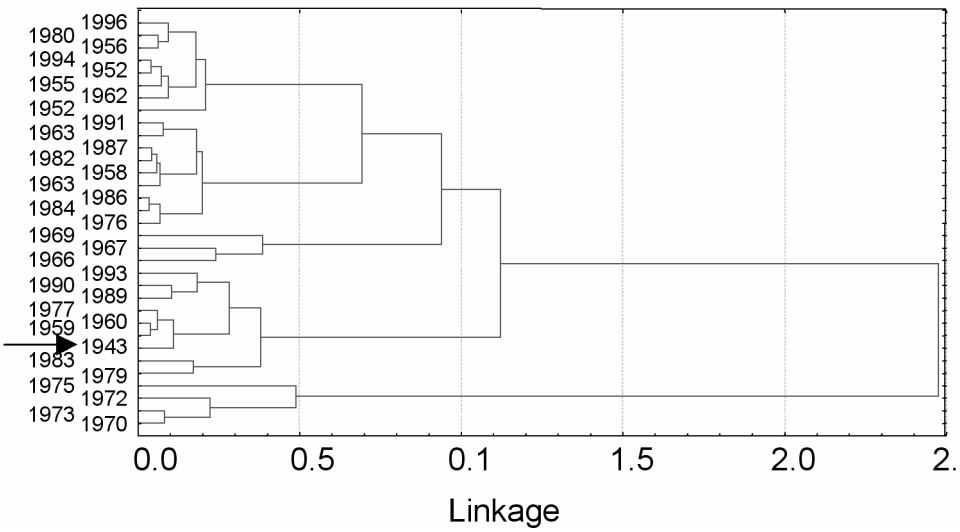

Figure 5.12. Cluster analysis of F35 foraminiferal data; dendrogram for 33 cases. Linkage procedure, Ward's Method; correlation coefficient, Euclidean distance. The arrow points to the core-bottom sample whose species richness differentiates it from the rest of the samples.

The scree plot of eigenvalues for the E60 data (Figure 5.13) reveals two significant factors that account for 64.7% of the total variance. However, given the relatively high proportion of variance (14.8%) explained by a third factor, that too was considered. As seen in Table 5.1, factor 1 accounts for almost half (46.7%) of the total variance and its "major parameters" (Table 5.2) are *Nonionella basiloba, Uvigerina hispido costata*, *Fursenkoina pontoni*, *Cancris sagra*, the agglutinated group, *Pyrgo*, and other porcelaneous taxa including *Quinqueloculina* and *Triloculina* (Q/T – ina). Factor 2 accounts for 18% of total variance. Significant loadings onto factor 2 are those of *Buliminella morgani* and *Epistominella vitrea*. Within factor 3, *Bulimina marginata*, *Bolivina lowmani*, and other species of *Bolivina* (*B.* spp), show significant loadings (Table 5.2). Thus, most of the variability in the data set is due to changes in the stratigraphic distribution of the agglutinated and porcelaneous taxa, and a few hyaline taxa. It is noticeable that in E60, *Buliminella morgani*, perhaps the most opportunistic species in the area of seasonal hypoxia of northwestern Gulf of Mexico (Blackwelder et al. 1996; Platon and Sen Gupta 2001), has a significant loading onto factor 2 which accounts for 18% of the total variance. Plots of loadings onto factor 1, 2, and 3 (Figures 5.14 and 5.15) reveal similar behavior of the data on *Fursenkoina pontoni*, *Cancris sagra*, *Uvigerina hispido-costata,* the agglutinated species group, the *Quinqueloculina-Triloculina* group, and *Pyrgo*. The data on *Nonionella basiloba* behave the opposite way.

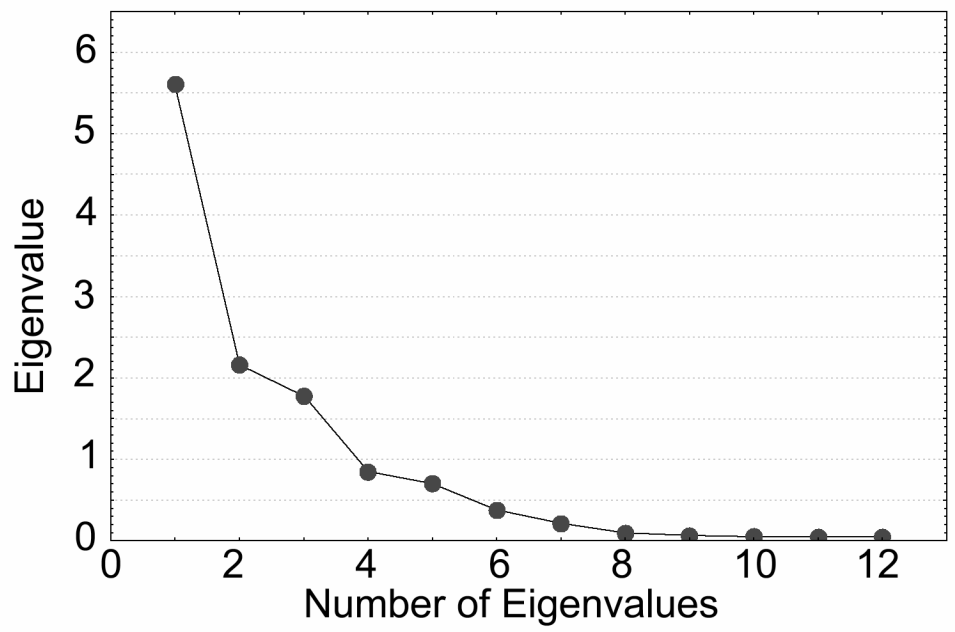

Figure 5.13. Eigenvalues scree plot for E60 foraminiferal data. Arrow marks a significant change in slope of curve and indicates the presence of two significant factors.

Table 5.1

Eigenvalues for E60 foraminiferal data. Extraction: principal components.

Factor	Eigenval	Variance	Eigenval	%
1	5.6070398	46.725332	5.6070398	46.725
2	2.1608055	18.006713	7.7678454	64.732
3	1.7773271	14.811059	9.5451724	79.543

Table 5.2

Factor loadings for 12 foraminiferal taxa in core E60.
Rotation: normalized Varimax; extraction: principal components.

Taxa	Factor 1	Factor 2	Factor 3
N. basiloba	**-0.71051**	0.3475779	0.0676453
E. vitrea	0.1329909	**0.7868568**	-0.250877
B. morgani	-0.066129	**-0.947769**	-0.102249
U. hispido costata	**0.7395553**	0.1880553	0.5665451
F. pontoni	**0.7402202**	0.2667797	-0.219597
B. marginata	0.0028491	0.4325385	**0.7023258**
C. sagra	**0.9486338**	-0.040595	0.0333846
B. lowmani	-0.026707	0.2134872	**-0.770596**
B. spp.	0.3590785	-0.281262	**0.7904396**
Agglutinated	**0.8520473**	0.2180553	0.3812768
Pyrgo	**0.7512396**	0.1741379	0.5153114
Q/T - ina	**0.8778652**	0.0941215	0.3418745
Expl.Var	4.7123098	2.1449108	2.6879519
Prp.Totl	0.3926925	0.1787426	0.223996

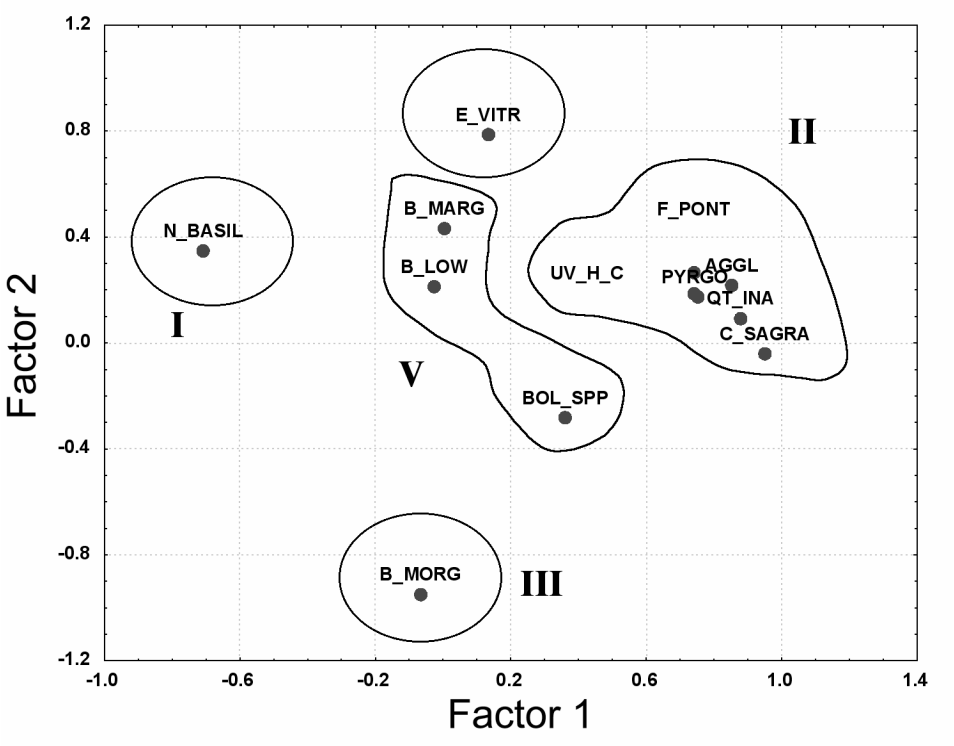

Figure 5.14. Factor loadings, Factor 1/Factor 2 core E60.

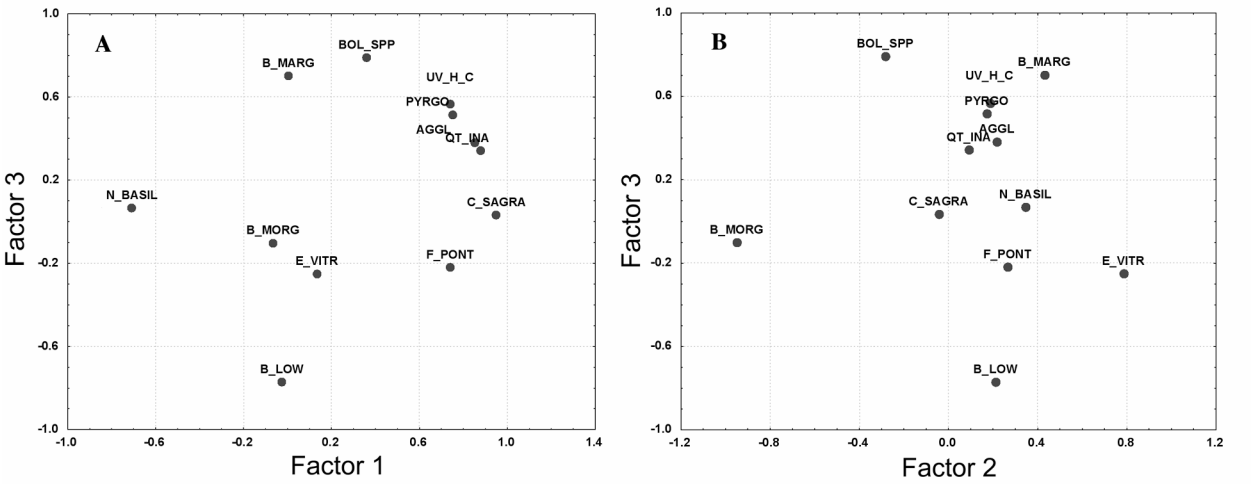

Figure 5.15. Factor loadings, Factor 1/Factor3 (A) and Factor 2/Factor 3 (B), core E60.

Figure 5.16 depicts the temporal distribution of factor 1 and factor 2 scores (data in Table 5.3). A change from positive to negative values of factor 1 scores took place after 1938. This trend is related to the reduced abundances or even disappearance of taxa with positive scores in younger sediments (Table 5.2). The factor 2 scores vary less in time. A very negative value of the score calculated for the core-top sample is due to the high abundance of *Buliminella morgani* associated with reduced proportions of *Epistominella vitrea* and *Nonionella basiloba*.

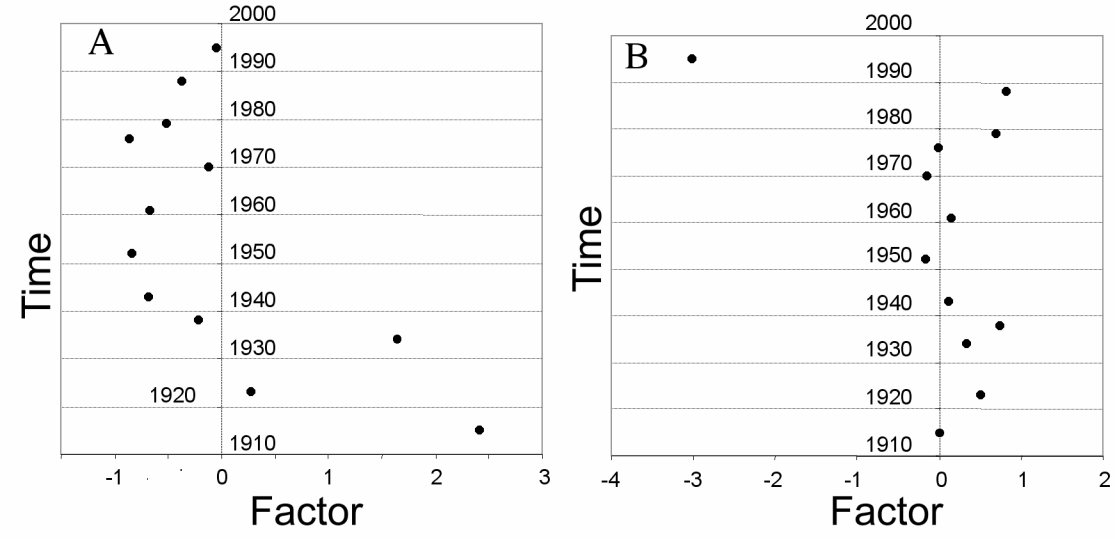

Figure 5.16. Plots of factor scores against time, core E60. A, Factor 1. B, Factor 2.

Table 5.3

Factor scores for 12 samples in core E60.

Obs.	Factor 1	Factor 2	Factor 3
1	-0.048191	-3.023071	-0.121067
2	-0.368304	0.8202798	-1.051938
3	-0.520913	0.6882466	-0.465986
4	-0.85864	-0.016316	0.2509972
5	-0.12036	-0.152501	-1.422886
6	-0.670037	0.141852	-0.56499
7	-0.840622	-0.160083	1.1244943
8	-0.68357	0.1101386	0.4775404
9	-0.211689	0.7416906	0.9235517
10	1.6443484	0.3358802	-1.535607
11	0.2702164	0.5065064	1.2350393
12	2.4077612	0.0073767	1.1508508

Additional Data

Published data (Blackwelder et al. 1996; Rabalais et al. 1996, Sen Gupta et al. 1996) from two cores from shallower sites in the study area (Figure 5.1; BL10 and G27, water depths 29 m and 27 m, respectively) were also examined and analyzed for comparison with data from F35 and E60. Figure 5.17 depicts the temporal distribution of the relative abundance of *Quinqueloculina* in G27. Its historical decline and its disappearance in the1890s suggests a progressively worsened environmental condition for this genus. Trends similar to those observed in the E60 and G27 data have been noticed by Blackwelder et al. (1996) in BL10. They report a decreasing trend for both the pocelaneous and agglutinated groups.

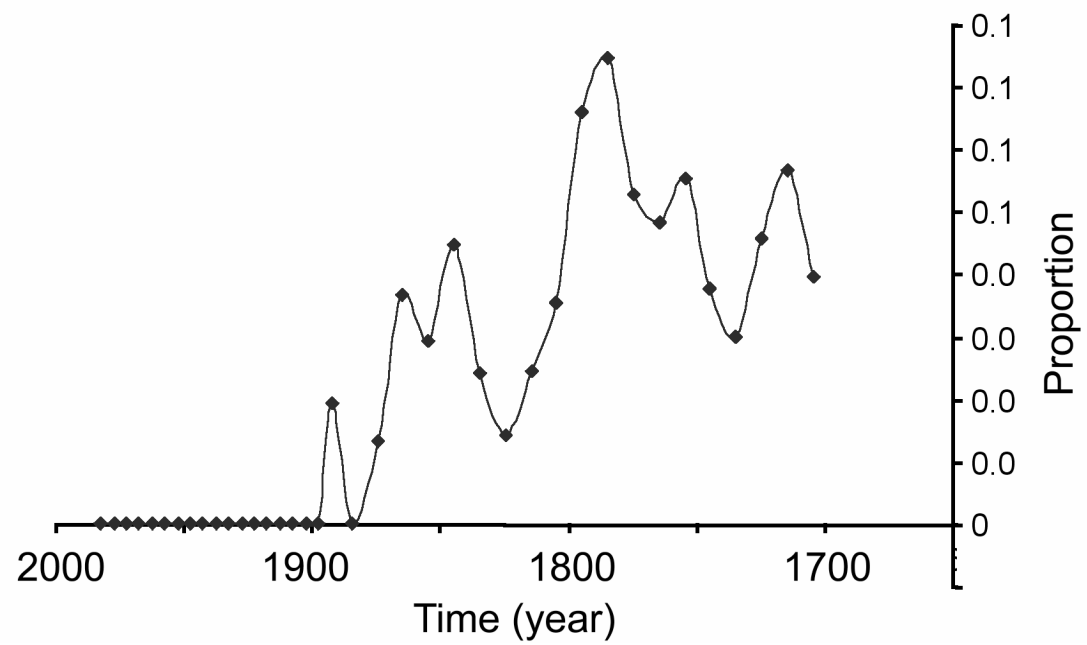

Figure 5.17. Distribution of relative abundance of *Quinqueloculina*; core G27.

The raw foraminiferal data of Blackwelder et al. (1996) were subjected to multivariate analyses (CA and PCA). The results of this CA are depicted in Figure 5.18. Two major clusters, placed at a relatively large linkage distance one from another, suggest a major change in the foraminiferal assemblage taking place in late 1940s or early 1950s.

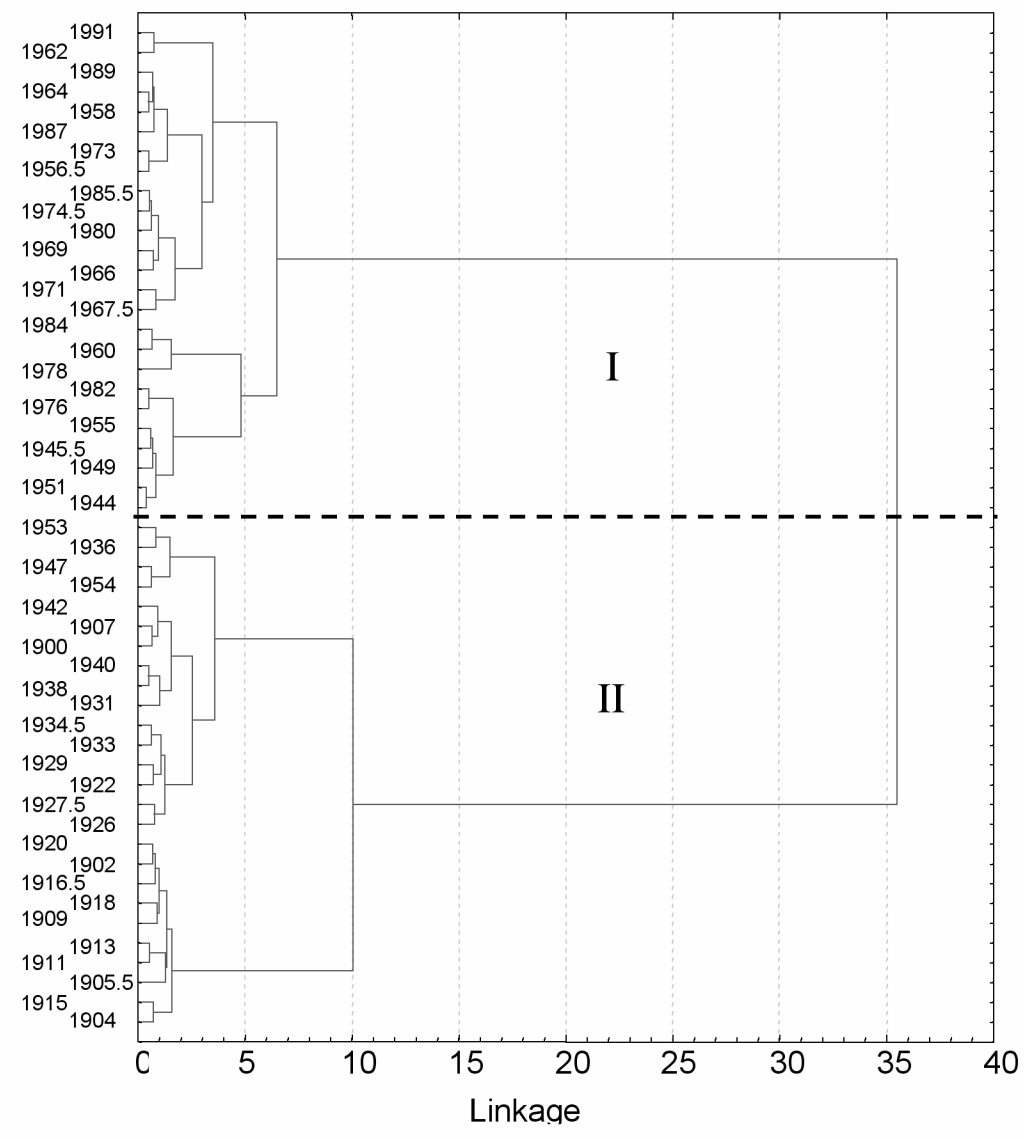

Figure 5.18. Cluster analysis of BL10 core data, dendrogram for 51 cases. Linkage procedure, Ward's Method; correlation coefficient, Euclidean distance.

Successive runs of PCA against foraminiferal data from BL10 core revealed the existence of four factors that explain 68.32% of the total variance, the first two factors accounting for 50.26% of the variance (Table 5.4). Important high loadings of considered variables (foraminiferal species) on factor 1 are those of *Buliminella morgani, Nonionella opima*, *Quinqueloculina tanagos*, *Bigenerina irrelgularis*, *Textularia mayori*, and *Quinqueloculina horrida* (Table 5.5). Among loadings on factor 2, those of *Buliminella morgani, Epistominella vitrea*, *Ammonia parkinsoniana*, *A. pauciloculata*, *Nonionella atlantica,* and *Pyrgo nasutus* show significant (> 0.6) values. Noticeable loads in the next two sets of loadings include those of *Epistominella vitrea, Hanzawaia concentrica* (factor 3), and *Ammonia parkinsoniana typica* (factor 4). [Taxonomic note: "*Ammonia pauciloculata*" of Blackwelder et al. (1996) may have been

included within *A. parkinsoniana* in this study, because the distinction is subtle and controversial.]

Table 5.4

Eigenvalues for BL10 foraminiferal data (raw data from Blackwelder et al. 1996). Extraction: principal components.

Factor	Eigenval	% total Variance	Cumululative .Eigenval	Cumululative %
1	6.975127	38.75071	6.975127	38.75071
2	2.071704	11.50947	9.046831	50.26017
3	1.659239	9.217992	10.70607	59.47817
4	1.591264	8.840354	12.29733	68.31852

Table 5.5

Factor loadings for 18 foraminiferal species from core BL10 (raw data from Blackwelder et al. 1996). Rotation: normalized Varimax; extraction: principal components.

Species	**Factor 1**	**Factor 2**	**Factor 3**	**Factor 4**
B. morgani	**-0.64443**	**-0.67949**	-0.04239	-0.09684
E. vitrea	0.008331	**-0.69939**	**-0.60564**	0.023484
E. gunteri	0.218805	0.47532	0.55822	0.041476
B. lowmani	-0.14123	0.337416	-0.58652	0.040451
A. parkinsoniana	0.220137	**0.820384**	-0.18493	0.132664
N. opima	**-0.85387**	0.161868	0.02265	0.179732
A. pauciloculata	0.281875	**0.696989**	0.051267	0.031923
N. atlantica	-0.05035	**0.761433**	0.122944	-0.0019
H. concentrica	0.239366	0.15558	**0.762594**	0.039075
A. parkinsoniana typica	-0.13212	-0.22732	0.392379	-0.6875
Q. tanagos	**0.803254**	0.232209	0.123191	-0.00185
P. nasutus	0.523701	**0.67358**	0.1062	-0.11404
Q. bicarinata	0.398886	0.527317	0.05401	-0.31529
Q. poeyanum	0.138989	0.331983	-0.03012	**-0.66056**
B. irregularis	**0.729607**	0.156321	0.258504	0.194536
T. mayori	**0.714906**	0.423283	0.329993	0.099306
D. compressa	0.199352	0.164346	0.378003	**0.652702**
Q. horrida	**0.658773**	0.355881	0.294589	0.267591
Expl.Var	4.032517	4.384495	2.247846	1.632476
Prp.Totl	0.224029	0.243583	0.12488	0.090693

Significant Stratigraphic Trends and Interpretations

Relationship with Contaminant Loading

Data on chemical contaminants are available for both F35 and E60 (Overton et al., this report). In F35, PAH peaks are at 26-30 cm (years 1956-1962) and 16-20 cm (1970-1975); an organochlorine (OC) pesticide peak is also present at 16-20 cm, but not at 26-30 cm. In E60, both the PAH and OC pesticide high values (not necessarily peaks) are in the oldest sample (46-47 cm, 1915-1917). We compared the stratigraphic locations of these contaminant peaks or high values with low and high values of foraminiferal parameters in the same cores (but different subcores).

In F35, the foraminiferal diversity trends (species richness and Shannon-Wiener function) do show a dip in the 16-20 cm section, within a relatively steady (but noisy) post-1945 pattern. The relative abundances of two dominant species (*Bolivina lowmani and Bulimina marginata*) also show this dip, but in addition, they show comparable dips at levels where neither PAH nor OC pesticides show any conspicuous shift. The A-E index shows a dip at 17-18 cm, but, as explained earlier, this index shows erratic shifts in F35 because of very low absolute abundances of these two taxa. The agglutinated group shows a peak in relative abundance (after the initial decline) at 20 cm, but this is a computing artifact, due to the fact that the much larger calcareous group was reduced at this level (reflected in the overall diversity drop). The porcelaneous group is absent in the large 16-35 cm interval.

In E60, various foraminiferal parameters show a decline from the oldest sample, but we cannot ascertain when the decline began, and the values (of diversity, several dominant species, and agglutinated and porcelaneous groups) are much lower at younger levels. So the PAH and OC pesticide high values in this sample do not imply a link with foraminiferal parameters. In any case, even the highest values of PAH in E60 (~30 ng g^{-1}) is rather low when compared to the values in F35. In contrast, the maximum OC pesticide value in E60 is higher than any in F35. Judging by the highest values of PAH in three other cores (500-1200 ng g^{-1} in D50G, D80, G40), however, even the highest values of PAH in both F35 (70 ng g^{-1}) and E60 (30 ng g^{-1}) are modest. (The PAH measure for the 16-20 cm segment, where some foraminiferal parameters show a decline, is only 37 ng g^{-1}.) The same inference can be made regarding the highest values of OC pesticides in F35 (35 ng g^{-1}) and E60 (80 ng g^{-1}) when comparisons are made with the highest values in cores in D80, E30, and G50 (2000-3500 ng g^{-1}).

Thus, the distributions of chemical and foraminiferal data from F35 and E60 suggest either a minor effect (in F35, 1970-1975 levels) or (more likely) no traceable effect of chemical contaminants on the historical change in foraminiferal assemblages. We did not find any deformed shells of benthic Foraminifera in our samples, as has been reported for coastal environments with severe chemical (especially metal) pollution (Yanko et al. 1999).

Relationship with Seasonal Hypoxia

Change of foraminiferal species diversity as a consequence of spatial or temporal environmental change is frequently reported in the literature (e.g., Bandy et al. 1964a; 1964b; Sen Gupta and Kilbourne 1974; Alve 1990 1995; Nelsen et al. 1994; Jannink et al. 1998). Both species richness

and Shannon-Wiener Index decreased from older to younger samples in F35 and E60. This suggests a possible connection with worsening seasonal hypoxia in the study area, as has been previously reported for the *Ammonia-Elphidium* (A-E) Index (Sen Gupta et al. 1996). This A-E Index becomes rather erratic or meaningless in deeper (>30 m) shelf waters, because the paucity or absence of these two taxa in these water depths. Thus, the trend of the A-E Index in F35 cannot be confidently interpreted as a clear proxy signal of progressive seasonal hypoxia, although persistently high values (80-100%) are confined to the youngest time interval (1981-1997).

Several other foraminifers commonly reported from this area seemingly tolerate oxygen deficiency, and prefer organic rich sediments in other marine areas. These taxa include *Bulimina marginata* (Bandy et al. 1964b), *Uvigerina peregrina* (Miller and Lohman 1982; Lutze 1980; Van der Zwaan et al. 1986), *Bolivina lowmani* (Bizon and Bizon 1984), *Fursenkoina* (Seiglie 1968, 1971), *Nonionella* (Seiglie 1968; Sen Gupta and Machain-Castillo 1993; Bernhard and Sen Gupta 1999), *Cancris* (Seiglie 1968; Jonkers 1984; Van der Zwaan and Jorissen 1991), *Epistominella* (Verhallen 1997), and *Buliminella* (Bandy et al. 1964a, b 1965). In a previous study (Platon and Sen Gupta 2001), we showed that *Buliminella morgani* dominates living assemblages of benthic Foraminifera from the sediment-water interface down to a substrate depth of 5-10 cm, possibly in severely dysoxic, or even anoxic, microhabitats. Given this adaptation, it is expected that the biostratigraphical record would reveal an increasing trend in relative abundances of *Buliminella morgani* as a consequence of progressive hypoxia, which is indeed the case.

Laboratory experiments on foraminiferal subsurface activity under oxygen-stress conditions suggest that the miliolid *Quinqueloculina* prefers oxic environments and has the ability of moving away from the anoxic sediment layers (Moodley et al. 1998). In both F35 and E60, *Quinqueloculina* is absent or virtually absent after 1945, which may indicate the attainment of a critical threshold of hypoxia, in intensity or duration.

Results of cluster analysis of the E60 data bring further insight into foraminiferal responses to progressive seasonal oxygen depletion on the Louisiana shelf. Three stratigraphically-separated assemblages (for 1915-1936, 1938-1978 and 1979-1997 time intervals, marked by reduction of species diversity and increase in species dominance, can be recognized in core E60. This pattern agrees with the three-stage foraminiferal assemblage evolution under seasonal hypoxia suggested by Blackwelder et al. (1996) for the BL10 core. Furthermore, cluster analysis of published data from BL 10 (Blackwelder et al. 1996) reveals a significant change in foraminiferal composition in the middle of the 20th century.

SUMMARY AND CONCLUSIONS

Various aspects of the numerical data on foraminiferal distribution in cores F35 and E60— diversity, relative abundances of key species, and sample groupings identified by cluster and factor analysis— indicate progressive changes from the oldest to the youngest stratigraphic level. For E60, which covers a longer time span (1915-1997) than F35 (1943-1997), the diversity measures (species richness and Shannon-Wiener index) and the cluster pattern indicate

significant changes in the foraminiferal assemblage in between the 1915-1936, 1938-1978, and 1979-1997 time intervals, but not within them. These changes are imprinted on a background of overall diversity reduction and dominance increase.

No unequivocal relationship could be detected between contaminant concentration in sediments and composition of the foraminiferal assemblage. The only match between a contaminant high and a diversity low was at the 1970-1975 segment in core F35, and that may indicate a connection, but we note that the values of both PAH (37 ng g^{-1}) and OC pesticides (35 ng g^{-1}) are more than an order of magnitude lower than those recorded in some other cores from the study area. Deformed Foraminifera, one indicator of extreme chemical pollution, are not present in either of the cores.

The overall decline in foraminiferal species diversity and increase in species dominance during the time intervals represented in cores F35 and E60 agree with the results of previous foraminiferal studies of paleohypoxia in the study area. The extreme decline of porcelaneous taxa, especially of *Quinqueloculina,* in the younger parts of the cores also conforms to the results of these earlier studies. The same is true of the increase in the relative abundance of *Buliminella morgani* in F35. The stratigraphic signal of the *Ammonia-Elphidium* index (indicator of nearshore oxygen stress on the Louisiana shelf and elsewhere) is noisy in F35, putatively because of the paucity of these two taxa at the water depth of this site (35 m).

CHAPTER 6

LITERATURE CITED

Abele-Oeschger, D. 1991. Potential of some carotenoids in two recent sediments of Kiel Bight as biogenic indicators of phytodetritus. *Marine Ecology Progress Series* 70:83-92.

Ashton, B.M., R.S. East, M.M. Walsh, M.S. Miles, and E.B. Overton. 2000. Studying and verifying the use of chemical biomarkers for identifying and quantitating oil residues in the environment. U.S. Dept. of the Interior, Minerals Management Service, Gulf of Mexico OCS Region, New Orleans, LA. OCS Study MMS 2000-086.

Alve, E. 1990. Variations in estuarine foraminiferal biofacies within diminishing oxygen conditions in Drammensfjord, SE Norway. In: Hemleben, C., M. Kaminski, W. Kuhnt, and D.B. Scott (eds.). Paloecology, Biostratigraphy, and Taxonomy of Agglutinated Foraminifera, Kluwer, Dordrecht. Pp. 661-694.

Alve, E. 1995. Benthic foraminiferal responses to estuarine pollution: A review. *Journal of Foraminiferal Research* 25:190-203.

Bandy, O.L., J.C. Ingle, Jr., and J.M. Resig. 1964a. Foraminiferal trends, Laguna Beach outfall area, California. *Limnology and Oceanography* 9:112-123.

Bandy, O.L., J.C. Ingle, Jr., and J.M. Resig.1964b. Foraminifera, Los Angeles County outfall area, California. *Limnology and Oceanography* 9:124-137.

Bandy, O. L., J.C. Ingle, Jr., and J.M. Resig.1965. Foraminiferal trends, Hyperion Outfall, California. *Limnology and Oceanography* 10:314-322.

Barrie, A. and S.J. Prosser. 1996. Automated analysis of light-element stable isotopes by isotope ratio mass spectrometry. In: T.W. Boutton and S. Yamasaki (eds.). Mass spectrometry of soils, Marcel Dekker Inc., New York. Pp. 1-46.

Bender, M.E., D.J. Reish, and C.H. Ward. 1979. Rice University Studies. 65(5&6):35-116.

Bernhard, J.M. and B.K. Sen Gupta. 1999. Foraminifera of oxygen depleted environments. In: B.K. Sen Gupta (ed.). Modern Foraminifera, Kluwer Academic Publishers, Dordrecht. Pp. 201-216.

Barber, L.B. and J.H. Writer. 1998. Impact of the 1993 flood on the distribution of organic contaminants in bed sediments of the Upper Mississippi River. *Environmental Science and Technology* 32:2077-2083.

Bianchi, T.S., S. Findlay, and R. Dawson. 1991. Organic matter sources in the water column and sediments of the Hudson River Estuary: The use of plant pigments as tracers. *Estuarine, Coastal and Shelf Science* 36:359-376.

Bianchi, T.S., E. Engelhaupt, P. Westman, T. Andrén, C. Rolff, and R. Elmgren. 2000. Cyanobacterial blooms in the Baltic Sea: Natural or human-induced? *Limnology and Oceanography* 45:716-726.

Bianchi, T.S., C. Rolff, B. Widbom, and R. Elmgren. 2002. Phytoplankton pigments in Baltic Sea seston and sediments: Seasonal variability, fluxes and transformations. *Estuarine, Coastal and Shelf Science* 55:369-383.

Bizon, G. and J.J. Bizon. 1984. Distribution des foraminifères sur le plateau continental au large du Rhone. In: Bizon, J.J. and P.F. Burollet (eds.). Ecologie des microorganismes en Méditeranee occidentale 'ECOMED'. Association Français des Techniciens du Pétrole, Paris. Pp. 84-94.

Blackwelder, P., T. Hood, C. Alvarez-Zarikian, T.A. Nelsen, and B. McKee. 1996. Benthic Foraminifera from the NECOP study area impacted by the Mississippi River plume and seasonal hypoxia. *Quaternary International* 31:19-36.

Boehm, P.D. and J.W. Farrington. 1984. Aspects of the polycyclic aromatic hydrocarbon geochemistry of recent sediments in the Georges Bank region. *Environmental Science and Technology* 18:840-845.

Bricker, S.B. 1993. The history of Cu, Pb, and Zn inputs to Narragansett Bay, Rhode Island as recorded by salt-marsh sediments. *Estuaries* 16:589-607.

Buffan-Dubau, E. and K.R. Carman. 2000a. Diel feeding behavior of meiofauna and their relationships with microalgal resources. *Limnology and Oceanography* 45:381-395.

Buffan-Dubau, E. and K.R. Carman. 2000b. Extraction of benthic microalgal pigments for HPLC analyses. *Marine Ecology Progress Series* 204:293-297.

Cariou-Le Gall, V. and G.F. Blanchard. 1995. Monthly HPLC measurements of pigment concentration from an intertidal muddy sediment of Marennes-Oléron Bay, France. *Marine Ecology Progress Series* 121:171-179.

Carr, R.S., E.R. Long, H.L. Windom, D.C. Chapman, G. Tursby, G.M. Sloane, and D.A. Wolfe. 1996. Sediment quality assessment studies of Tampa Bay, Florida. *Environmental Toxicology and Chemistry* 15:1218-1231.

Chen, N., T.S. Bianchi, B.A. McKee. and J.M. Bland. 2001. Historical trends of hypoxia on the Louisiana shelf: Application of pigments as biomarkers. *Organic Geochemistry* 32:543-561.

Cochran, J.K., D.J. Hirschberg, J. Wang, and C. Dere. 1998. Atmospheric deposition of metals to coastal waters (Long Island Sound, New York, U.S.A.): Evidence from salt marsh deposits. *Estuarine, Coastal and Shelf Science* 46:503-522.

DeMasters, D.J. 1981. The supply and accumlation of silica in the marine environment. *Geochimica et Cosmochimica Acta* 45:1715-1732.

Dortch, Q., R.E. Turner, M.L. Parsons, and N.N. Rabalais. 1999. What is the threat of harmful algal blooms in Louisiana coastal waters? In: Rozas, L.P., J.A Nyman, C.E. Proffitt, N.N. Rabalais, D.J. Reed, and R.E. Turner (eds.). Recent Research in Coastal Louisiana: Natural System Function and Response to Human Influence, Louisiana Sea Grant College Program, Baton Rouge, Louisiana. Pp. 134-144.

Eadie, B.J., B.A. McKee, M.B. Lansing, J.A. Robbins, S. Metz, and J.H. Trefry. 1994. Records of nutrient-enhanced coastal productivity in sediments from the Louisiana continental shelf. *Estuaries* 17:754-765.

Folk, R.L. 1974. Petrology of sedimentary rocks. Austin, Texas: Hemphill Publishing Co. 182 pp.

Goolsby, D.A. and W.E. Pereira. 1995. Pesticides in the Mississippi River. Contaminants in the Mississippi River. U.S. Geological Survey Circular 1133.

Harper, D.E., Jr. and G. Guillen. 1989. Occurrence of a dinoflagellate bloom associated with an influx of low salinity water at Galveston, Texas, and coincident mortalities of demersal fish and benthic invertebrates. *Contributions in Marine Science* 31:147-161.

Hodgson, D.A, S.W. Wright, and N. Davies. 1997. Mass spectrometry and reverse phase HPLC techniques for the identification of degraded fossil pigments in lake sediments and their application in paleolimnology. *Journal of Paleolomnology* 18:335-350.

Hodgson, D.A., S.W. Wright, P.A. Tyler, and N. Davies. 1998. Analysis of fossil pigments from algae and bacteria in merimictic Lake Fidler, Tasmania, and its application to lake management. *Journal of Paleolomnology* 19:1-22.

Jannink., N.T., W.J. Zachariasse, and G.J. Van der Zwaan. 1998. Living (Rose Bengal stained) benthic Foraminifera from Pakistan continental margin (northern Arabian Sea). *Deep-Sea Research I* 45:1483-1513.

Jeffrey, S.W. and R.F.C. Mantoura. 1997. Development of pigment methods for oceanography: SCOR-supported Working Groups and objectives. In: Jeffrey, S.W., R.F.C. Mantoura, and S.W. Wright (eds.). Phytoplankton Pigments in Oceanography: Guidelines to Modern Methods. Paris: UNESCO Publishing. Pp. 19-36.

Jeffrey, S.W., R.F.C. Mantoura, and S.W. Wright (eds.). 1997. Phytoplankton pigments in oceanography: Guidelines to modern methods. Paris: UNESCO Publishing. 638 pp.

Jonkers, H.A. 1984. Pliocene benthic Foraminifera from homogenous and laminated marls on Crete. Utrecht *Micropaleontological Bulletins* 31:1-179.

Justic', D., N.N. Rabalais, R.E. Turner, and W.J. Wiseman, Jr. 1993. Seasonal coupling between riverborne nutrients, net productivity and hypoxia. *Marine Pollution Bulletin* 26:184-189.

Justic', D., N.N. Rabalais, and R.E. Turner. 1996. Effects of climate change on hypoxia in coastal waters: A doubled CO_2 scenario for the northern Gulf of Mexico. *Limnology and Oceanography* 41:992-1003.

Kelly, T., D. Buckingham, C. DiFrancesco, K. Porter, T. Goonan, J. Sznopek, C. Berry, and M. Crane. 2001. Historical statistics for mineral commodities in the United States. USGS Open-File Report 01-006. Internet Website at http://minerals.usgs.gov/minerals/pubs/of01-006/

Klein B. and C. Riaux-Gobin. 1991. Algal pigment diversity in coastal sediments from Kerguelen (sub-Antarctic Islands) reflecting local dominance of green algae, euglenoids and diatoms. *Polar Biology* 11:439-448.

Laska, A.L., C.K. Bartell, and J.L. Laseter. 1976. Distribution of hexachlorobutadiene in water, soil and selected aquatic organisms along the Lower Mississippi River, Louisiana. *Bulletin of Environmental Contamination and Toxicology* 15:535-542.

Leavitt, P.R. 1993. A review of factors that regulate carotenoid and chlorophyll deposition and fossil pigment abundance. *Journal of Paleolimnology* 9:109-127.

Lutze, G.F. 1980. Depth distribution of benthic foraminifera on the continental margin off NW Africa. 'Meteor' *Forschungs-Ergebnisse, Reihe C*. 32:31-80.

Meade, R.H. (ed.). 1995. Contaminants in the Mississippi River, 1987-1992. U.S. Geological Survey Circular 1133. U.S. Dept. of the Interior, Geological Survey, Denver, Colorado.

Miller, K.G. and G.P. Lohmann. 1982. Environmental distribution of Recent benthic Foraminifera on the northeast United States continental slope. *Geological Society of America Bulletin* 93:200-206.

Moodley, L., G.J. Van der Zwaan, M.W. Rutten, R.C.E. Boom, and L. Kempers. 1998. Subsurface activity of benthic Foraminifera in relation to porewater oxygen content: laboratory experiments. *Marine Micropaleontology* 34:91-106.

Murray, H.E., L.E. Ray, and C.S. Giam. 1981. Analysis of marine sediment, water and biota for selected organic pollutants. *Chemosphere* 10(11/12):1327-1334.

National Research Council. 2003. Oil in the sea III: Inputs, fates, and effects. Ocean Studies and Marine Board, Divisions of Earth and Life Studies and Transportation Research Board, NRC. Washington, DC: National Academy Press.

Nelsen, T.A., P. Blackwelder, T. Hood, B. McKee, N. Romer, C. Alvarez-Zarikian, and S. Metz. 1994. Time-based correlation of biogenic, lithogenic and authigenic sediment components with anthropogenic inputs in the Gulf of Mexico NECOP study area. *Estuaries* 17:873-885.

Nichols, B.W. 1973. Lipid composition and metabolism. In: Carr. N.G. and B.A. Whitton (eds.). The Biology of Blue-green Algae, Blackwells, Oxford. Pp. 144-161.

Nittrouer, C.A., R.W. Strernberg, R. Carpenter, and T. Bennett. 1979. The use of Pb-210 geochronology as a sedimentological tool: Application to the Washington continental shelf. *Marine Geology* 31:297-316.

Overton, E.B., M.H. Schultz, K.M. St. Pé, and C. Byrne. 1986. Distribution of trace organics, heavy metals, and conventional pollutants in Lake Pontchartrain, Louisiana. Organic Marine Geochemistry, Chapter 15.

Parsons, M.L., Q. Dortch, and R.E. Turner. 2002. Sedimentological evidence of an increase in *Pseudo-nitzschia* (Bacillariophyceae) abundance in response to coastal eutrophication. *Limnology and Oceanography* 47:551-558.

Philip, R.P. and J.N. Oung. 1988. Biomarkers: Occurrence, utility and detection. *Analytical Chemistry* 60:887A-896A.

Platon, E. and B.K. Sen Gupta. 2001. Foraminiferal communities of oxygen-stressed environments on the Louisiana continental shelf. In: Rabalais, N.N. and R.E. Turner. (eds.). Coastal Hypoxia: Consequences for Living Resources and Ecosystems. Coastal and Estuarine Studies 58. American Geophysical Union, Washington, DC. Pp. 147-163.

Rabalais, N.N., R.E. Turner, D. Justic´, Q. Dortch, W.J. Wiseman, Jr., and B.K. Sen Gupta. 1996. Nutrient changes in the Mississippi River and system responses on the adjacent continental shelf. *Estuaries* 19:386-407.

Rabalais, N.N., R.E. Turner, and D. Scavia. 2002a. Beyond science into policy: Gulf of Mexico hypoxia and the Mississippi River. *BioScience* 52:129-142.

Rabalais, N.N., R.E. Turner, and W.J. Wiseman, Jr. 2002b. Hypoxia in the Gulf of Mexico, a.k.a. "The Dead Zone." *Annual Review of Ecology and Systematics* 33:235-263.

Rabalais, N.N., R.E. Turner, Q. Dortch, D. Justic', V.J. Bierman, Jr., and W.J. Wiseman, Jr. 2002c. Review. Nutrient-enhanced productivity in the northern Gulf of Mexico: past, present and future. *Hydrobiologia* 475/476:39-63.

Ravichandran, M., M. Baskaran, P.H. Santschi, and T.S. Bianchi. 1995. History of trace metal pollution in Sabine-Neches estuary, Beaumont, Texas. *Environmental Science and Technology* 29:1495-1503.

Reich, A.R., J.L. Perkins, and G. Cutter. 1986. DDT contamination of a north Alabama aquatic ecosystem. *Environmental Toxicology and Chemistry* 5:725-736.

Riaux-Gobin, C., C.A. Llewellyn, and B. Klein. 1987. Microphytobenthos from two subidal sediments from North Brittany. II. Variations of pigment compositions and concentrations determined by HPLC and conventional techniques. *Marine Ecology Progress Series* 40:275-283.

Rose, G.J. 1963. Crop Protection. New York, NY: Chemical Publishing Co., Inc.

Rowe, G.T. and R.E. Turner. 1989. Minerals Management Planning Workshop Report: Texas-Louisiana Marine Ecosystem Study. U.S. Department of the Interior, Minerals Management Service, Gulf of Mexico OCS Region, New Orleans, LA.

Santschi, P.H., B.J. Presley, T.L. Wade, B. Garcia-Romero, and M. Baskaran. 2001. Historical contamination of PAHs, PCBs, DDTs, and heavy metals in Mississippi River Delta,

Galveston Bay and Tampa Bay sediment cores. *Marine Environmental Research* 52:51-79.

Sassen, R., H. Roberts, A.V. Milkov, and D.A. DeFreitas. 2001. Sea floor vents, seeps, and gas hydrate: Relation to flux rate from the deep Gulf of Mexico petroleum system. 21st annual Bob F. Perkins Research Conference Program and Abstracts, Gulf Coast Section Society of Economic Paleontologists and Mineralogists Foundation.

Scavia, D., N.N. Rabalais, R.E. Turner, D. Justic', and W.J. Wiseman, Jr. 2003. Predicting the response of Gulf of Mexico hypoxia to variations in Mississippi River nitrogen load. *Limnology and Oceanography* 48:951-956.

Seiglie, G.A. 1968. Foraminiferal assemblages as indicators of high organic carbon content in sediments and of polluted waters. *American Association of Petroleum Geologists Bulletin* 52:2231-2241.

Seiglie, G.A. 1971. A preliminary note on the relationships between foraminifers and pollution in two Puerto Rican bays, *Caribbean Journal of Science* 11:93-98.

Sen Gupta, B.K. and R.T. Kilbourne. 1974. Depth distribution of benthic Foraminifera on the Georgia continental shelf. In: Schafer, C.T. and B.R. Pelletier (eds.). First International Symposium on Benthic Foraminifera of Continental Margins, Part A: Ecology and Biology, Maritime Sediments, Special Publication 1. Pp. 25-38.

Sen Gupta, B.K. and M.L. Machain-Castillo. 1993. Benthic foraminifera in oxygen-poor habitats. *Marine Micropaleontology* 20:183-201.

Sen Gupta, B.K., R.E. Turner, and N.N. Rabalais. 1996. Seasonal oxygen depletion in continental-shelf waters of Louisiana: Historical record of benthic foraminifers. *Geology* 24:227-230.

Sun, M.-Y., R.C. Aller, and C. Lee. 1991. Early diagenesis of chlorophyll *a* in Long Island Sound sediments: A measure of carbon flux and particle reworking. *Journal of Marine Research* 49:379-401.

Sun, M.-Y., C. Lee, and R.C. Aller. 1993. Anoxic and oxic degradation of ^{14}C-labeled chloropigments and a ^{14}C-labeled diatom in Long Island Sound sediments. *Limnology and Oceanography* 38:1438-1451.

Thomson, W.T. 1979. Agricultural chemicals: Book I. Insecticides, Acaricides and Ovicides. 1979-80 Revision. Fresno, CA: Thomson Publications.

Treffry J.H, S. Metz, R.P. Trocine, and T.A. Nelsen. 1985. A decline in lead transport by the Mississippi River. *Science* 230:439-441.

Turner, R.E. and N.N. Rabalais. 1994a. Coastal eutrophication near the Mississippi river delta. *Nature* 368:619-621.

Turner, R.E. and N.N. Rabalais. 1994b. Changes in the Mississippi River nutrient supply and offshore silicate-based phytoplankton community responses. In: Dyer, K.R. and R.J. Orth (eds.). Changes in Fluxes in Estuaries: Implications from Science to Management. Fredensborg, Denmark: Olsen & Olsen. Pp. 147-150.

Turner, R.E., N.N. Rabalais, N. Atilla, C. Normandeau, B. Fry, J.J. Lee, C.S. Milan, T.A. Oswald, and E.M. Swenson. 2001. Paleo-reconstruction of water quality in Charlotte Harbor estuary (Florida). Final report to the Southwest Florida Water Management District, Coastal Ecology Institute, Louisiana State University, Baton Rouge, LA. 61 pp. + apps.

U.S. Department of the Interior, Minerals Management Service. 2003. Production Data Online Query. Internet website: http://www.gomr.mms.gov/homepg/fastfacts/production/master.asp (data are in barrels).
U.S. Department of Transportation, Coast Guard. 2003. Oil compendium data. Internet wetsite: http://www.uscg.mil/hq/g-m/nmc/response/stats/C4Data.htm (data are in gallons).
Van der Zwaan, G.J. and F.J. Jorissen. 1991. Biofacial patterns in river-induced shelf hypoxia. In: Tyson, R.V. and T.H. Pearson (eds.). Modern and Ancient Continental Shelf Anoxia. *Geological Society Special Publication* 58. Pp. 65-82.
Van der Zwaan, G.J., F.J. Jorissen, P.J.J.M. Verhallen, and C.H. Von Daniels. 1986. Uvigerina from the eastern Atlantic, North Sea basin, Paratethys and Mediterranean. In: Van der Zwaan, G.J., F.J. Jorissen, P.J.J.M. Verhallen, and C.H. Von Daniels (eds.). Atlantic-European Oligocene to Recent Uvigerina. *Utrecht Micropaleontological Bulletins* 35:7-20.
Verhallen, P.J.J.M. 1997. *Epistominella tricarinata*, a new species from sapropelitic layers in the Upper Pliocene of Italy. *Proceedings Koninklijke Nederlandse Akademie van Wetenschappen, Series B* 90:307-313.
Wright, S.W., S.W. Jeffrey, R.F.C. Mantoura, C.A. Llewellyn, T. Bjornland, D. Repeta, and N. Welschmeyer. 1991. Improved HPLC method for the analysis of chlorophylls and carotenoids from marine phytoplankton. *Marine Ecology Progress Series* 77:183-196.
Yanko, V., A.J. Arnold, and W.C. Parker. 1999. Effects on marine pollution on benthic Foraminifera. In: Sen Gupta, B.K. (ed.). Modern Foraminifera, Kluwer Academic Publishers, Dortrecht. Pp. 217-235.
Züllig, H. 1981. On the use of carotenoid stratigraphy in lake sediments for detecting past developments of phytoplankton. *Limnology and Oceanography* 26:970-976.

CHAPTER 7

APPENDICES

APPENDIX A

Total Organochlorine Pesticide Histograms

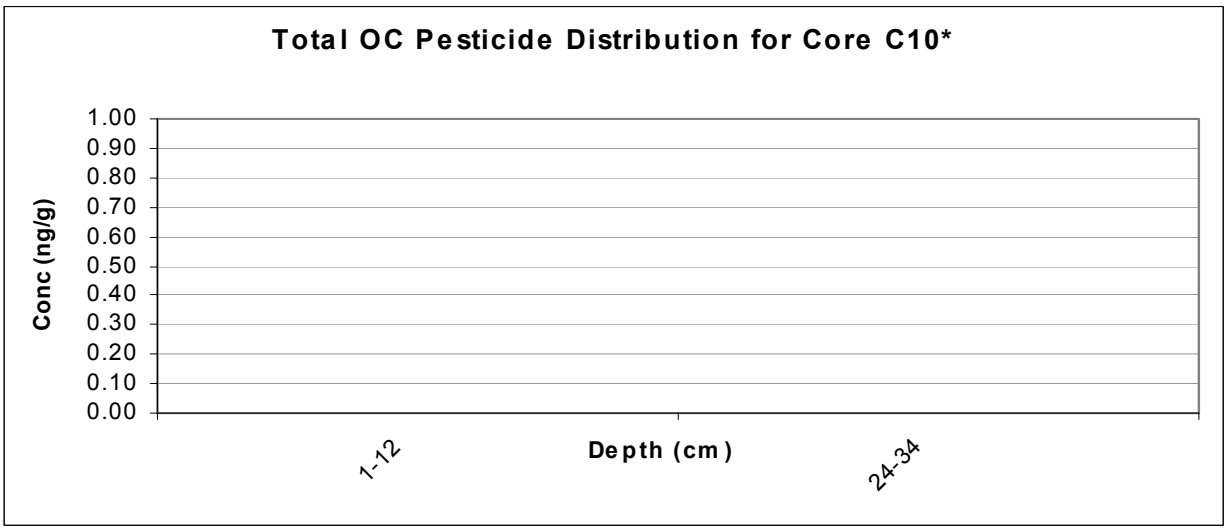
Total OC Pesticide Distribution for Core C10*
Conc (ng/g)
1.00
0.90
0.80
0.70
0.60
0.50
0.40
0.30
0.20
0.10
0.00
1-12
Depth (cm)
24-34

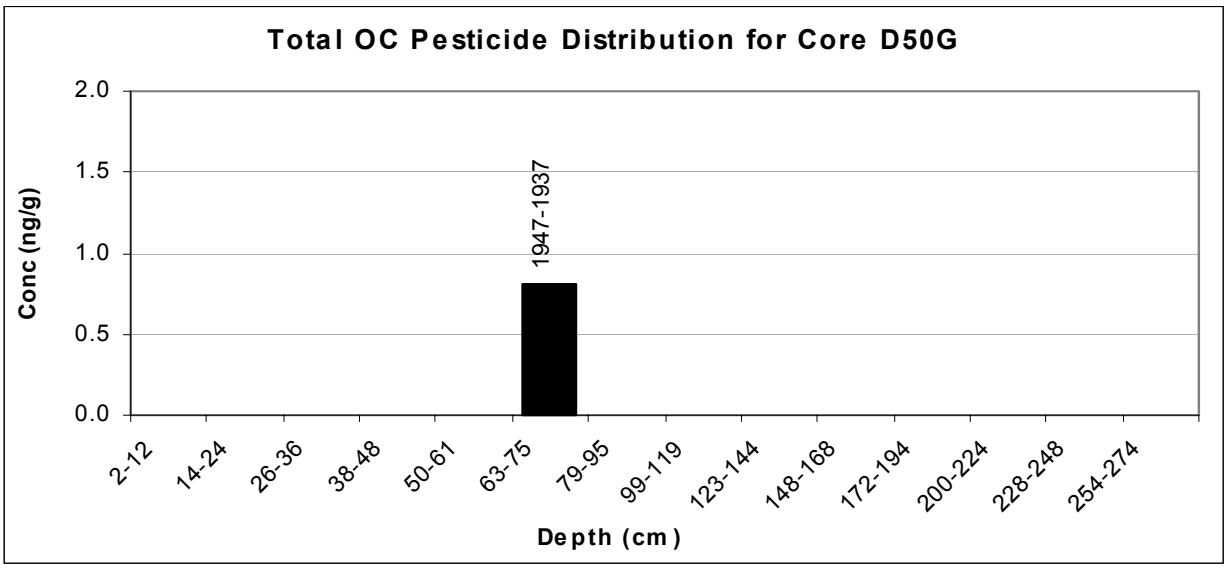
Total OC Pesticide Distribution for Core D50G
Conc (ng/g)
2.0
1.5
1.0
0.5
0.0
1947-1937
2-12
14-24
26-36
38-48
50-61
63-75
79-95
99-119
123-144
148-168
172-194
200-224
228-248
254-274
Depth (cm)

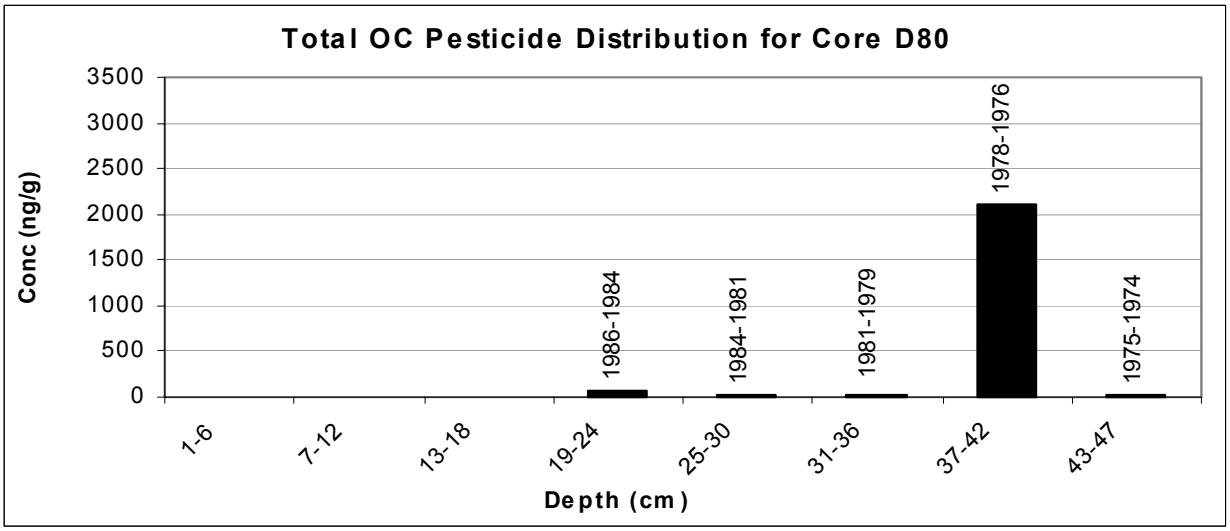
Total OC Pesticide Distribution for Core D80
Conc (ng/g)
3500
3000
2500
2000
1500
1000
500
0
1986-1984
1984-1981
1981-1979
1978-1976
1975-1974
1-6
7-12
13-18
19-24
25-30
31-36
37-42
43-47
Depth (cm)

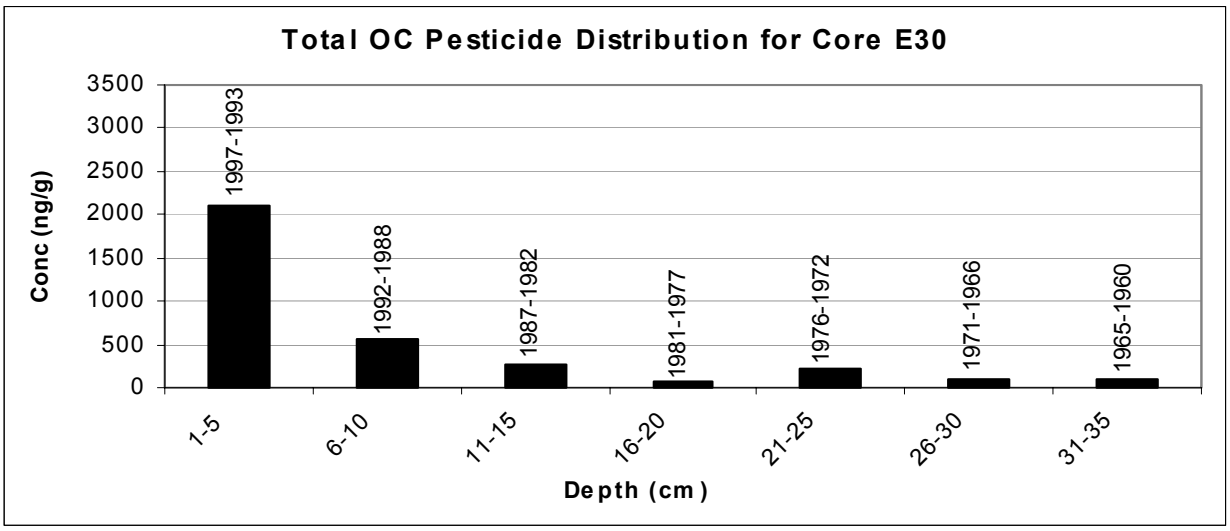
Total OC Pesticide Distribution for Core E30
Conc (ng/g)
3500
3000
2500
2000
1500
1000
500
0
1997-1993
1992-1988
1987-1982
1981-1977
1976-1972
1971-1966
1965-1960
1-5
6-10
11-15
16-20
21-25
26-30
31-35
Depth (cm)

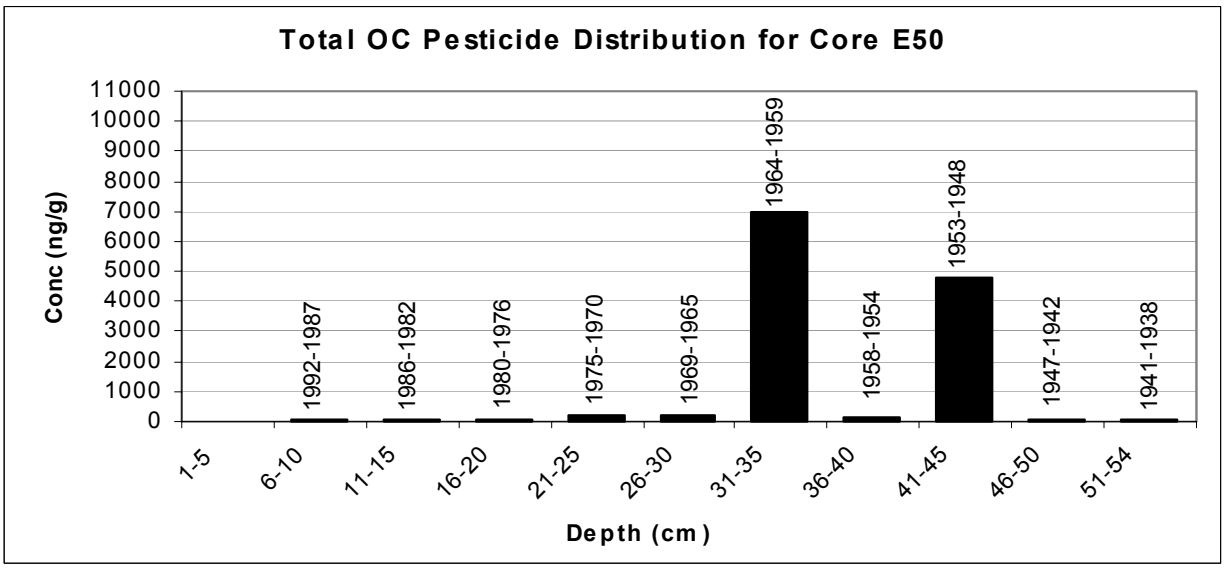
Total OC Pesticide Distribution for Core E50
Conc (ng/g)
11000
10000
9000
8000
7000
6000
5000
4000
3000
2000
1000
0
1992-1987
1986-1982
1980-1976
1975-1970
1969-1965
1964-1959
1958-1954
1953-1948
1947-1942
1941-1938
1-5
6-10
11-15
16-20
21-25
26-30
31-35
36-40
41-45
46-50
51-54
Depth (cm)

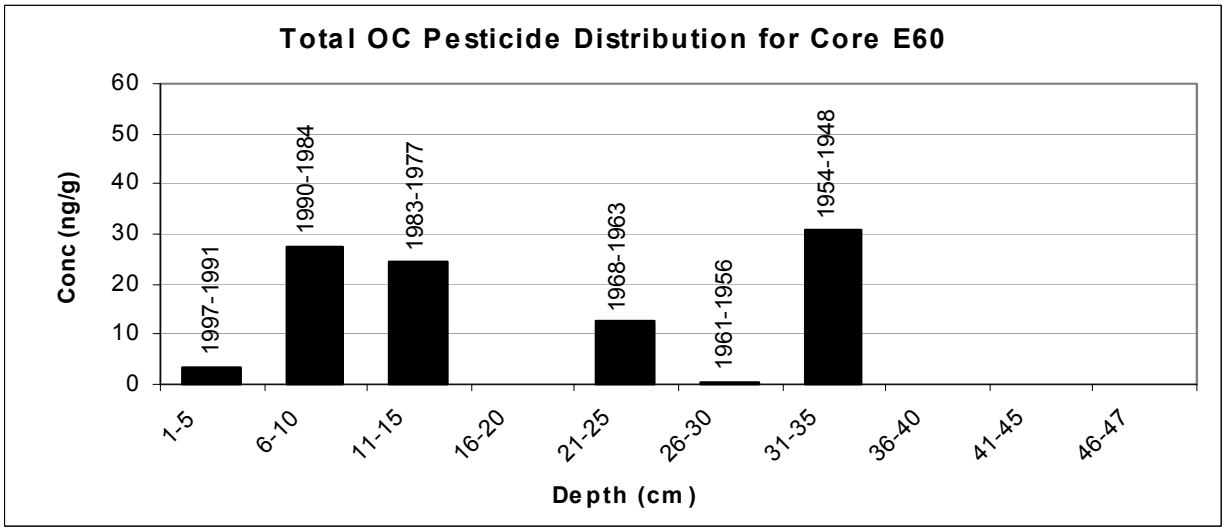
Total OC Pesticide Distribution for Core E60
Conc (ng/g)
60
50
40
30
20
10
0
1997-1991
1990-1984
1983-1977
1968-1963
1961-1956
1954-1948
1-5
6-10
11-15
16-20
21-25
26-30
31-35
36-40
41-45
46-47
Depth (cm)

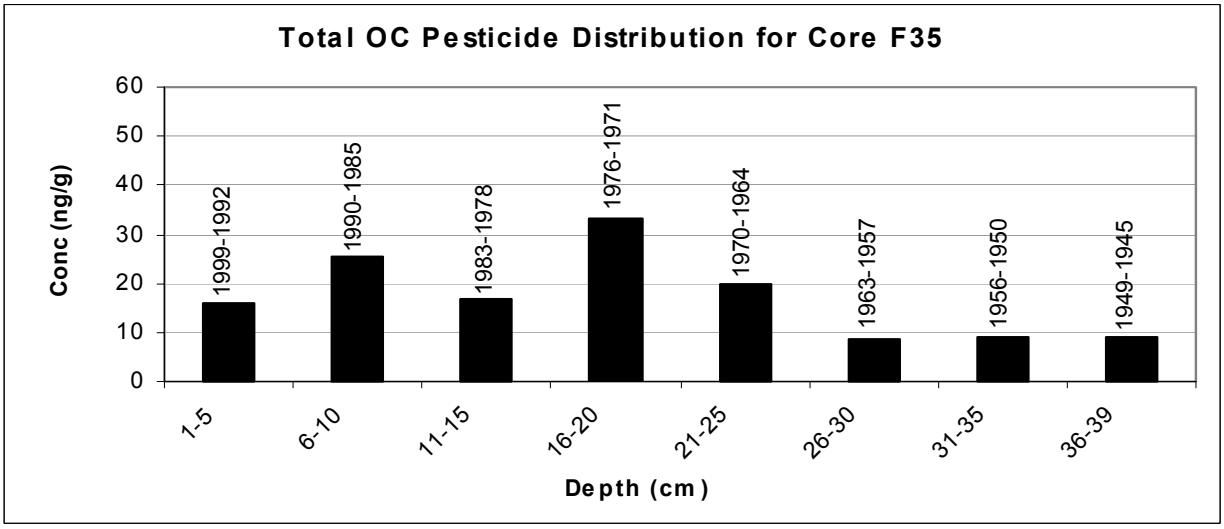
Total OC Pesticide Distribution for Core F35
Conc (ng/g)
60
50
40
30
20
10
0
1999-1992
1990-1985
1983-1978
1976-1971
1970-1964
1963-1957
1956-1950
1949-1945
1-5
6-10
11-15
16-20
21-25
26-30
31-35
36-39
Depth (cm)

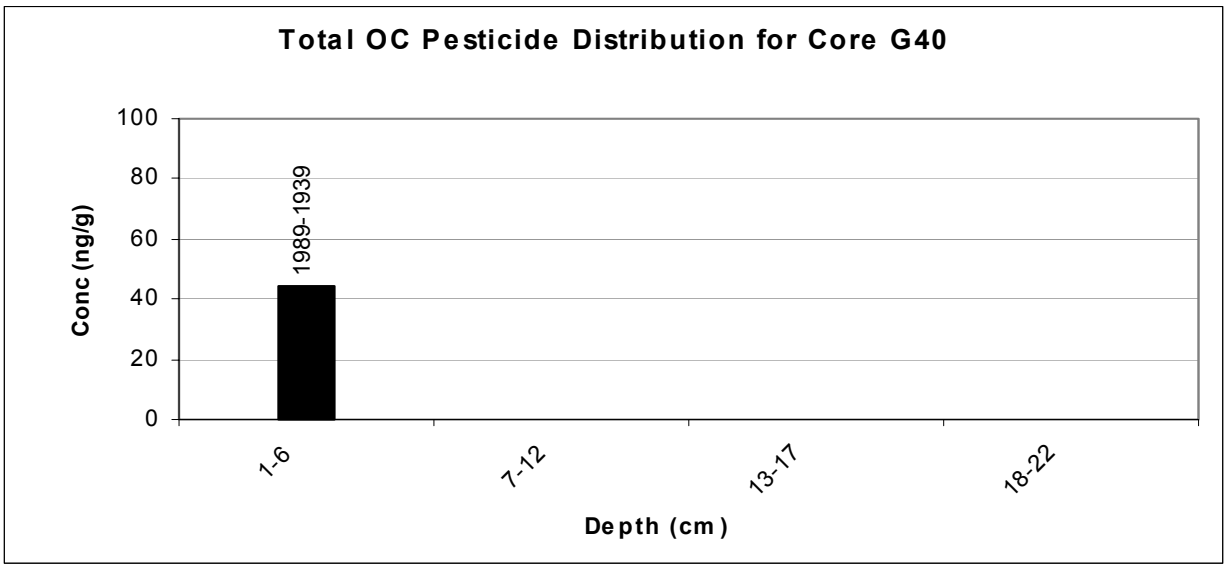
Total OC Pesticide Distribution for Core G40
Conc (ng/g)
100
80
60
40
20
0
1989-1939
1-6
7-12
13-17
18-22
Depth (cm)

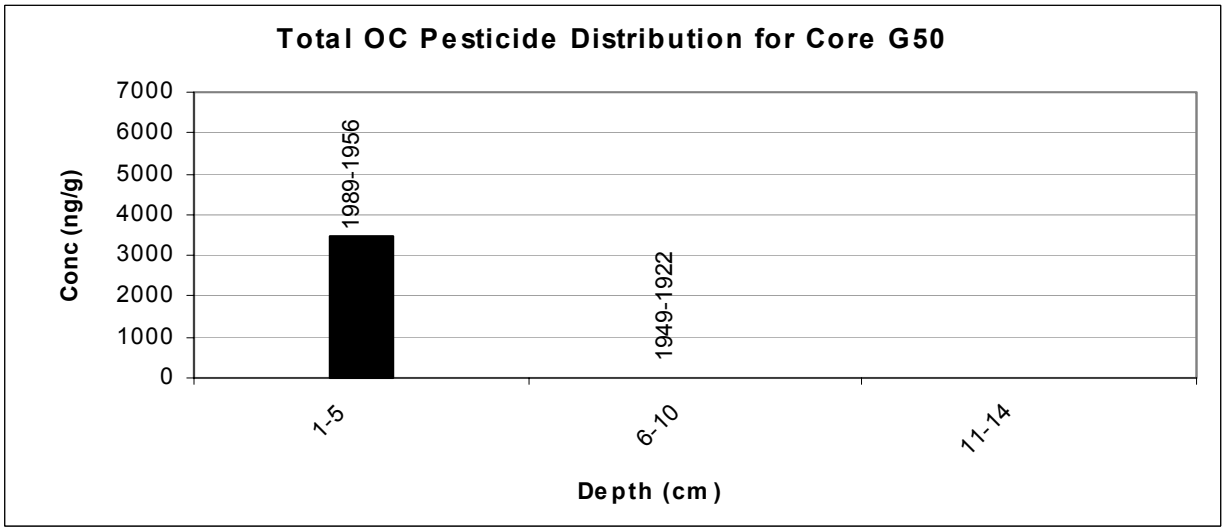
Total OC Pesticide Distribution for Core G50
Conc (ng/g)
7000
6000
5000
4000
3000
2000
1000
0
1989-1956
1949-1922
1-5
6-10
11-14
Depth (cm)

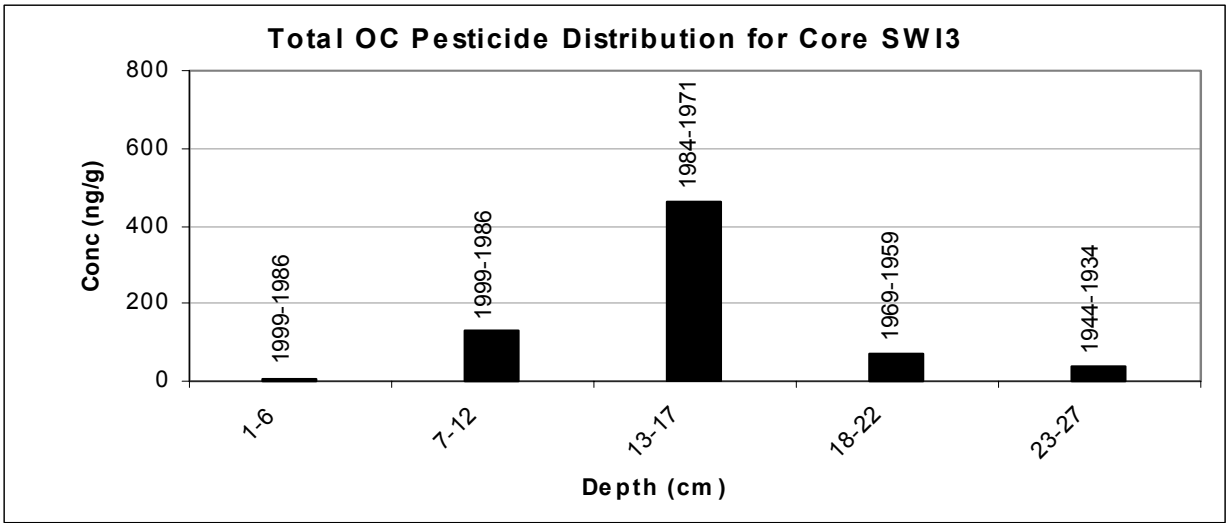
Total OC Pesticide Distribution for Core SWI3
Conc (ng/g)
800
600
400
200
0
1999-1986
1999-1986
1984-1971
1969-1959
1944-1934
1-6
7-12
13-17
18-22
23-27
Depth (cm)

APPENDIX B

Organochlorine Pesticide Concentrations for Sediment Cores

Sample Name	4A	4C	2A	2B	2C	2D	2E
Core	C10	C10	D50G	D50G	D50G	D50G	D50G
Depth	1-12	24-34	2-12	14-24	26-36	38-48	50-61
Date Range	1989-1984	1978-1974	1996-1988	1987-1979	1977-1969	1967-1959	1958-1949
Compounds	**Conc (ng/g)**	**Conc (ng/g)**	**Conc (ng/g)**	**Conc (ng/g)**	**Conc (ng/g)**	**Conc (ng/g)**	**Conc (ng/g)**
Hexachlorobenzene	nd	nd	nd	nd	nd	nd	nd
Lindane (g-BHC)	nd	nd	nd	nd	nd	nd	nd
Heptachlor	nd	nd	nd	nd	nd	nd	nd
Aldrin	nd	nd	nd	nd	nd	nd	nd
Heptachlor Epoxide	nd	nd	nd	nd	nd	nd	nd
trans-Nonachlor	nd	nd	nd	nd	nd	nd	nd
cis-Chlordane	nd	nd	nd	nd	nd	nd	nd
4, 4' DDE	nd	nd	nd	nd	nd	nd	nd
Dieldrin	nd	nd	nd	nd	nd	nd	nd
Endrin	nd	nd	nd	nd	nd	nd	nd
4, 4' DDD	nd	nd	nd	nd	nd	nd	nd
4,4' DDT	nd	nd	nd	nd	nd	nd	nd
TOTAL OCPs (ng/g)	**0.00**	**0.00**	**0.00**	**0.00**	**0.00**	**0.00**	**0.00**

Sample Name	2F	2G	2H	1A	1B	1C	1D
Core	D50G	D50G	D50G	D50G	D50G	D50G	D50G
Depth	63-75	79-95	99-119	123-144	148-168	172-194	200-224
Date Range	1947-1937	1934-1921	1918-1902	1899-1882	1879-1862	1859-1842	1837-1817
Compounds	**Conc (ng/g)**	**Conc (ng/g)**	**Conc (ng/g)**	**Conc (ng/g)**	**Conc (ng/g)**	**Conc (ng/g)**	**Conc (ng/g)**
Hexachlorobenzene	nd	nd	nd	nd	nd	nd	nd
Lindane (g-BHC)	nd	nd	nd	nd	nd	nd	nd
Heptachlor	nd	nd	nd	nd	nd	nd	nd
Aldrin	nd	nd	nd	nd	nd	nd	nd
Heptachlor Epoxide	nd	nd	nd	nd	nd	nd	nd
trans-Nonachlor	nd	nd	nd	nd	nd	nd	nd
cis-Chlordane	nd	nd	nd	nd	nd	nd	nd
4, 4' DDE	nd	nd	nd	nd	nd	nd	nd
Dieldrin	nd	nd	nd	nd	nd	nd	nd
Endrin	nd	nd	nd	nd	nd	nd	nd
4, 4' DDD	nd	nd	nd	nd	nd	nd	nd
4,4' DDT	0.81	nd	nd	nd	nd	nd	nd
TOTAL OCPs (ng/g)	**0.81**	**0.00**	**0.00**	**0.00**	**0.00**	**0.00**	**0.00**

Sample Name	3A	3B	4D	4E	4F	4G	4H
Core	D50G	D50G	D80	D80	D80	D80	D80
Depth	228-248	254-274	1-6	7-12	13-18	19-24	25-30
Date Range	1814-1798	1793-1777	1995-1992	1992-1990	1989-1987	1986-1984	1984-1981
Compounds	**Conc (ng/g)**	**Conc (ng/g)**	**Conc (ng/g)**	**Conc (ng/g)**	**Conc (ng/g)**	**Conc (ng/g)**	**Conc (ng/g)**
Hexachlorobenzene	nd	nd	nd	nd	nd	nd	nd
Lindane (g-BHC)	nd	nd	nd	nd	nd	nd	nd
Heptachlor	nd	nd	nd	nd	nd	35	nd
Aldrin	nd	nd	nd	nd	nd	20	12
Heptachlor Epoxide	nd	nd	nd	nd	nd	nd	nd
trans-Nonachlor	nd	nd	nd	nd	nd	nd	nd
cis-Chlordane	nd	nd	nd	nd	nd	nd	5.8
4, 4' DDE	nd	nd	nd	nd	nd	nd	nd
Dieldrin	nd	nd	nd	nd	nd	nd	4.4
Endrin	nd	nd	nd	nd	nd	nd	nd
4, 4' DDD	nd	nd	nd	nd	nd	12	nd
4,4' DDT	nd	nd	nd	nd	nd	nd	1.2
TOTAL OCPs (ng/g)	**0.00**	**0.00**	**0.00**	**0.00**	**0.00**	**67**	**24**

Sample Name	4I	4J	4K	2N1235-16	2N1235-12	2N1235-18	2N1235-36
Core	D80	D80	D80	E30	E30	E30	E30
Depth	31-36	37-42	43-47	1-5	6-10	11-15	16-20
Date Range	1981-1979	1978-1976	1975-1974	1997-1993	1992-1988	1987-1982	1981-1977
Compounds	**Conc (ng/g)**	**Conc (ng/g)**	**Conc (ng/g)**	**Conc (ng/g)**	**Conc (ng/g)**	**Conc (ng/g)**	**Conc (ng/g)**
Hexachlorobenzene	nd	nd	nd	nd	290	140	nd
Lindane (g-BHC)	nd	nd	nd	230	nd	nd	nd
Heptachlor	nd	nd	nd	450	nd	nd	nd
Aldrin	nd	nd	nd	480	77	nd	nd
Heptachlor Epoxide	nd	32	nd	nd	nd	62	nd
trans-Nonachlor	2.0	370	nd	nd	90	nd	nd
cis-Chlordane	25	320	9.0	680	100	69	79
4, 4' DDE	nd	140	nd	nd	nd	nd	nd
Dieldrin	nd	310	nd	250	nd	nd	nd
Endrin	1.2	390	nd	nd	nd	nd	nd
4, 4' DDD	2.0	310	10	nd	nd	nd	nd
4,4' DDT	nd	190	nd	nd	nd	nd	nd
TOTAL OCPs (ng/g)	**30**	**2100**	**19**	**2100**	**560**	**270**	**79**

Sample Name	2N1235-35	2N1235-08	2N1235-15	2N1235-01	2N1235-05	2N1235-22	2N1235-23
Core	E30	E30	E30	E50	E50	E50	E50
Depth	21-25	26-30	31-35	1-5	6-10	11-15	16-20
Date Range	1976-1972	1971-1966	1965-1960	1997-1993	1992-1987	1986-1982	1980-1976
Compounds	**Conc (ng/g)**	**Conc (ng/g)**	**Conc (ng/g)**	**Conc (ng/g)**	**Conc (ng/g)**	**Conc (ng/g)**	**Conc (ng/g)**
Hexachlorobenzene	nd	nd	nd	nd	nd	nd	nd
Lindane (g-BHC)	nd	nd	nd	nd	nd	nd	nd
Heptachlor	nd	nd	nd	nd	nd	nd	7.0
Aldrin	nd	nd	nd	nd	nd	71	nd
Heptachlor Epoxide	nd	nd	nd	nd	nd	nd	22
trans-Nonachlor	nd	nd	nd	nd	nd	nd	1.3
cis-Chlordane	220	100	86	nd	38	nd	26
4, 4' DDE	nd	nd	nd	nd	nd	nd	3.3
Dieldrin	nd	nd	nd	nd	nd	nd	nd
Endrin	nd	nd	nd	nd	nd	nd	nd
4, 4' DDD	nd	nd	nd	nd	nd	20	nd
4,4' DDT	nd	nd	nd	nd	nd	nd	nd
TOTAL OCPs (ng/g)	**220**	**100**	**86**	**0.00**	**38**	**91**	**60**

Sample Name	2N1235-27	2N1235-02	2N1235-04	2N1235-06	2N1235-17	2N1235-28	2N1235-03
Core	E50	E50	E50	E50	E50	E50	E50
Depth	21-25	26-30	31-35	36-40	41-45	46-50	51-54
Date Range	1975-1970	1969-1965	1964-1959	1958-1954	1953-1948	1947-1942	1941-1938
Compounds	**Conc (ng/g)**	**Conc (ng/g)**	**Conc (ng/g)**	**Conc (ng/g)**	**Conc (ng/g)**	**Conc (ng/g)**	**Conc (ng/g)**
Hexachlorobenzene	55	nd	550	3.1	420	nd	nd
Lindane (g-BHC)	230	nd	540	39	460	3.5	nd
Heptachlor	2.1	3.5	520	26	370	nd	nd
Aldrin	2.4	17	640	9.9	530	nd	nd
Heptachlor Epoxide	nd	51	690	nd	600	nd	nd
trans-Nonachlor	7.1	nd	740	nd	620	12	nd
cis-Chlordane	30	94	640	16	510	37	nd
4, 4' DDE	nd	nd	120	2.1	56	nd	2.1
Dieldrin	3.8	6.5	610	1.9	540	nd	nd
Endrin	9.1	13	780	6.8	660	nd	nd
4, 4' DDD	2.9	25	830	nd	67	nd	59
4,4' DDT	nd	nd	310	nd	nd	nd	nd
TOTAL OCPs (ng/g)	**240**	**210**	**7000**	**110**	**4800**	**53**	**61**

Sample Name	2N1235-26	2N1235-31	2N1235-24	2N1235-29	2N1235-10	2N1235-33	2N1235-32
Core	E60	E60	E60	E60	E60	E60	E60
Depth	1-5	6-10	11-15	16-20	21-25	26-30	31-35
Date Range	1997-1991	1990-1984	1983-1977	1976-1970	1968-1963	1961-1956	1954-1948
Compounds	**Conc (ng/g)**	**Conc (ng/g)**	**Conc (ng/g)**	**Conc (ng/g)**	**Conc (ng/g)**	**Conc (ng/g)**	**Conc (ng/g)**
Hexachlorobenzene	nd	nd	nd	nd	nd	nd	nd
Lindane (g-BHC)	nd	nd	nd	nd	nd	nd	nd
Heptachlor	nd	0.67	nd	nd	nd	nd	1.2
Aldrin	nd	nd	nd	nd	1.2	0.48	4.3
Heptachlor Epoxide	1.8	nd	1.6	nd	0.85	nd	1.6
trans-Nonachlor	nd	4.0	9.9	nd	4.0	nd	14
cis-Chlordane	nd	19	13	nd	nd	nd	nd
4, 4' DDE	nd	nd	nd	nd	nd	nd	nd
Dieldrin	nd	nd	nd	nd	nd	nd	nd
Endrin	1.4	2.1	nd	nd	2.6	nd	nd
4, 4' DDD	nd	1.2	nd	nd	nd	nd	9.5
4,4' DDT	nd	nd	nd	nd	4.1	nd	nd
TOTAL OCPs (ng/g)	**3.2**	**27**	**24**	**0.0**	**13**	**0.48**	**31**

Sample Name	2N1235-34	2N1235-30	2N1235-07	2N1235-13	2N1235-20	2N1235-25	2N1235-09
Core	E60	E60	E60	F35	F35	F35	F35
Depth	36-40	41-45	46-47	1-5	6-10	11-15	16-20
Date Range	1947-1941	1940-1934	1933-1931	1999-1992	1990-1985	1983-1978	1976-1971
Compounds	**Conc (ng/g)**	**Conc (ng/g)**	**Conc (ng/g)**	**Conc (ng/g)**	**Conc (ng/g)**	**Conc (ng/g)**	**Conc (ng/g)**
Hexachlorobenzene	nd	nd	nd	nd	nd	nd	nd
Lindane (g-BHC)	nd	nd	nd	nd	nd	nd	nd
Heptachlor	nd	nd	nd	nd	nd	nd	nd
Aldrin	nd	nd	nd	nd	nd	nd	nd
Heptachlor Epoxide	nd	nd	nd	nd	1.3	nd	1.2
trans-Nonachlor	nd	nd	nd	nd	9.1	nd	2.9
cis-Chlordane	nd	nd	nd	14	14	16	29
4, 4' DDE	nd	nd	nd	nd	nd	nd	nd
Dieldrin	nd	nd	nd	nd	nd	nd	nd
Endrin	nd	nd	nd	2.3	1.1	1.1	nd
4, 4' DDD	nd	nd	nd	nd	nd	nd	nd
4,4' DDT	nd	nd	nd	nd	nd	nd	nd
TOTAL OCPs (ng/g)	**0.0**	**0.0**	**0.0**	**16**	**25**	**17**	**33**

Sample Name	2N1235-21	2N1235-19	2N1235-11	2N1235-14	3H	3I	3J
Core	F35	F35	F35	F35	G40	G40	G40
Depth	21-25	26-30	31-35	36-39	1-6	7-12	13-17
Date Range	1970-1964	1963-1957	1956-1950	1949-1945	1989-1939	1939-1889	1889-1847
Compounds	**Conc (ng/g)**	**Conc (ng/g)**	**Conc (ng/g)**	**Conc (ng/g)**	**Conc (ng/g)**	**Conc (ng/g)**	**Conc (ng/g)**
Hexachlorobenzene	nd	nd	nd	nd	39	nd	nd
Lindane (g-BHC)	nd	nd	nd	nd	nd	nd	nd
Heptachlor	nd	nd	nd	nd	nd	nd	nd
Aldrin	nd	nd	nd	nd	nd	nd	nd
Heptachlor Epoxide	1.7	nd	0.19	0.67	nd	nd	nd
trans-Nonachlor	2.8	nd	nd	0.12	nd	nd	nd
cis-Chlordane	12	7.3	6.2	6.7	nd	nd	nd
4, 4' DDE	nd	nd	nd	nd	nd	nd	nd
Dieldrin	nd	nd	nd	nd	nd	nd	nd
Endrin	nd	nd	0.31	nd	nd	nd	nd
4, 4' DDD	3.3	1.3	2.5	1.5	5.2	nd	nd
4,4' DDT	nd	nd	nd	nd	nd	nd	nd
TOTAL OCPs (ng/g)	**20**	**8.6**	**9.2**	**9.0**	**44**	**0.00**	**0.00**

Sample Name	3K	4L	4M	4N	3C	3D	3E
Core	G40	G50	G50	G50	SWI3	SWI3	SWI3
Depth	18-22	1-5	6-10	11-14	1-6	7-12	13-17
Date Range	1847-1805	1989-1956	1956-1922	1922-1892	1999-1986	1984-1971	1969-1959
Compounds	**Conc (ng/g)**	**Conc (ng/g)**	**Conc (ng/g)**	**Conc (ng/g)**	**Conc (ng/g)**	**Conc (ng/g)**	**Conc (ng/g)**
Hexachlorobenzene	nd	nd	nd	nd	nd	nd	nd
Lindane (g-BHC)	nd	190	nd	nd	nd	nd	nd
Heptachlor	nd	16	nd	nd	nd	nd	37
Aldrin	nd	22	nd	nd	0.76	nd	nd
Heptachlor Epoxide	nd	nd	0.71	nd	2.7	nd	61
trans-Nonachlor	nd	590	nd	nd	nd	nd	nd
cis-Chlordane	nd	540	nd	nd	nd	nd	nd
4, 4' DDE	nd	170	nd	nd	nd	nd	nd
Dieldrin	nd	380	nd	nd	nd	100	360
Endrin	nd	650	0.77	nd	nd	7.3	nd
4, 4' DDD	nd	510	1.1	nd	nd	1.9	nd
4,4' DDT	nd	469	1.6	nd	nd	20	1.3
TOTAL OCPs (ng/g)	**0.00**	**3500**	**4.2**	**0.00**	**3.5**	**130**	**460**

Sample Name	3F	3G
Core	SWI3	SWI3
Depth	18-22	23-27
Date Range	1956-1946	1944-1934
Compounds	**Conc (ng/g)**	**Conc (ng/g)**
Hexachlorobenzene	4.0	nd
Lindane (g-BHC)	nd	38
Heptachlor	1.8	nd
Aldrin	nd	nd
Heptachlor Epoxide	nd	nd
trans-Nonachlor	nd	nd
cis-Chlordane	nd	nd
4, 4' DDE	nd	nd
Dieldrin	58	nd
Endrin	2.0	nd
4, 4' DDD	2.9	1.2
4,4' DDT	1.4	nd
TOTAL OCPs (ng/g)	**70**	**39**

APPENDIX C

Total Organochlorine Pesticide Histograms by Decade

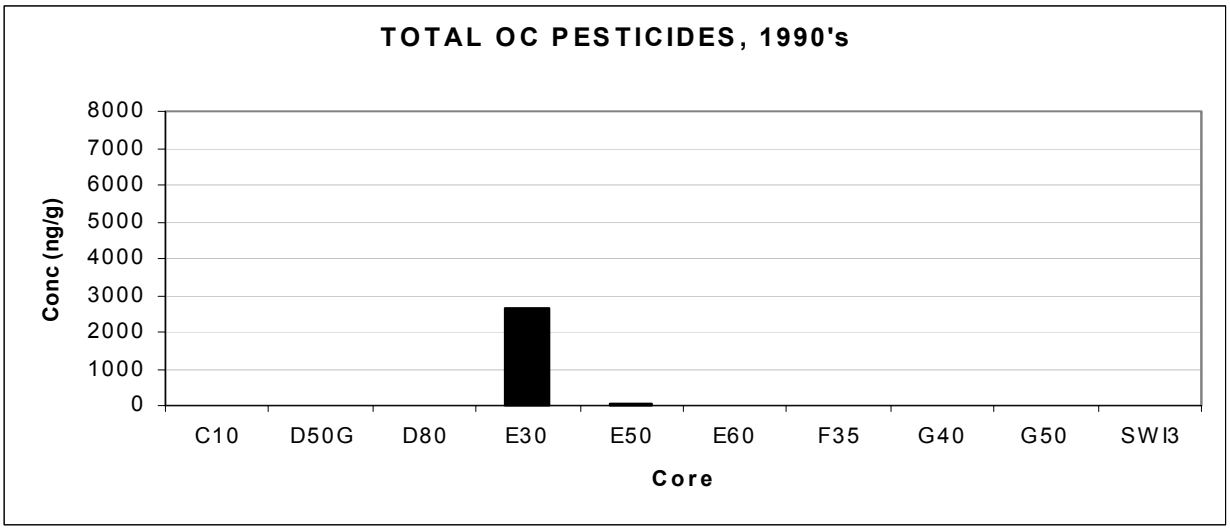
TOTAL OC PESTICIDES, 1990's
Conc (ng/g)
8000
7000
6000
5000
4000
3000
2000
1000
0
C10
D50G
D80
E30
E50
E60
F35
G40
G50
SWI3
Core

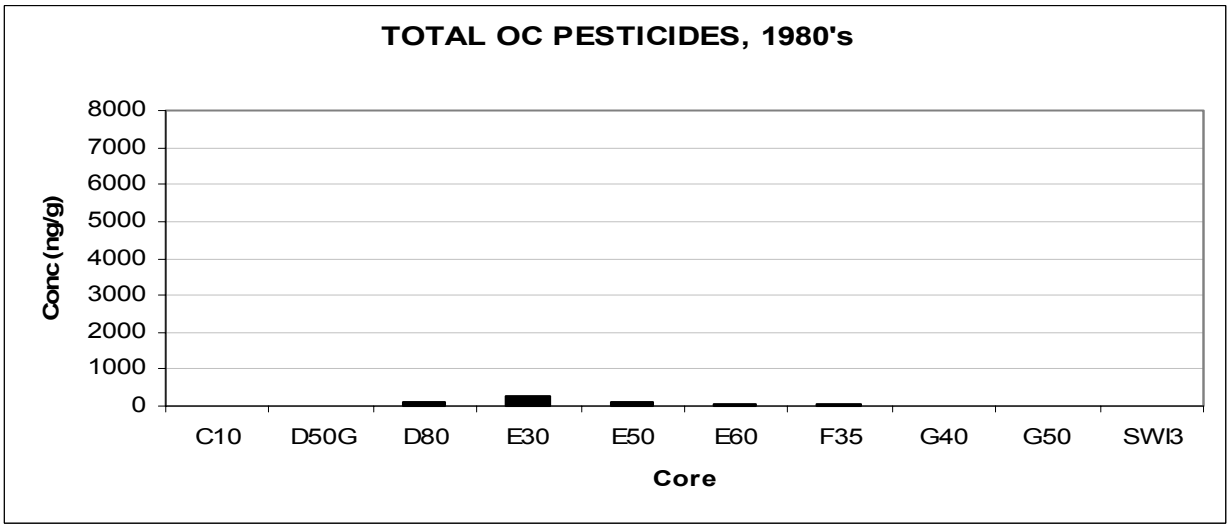
TOTAL OC PESTICIDES, 1980's
Conc (ng/g)
8000
7000
6000
5000
4000
3000
2000
1000
0
C10
D50G
D80
E30
E50
E60
F35
G40
G50
SWI3
Core

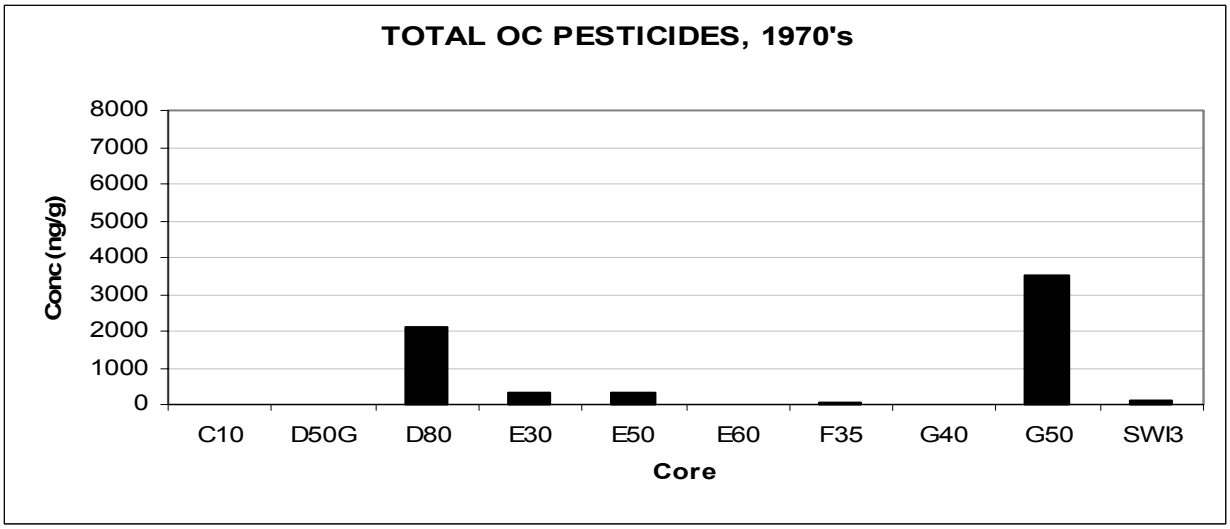
TOTAL OC PESTICIDES, 1970's
Conc (ng/g)
8000
7000
6000
5000
4000
3000
2000
1000
0
C10
D50G
D80
E30
E50
E60
F35
G40
G50
SWI3
Core

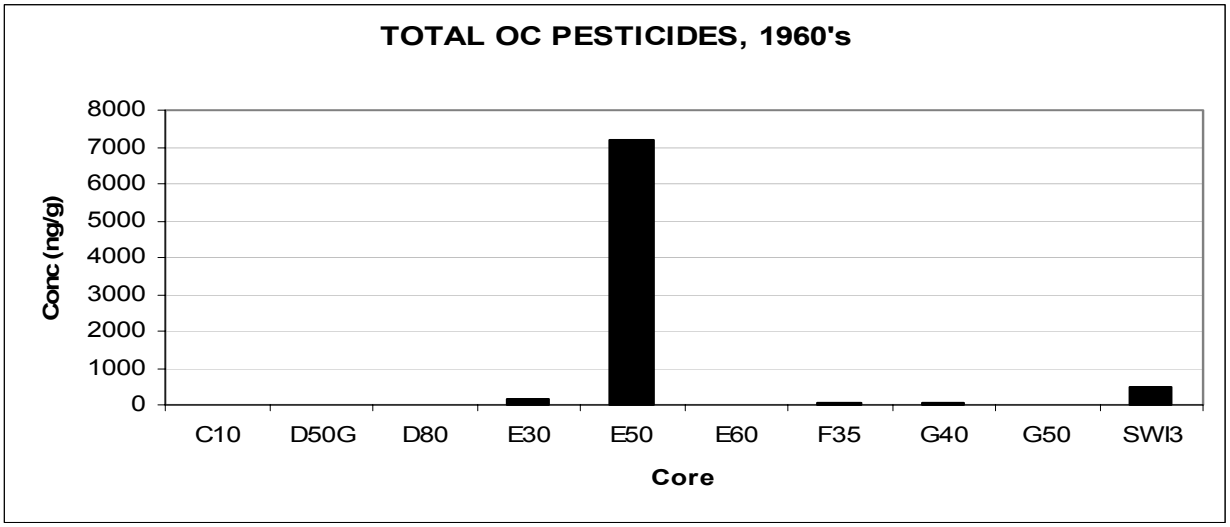
TOTAL OC PESTICIDES, 1960's
Conc (ng/g)
8000
7000
6000
5000
4000
3000
2000
1000
0
C10
D50G
D80
E30
E50
E60
F35
G40
G50
SWI3
Core

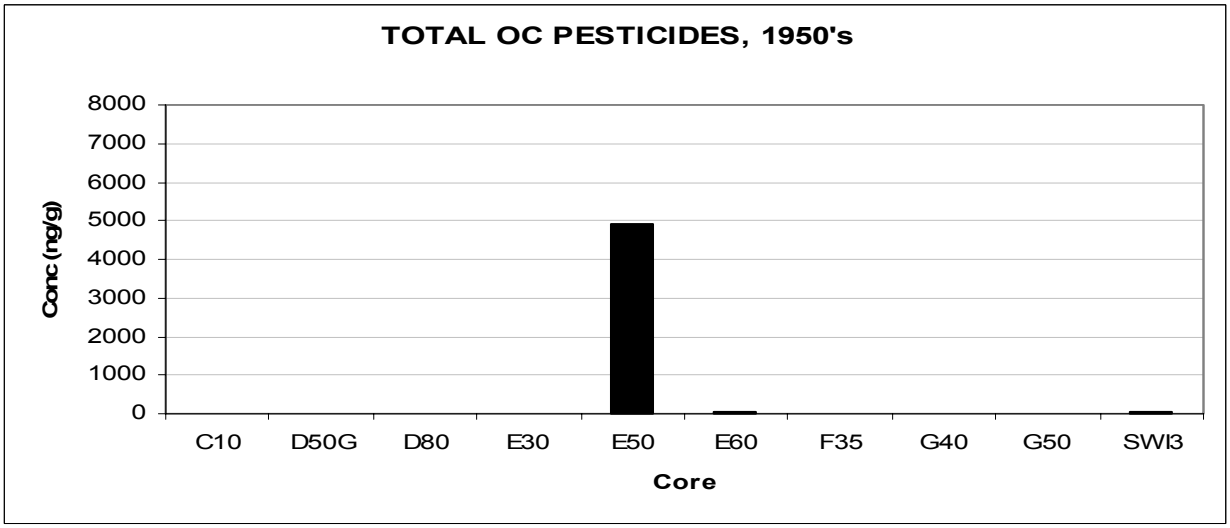
TOTAL OC PESTICIDES, 1950's
Conc (ng/g)
8000
7000
6000
5000
4000
3000
2000
1000
0
C10
D50G
D80
E30
E50
E60
F35
G40
G50
SWI3
Core

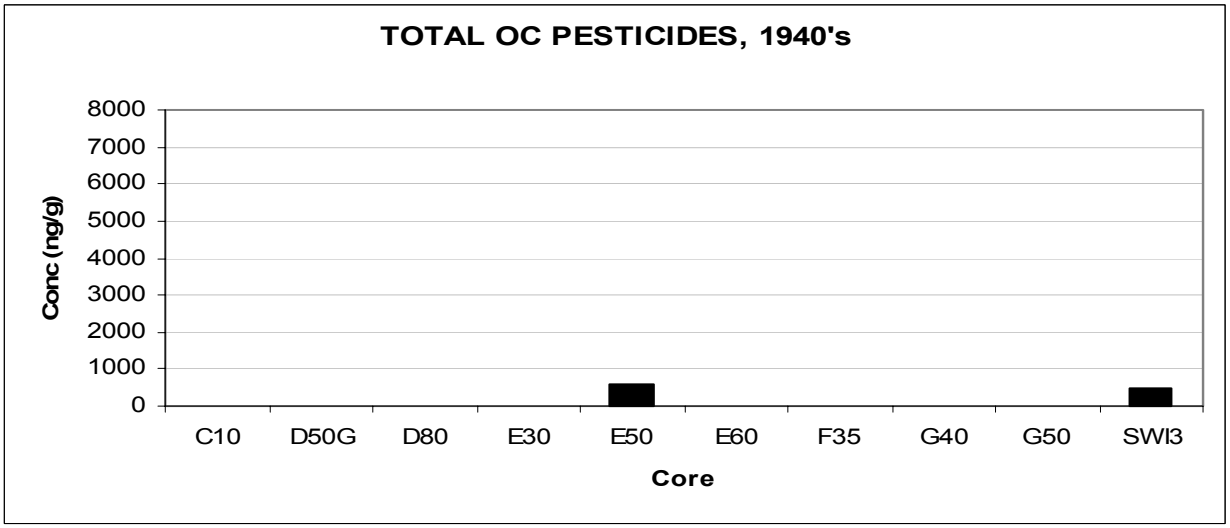
TOTAL OC PESTICIDES, 1940's
Conc (ng/g)
8000
7000
6000
5000
4000
3000
2000
1000
0
C10
D50G
D80
E30
E50
E60
F35
G40
G50
SWI3
Core

APPENDIX D

Total PAH Histograms

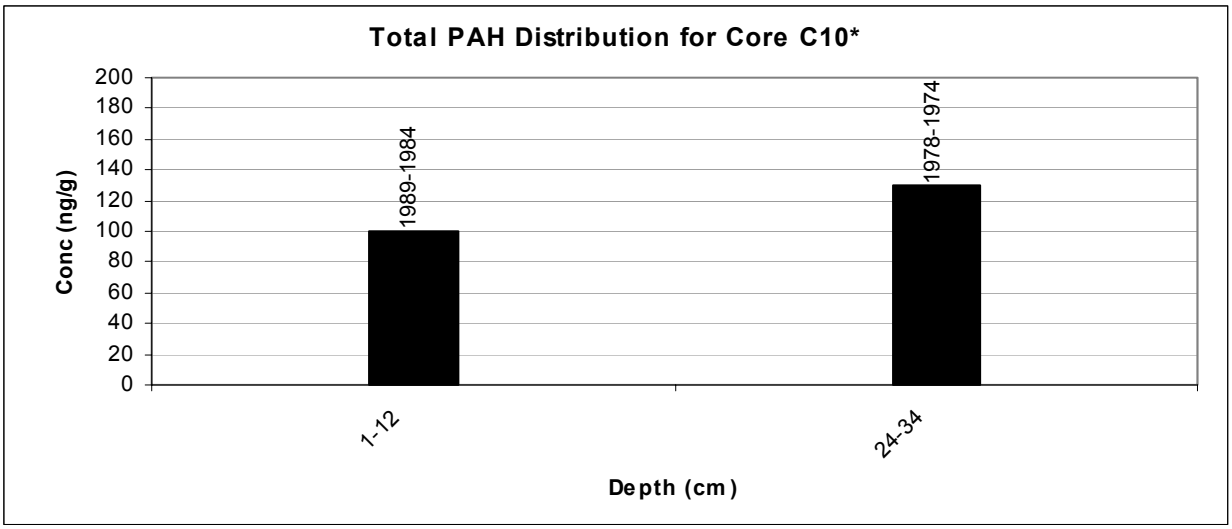

*Missing sections 13-23

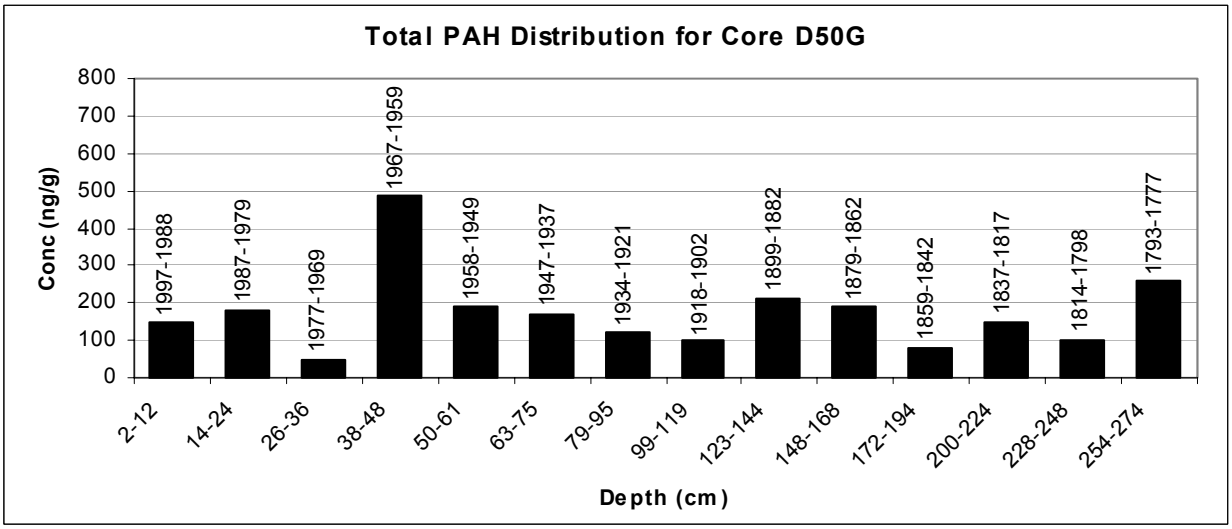

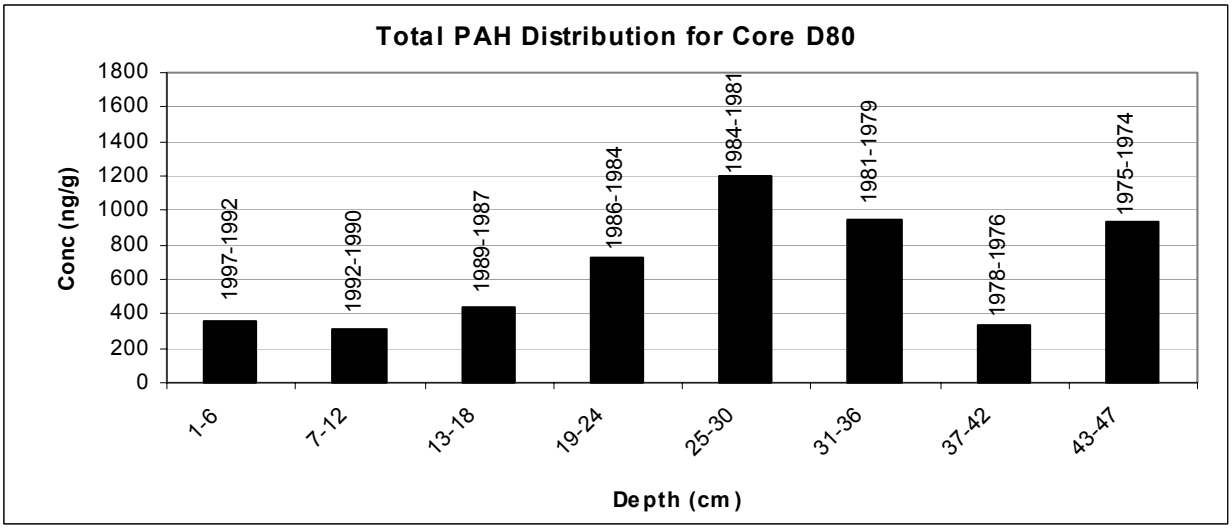

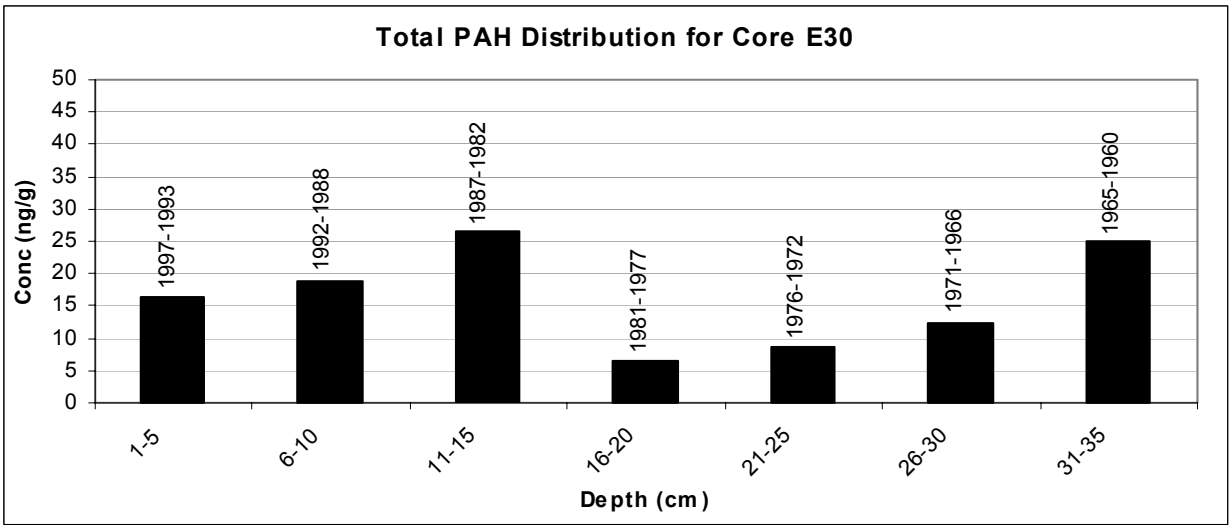
Total PAH Distribution for Core E30
Conc (ng/g)
50
45
40
35
30
25
20
15
10
5
0
1997-1993
1992-1988
1987-1982
1981-1977
1976-1972
1971-1966
1965-1960
1-5
6-10
11-15
16-20
21-25
26-30
31-35
Depth (cm)

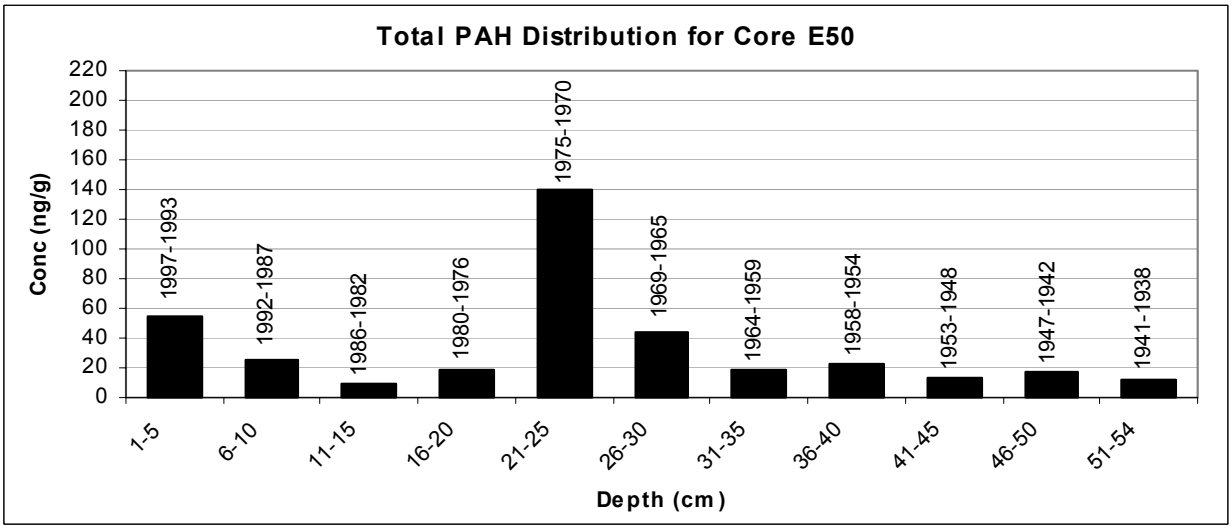
Total PAH Distribution for Core E50
Conc (ng/g)
220
200
180
160
140
120
100
80
60
40
20
0
1997-1993
1992-1987
1986-1982
1980-1976
1975-1970
1969-1965
1964-1959
1958-1954
1953-1948
1947-1942
1941-1938
1-5
6-10
11-15
16-20
21-25
26-30
31-35
36-40
41-45
46-50
51-54
Depth (cm)

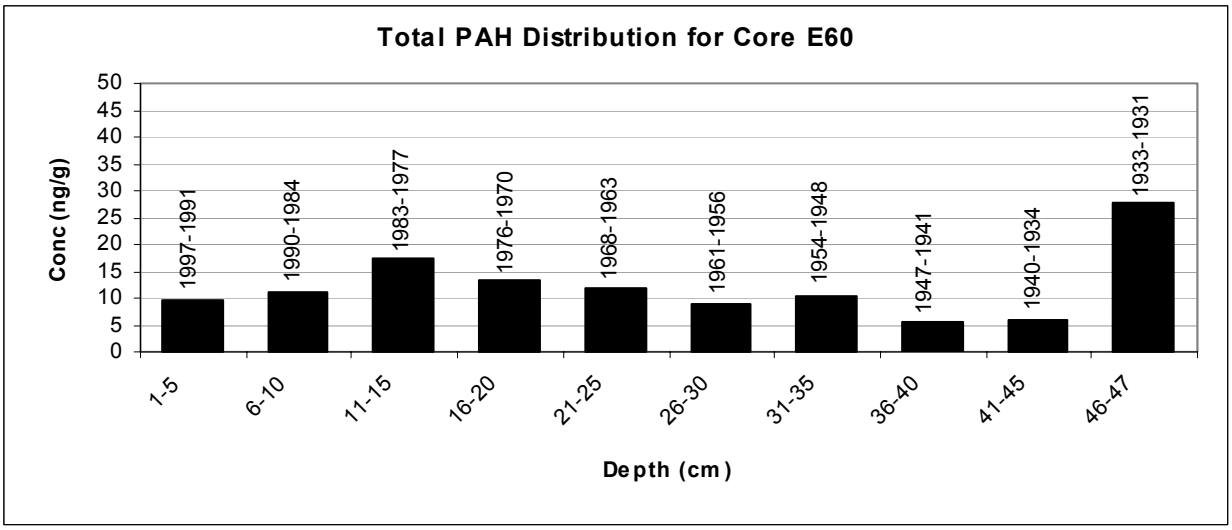
Total PAH Distribution for Core E60
Conc (ng/g)
50
45
40
35
30
25
20
15
10
5
0
1997-1991
1990-1984
1983-1977
1976-1970
1968-1963
1961-1956
1954-1948
1947-1941
1940-1934
1933-1931
1-5
6-10
11-15
16-20
21-25
26-30
31-35
36-40
41-45
46-47
Depth (cm)

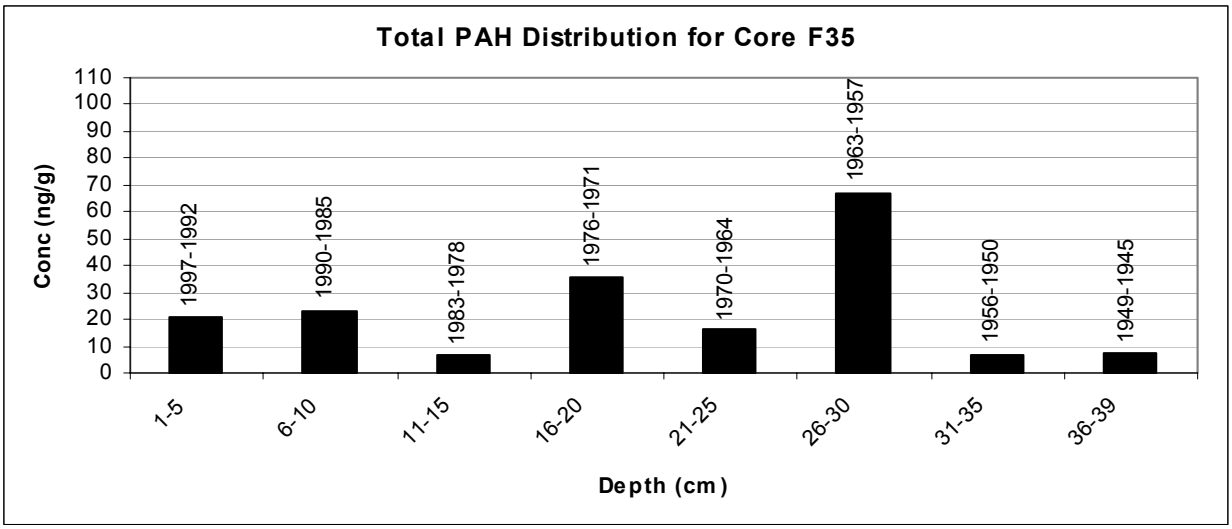
Total PAH Distribution for Core F35
Conc (ng/g)
110
100
90
80
70
60
50
40
30
20
10
0
1997-1992
1990-1985
1983-1978
1976-1971
1970-1964
1963-1957
1956-1950
1949-1945
1-5
6-10
11-15
16-20
21-25
26-30
31-35
36-39
Depth (cm)

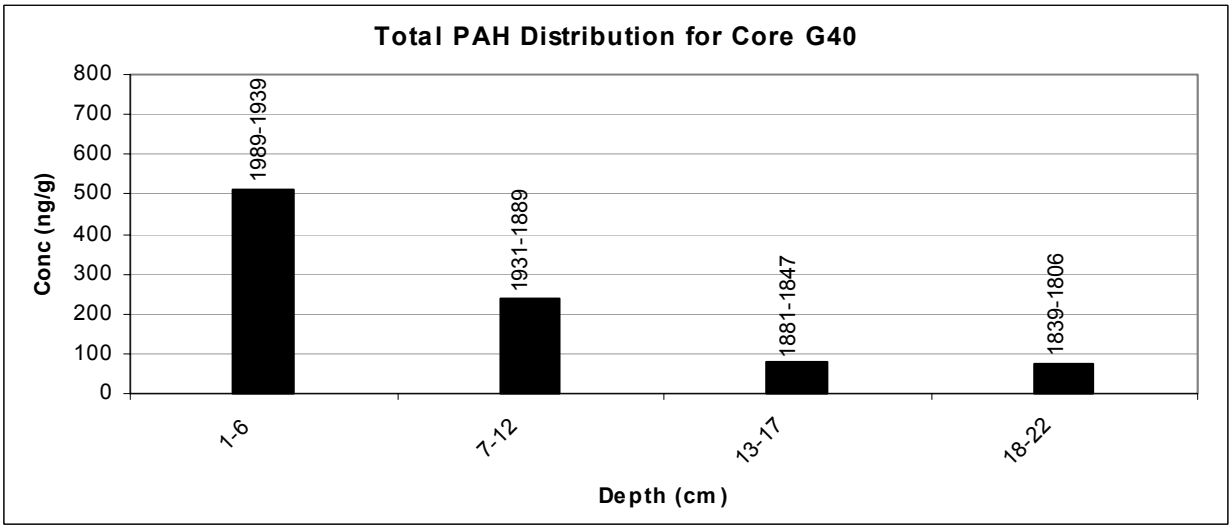
Total PAH Distribution for Core G40
Conc (ng/g)
800
700
600
500
400
300
200
100
0
1989-1939
1931-1889
1881-1847
1839-1806
1-6
7-12
13-17
18-22
Depth (cm)

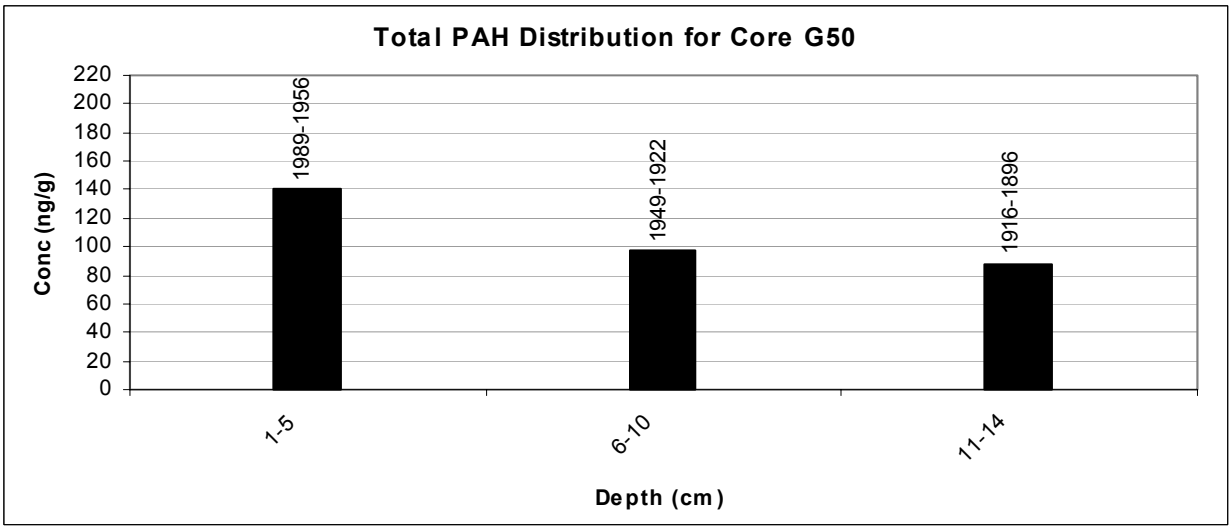
Total PAH Distribution for Core G50
Conc (ng/g)
220
200
180
160
140
120
100
80
60
40
20
0
1989-1956
1949-1922
1916-1896
1-5
6-10
11-14
Depth (cm)

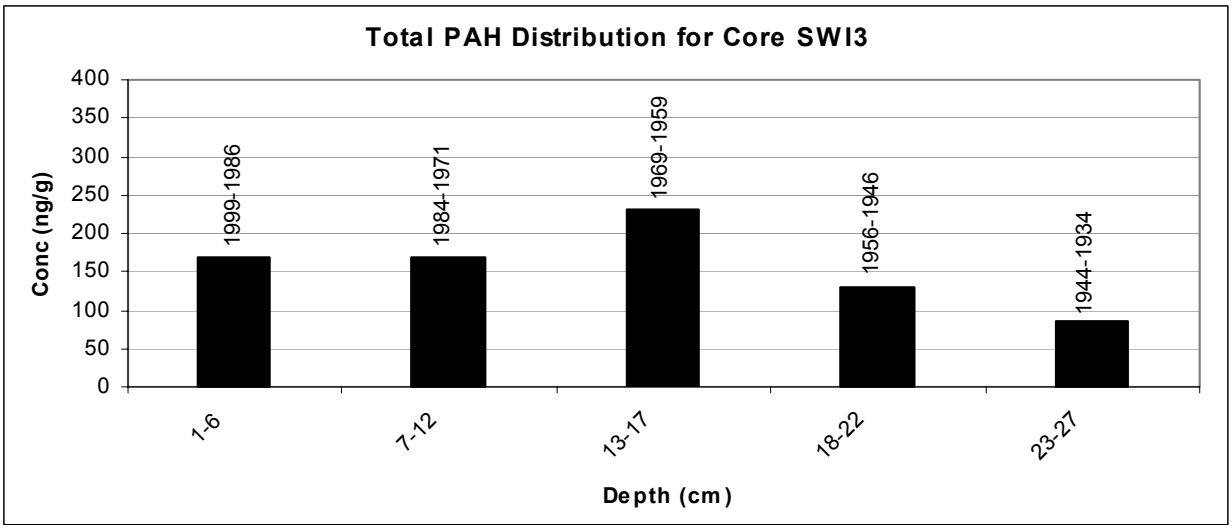
Total PAH Distribution for Core SWI3
Conc (ng/g)
400
350
300
250
200
150
100
50
0
1999-1986
1984-1971
1969-1959
1956-1946
1944-1934
1-6
7-12
13-17
18-22
23-27
Depth (cm)

APPENDIX E

PAH Concentrations for Sediment Cores

Sample Name	4A	4C	2A	2B	2C	2D	2E
Core	C10	C10	D-50G	D-50G	D-50G	D-50G	D-50G
Depth (cm)	1-12	24-34	2-12	14-24	26-36	38-48	50-61
Date Range	1989-1984	1978-1974	1997-1988	1987-1979	1977-1969	1967-1959	1958-1949
Name	**Conc (ng/g)**	**Conc (ng/g)**	**Conc (ng/g)**	**Conc (ng/g)**	**Conc (ng/g)**	**Conc (ng/g)**	**Conc (ng/g)**
Naphthalene	nd	nd	nd	nd	nd	nd	nd
2-Methyl Naphthalene	0.89	1.0	1.6	3.1	1.3	11	1.8
1-Methyl Naphthalene	0.15	0.17	0.48	0.88	0.17	2.3	0.54
2,3,5-Trimethyl Naphthalene*	--	--	--	--	--	--	--
2,6-Dimethyl Naphthalene	1.4	0.31	1.7	2.1	0.27	9.0	0.54
Acenaphthylene	2.5	6.3	5.1	5.2	3.1	18	7.2
Acenaphthene	3.2	1.9	3.2	2.6	0.87	12	4.2
Biphenyl	nd	nd	nd	nd	nd	nd	nd
Fluorene	0.74	1.3	1.9	1.6	0.62	8.8	4.2
Phenanthrene	15	21	22	15	5.9	94	46
Anthracene	1.1	0.56	4.0	2.7	1.5	20	8.5
1-Methyl Phenanthrene	9.5	4.9	nd	nd	nd	nd	nd
Fluoranthene	23	42	26	23	8.0	120	45
Pyrene	23	38	30	30	15	150	50
Benzo (a) Anthracene	2.7	2.5	4.5	7.0	0.79	5.5	2.0
Chrysene	2.4	1.7	5.1	6.5	0.83	6.1	2.0
Benzo (b) Fluoranthene	1.7	1.7	6.2	11	1.3	6.6	3.1
Benzo (k) Fluoranthene	3.1	2.5	7.5	16	1.4	8.7	4.0
Benzo (e) Pyrene	2.1	1.8	6.1	11	1.3	6.2	3.2
Benzo (a) Pyrene	1.4	0.81	4.5	8.9	1.0	3.5	2.3
Perylene	6.4	4.3	10	13	1.1	6.0	3.6
Indeno (1,2,3 - cd) Pyrene	0.72	0.52	2.1	5.8	0.42	2.0	1.7
Dibenzo (a,h) anthracene	0.39	0.28	1.0	3.2	0.21	1.1	1.0
Benzo (g,h,i) perylene	1.1	1.0	3.1	12	1.0	3.4	2.9
TOTAL PAHs (ng/g)	**100**	**130**	**150**	**180**	**46**	**490**	**190**
*Co-eluting with internal standard							

Sample Name	2F	2G	2H	1A	1B	1C	1D
Core	D-50G	D-50G	D-50G	D-50G	D-50G	D-50G	D-50G
Depth (cm)	63-75	79-95	99-119	123-144	148-168	172-194	200-224
Date Range	1947-1937	1934-1921	1918-1902	1899-1882	1879-1862	1859-1842	1837-1817
Name	**Conc (ng/g)**	**Conc (ng/g)**	**Conc (ng/g)**	**Conc (ng/g)**	**Conc (ng/g)**	**Conc (ng/g)**	**Conc (ng/g)**
Naphthalene	nd	nd	nd	nd	nd	nd	nd
2-Methyl Naphthalene	1.2	1.1	1.2	0.35	0.21	0.40	1.8
1-Methyl Naphthalene	0.40	0.26	0.33	0.31	0.21	0.07	0.45
2,3,5-Trimethyl Naphthalene*	--	--	--	--	--	--	--
2,6-Dimethyl Naphthalene	0.53	0.24	0.28	0.88	0.35	0.21	1.3
Acenaphthylene	6.0	4.4	4.6	7.8	8.1	1.7	4.7
Acenaphthene	4.3	1.7	2.1	5.1	2.8	1.7	2.0
Biphenyl	nd	nd	nd	nd	nd	nd	nd
Fluorene	2.2	2.0	1.2	3.4	2.8	1.2	1.8
Phenanthrene	34	25	18	52	43	15	23
Anthracene	6.8	4.9	3.8	2.3	5.8	2.1	3.3
1-Methyl Phenanthrene	nd	nd	nd	nd	nd	nd	nd
Fluoranthene	47	34	23	61	47	17	31
Pyrene	44	34	26	53	56	22	31
Benzo (a) Anthracene	2.6	1.7	1.9	2.9	3.3	1.9	4.4
Chrysene	2.8	1.7	2.0	3.0	2.6	2.0	5.3
Benzo (b) Fluoranthene	2.9	1.6	1.8	2.5	2.9	2.0	5.5
Benzo (k) Fluoranthene	3.6	2.3	2.8	3.5	3.8	2.4	7.8
Benzo (e) Pyrene	2.8	1.7	2.0	2.8	3.0	2.1	6.0
Benzo (a) Pyrene	2.3	1.2	1.6	1.7	2.3	1.8	4.4
Perylene	4.4	3.1	3.9	3.5	6.2	4.9	8.3
Indeno (1,2,3 - cd) Pyrene	1.0	0.56	0.59	1.2	1.5	1.0	2.6
Dibenzo (a,h) anthracene	0.56	0.29	0.38	0.75	0.86	0.63	1.5
Benzo (g,h,i) perylene	1.5	0.77	1.1	1.5	1.8	1.3	4.3
TOTAL PAHs (ng/g)	**170**	**120**	**99**	**210**	**190**	**81**	**150**
*Co-eluting with internal standard							

Sample Name	3A	3B	4D	4E	4F	4G	4H
Core	D-50G	D-50G	D80	D80	D80	D80	D80
Depth (cm)	228-248	254-274	1-6	7-12	13-18	19-23	25-30
Date Range	1814-1798	1793-1777	1997-1992	1992-1990	1989-1987	1986-1984	1984-1981
Name	**Conc (ng/g)**	**Conc (ng/g)**	**Conc (ng/g)**	**Conc (ng/g)**	**Conc (ng/g)**	**Conc (ng/g)**	**Conc (ng/g)**
Naphthalene	nd	nd	nd	nd	nd	nd	nd
2-Methyl Naphthalene	0.76	1.9	1.5	1.6	1.0	6.7	10
1-Methyl Naphthalene	0.34	0.72	0.17	0.21	0.20	1.8	1.5
2,3,5-Trimethyl Naphthalene*	--	--	--	--	--	--	--
2,6-Dimethyl Naphthalene	0.27	1.0	3.4	3.5	3.1	2.3	2.2
Acenaphthylene	2.0	3.0	8.7	9.8	14	22	44
Acenaphthene	3.3	4.2	8.8	8.2	8.2	8.1	10
Biphenyl	nd	nd	nd	nd	nd	nd	nd
Fluorene	1.2	2.8	30	30	38	4.0	6.4
Phenanthrene	21	73	54	45	57	120	200
Anthracene	2.5	5.4	3.8	4.2	5.6	9.5	21
1-Methyl Phenanthrene	nd	nd	48	14	14	92	43
Fluoranthene	22	65	87	77	140	200	450
Pyrene	37	94	88	77	120	220	410
Benzo (a) Anthracene	1.7	1.5	4.8	4.6	3.9	3.7	2.4
Chrysene	0.82	0.49	4.6	4.8	5.0	4.4	3.2
Benzo (b) Fluoranthene	1.0	0.68	3.6	5.5	5.3	5.1	3.0
Benzo (k) Fluoranthene	1.5	1.0	3.8	3.5	4.0	5.8	3.5
Benzo (e) Pyrene	1.0	0.71	3.2	5.0	5.2	5.5	2.6
Benzo (a) Pyrene	0.82	0.55	1.8	2.6	2.4	2.5	1.3
Perylene	3.7	3.3	6.4	8.7	6.4	6.4	3.3
Indeno (1,2,3 - cd) Pyrene	0.38	0.29	1.0	1.9	1.8	1.7	1.0
Dibenzo (a,h) anthracene	0.25	0.14	0.55	1.0	0.84	0.95	0.60
Benzo (g,h,i) perylene	0.59	0.37	1.7	3.0	3.1	3.3	1.6
TOTAL PAHs (ng/g)	**100**	**260**	**360**	**310**	**440**	**730**	**1200**
*Co-eluting with internal standard							

Sample Name	4I	4J	4K	2N1235-16	2N1235-12	2N1235-18	2N1235-36
Core	D80	D80	D80	E30	E30	E30	E30
Depth (cm)	31-36	37-42	43-47	1-5	6-10	11-15	16-20
Date Range	1981-1979	1978-1976	1975-1974	1997-1993	1992-1988	1987-1982	1981-1977
Name	**Conc (ng/g)**	**Conc (ng/g)**	**Conc (ng/g)**	**Conc (ng/g)**	**Conc (ng/g)**	**Conc (ng/g)**	**Conc (ng/g)**
Naphthalene	nd	nd	nd	nd	nd	nd	nd
2-Methyl Naphthalene	12	12	13	0.13	0.24	0.16	0.05
1-Methyl Naphthalene	1.3	1.6	1.6	0.07	0.12	0.14	0.04
2,3,5-Trimethyl Naphthalene*	--	--	--	--	--	--	--
2,6-Dimethyl Naphthalene	2.3	2.3	1.4	0.10	0.06	0.14	0.02
Acenaphthylene	41	17	16	0.06	0.05	0.12	0.02
Acenaphthene	3.8	3.7	3.6	0.12	0.29	0.20	0.06
Biphenyl	nd	nd	nd	nd	nd	nd	nd
Fluorene	5.0	4.1	2.6	0.13	0.17	0.25	0.03
Phenanthrene	160	64	170	0.76	1.3	1.1	0.22
Anthracene	15	11	4.7	0.03	0.05	0.02	0.01
1-Methyl Phenanthrene	17	13	10	0.67	0.69	0.75	0.06
Fluoranthene	340	83	310	1.4	1.9	2.2	0.56
Pyrene	330	110	380	1.3	2.0	2.4	0.57
Benzo (a) Anthracene	2.2	2.3	2.0	1.5	2.1	2.5	0.78
Chrysene	2.8	2.1	2.2	1.8	2.1	2.6	0.93
Benzo (b) Fluoranthene	2.7	3.2	2.8	1.4	1.3	1.6	0.40
Benzo (k) Fluoranthene	3.7	3.4	3.4	1.5	1.6	2.0	0.35
Benzo (e) Pyrene	2.8	2.6	2.6	1.5	0.93	1.9	0.48
Benzo (a) Pyrene	1.6	1.3	1.3	0.68	0.78	1.6	0.29
Perylene	3.5	3.3	2.2	1.2	1.4	3.3	0.63
Indeno (1,2,3 - cd) Pyrene	1.3	1.4	0.92	0.63	0.80	0.93	0.45
Dibenzo (a,h) anthracene	0.66	0.53	0.46	nd	0.06	0.31	0.14
Benzo (g,h,i) perylene	2.0	1.9	1.8	1.5	0.88	2.0	0.46
TOTAL PAHs (ng/g)	**950**	**340**	**930**	**16**	**19**	**26**	**6.5**
*Co-eluting with internal standard							

Sample Name	2N1235-35	2N1235-08	2N1235-15	2N1235-01	2N1235-05	2N1235-22	2N1235-23
Core	E30	E30	E30	E50	E50	E50	E50
Depth (cm)	21-25	26-30	31-35	1-5	6-10	11-15	16-20
Date Range	1976-1972	1971-1966	1965-1960	1997-1993	1992-1987	1986-1982	1980-1976
Name	**Conc (ng/g)**	**Conc (ng/g)**	**Conc (ng/g)**	**Conc (ng/g)**	**Conc (ng/g)**	**Conc (ng/g)**	**Conc (ng/g)**
Naphthalene	nd	nd	nd	nd	nd	nd	nd
2-Methyl Naphthalene	0.09	0.18	0.25	0.43	0.16	0.06	0.12
1-Methyl Naphthalene	0.05	0.16	0.17	0.19	0.11	0.06	0.07
2,3,5-Trimethyl Naphthalene*	--	--	--	--	--	--	--
2,6-Dimethyl Naphthalene	0.02	0.09	0.09	0.17	0.08	0.07	0.06
Acenaphthylene	0.03	0.06	0.19	0.01	0.08	0.05	0.14
Acenaphthene	0.08	0.20	0.36	0.28	0.31	0.19	0.32
Biphenyl	nd	nd	nd	nd	nd	nd	nd
Fluorene	0.02	0.17	0.22	0.30	0.33	0.07	0.11
Phenanthrene	0.15	0.76	1.7	2.4	1.6	0.52	0.71
Anthracene	0.02	0.03	0.04	0.15	0.09	0.01	0.02
1-Methyl Phenanthrene	0.25	0.44	1.2	1.1	1.1	0.26	0.56
Fluoranthene	0.84	0.82	2.1	2.6	2.7	0.66	1.5
Pyrene	0.75	1.0	3.4	2.3	2.6	0.58	1.5
Benzo (a) Anthracene	0.70	1.6	2.4	3.4	2.3	0.86	1.6
Chrysene	1.4	1.2	2.4	2.7	2.1	0.89	2.4
Benzo (b) Fluoranthene	0.35	0.72	1.8	2.5	1.4	0.49	1.1
Benzo (k) Fluoranthene	0.59	0.86	1.8	3.0	2.0	0.60	1.4
Benzo (e) Pyrene	0.72	0.65	1.1	2.8	1.6	0.50	1.2
Benzo (a) Pyrene	0.43	0.71	1.3	3.3	1.4	0.35	1.2
Perylene	0.72	1.5	1.9	3.6	2.2	0.71	1.7
Indeno (1,2,3 - cd) Pyrene	0.43	0.31	0.85	6.7	1.5	0.56	1.3
Dibenzo (a,h) anthracene	nd	0.12	nd	5.5	0.56	0.65	0.51
Benzo (g,h,i) perylene	0.93	0.71	1.9	11	1.6	0.93	1.1
TOTAL PAHs (ng/g)	**8.5**	**12**	**25**	**54**	**26**	**9.1**	**19**
*Co-eluting with internal standard							

Sample Name	2N1235-27	2N1235-02	2N1235-04	2N1235-06	2N1235-17	2N1235-28	2N1235-03
Core	E50	E50	E50	E50	E50	E50	E50
Depth (cm)	21-25	26-30	31-35	36-40	41-45	46-50	51-54
Date Range	1975-1970	1969-1965	1964-1959	1958-1954	1953-1948	1947-1942	1941-1938
Name	**Conc (ng/g)**	**Conc (ng/g)**	**Conc (ng/g)**	**Conc (ng/g)**	**Conc (ng/g)**	**Conc (ng/g)**	**Conc (ng/g)**
Naphthalene	nd	nd	nd	nd	nd	nd	nd
2-Methyl Naphthalene	0.13	0.13	0.11	0.14	0.14	0.04	0.17
1-Methyl Naphthalene	0.08	0.09	0.09	0.25	0.10	0.03	0.12
2,3,5-Trimethyl Naphthalene*	--	--	--	--	--	--	--
2,6-Dimethyl Naphthalene	0.08	0.06	0.07	0.06	0.08	0.04	0.08
Acenaphthylene	0.06	0.20	0.10	0.06	0.12	0.04	nd
Acenaphthene	0.27	0.31	0.30	0.12	0.11	0.07	0.22
Biphenyl	nd	nd	nd	nd	nd	nd	nd
Fluorene	0.70	0.33	0.09	0.26	0.18	0.04	0.11
Phenanthrene	3.6	2.2	1.0	0.99	1.2	0.19	0.79
Anthracene	0.32	0.10	0.06	0.03	0.02	0.01	0.04
1-Methyl Phenanthrene	4.5	1.7	0.87	0.86	0.55	0.29	0.83
Fluoranthene	20	2.6	1.3	1.5	1.2	1.3	0.95
Pyrene	14	2.9	1.7	2.1	1.4	1.2	0.85
Benzo (a) Anthracene	12	2.7	1.5	2.3	1.4	0.87	1.0
Chrysene	15	2.8	1.9	1.6	1.9	1.8	1.2
Benzo (b) Fluoranthene	11	2.8	1.0	2.1	0.90	1.2	0.58
Benzo (k) Fluoranthene	13	3.1	1.2	1.3	1.0	0.94	0.78
Benzo (e) Pyrene	11	3.0	1.0	1.4	0.67	1.9	0.51
Benzo (a) Pyrene	11	3.2	1.0	1.6	0.56	1.2	0.67
Perylene	5.1	3.6	1.6	1.8	1.3	2.1	0.72
Indeno (1,2,3 - cd) Pyrene	7.0	3.2	0.83	1.2	0.47	1.5	0.61
Dibenzo (a,h) anthracene	2.6	2.0	0.50	0.64	0.07	0.66	0.50
Benzo (g,h,i) perylene	12	6.8	1.8	2.1	0.67	1.9	1.4
TOTAL PAHs (ng/g)	**140**	**44**	**18**	**23**	**14**	**17**	**12**
*Co-eluting with internal standard							

Sample Name	2N1235-26	2N1235-31	2N1235-24	2N1235-29	2N1235-10	2N1235-33	2N1235-32
Core	E60	E60	E60	E60	E60	E60	E60
Depth (cm)	1-5	6-10	11-15	16-20	21-25	26-30	31-35
Date Range	1997-1991	1990-1984	1983-1977	1976-1970	1968-1963	1961-1956	1954-1948
Name	**Conc (ng/g)**	**Conc (ng/g)**	**Conc (ng/g)**	**Conc (ng/g)**	**Conc (ng/g)**	**Conc (ng/g)**	**Conc (ng/g)**
Naphthalene	nd	nd	nd	nd	nd	nd	nd
2-Methyl Naphthalene	0.10	0.14	0.12	0.10	0.17	0.08	0.11
1-Methyl Naphthalene	0.05	0.04	0.11	0.05	0.09	0.05	0.09
2,3,5-Trimethyl Naphthalene*	--	--	--	--	--	--	--
2,6-Dimethyl Naphthalene	0.05	0.04	0.04	0.03	0.09	0.04	0.05
Acenaphthylene	0.06	0.02	0.04	0.04	0.05	0.07	0.04
Acenaphthene	0.14	0.06	0.23	0.07	0.18	0.12	0.14
Biphenyl	nd	nd	nd	nd	nd	nd	nd
Fluorene	0.08	0.05	0.11	0.05	0.19	0.04	0.03
Phenanthrene	0.36	0.29	0.71	0.38	0.51	0.21	0.35
Anthracene	0.02	0.01	0.02	0.02	0.04	0.01	0.02
1-Methyl Phenanthrene	0.23	0.19	0.47	0.22	0.46	0.13	0.16
Fluoranthene	1.3	1.8	2.2	1.8	1.0	1.0	1.1
Pyrene	1.0	1.7	2.0	1.7	1.1	1.2	1.5
Benzo (a) Anthracene	0.66	1.0	1.4	1.6	1.4	0.78	0.74
Chrysene	1.4	1.3	1.9	1.4	1.7	1.1	1.4
Benzo (b) Fluoranthene	0.40	0.75	1.0	0.69	0.66	0.50	0.51
Benzo (k) Fluoranthene	0.54	0.86	1.2	0.92	0.77	0.57	0.69
Benzo (e) Pyrene	0.76	0.68	1.1	0.80	0.80	0.62	0.72
Benzo (a) Pyrene	0.49	0.46	1.0	0.43	0.62	0.41	0.59
Perylene	0.72	0.57	1.1	0.73	0.94	0.69	0.63
Indeno (1,2,3 - cd) Pyrene	0.55	0.47	0.86	0.93	0.39	0.47	0.42
Dibenzo (a,h) anthracene	0.16	0.05	0.53	nd	0.33	0.06	0.09
Benzo (g,h,i) perylene	0.60	0.65	1.4	1.4	0.39	0.66	0.83
TOTAL PAHs (ng/g)	**9.6**	**11**	**18**	**13**	**12**	**8.8**	**10**
*Co-eluting with internal standard							

Sample Name	2N1235-34	2N1235-30	2N1235-07	2N1235-13	2N1235-20	2N1235-25	2N1235-09
Core	E60	E60	E60	F35	F35	F35	F35
Depth (cm)	36-40	41-45	46-47	1-5	6-10	11-15	16-20
Date Range	1947-1941	1940-1934	1933-1931	1997-1992	1990-1985	1983-1978	1976-1971
Name	**Conc (ng/g)**	**Conc (ng/g)**	**Conc (ng/g)**	**Conc (ng/g)**	**Conc (ng/g)**	**Conc (ng/g)**	**Conc (ng/g)**
Naphthalene	nd	nd	nd	nd	nd	nd	nd
2-Methyl Naphthalene	0.08	0.06	0.59	0.26	0.11	0.05	0.17
1-Methyl Naphthalene	0.05	0.03	0.39	0.10	0.17	0.03	0.13
2,3,5-Trimethyl Naphthalene*	--	--	--	--	--	--	--
2,6-Dimethyl Naphthalene	0.03	0.04	0.26	0.06	0.07	0.07	0.06
Acenaphthylene	0.04	0.03	0.18	0.09	0.08	0.03	0.07
Acenaphthene	0.15	0.11	1.0	0.44	0.20	0.19	0.18
Biphenyl	nd	nd	nd	nd	nd	nd	nd
Fluorene	0.03	0.05	0.58	0.30	0.14	0.05	0.25
Phenanthrene	0.20	0.29	2.4	1.0	0.50	0.33	0.95
Anthracene	0.01	0.02	0.07	0.04	0.01	0.02	0.05
1-Methyl Phenanthrene	0.07	0.19	1.7	0.91	0.34	0.19	0.84
Fluoranthene	0.44	0.49	1.9	1.8	0.88	0.64	1.3
Pyrene	0.50	0.61	2.1	1.8	0.87	0.72	1.7
Benzo (a) Anthracene	0.79	0.81	2.9	2.8	1.4	0.82	2.4
Chrysene	0.81	0.77	3.8	1.5	1.4	0.79	2.0
Benzo (b) Fluoranthene	0.28	0.26	1.5	1.2	1.0	0.29	2.5
Benzo (k) Fluoranthene	0.31	0.35	1.5	1.5	0.93	0.50	2.4
Benzo (e) Pyrene	0.28	0.36	1.6	1.3	1.1	0.33	3.8
Benzo (a) Pyrene	0.25	0.23	1.2	1.1	1.2	0.24	5.2
Perylene	0.40	1.0	1.7	2.6	1.6	0.27	4.4
Indeno (1,2,3 - cd) Pyrene	0.38	0.25	1.2	0.72	3.1	0.40	1.4
Dibenzo (a,h) anthracene	0.05	0.09	nd	0.08	2.5	0.46	1.7
Benzo (g,h,i) perylene	0.39	0.08	1.5	1.3	5.4	0.58	3.8
TOTAL PAHs (ng/g)	**5.5**	**6.1**	**28**	**21**	**23**	**7.0**	**35**
*Co-eluting with internal standard							

Sample Name	2N1235-21	2N1235-19	2N1235-11	2N1235-14	3H	3I	3J
Core	F35	F35	F35	F35	G40	G40	G40
Depth (cm)	21-25	26-30	31-35	36-39	1-6	7-12	13-17
Date Range	1970-1964	1963-1957	1956-1950	1949-1945	1989-1939	1931-1889	1881-1847
Name	**Conc (ng/g)**	**Conc (ng/g)**	**Conc (ng/g)**	**Conc (ng/g)**	**Conc (ng/g)**	**Conc (ng/g)**	**Conc (ng/g)**
Naphthalene	nd	nd	nd	nd	nd	nd	nd
2-Methyl Naphthalene	0.08	0.14	0.23	0.16	2.2	0.92	0.85
1-Methyl Naphthalene	0.07	0.08	0.08	0.09	0.93	0.15	0.28
2,3,5-Trimethyl Naphthalene*	--	--	--	--	--	--	--
2,6-Dimethyl Naphthalene	0.07	0.09	0.08	0.08	1.2	0.44	0.28
Acenaphthylene	0.07	0.08	0.04	0.05	17	6.0	1.5
Acenaphthene	0.24	0.38	0.54	0.20	13	8.0	1.1
Biphenyl	nd	nd	nd	nd	nd	nd	nd
Fluorene	0.09	0.08	0.14	0.16	3.2	2.1	0.69
Phenanthrene	0.57	0.41	0.51	0.61	109	43	7.1
Anthracene	0.04	0.02	0.03	0.02	2.5	1.3	0.85
1-Methyl Phenanthrene	0.44	0.29	0.15	0.56	35	18	15
Fluoranthene	0.91	0.51	0.43	0.57	139	72	8.3
Pyrene	1.3	0.65	0.44	0.67	166	70	10
Benzo (a) Anthracene	1.3	1.8	0.86	0.92	2.5	1.7	0.88
Chrysene	1.4	1.6	1.1	1.2	1.9	1.0	0.72
Benzo (b) Fluoranthene	1.0	1.6	0.16	0.26	1.3	1.2	0.64
Benzo (k) Fluoranthene	1.2	1.7	0.26	0.53	1.5	0.91	0.91
Benzo (e) Pyrene	1.0	2.4	0.20	0.47	1.2	0.92	0.67
Benzo (a) Pyrene	0.75	1.5	0.22	0.24	0.68	0.49	0.34
Perylene	2.2	2.0	0.70	0.43	9.5	7.4	29
Indeno (1,2,3 - cd) Pyrene	0.69	15	0.22	0.18	0.39	0.29	0.26
Dibenzo (a,h) anthracene	0.90	13	nd	0.07	0.18	0.16	0.19
Benzo (g,h,i) perylene	1.7	24	0.36	0.26	0.63	0.50	0.53
TOTAL PAHs (ng/g)	**16**	**67**	**6.7**	**7.7**	**510**	**240**	**80**
*Co-eluting with internal standard							

Sample Name	3K	4L	4M	4N	3C	3D	3E
Core	G40	G50	G50	G50	SWI3	SWI3	SWI3
Depth (cm)	18-22	1-5	6-10	11-14	1-6	7-12	13-17
Date Range	1839-1806	1989-1956	1949-1922	1916-1896	1999-1986	1984-1971	1969-1959
Name	**Conc (ng/g)**	**Conc (ng/g)**	**Conc (ng/g)**	**Conc (ng/g)**	**Conc (ng/g)**	**Conc (ng/g)**	**Conc (ng/g)**
Naphthalene	nd	nd	nd	nd	nd	nd	nd
2-Methyl Naphthalene	0.60	7.3	6.9	5.4	3.3	2.6	1.9
1-Methyl Naphthalene	0.22	1.6	1.5	1.3	0.91	0.73	0.74
2,3,5-Trimethyl Naphthalene*	--	--	--	--	--	--	--
2,6-Dimethyl Naphthalene	0.37	0.77	0.60	0.54	1.3	1.3	1.6
Acenaphthylene	0.49	2.0	2.1	2.1	3.6	4.4	5.9
Acenaphthene	0.67	3.7	3.8	3.8	7.8	14	10
Biphenyl	nd	nd	nd	nd	nd	nd	nd
Fluorene	0.80	2.6	2.4	2.4	5.0	5.1	5.6
Phenanthrene	8.3	32	21	18	25	28	48
Anthracene	0.60	3.2	2.6	2.0	2.3	2.4	2.9
1-Methyl Phenanthrene	13	0.00	0.00	0.00	29	32	35
Fluoranthene	7.6	35	20	15	28	36	50
Pyrene	10	44	25	19	48	40	51
Benzo (a) Anthracene	0.47	0.47	0.37	0.23	2.3	1.9	2.8
Chrysene	0.68	0.60	0.50	0.36	1.3	0.31	0.71
Benzo (b) Fluoranthene	0.51	0.42	0.33	0.21	2.6	0.64	1.2
Benzo (k) Fluoranthene	0.36	0.50	0.42	0.29	3.2	0.43	1.4
Benzo (e) Pyrene	0.32	0.33	0.36	0.30	2.2	0.46	0.74
Benzo (a) Pyrene	0.08	0.28	0.20	0.17	2.3	0.42	0.92
Perylene	28	8.0	9.2	16	2.3	2.4	3.9
Indeno (1,2,3 - cd) Pyrene	0.13	0.13	0.17	0.07	1.1	0.17	0.43
Dibenzo (a,h) anthracene	0.06	0.08	0.00	0.07	0.62	0.09	0.26
Benzo (g,h,i) perylene	0.20	0.25	0.25	0.19	1.3	0.25	0.60
TOTAL PAHs (ng/g)	**73**	**140**	**98**	**87**	**170**	**170**	**230**
*Co-eluting with internal standard							

Sample Name	3F	3G
Core	SWI3	SWI3
Depth (cm)	18-22	23-27
Date Range	1956-1946	1944-1934
Name	**Conc (ng/g)**	**Conc (ng/g)**
Naphthalene	nd	nd
2-Methyl Naphthalene	1.7	1.9
1-Methyl Naphthalene	0.86	0.79
2,3,5-Trimethyl Naphthalene*	--	--
2,6-Dimethyl Naphthalene	1.1	1.6
Acenaphthylene	2.6	1.0
Acenaphthene	3.1	8.0
Biphenyl	nd	nd
Fluorene	2.5	2.8
Phenanthrene	31	25
Anthracene	1.8	1.5
1-Methyl Phenanthrene	30	14
Fluoranthene	26	12
Pyrene	25	11
Benzo (a) Anthracene	1.9	0.81
Chrysene	1.3	0.72
Benzo (b) Fluoranthene	0.76	0.41
Benzo (k) Fluoranthene	0.92	0.35
Benzo (e) Pyrene	0.42	0.20
Benzo (a) Pyrene	0.44	0.23
Perylene	3.5	2.3
Indeno (1,2,3 - cd) Pyrene	0.25	0.14
Dibenzo (a,h) anthracene	0.22	0.08
Benzo (g,h,i) perylene	0.40	0.25
TOTAL PAHs (ng/g)	**130**	**85**

*Co-eluting with internal standard

APPENDIX F

Total PAH Histograms by Decade

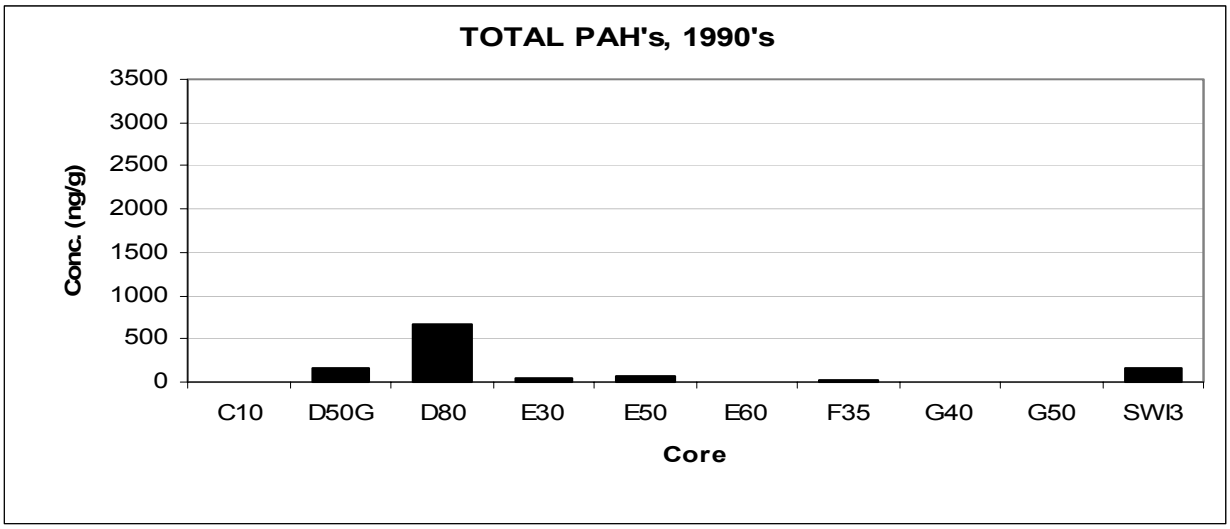
TOTAL PAH's, 1990's
Conc. (ng/g)
3500
3000
2500
2000
1500
1000
500
0
C10
D50G
D80
E30
E50
E60
F35
G40
G50
SWI3
Core

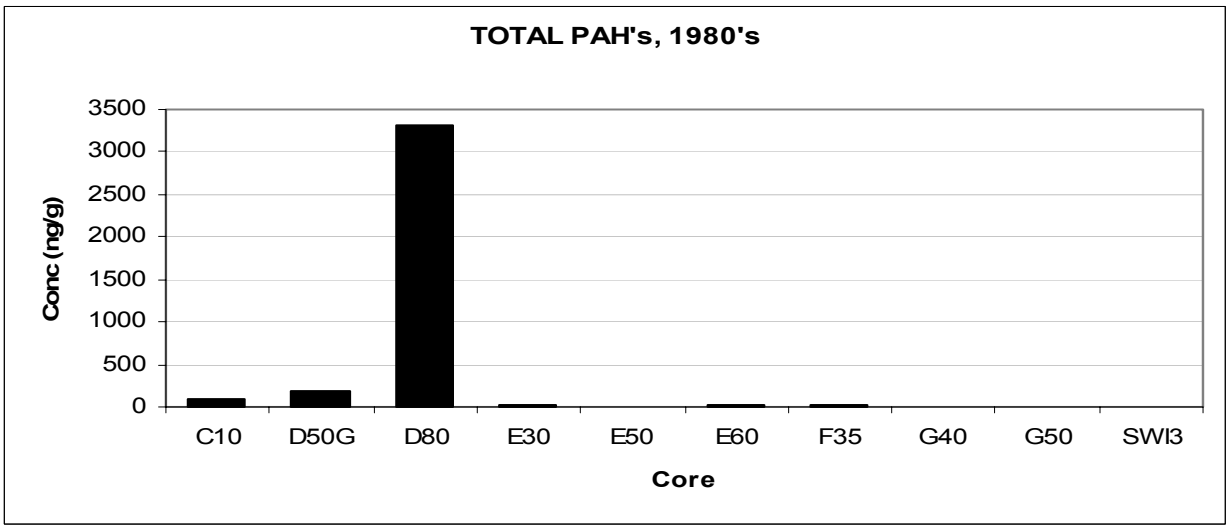
TOTAL PAH's, 1980's
Conc (ng/g)
3500
3000
2500
2000
1500
1000
500
0
C10
D50G
D80
E30
E50
E60
F35
G40
G50
SWI3
Core

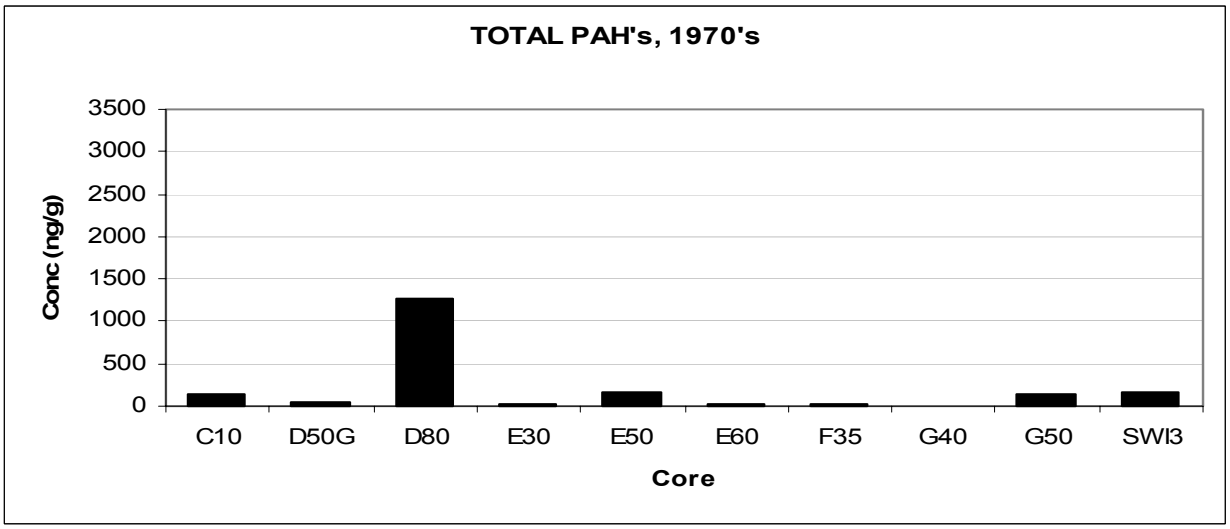
TOTAL PAH's, 1970's
Conc (ng/g)
3500
3000
2500
2000
1500
1000
500
0
C10
D50G
D80
E30
E50
E60
F35
G40
G50
SWI3
Core

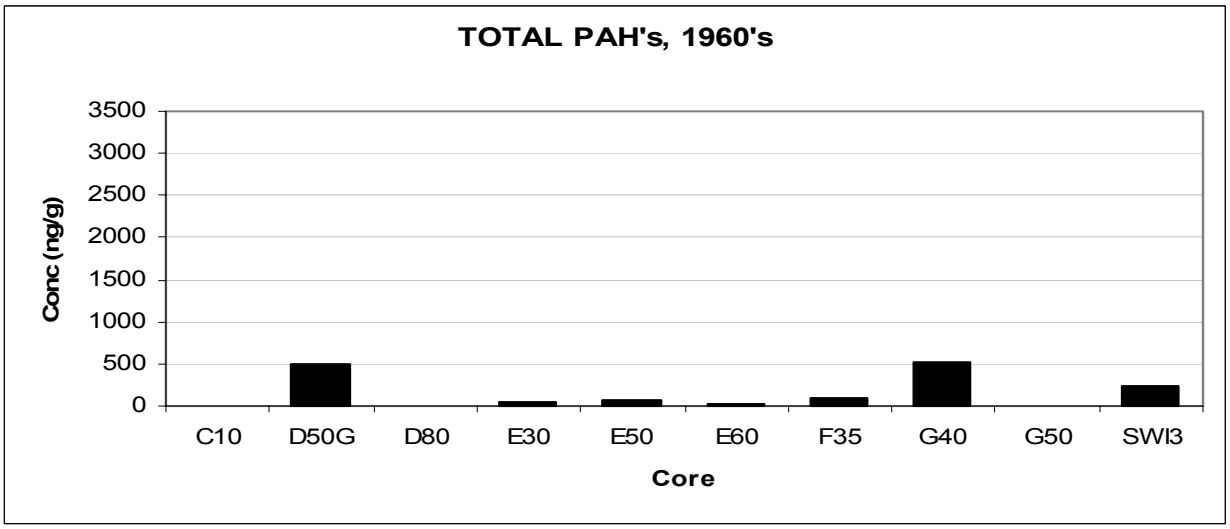
TOTAL PAH's, 1960's
Conc (ng/g)
3500
3000
2500
2000
1500
1000
500
0
C10
D50G
D80
E30
E50
E60
F35
G40
G50
SWI3
Core

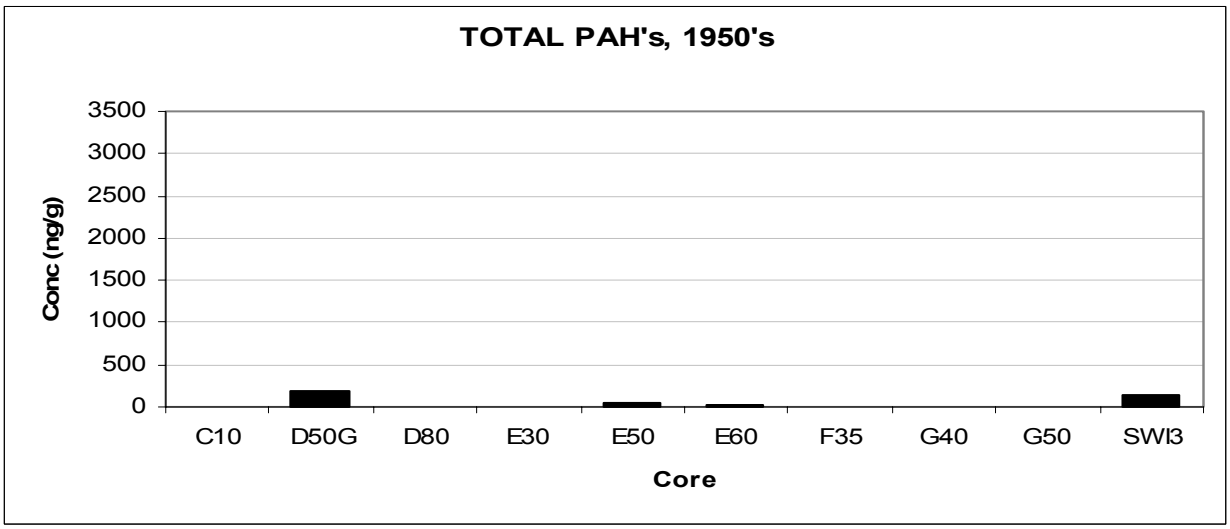
TOTAL PAH's, 1950's
Conc (ng/g)
3500
3000
2500
2000
1500
1000
500
0
C10
D50G
D80
E30
E50
E60
F35
G40
G50
SWI3
Core

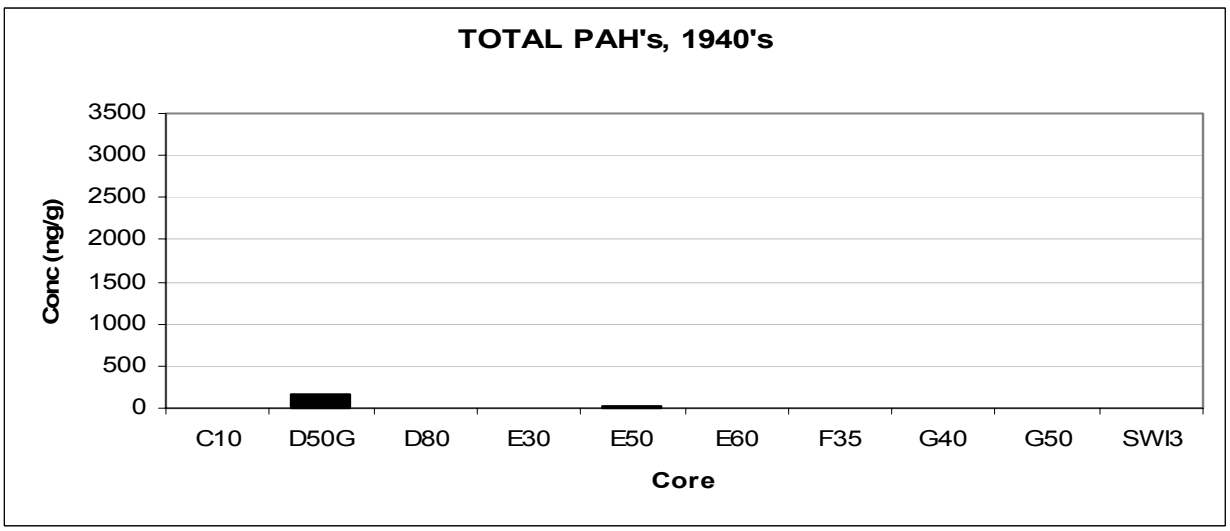
TOTAL PAH's, 1940's
Conc (ng/g)
3500
3000
2500
2000
1500
1000
500
0
C10
D50G
D80
E30
E50
E60
F35
G40
G50
SWI3
Core

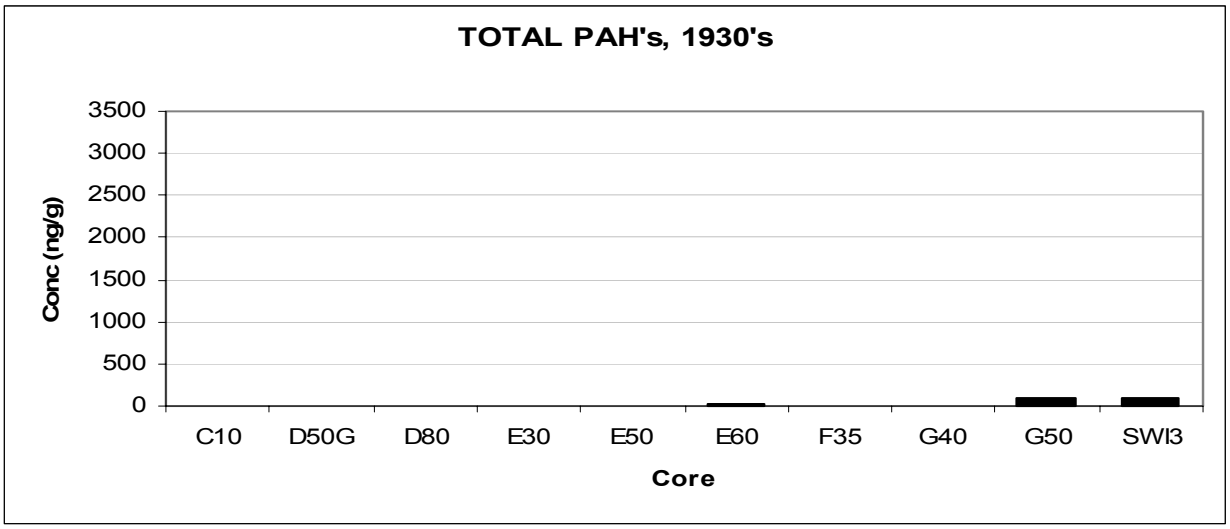
TOTAL PAH's, 1930's
Conc (ng/g)
3500
3000
2500
2000
1500
1000
500
0
C10
D50G
D80
E30
E50
E60
F35
G40
G50
SWI3
Core

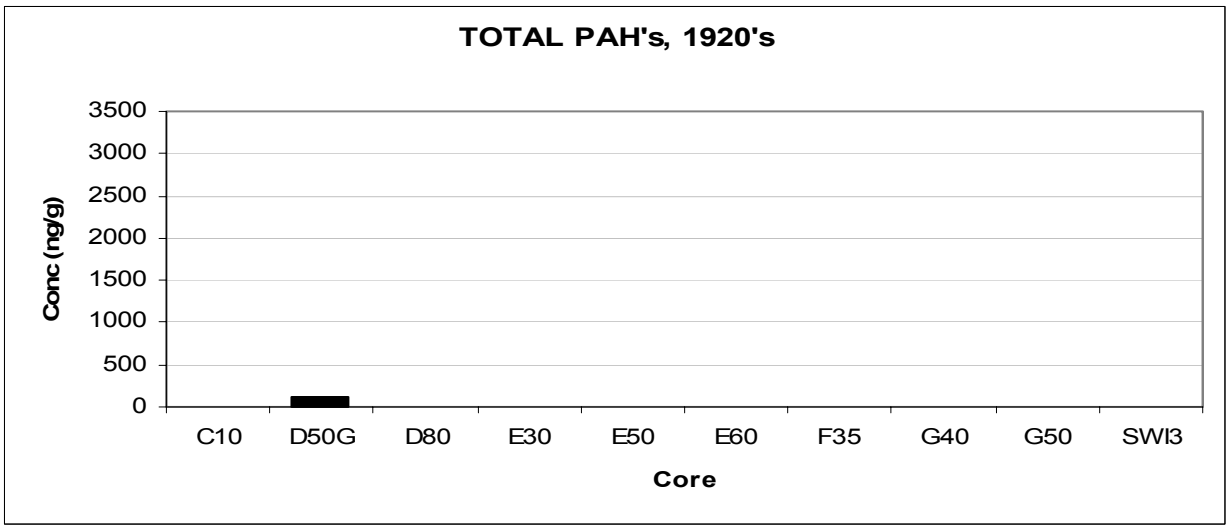
TOTAL PAH's, 1920's
Conc (ng/g)
3500
3000
2500
2000
1500
1000
500
0
C10
D50G
D80
E30
E50
E60
F35
G40
G50
SWI3
Core

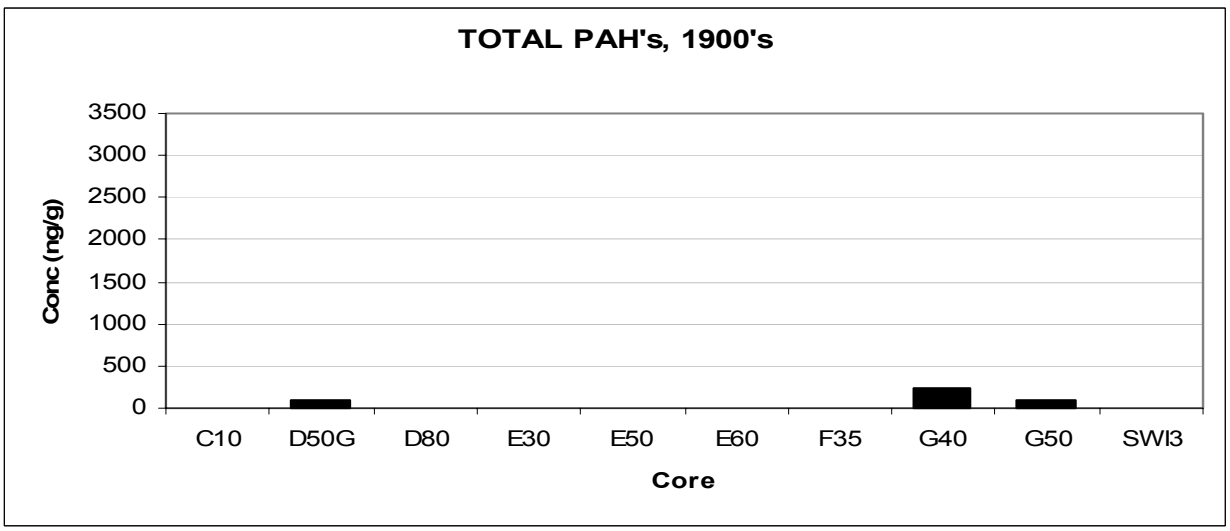
TOTAL PAH's, 1900's
Conc (ng/g)
3500
3000
2500
2000
1500
1000
500
0
C10
D50G
D80
E30
E50
E60
F35
G40
G50
SWI3
Core

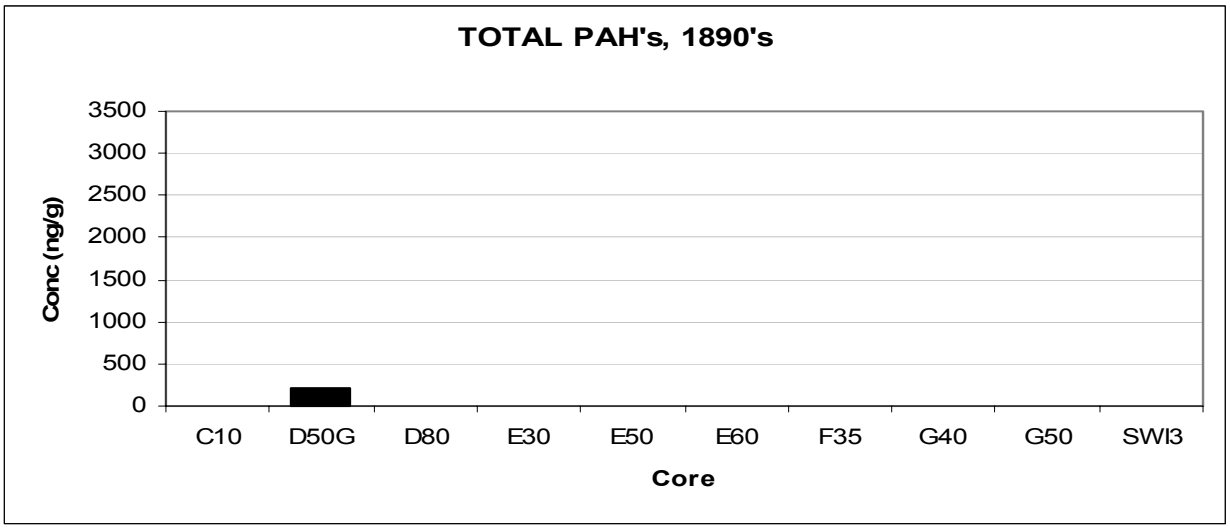
TOTAL PAH's, 1890's
Conc (ng/g)
3500
3000
2500
2000
1500
1000
500
0
C10
D50G
D80
E30
E50
E60
F35
G40
G50
SWI3
Core

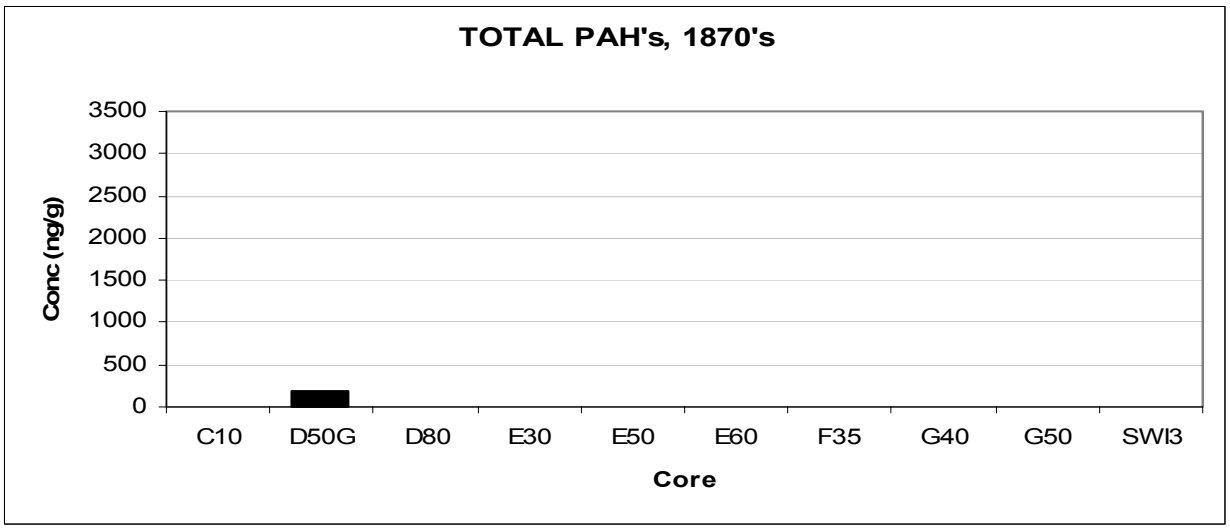
TOTAL PAH's, 1870's
Conc (ng/g)
3500
3000
2500
2000
1500
1000
500
0
C10
D50G
D80
E30
E50
E60
F35
G40
G50
SWI3
Core

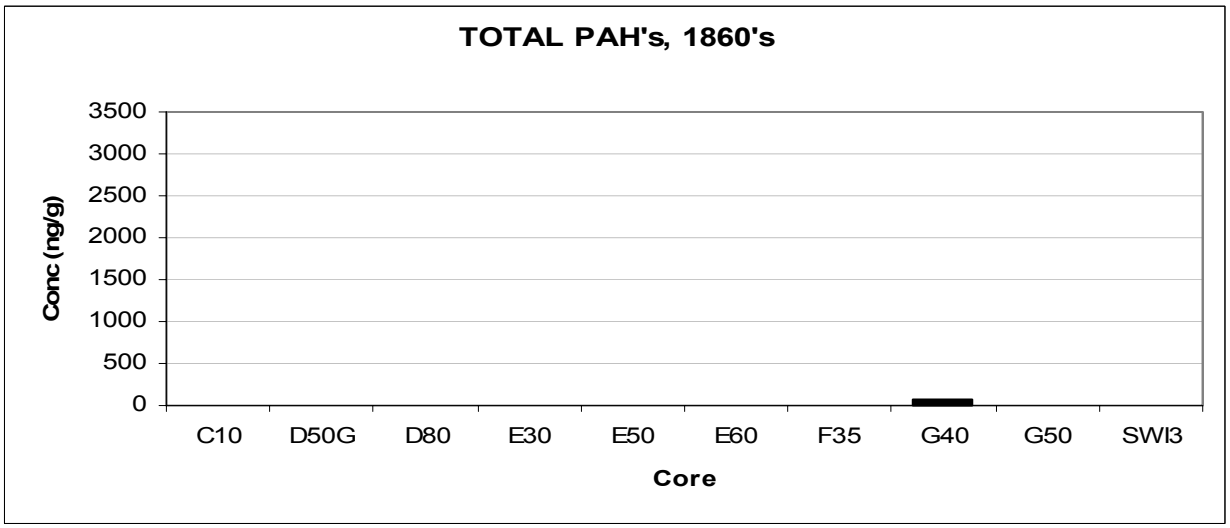
TOTAL PAH's, 1860's
Conc (ng/g)
3500
3000
2500
2000
1500
1000
500
0
C10
D50G
D80
E30
E50
E60
F35
G40
G50
SWI3
Core

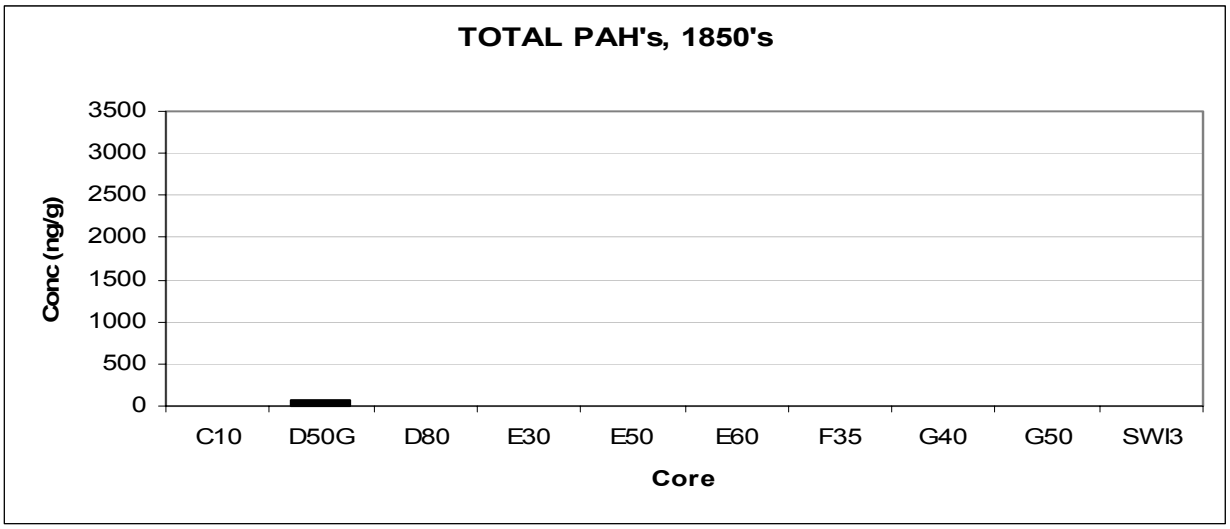
TOTAL PAH's, 1850's
Conc (ng/g)
3500
3000
2500
2000
1500
1000
500
0
C10
D50G
D80
E30
E50
E60
F35
G40
G50
SWI3
Core

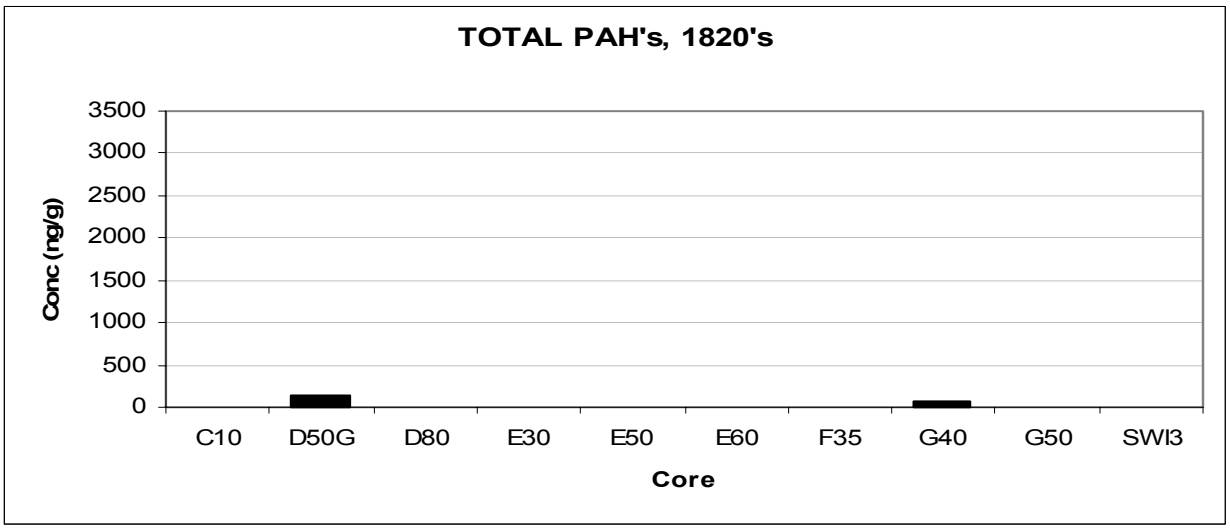
TOTAL PAH's, 1820's
Conc (ng/g)
3500
3000
2500
2000
1500
1000
500
0
C10
D50G
D80
E30
E50
E60
F35
G40
G50
SWI3
Core

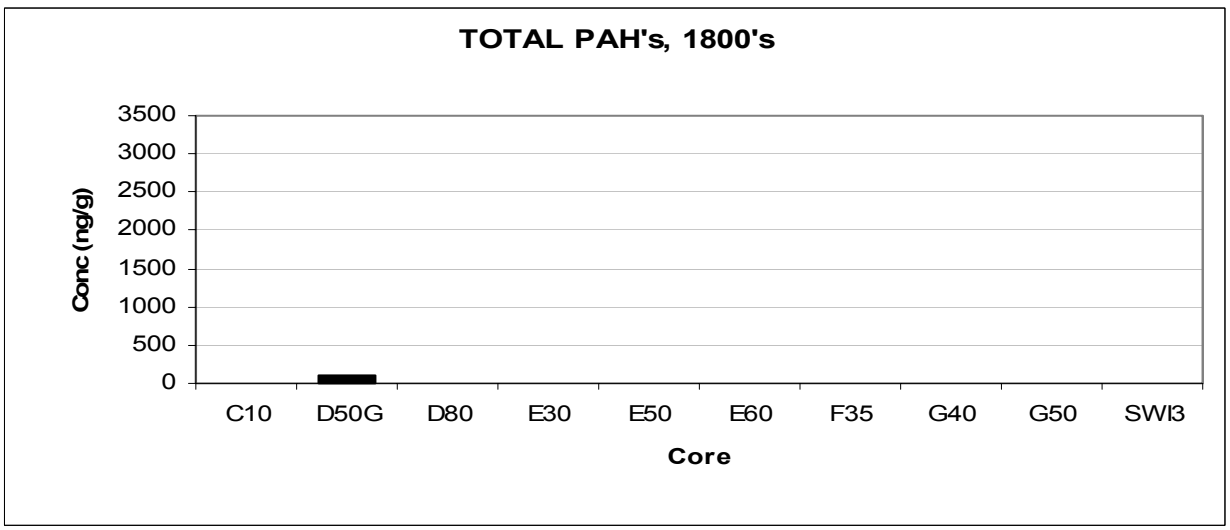
TOTAL PAH's, 1800's
Conc (ng/g)
3500
3000
2500
2000
1500
1000
500
0
C10
D50G
D80
E30
E50
E60
F35
G40
G50
SWI3
Core

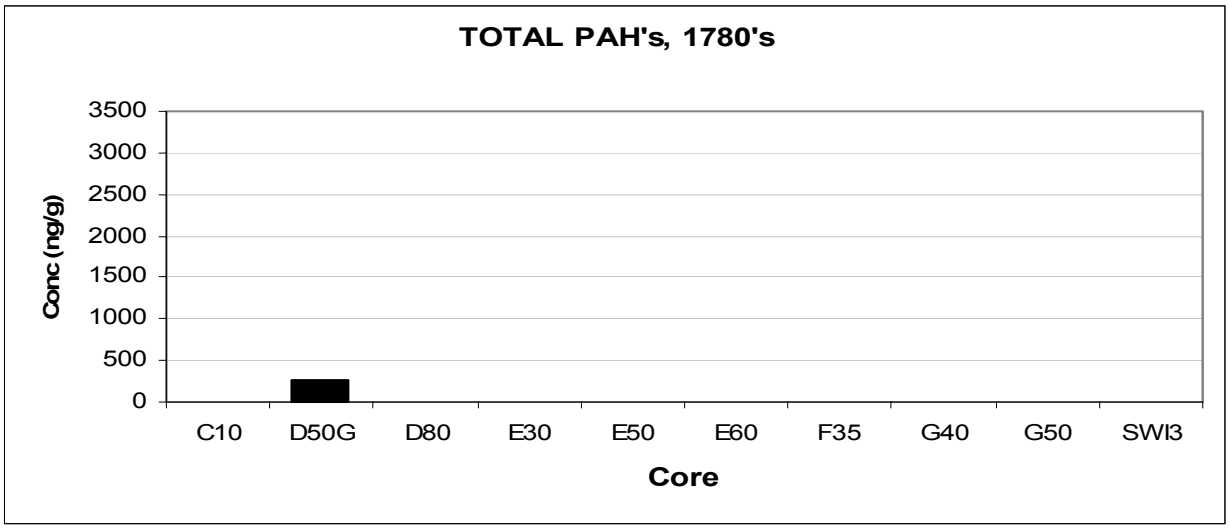
TOTAL PAH's, 1780's
Conc (ng/g)
3500
3000
2500
2000
1500
1000
500
0
C10
D50G
D80
E30
E50
E60
F35
G40
G50
SWI3
Core

APPENDIX G

Total PAH vs. Estimated Total Hopane Concentrations by Core and Date

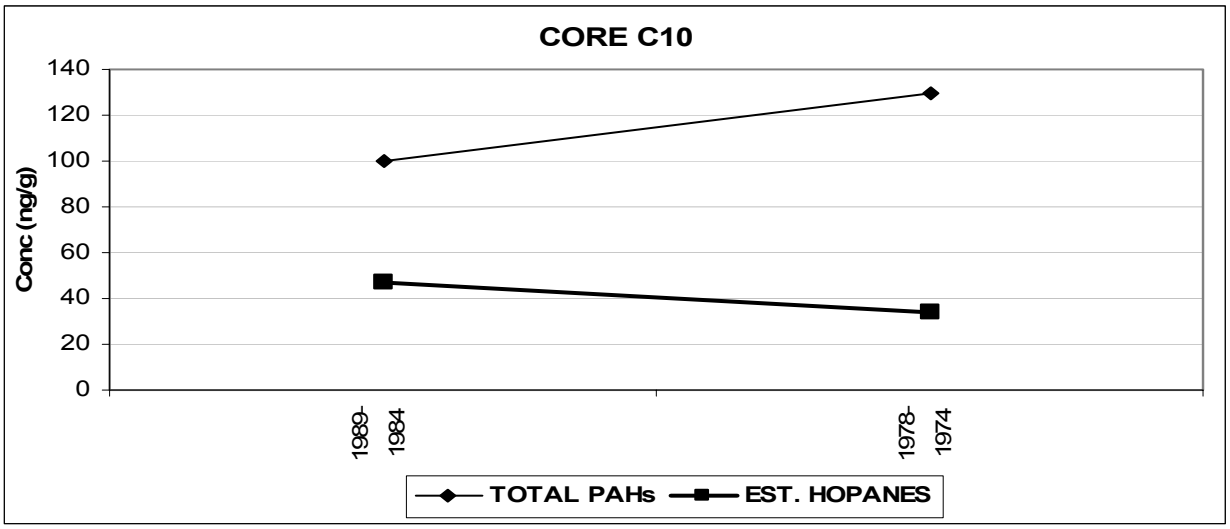
CORE C10
Conc (ng/g)
140
120
100
80
60
40
20
0
1989-1984
1978-1974
TOTAL PAHs
EST. HOPANES

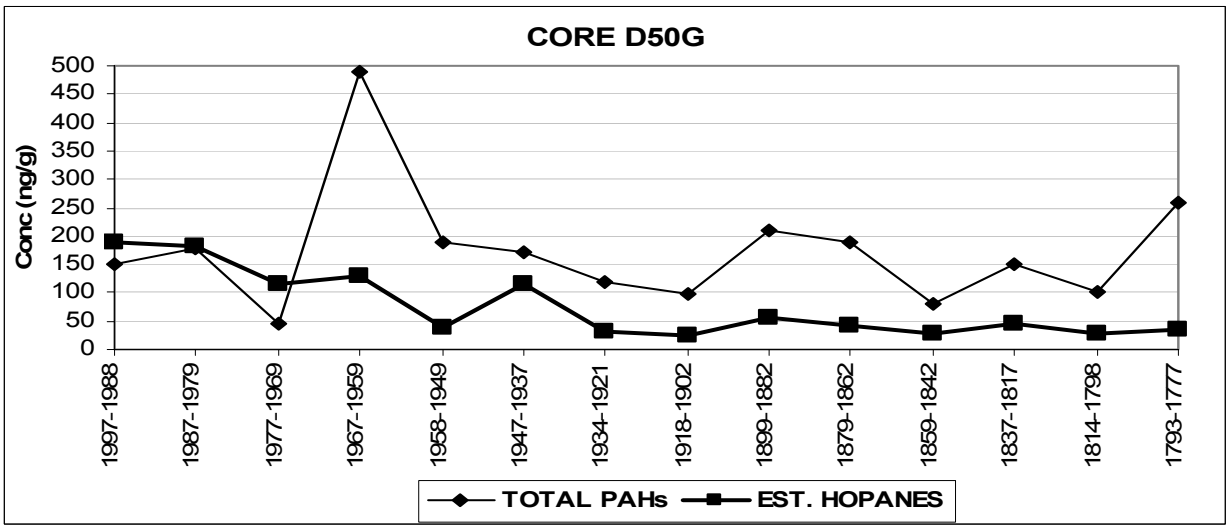
CORE D50G
Conc (ng/g)
500
450
400
350
300
250
200
150
100
50
0
1997-1988
1987-1979
1977-1969
1967-1959
1958-1949
1947-1937
1934-1921
1918-1902
1899-1882
1879-1862
1859-1842
1837-1817
1814-1798
1793-1777
TOTAL PAHs
EST. HOPANES

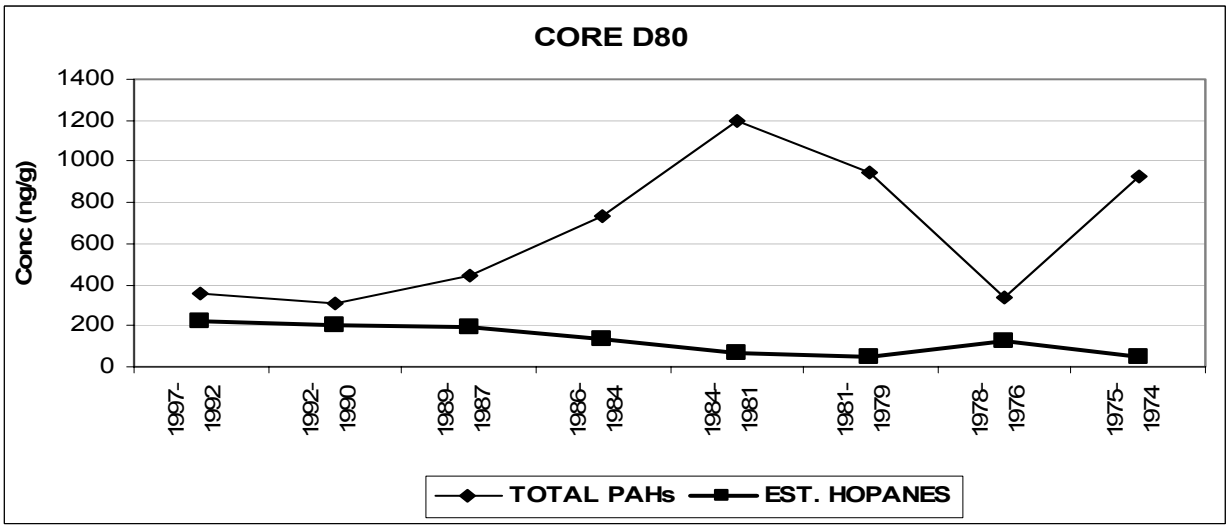
CORE D80
Conc (ng/g)
1400
1200
1000
800
600
400
200
0
1997-1992
1992-1990
1989-1987
1986-1984
1984-1981
1981-1979
1978-1976
1975-1974
TOTAL PAHs
EST. HOPANES

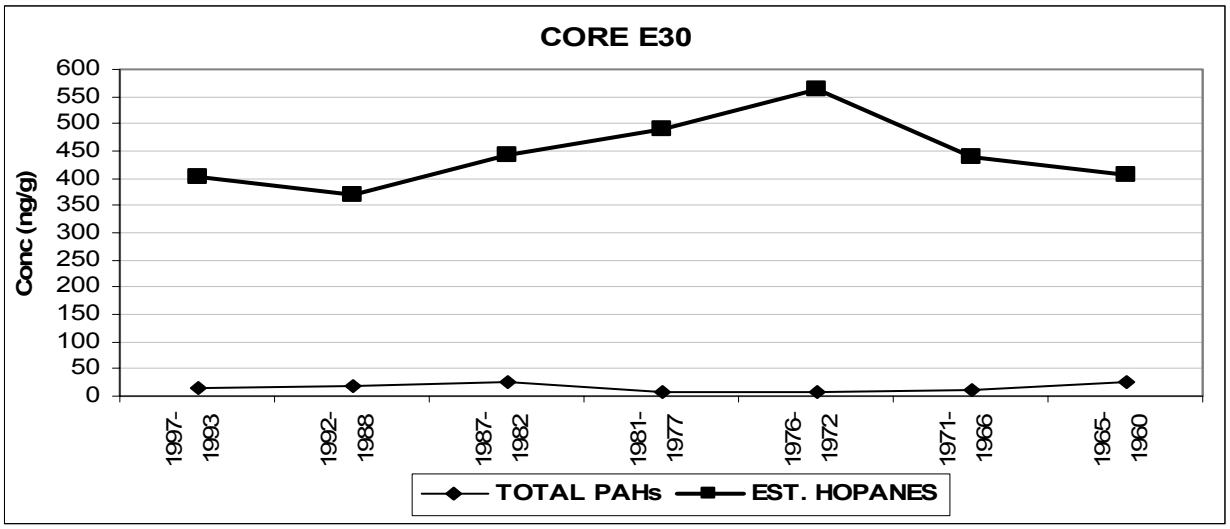
CORE E30
Conc (ng/g)
600
550
500
450
400
350
300
250
200
150
100
50
0
1997-1993
1992-1988
1987-1982
1981-1977
1976-1972
1971-1966
1965-1960
TOTAL PAHs
EST. HOPANES

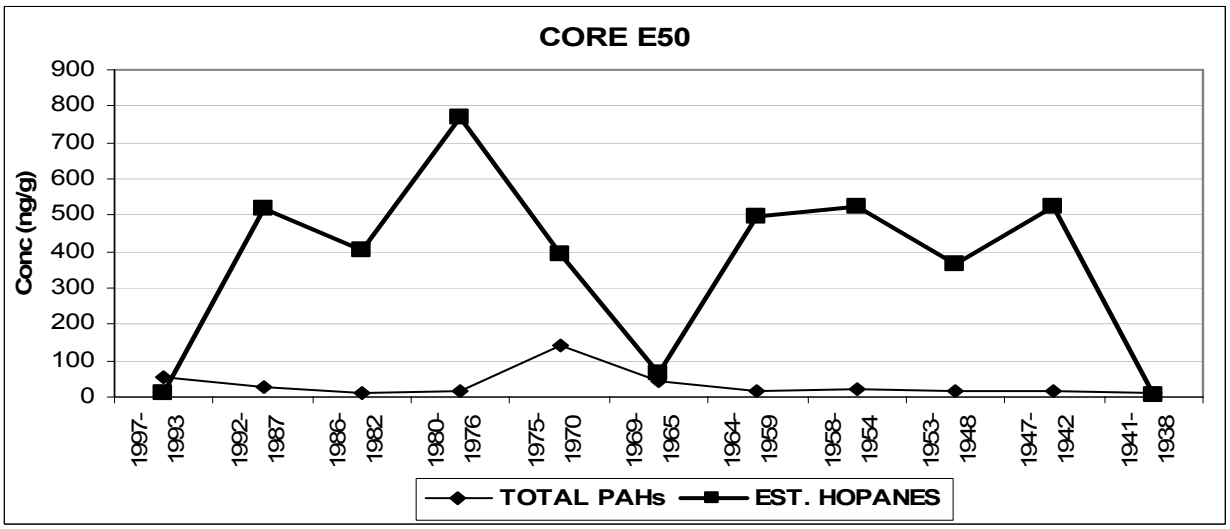
CORE E50
Conc (ng/g)
900
800
700
600
500
400
300
200
100
0
1997-1993
1992-1987
1986-1982
1980-1976
1975-1970
1969-1965
1964-1959
1958-1954
1953-1948
1947-1942
1941-1938
TOTAL PAHs
EST. HOPANES

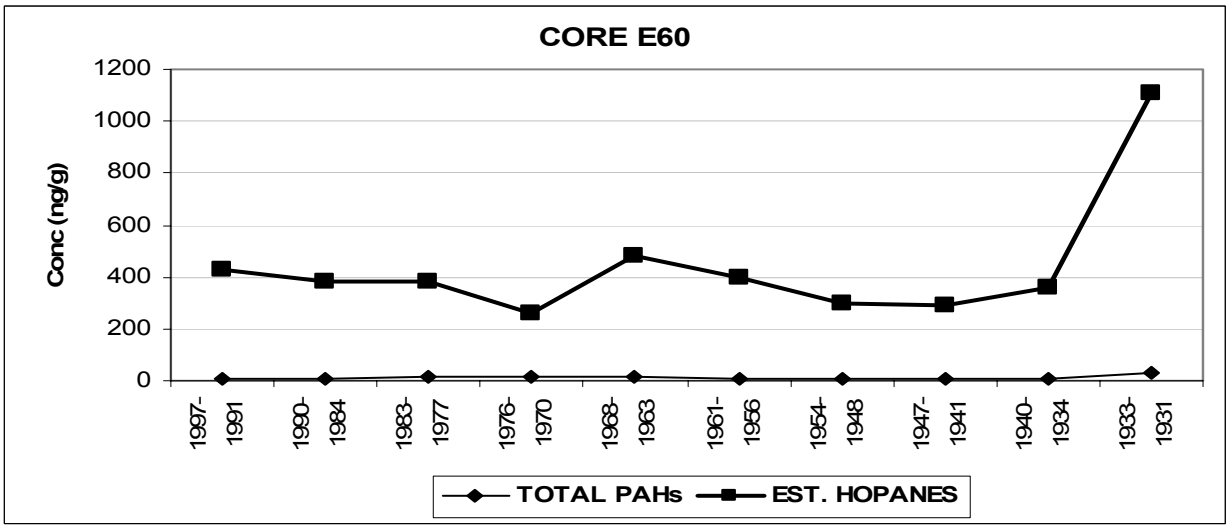
CORE E60
Conc (ng/g)
1200
1000
800
600
400
200
0
1997-1991
1990-1984
1983-1977
1976-1970
1968-1963
1961-1956
1954-1948
1947-1941
1940-1934
1933-1931
TOTAL PAHs
EST. HOPANES

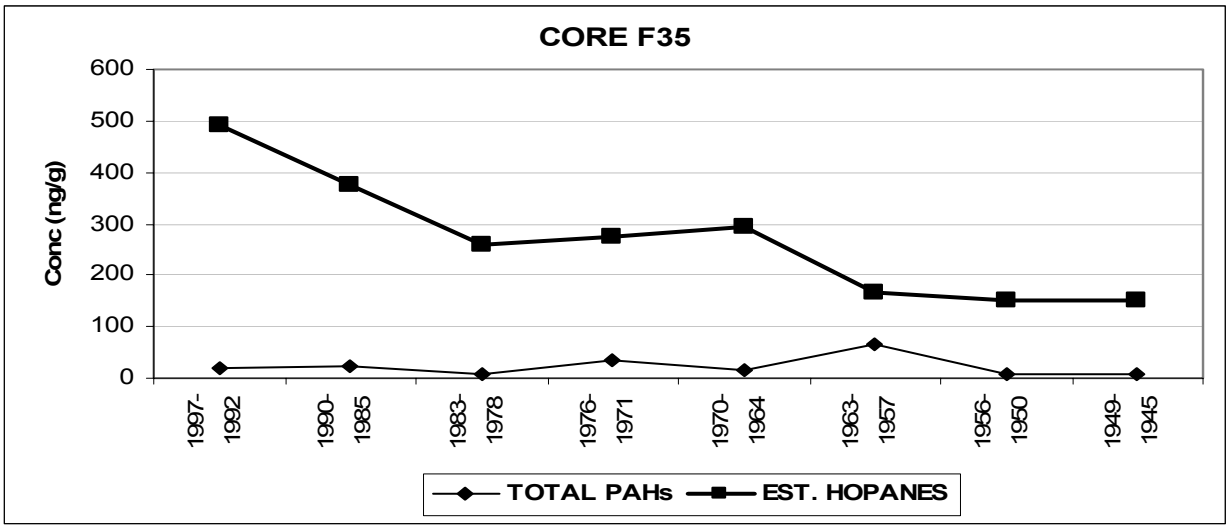

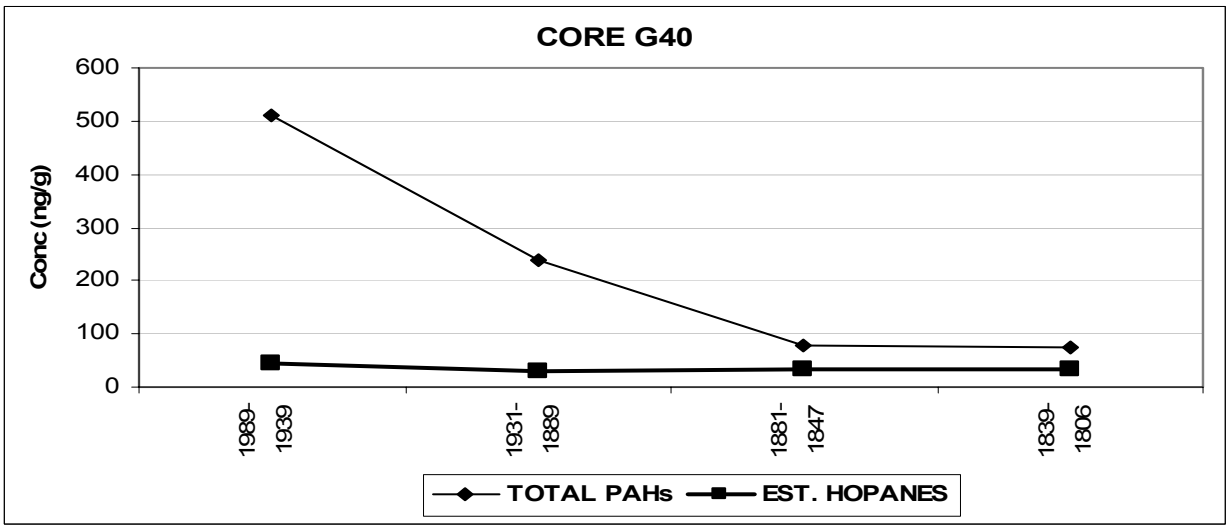

*Analysis not performed on CORE G50 due to only two data points

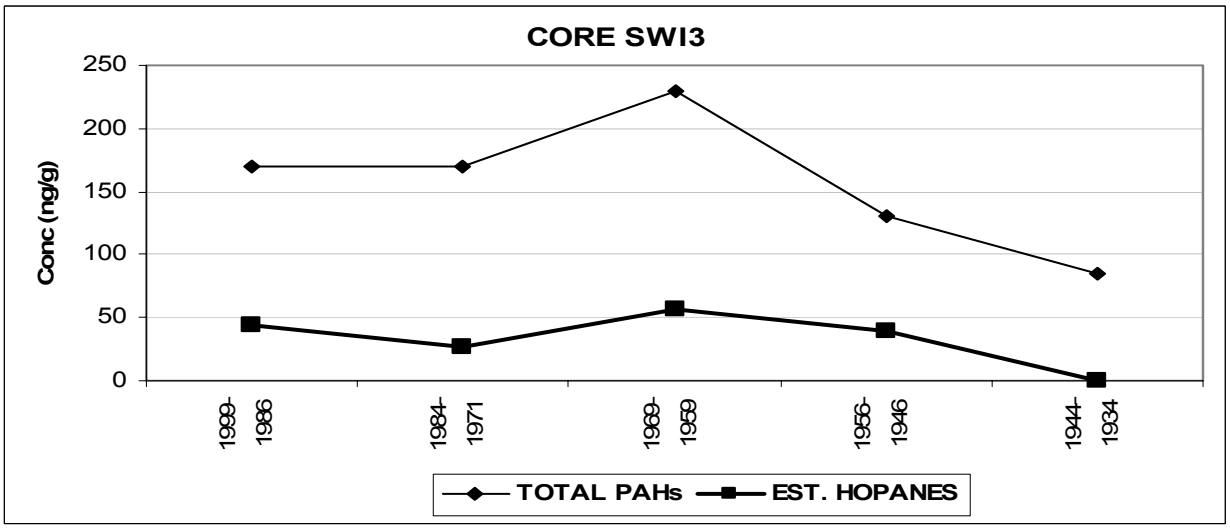

The Department of the Interior Mission

As the Nation's principal conservation agency, the Department of the Interior has responsibility for most of our nationally owned public lands and natural resources. This includes fostering sound use of our land and water resources; protecting our fish, wildlife, and biological diversity; preserving the environmental and cultural values of our national parks and historical places; and providing for the enjoyment of life through outdoor recreation. The Department assesses our energy and mineral resources and works to ensure that their development is in the best interests of all our people by encouraging stewardship and citizen participation in their care. The Department also has a major responsibility for American Indian reservation communities and for people who live in island territories under U.S. administration.

The Minerals Management Service Mission

As a bureau of the Department of the Interior, the Minerals Management Service's (MMS) primary responsibilities are to manage the mineral resources located on the Nation's Outer Continental Shelf (OCS), collect revenue from the Federal OCS and onshore Federal and Indian lands, and distribute those revenues.

Moreover, in working to meet its responsibilities, the **Offshore Minerals Management Program** administers the OCS competitive leasing program and oversees the safe and environmentally sound exploration and production of our Nation's offshore natural gas, oil and other mineral resources. The MMS **Minerals Revenue Management** meets its responsibilities by ensuring the efficient, timely and accurate collection and disbursement of revenue from mineral leasing and production due to Indian tribes and allottees, States and the U.S. Treasury.

The MMS strives to fulfill its responsibilities through the general guiding principles of: (1) being responsive to the public's concerns and interests by maintaining a dialogue with all potentially affected parties and (2) carrying out its programs with an emphasis on working to enhance the quality of life for all Americans by lending MMS assistance and expertise to economic development and environmental protection.